“The generation of anti-prostate cancer-specific antibodies for improved disease diagnosis”

Hannah Byrne B. Sc. (Hons)

A thesis submitted for the degree of Ph.D.

Feb 2016

Based on research carried out at
School of Biotechnology,
Dublin City University,
Dublin 9,
Ireland.

Under the supervision of Professor Richard O’ Kennedy and Professor Elaine Kay (Co-Supervisor)

Declaration

I hereby certify that this material, which I now submit for assessment on the programme of study leading to the award of Doctor of Philosophy, is entirely my own work. I have exercised reasonable care to ensure that the work is original. This work does not to the best of my knowledge breach any law of copyright, and has not been taken from the work of others save and to the extent that such work has been cited and acknowledged within the text of my work.

Signed:

Student number: 57508590

Date:

Dedication

This thesis is lovingly dedicated to my Mum, Maureen Byrne, and my Sister, Ruth Byrne. Their support, encouragement, and constant love, have sustained me throughout my life.

"Courage doesn't always roar. Sometimes courage is the quiet voice at the end of the day saying, I will try again tomorrow."

Acknowledgements

Firstly, I wish to express my appreciation and gratitude to Prof. Richard O' Kennedy. This thesis would not have been possible without the expert knowledge, direction, support and patience of my supervisor. It has been an invaluable experience working with you on both an academic and personal level, for which I am extremely grateful.

I also wish to acknowledge the support, guidance, encouragement and direction provided to me for the last number of years by Dr. Stephen Hearty, Dr. Paul Conroy, and Dr. Jenny Fitzgerald. It has been my pleasure to work with and learn from three of the most talented scientists I have ever met.

A word of thanks to everyone in the Applied Biochemistry Group, both past and present, for their friendship and support over the past four years. Aoife, Jenny, Kara, and Sarah, thank you for the many, many cups of coffee and chats. Without you girls, my Ph.D. experience would not have been the same.

I owe an immense debt of gratitude to my Mum, my Sister and my Brother in-law, Kevin, for their support, encouragement and total belief in me. Without their unwavering commitment to my education (over many years!) I could never have achieved so much.

Finally, I would like to say a special word of thanks to my best friends, Debi, Emily and Jen. You guys have been there for me through everything and have always believed in me. For this, I will be forever grateful.

Table of Contents

Table of Tables

Table of Figures

Abbreviations

AA	Amino acid
Ab	Antibody
ADCC	Antibody-dependent cell-mediated cytotoxicity
Ag	Antigen
AMACR	Alpha-methylacyl-CoA racemase
AMC	American Cancer Society
APC	Adenomatous polyposis coli
BCR	Biochemical Recurrence
BDI	Biomedical Diagnostics Unit
BiTE	Bispecific T-cell engager
BM	Bone marrow
BMI	Body-mass index
BPH	Benign prostatic hyperplasia
bPSA	Benign prostate specific antigen
BsAb	Bispecific antibody
BSA	Bovine serum albumin
C	Control
CamKII	Calcium/calmodulin-dependent kinase II
CDC	Complement dependent cytotoxicity
cDNA	Complementary DNA
CDR	Complementarity determining region
cPSA	Complexed prostate specific antigen
CP-CPPS	Chronic prostatitis/chronic pelvic pain syndrome
CEA	Carcinoembryonic antigen
C-FABP	C-terminal positioned FABP protein
C_H	Constant heavy (region of antibody)
CHO	Chinese hamster ovary
CIN	Control induced
C_L	Constant light (region of antibody)
Conc.	Concentration
CP	Concentrated protein
CRD	'Cysteine-rich' domain

CRPC	Castration resistant prostate cancer
CSF	Control soluble fraction
CSOC	Cleavage site of choice
CTnI	Cardiac troponin I
CInF	Control insoluble fraction
CUIN	Control uninduced
CVD	Cardiovascular
DAAM	Dishevelled associated activator of morphogenesis
DART	Dual affinity retargeting
DAUDA	(Dansylamino) undecanoic Acid
Db	Diabody
DKK	Dickkopf
DMSO	Dimethyl sulfoxide
DNA	Deoxyribonucleic acid
DRE	Digital rectal examination
dNTP	Deoxyribonucleotide triphosphate
DNMT	DNA methyltransferase
DVD	Dual-variable-domain
DVL	Dishevelled
E. coli	*Escherichia coli*
EF	Eluted fraction
EGFR	Epidermal growth factor receptor
ELISA	Enzyme-linked immunosorbent assay
EP	Eluted protein
EpCam	Epithelial cell adhesion molecule
ERB	Epidermal growth factor
FABP	Fatty acid binding protein
Fab	Antigen-binding fragment (region of antibody)
Fc	Constant fragment (region of antibody)
FDA	Food and Drug Administration
Ff	Filamentous
Fmi	Flamingo
Fh8	*Fasciola hepatica* 8-kDa antigen
FOLH	Folate hydrolase

fPSA	Free prostate specific antigen
FT	‘Flow-through’
Fv	Fragment variable (region of antibody)
FXa	Factor Xa
FZD	Frizzled
G3	Gleason grade 3
G4	Gleason grade 4
G5	Gleason grade 5
GSK	Glycogen synthase kinase
GS-rich	Glycine-serine rich
GST	Glutathione-S-transferase
GSTP	Glutathione S-transferase P
HA	Haemagglutinin
HAT	Histone acetyltransferase
HBD	Human beta-defensin
HBS	Hepes buffered saline
HDACs	Histone deacetylase
hFABP	Heart fatty acid binding protein
His	Histidine
H/L	Heavy/light (regions of antibody)
HIV	Human Immunodeficiency virus
HRP	Horseradish peroxidase
hrs	Hours
Ig	Immunoglobulin
IGFR	Insulin-like growth factor
IHC	Immunohistochemistry
IMAC	Immobilised metal affinity chromatography
IN	Induced
InF	Insoluble fraction
iPSA	Intact prostate specific antigen
IPTG	Isopropyl β-D-1-thiogalactopyranoside
JNK	JUN-N-terminal kinase
L	Ladder
LEF	Lymphocyte enhancer factor

LRP	Lipoprotein receptor-related protein
Luks-PV	PantonñValentine leukocidin
mAb	Monoclonal antibody
MBD	Methyl-CpG-binding domain
MBP	Maltose binding protein
$MgCl_2$	Magnesium chloride
$MgSO_4$	Magnesium sulphate
MHC	Major histocompatibility complex
MM	Milk Marvel
Mol. G H_2O	Molecular grade water
MPD	Methylation patterns during
MPO	Myeloperoxidase
mRNA	Messenger ribonucleic acid
MWCO	Molecular weight ‘cut-off’
N	Negative
N-FABP	N-terminal positioned FABP protein
NIH	National Institutes of Health
Nkd	Naked
Non-SupE	Non suppressor
NSCLC	Non-small cell lung cancer
NTR	Netrin
NusA	N-utilization substance
OD	Optical density
O/N	Overnight
pAb	Polyclonal antibody
PBS	Phosphate buffered saline
PBSM	Milk marvel prepared in phosphate buffer saline
PBS-T	Phosphate buffered-saline containing (0.05% (v/v) Tween
PBSTM	MM prepared in phosphate buffered saline containing tween
PCa	Prostate cancer
PCR	Polymerase chain reaction
PCA3	Prostate cancer antigen 3
PCTA	Prostate cancer tumour antigen
PDZ	Post-synaptic Drosophila Zona

PIN	Prostatic intraepithelial neoplasia
PKC	Protein kinase C
POC	‘Point-of-care’
pPSA	Pro-prostate specific antigen
PSA	Prostate specific antigen
PSCA	Prostate stem cell antigen
PSAP/PAP	Human prostatic acid phosphatase
PSMA	Prostate-specific membrane antigen
QMSP	Quantitative methylation-specific PCR
rAb	Recombinant antibody
rbsAb	Recombinant bispecific antibody
RNA	Ribonucleic acid
Rock	Rho-associated kinase
RT	Room temperature
RU	Response units
SB	Super broth
scAb	Single chain antibody
scFv	Single chain fragment variable
SCNC	Small-cell (neuroendocrine) carcinoma
SDS-PAGE	Sodium dodecyl sulfate-polyacrylamide gel electrophoresis
SE	Stability early
SF	Soluble fraction
SFRP-2	Secreted Frizzled Related Protein-2
SL	Stability late
SOE	Splice-by-overlap
SP	Spleen
SPR	Surface plasmon resonance
SS	Stuffer
ssDNA	Single stranded DNA
STEAP	Six transmembrane epithelial antigen of the prostate
SUMO	Small ubiquitin modified
SupE	Suppressor strain
T	Tween
taFv	Tandem Fv

T-cells	Thymus cells
TCF	T-cell factor
TE	Tris EDTA
TEMED	Tetramethylethlenediamine
TEV	Tobacco Etch Virus
TF	Transcription factor
TMA	Tissue micro-arrays
TMB	Tetramethylbenzidine
TMPRSS2	Transmembrane protease, serine 2
TNF	Tumour necrosis factor
TOC	Tag-of-choice
tPSA	Total PSA
TRAIL	Tumour necrosis factor-related apoptosis-inducing ligand
Trx	Thioredoxin
TURP	Transurethral resection of the prostate
UCC	Urothelial cell carcinoma
UN	Uninduced
USA	United States of America
VEGFR	Vascular endothelial growth factor
V_H	Variable Heavy (region of antibody)
V_L	Variable Light (region of antibody)
WA	Wash A
WB	Wash B
WB	Western blotting
WHO	World Health Organization
WIF	WNT Inhibitory factor
WNT	Wingless
WTX	Wilms tumour gene on the X-chromosome

Units

µg	Microgram
µL	Microlitre
µM	Micromolar
g	Gram
kDa	Kiladaltons
L	Litre
M	Molar
mg	Milligram
mL	Millilitre
min	Minute
mM	Millimolar
ng	Nanogram
°C	Degrees Celsius
rpm	Revolutions per minute
U	Unit
V	Volts
v/v	Volume per unit volume
w/v	Weight per unit volume
x g	Centrifugal acceleration

Publications and Presentations

Publications:

Byrne, H., Conroy, P. J., Whisstock, J. C., O'Kennedy, R. J. A tale of two specificities: bispecific antibodies for therapeutic and diagnostic applications." *Trends Biotechnol.* 2013; 31: 621-632.

Byrne, H., Conroy, P. J., O'Kennedy, R. .J. "Approaches for the detection of prostate cancer. Nano-Inspired Biosensors for improved healthcare. (Submitted to CRC press for publication).

Sharma, S., Byrne, H., O'Kennedy, R. J. Antibodies and antibody-derived analytical biosensors. (Submitted for publication in Biosensor technologies for detection of biomolecules), Essays in Biochemistry series, Portland Press, London.

Presentations:

Byrne, H, O'Kennedy, R.J. "Generation of novel antibodies and approaches for the detection of prostate cancer.' BioAT research day 11th June 2012, Royal College of Surgeons, Dublin, Ireland. (Oral presentation)

Byrne, H, Conroy, PJ, O'Kennedy R.J. "The generation of a bispecific antibody using a novel generation strategy. BioAT research day 12th June 2013, National University of Ireland, Maynooth, Co. Kildare, Ireland. (Poster presentation)

Byrne, H, Gilgunn, S, Fitzgerald, S. Antibody expression, purification and application. PROSENSE workshop. 2nd – 4th July 2013. Dublin City University, Dublin, Ireland. (Oral presentation)

Byrne, H, Gilgunn, S. "The generation and characterisation of recombinant antibodies." PROSENSE workshop. 2nd – 4th July 2013. Dublin City University, Dublin, Ireland. (Poster presentation)

Gilgunn, S, Byrne, H. "Screening avian scFv libraries through phage display." PROSENSE workshop. 2nd – 4th July 2013. Dublin City University, Dublin, Ireland. (Poster presentation)

Abstract

Prostate Cancer (PCa) is one of the leading medical issues faced by men worldwide and is the most prevalent cancer diagnosed in men in both Europe and the United States. Some prostatic cancers present as an indolent disease with no clinical symptoms during the lifetime of the patient, and in many cases, men die with the disease rather than from it (insignificant PCa). However, for some PCa patients the disease takes a much more aggressive route, spreading into the seminal vesicles, bladder, and rectum and further metastasising to the lymph nodes, bone and other organs. Measurement of prostate specific antigen (PSA) levels in serum is routinely used for PCa diagnosis and monitoring disease progression (Lilja, H., *et al*. 1987; *J. Clin. Invest* 80: 281-285). Conversely, PSA levels can also rise as a result of Benign Prostatic Hyperplasia (BPH) and hence this marker provides little or no insight into the biology of an individual's prostatic disorder. There is no outright test that can distinguish between significant and insignificant disease. There is an unmet need for better biomarkers to stratify patients into the most appropriate treatment option for their individual prostatic disease. The overall aim of this research was to generate PCa-specific antibodies, namely anti-prostate-specific membrane antigen (PSMA) and anti-secreted frizzled related protein-2 (SFRP2) antibodies, for application in Immunohistochemistry (IHC) to enhance or improve prostate cancer diagnosis.

Using a specific targeting strategy, anti-SFRP-2 and anti-PSMA fragment antibodies were successfully produced and characterised. The generation and characterisation approach applied required a combination of the use of a novel antigen expression strategy (for the production of SFRP2), high-throughput assay screening with 'state-of-the-art' multiplexed surface-plasmon resonance-based instrumentation and standard analytical techniques. The selected recombinant antibodies were demonstrated to match the performance of current commercially available polyclonal antibodies.

In addition, the use of bispecific antibodies for therapeutic and diagnostic application was described and the first step in 'proof-of-concept' studies establishing a novel bispecific antibody generation approach is presented.

Chapter 1

Introduction and aims of the study

1.1 Histology of the Prostate

The prostate is the largest accessory gland in the male reproductive system. It is a compound tubuloalveolar exocrine gland, which is located under the bladder in front of the rectum and is pierced by the urethra and the ejaculatory ducts (Figure 1.1) (Gartner & Hiatt, 2001). It is responsible for producing a slightly alkaline white fluid (pH 7.29) that makes up 25-30% of male semen. This fluid, which protects, carries and nourishes sperm cells, is rich in lipids, proteolytic enzymes, acid phosphatase, fibrolysin and citric acids (Gartner & Hiatt, 2001). The majority of seminal fluid is produced by the seminal vesicles, located directly behind the prostate gland. The prostate also contains smooth muscle, which helps expel semen during ejaculation. The active form of testosterone, dihydrotestosterone, regulates the formation, synthesis and release of prostate secretions (Gartner & Hiatt 2001).

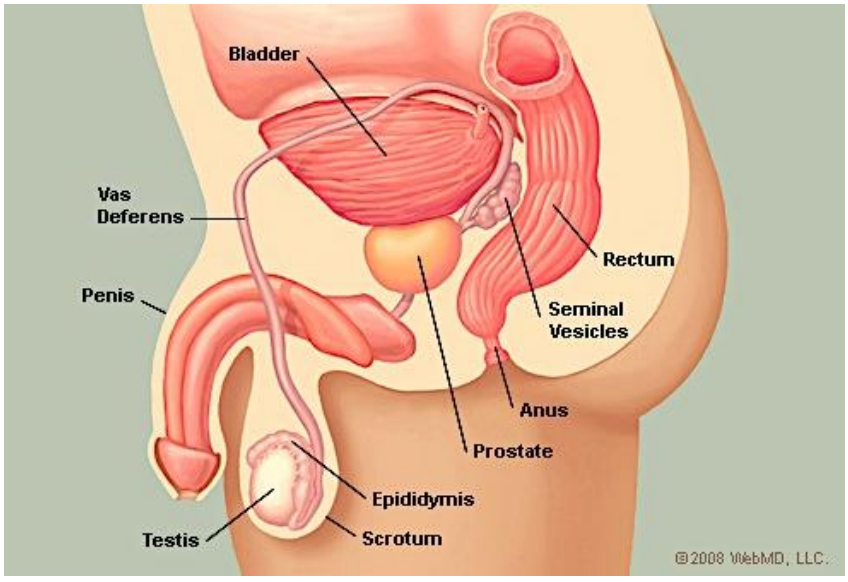

Figure 1.1. Location of the prostate gland in the male reproductive system.

The prostate is a walnut-sized gland located between the bladder and the penis. The prostate is just in front of the rectum. The urethra runs through the center of the prostate, from the bladder to the penis, letting urine flow out of the body. (Adapted from: http://www.webmd.com/urinary-incontinence-oab/picture-of-the-prostate)

There are three major glandular regions within the prostate gland (see Figure 1.2); the peripheral zone, which is the sub-capsular portion of the posterior aspect of the prostate gland that surrounds the distal urethra, the central zone, which surrounds the ejaculatory ducts and the transition zone, which surrounds the proximal urethra. Each

zone differs from the next both biologically and histologically (McNeal, 1988). The anterior fibro-muscular zone is the fourth zone of the prostate but is usually devoid of glandular components and is composed only of muscle and fibrous tissue. Each glandular zone has specific architectural and stromal features. The stroma of the gland is derived from the capsule (membrane covering the prostate that merges with surrounding soft tissues, including nerves) and is enriched by smooth muscle fibres in addition to connective tissue cells. A layer of basal cells beneath the secretory lining exists in each zone in addition to interspersed endocrine-paracrine cells (McNeal, 1988). The lumina of the tubuloalveolar glands often contain oval prostatic concretions, called corpora amylacea, which are composed of calcified glycoproteins. The number of calcified glycoproteins increases with a man's age (Gartner & Hiatt, 2001).

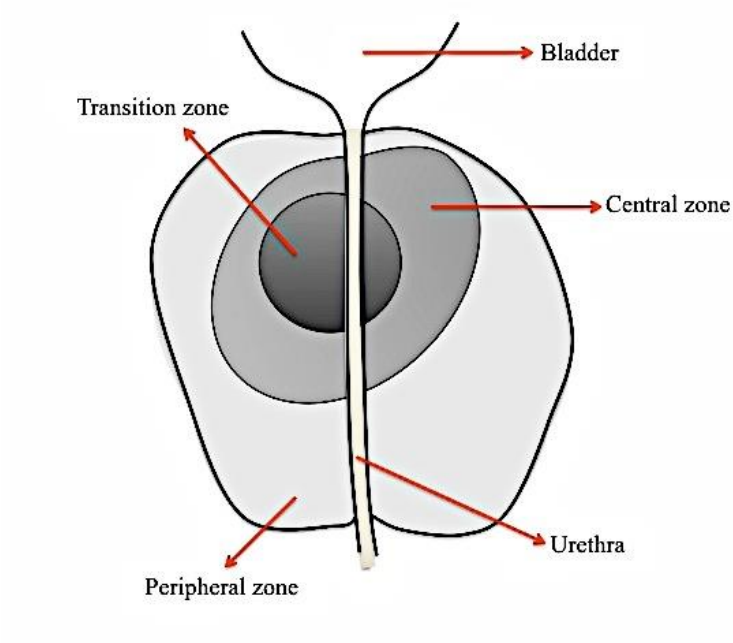

Figure 1.2. Glandular regions within the prostate gland.

The peripheral zone is the area of the prostate that lies closest to the rectum and can be easily felt by the doctor during a digital rectal examination (DRE). It is the largest zone of the prostate and approximately 75% of all PCa occur in this zone. The transition zone is located in the middle area of the prostate. It surrounds the urethra as it passes through the prostate. 10-20% of all PCa occur in this zone. This zone makes up about 5 - 20% of the prostate gland until the age of 40. During aging in men, the transition zone begins to enlarge, until it becomes the largest area of the prostate. This is called benign prostatic hyperplasia (BPH). The central zone surrounds the ejaculatory ducts and makes up 25% of the prostate gland. This zone accounts for approximately 2.5% of prostate cancers. (Adapted from: http://www.cancer.ca)

1.2 Pathology of the Prostate

Prostate disorders are usually associated with ageing and are the most common health complaint in men over the age of 50. In contrast, young men are rarely affected by prostate problems. The main prostate disorders include inflammatory disorders, hyperplasia and carcinoma.

1.2.1 Prostatitis

Prostatitis causes swelling and inflammation of the prostate. The four categories of prostatitis are acute prostatitis, chronic bacterial prostatitis, chronic prostatitis/chronic pelvic pain syndrome and asymptomatic inflammatory prostatitis. Symptoms of prostatitis include: painful or difficult urination, pain in the groin, pelvic or genital area, and sometimes 'flu-like' symptoms. Infection in the prostate from bacteria such as *Escherichia coli* (*E. coli*) and Proteus species, causes a condition known as acute prostatitis, which results in swelling of the acutely inflamed gland (Selius & Subedi, 2008). Chronic bacterial prostatitis is a rare condition, which presents as recurrent urinary tract infections originating from a bacterial infection in the prostate. The most common type of prostatitis is prostatitis/chronic pelvic pain syndrome (CP/CPPS) (Pontari & Ruggieri, 2004). The National Institute of Health (NIH) defines CP/CPPS as genitourinary pain with or without voiding symptoms in the absence of uropathogenic bacteria, as detected by standard microbiological methods, or due to, another identifiable cause such as malignancy. Asymptomatic inflammatory prostatitis is difficult to diagnose and the correct diagnosis is very important, because the treatment varies for the different types of prostatitis syndromes. In addition, it is extremely important to ensure the symptoms are not derived from other conditions such as urethritis, cystitis, an enlarged prostate or cancer. Prostatitis is usually diagnosed through a DRE, a cystoscopy, a uroflow test, transrectal ultrasound or biopsy. Infectious prostatitis requires anti-microbial treatment whereas non-infectious prostatitis cannot be treated with anti-microbial agents.

1.2.2 Benign prostatic hyperplasia (BPH)

Benign prostatic hyperplasia is a non-malignant enlargement of the prostate as a result of proliferation of epithelial cells within the basal cell layer, due to an alteration in hormone balance (accumulation of dihydrotestosterone). It is the most common benign tumour in men, is not considered a pre-malignant lesion, and is more prevalent in the Asian population (Prajapati *et al.*, 2013). The disease has stromal and glandular

components (Ziada *et al.*, 1999) and is characterised histologically by the presence of nodules on the periurethral zone/mucosal glands of the prostate (Edwards, 2008) but can extend to involve the lateral lobes. Men with BPH commonly have difficulty passing urine due to compression of periurethral nodules impeding the flow of urine. Obstructive and irritative symptoms associated with BPH are hesitancy urinating, weak stream, retention of urine in the bladder, very frequent urination, and small voided volumes. There is evidence of BPH in ~20%, 40%, 55%, 80%, and 90% of men aged 40-50, 50-60, 60-70, 70-80, and 80-90, respectively (Ziada *et al.*, 1999). Factors leading to BPH include hormone imbalance, oxidative stress, environmental pollutants, family history, age, race, ethnicity, cigarette smoking, and chronic disease.

BPH is usually diagnosed through the presence of clinical symptoms, a digital rectal examination (DRE) or the prostate specific antigen (PSA) test. However, there are major contentions in relation to how reliable the PSA test is for the differentiation between BPH and PCa. A PSA level that continues to increase over time does not necessarily mean PCa, but can be an indicator that the patient in question may have BPH or prostatitis. Patients with an increased PSA level are usually advised to undergo a transrectal prostatic needle biopsy for confirmation of PCa. The majority of patients that undergo this procedure do not have PCa. Therefore, biopsies are typically unnecessary and may cause the patient stress and discomfort. A more specific test with the ability to decipher between BPH and PCa is badly needed.

Treatment options for BPH are categorized as either surgical or non-surgical interventions. The choice of therapy administered to a patient is dependent on the nature, severity and duration of symptoms. Drug therapies for BPH include drugs that inhibit the 5-alpha reductase enzyme, which converts testosterone to dihydrotestosterone within cells and alpha-adrenergic blockers, which leads to relaxation of smooth muscle in the prostate and helps to relieve obstruction. The gold standard surgical treatment of BPH is transurethral resection of the prostate (TURP), which improves symptoms of BPH by 85-100%, and has an associated mortality risk of 2% (Ziada *et al.*, 1999). This surgical procedure involves removing tissue from the prostate via a resectoscope inserted through the urethra.

1.3 Prostate Cancer (PCa)

1.3.1 Epidemiology of Prostate Cancer

Prostate cancer (PCa) is the most commonly diagnosed male malignancy in Western Europe and North America, with 1 in 7 men diagnosed with the disease (www.cancer.org). The American Cancer Society's estimates for PCa in the United States for 2016 are that approximately 220,800 new cases will be diagnosed, of which 27,540 men will die of the disease (1 in 36 men worldwide). Taking these statistics into consideration, 75 men will die every day this year from PCa.

The first case of PCa, which was diagnosed by histological evaluation, was reported in 1853 (Lytton, 2001). It was initially regarded as a very rare form of cancer but this may well be due to the fact that PCa went largely unrecognized until the turn of the last century (Lytton, 2001). In Europe, an estimated 2.6 million new cases of cancer are diagnosed each year. Prostate cancer represents about 11% of all cancers in Europe and accounts for 9% of cancer deaths among the male population within the EU (Aus *et al.,* 2005). Annual incidence of PCa in the Republic of Ireland is approximately 2,500 with mortality in excess of 550 cases per annum (www.ncri.ie). In 2015, 3,172 men were diagnosed with PCa in Ireland, which accounted for 19.5% of total cancer diagnosis. It is predicted that the incidence of PCa will increase by 275%, with figures approaching 6,000 new cases by 2020, due to an ageing population, and an increased awareness of PCa. (www.ncri.ie).

1.3.2 Types of PCa

Prostatic adenocarcinoma is the most common form of all PCa (95%). Prostatic adenocarcinoma is an aggressive, uncontrolled malignant growth initially localized in the prostate gland, but, if not treated successfully at an early stage, can spread very rapidly to other parts of the body, in particular the lymph nodes and the bone. Other forms of prostate cancer are summarized in Table 1.

Table 1. Rare types of Prostate Cancer.

Type of Prostate Cancer	Disease Description	Incidence
Small-cell (neuroendocrine) carcinoma (SCNC)	A rare malignancy of neuroendocrine cell lineage arising in the human prostate. The aggressive form of SCNC gives a median survival time of 6 – 17 months following diagnosis. SCNC does not usually secrete prostate specific antigen (PSA) unlike adenocarcinomas and cannot be detected using the PSA test (Brownback *et al.*, 2009).	0.5% - 2% of all primary prostatic tumours (Brownback *et al.*, 2009)
Squamous cell carcinoma	A rare neoplasm of the prostate gland. This is a very aggressive tumour with very short survival time. It differs from adenocarcinomas in its biological behavior, therapeutic response and prognosis.	0.5% of all prostatic malignancies (John *et al.*, 2005)
Primary transitional cell carcinoma (TCC)/ urothelial cell carcinoma (UCC) of the prostate	A rare malignancy that originates in the transitional epithelial cells of the intra-prostatic periurethral ducts.	2-4% of all prostatic carcinomas (Rubenstein & Rubnitz, 1969)

1.3.3 Prostatic intraepithelial neoplasia (PIN)

Prostatic intraepithelial neoplasia (PIN) is a cytological alteration in architecturally normal glands that consists of an intraluminal proliferation of the secretory epithelium revealing a spectrum of atypical cytological changes ranging from minimal changes to those that are indistinguishable from carcinoma. PIN is divided into two grades; low grade PIN (formerly grade 1) and high grade PIN (formerly grade 2 and 3). PIN, especially high grade, is considered to be a precursor to malignancy. As high grade PIN has high predictive value as a marker for adenocarcinoma, repeat biopsies are warranted if detected on initial biopsy (Dabbs, 2006). It was reported that carcinoma will develop in most patients with high grade PIN within 10 years and that the

incidence (Bostwick *et al.*, 2004) and extent of PIN appears to increase with patient age (Dabbs, 2006).

1.4 Molecular Biology of Prostate Cancer

Every carcinoma focus is presumed to reflect a progressive and cumulative genetic alteration from a single cell, which affects regulatory genes resulting in a growth or survival advantage. Multiple classes of cancer-associated genes contribute to the carcinogenic process when their functions are perturbed by either genetic or epigenetic mechanisms (Isaacs & Kainu, 2001). Such classes of cancer-associated genes are oncogenes and tumour suppressor genes. Proto-oncogenes are involved in normal cell proliferation. They encode a variety of proteins that function as growth factors, growth factor receptors, modifiers of protein function, regulators of replication or transcription or other signalling pathways (Karayi & Markham, 2004). When a proto-oncogene is mutated, translocated or amplified, it becomes activated and is known as an oncogene. Oncogenes are pro-carcinogenic and only require the alteration of one allele as they function in a dominant manner (Karayi & Markham, 2004). Examples of oncogenes include *K-RAS*, which is widely studied in many cancers including urological neoplasms and *C-ERB-B2* (also called *HER-2/NEU*) in breast cancer.

Tumour suppressor genes are anti-oncogenes. They are protective genes that normally limit the growth of tumours. When tumour suppressor genes are inactivated there is a loss or reduction in their function contributing to cancer formation. Tumour suppressor genes function in a recessive manner. An example of a well-characterised tumour suppressor gene is the P53 gene, which is the cause of Li-Fraumeni syndrome when absent in the germ line and is implicated in many other cancers. ‘Gate-keeper’ genes directly regulate the growth of tumours through promoting cell death and inhibiting growth (Karayi & Markham, 2004). The inactivation of a ‘gate-keeper’ gene results in tissue-specific distribution of cancer. Examples of ‘gate-keeper’ genes include the APC gene in colon carcinoma and the RB gene in retinoblastoma. ‘Caretaker’ genes regulate genomic repair and genomic instability results from mutations in those genes. Tumour initiation is not promoted by the inactivation of ‘caretaker’ genes but the resulting genomic instability leads to the higher mutation rates in other genes such as ‘gatekeeper’ genes. Thus, an individual with a hereditary

mutation of a ‘caretaker’ gene is at greater risk of developing a tumour than the general population (Karayi & Markham, 2004). BRCA1 and BRCA2 are examples of “caretaker” genes associated with breast cancer.

Like all carcinomas, prostate cancer arises in differentiated epithelial cells and/or progenitor cells in which embryonic pathways are reactivated through the activation of oncogenes and the loss of tumour suppressor genes, which leads to a growth and survival advantage (Taichman *et al.*, 2007). The process of prostate carcinogenesis is the result of DNA damage that occurs in either a differentiated cell or a stem cell through a complex interplay of genes, the cellular micro-environment and the macro-environment such as external agents and/or ingestion of carcinogens (Taichman *et al.*, 2007). It is postulated that prostate carcinogenesis is a multi-step process requiring a subset of ‘hits’ or mutations in putative precursor lesions or latent cancers in order for progression to fully malignant phenotype (Isaacs & Kainu, 2001). Classic oncogenes and tumour suppressor genes are rarely mutated in prostate cancer. However, several molecular and genetic changes both inherited (e.g. *RNASEL* and *MSR1*) and somatic (e.g. *RB1* and *PTEN*) have been directly involved in prostate carcinogenesis but none have been explicitly linked to prostate cancer initiation or progression (DeMarzo *et al.*, 2003). These molecular and genetic changes in prostate cancer are summarized in Tables 2 and 3.

Table 2. Genes proposed to be involved in prostate cancer carcinogenesis or in modifying the risk of prostate cancer. (Adapted from DeMarzo *et al.*, 2003).

Gene	Proposed function
Mutations causing decreased activity	
MSR1	Anti-infectious, scavenger receptor
RNASEL	Anti-infectious, apoptosis
ELAC2	Metal-dependent hydrolase
Promotor hypermethylation resulting in gene silencing	
GSTP1	Carcinogen detoxification
Loss of heterozygosity and point mutation	
PTEN	Cell survival and proliferation
TP53 (also P53)	Cell survival and proliferation, genome stability
Loss of heterozygosity and haploinsufficiency	
NKX3-1	Cell differentiation and proliferation
CDKN1B (P27KIP1)	Cell differentiation
Point mutations	
COPEB (also KLR6)	Transcription regulator
AR	Cell proliferation, survival and differentiation
Amplification	
AR	Cell proliferation, survival and differentiation
Overexpressed at mRNA and protein level	
HTERT	Cell immortality
HPN	Transmembrane protease
FASN	Fatty-acid synthesis
AMACR	Fatty-acid metabolism, branched chain
EZH2	Transcription repressor, cell proliferation
MYC	Cell proliferation
BCL2	Cell survival
Polymorphism affecting prostate cancer risks	
AR	Cell proliferation/survival/differentiation
CYP17	Androgen metabolism
SRD5A2	Androgen metabolism

Table 3. Molecular progression in prostate cancer. (Adapted from Karayi & Markham, 2004).

Normal prostate cells

Presence of predisposed alleles (e.g. *RNASEL*)
Methylation of tumour suppressor gene promoters leading to epigenetic silencing
Chromosome 8p loss
AR CAG repeat alterations
Vitamin D Receptor reduced activity
5α reductase (*SRD4A2*) increased activity
CAPB (1p36) mutation
HPC1 (1q24-25) mutation
MSR1 (8p22-23) mutation
KLF6 (10p15) mutation
ELAC2 (17q11.2) mutation
HPC20 (20q13) mutation
HPCX mutation

Localised prostate cancer

Chromosome 16q loss
Altered E-Cadherin expression (16q)
RB1 (13q) loss
P53 (17p) inactivation
GSTP1 (11q13) inactivation

Metastatic prostate cancer

Overexpression of EZH2 polycomb protein
Transcriptional silencing of many genes by histone deacetylation
Increased BCL-2 expression
Increased availability of adrenal steroids
Loss of KAI-1 (11p)
PTEN mutation
AR gene amplification
AR mutation
Abnormal phosphorylation of AR by 2nd messenger systems

Androgen-independent prostate cancer

1.5 Causes, symptoms, and current approaches for diagnosis of PCa - (the limitations)

The incidence of PCa varies largely between racial/ethnic groups. PCa is highest among Africans, intermediate among Caucasians, and lowest among Asians (Ntais *et al.*, 2003). Black men have the highest incidence rate in the United States and are more inclined to receive an advanced PCa diagnosis than men in any other racial or ethnic group (Hoffman, 2011). The strongest risk factors associated with PCa are body-mass index (BMI), older age, a positive family history, and race. The median age of diagnosis for PCa is 67 years, and the median age of death is 81 years

(Hoffman, 2011). Men who have a first-degree relative with PCa are twice as a likely to be diagnosed with the disease in comparison to those who do not (Hoffman, 2011). The most common symptoms associated with PCa are difficulty passing urine, passing urine more often than usual, pain when passing urine, and blood in the urine.

The key to survival with every type of cancer is early and accurate diagnosis, followed by appropriate treatment. An effective cancer-screening test can be described as an accurate, reliable, and 'easy-to-use' test that detects clinically significant cancers at a pre-clinical stage. PCa screening is performed in an effort to detect unsuspected cancer, which may lead to more specific diagnostic follow-up tests such as a biopsy. For many years the digital rectal examination (DRE) was the primary screening test for PCa diagnosis. A DRE is a physical examination of the prostate gland carried out by a physician. During a DRE, a clinician detects hard nodules on the prostate or enlargement of the prostate by manual examination. The latter typically indicates BPH or prostatitis and the former typically relates to PCa (Baumgart *et al.*, 2010). Unfortunately, this test has considerable inter-examiner variability, the majority of cancers detected using this method are at an advanced stage (Hoffman, 2011), and it is not a very attractive form of examination for patients.

In the late 1980s, the prostate specific antigen (PSA) test, which was initially introduced for PCa surveillance, became widely adopted as the 'gold standard' for PCa screening. In 1994 the Food and Drug Administration (FDA) approved PSA in the United States for cancer detection (Nogueira *et al.*, 2009). PSA is a 34-kilo Dalton (kDa) glycoprotein and consists of 237 amino acids. It is an androgen-regulated serine protease and a member of the tissue kallikrein family of proteases. Prostate glands in humans consist of a single layer of secretory epithelial cells, surrounded by a continuous layer of basal cells and a basement membrane (Balk *et al.*, 2003). PSA is produced by prostate ductal and acinar epithelium and is secreted into the lumen, where its physiological function is to liquefy semen from its gel form. In normal conditions, PSA can only enter blood circulation by leaking into the extracellular fluid and diffusing into veins and capillaries. PSA circulates in serum in free and complexed forms, with free forms representing 5-35% of total PSA, and complexed forms representing 65-95% (Nogueira *et al.*, 2009). Figure 1.3 shows a schematic representation of the processing of PSA in the cell (Gilgunn *et al.*, 2013). A

characteristic early feature of PCa is disruption of the basal cell layer and basement membrane by tumour growth. This disruption in the architecture of the prostate appears to allow increased PSA levels in the peripheral circulation. A standard PSA test measures the ratio of free PSA (fPSA) to total PSA (tPSA). PSA is found in the serum in several isoforms including fPSA (complete PSA protein with no modifications), complexed PSA (cPSA - PSA that forms complexes with various serum proteins), pro-PSA (a precursor form of PSA), benign PSA (bPSA - contains two internal peptide bond cleavages at lysine 145 and 182), and intact non-native PSA (a non-native form of PSA that is not cleaved at lysines 145 and/or 182). An increased level of PSA (4.0 ng/ml of total PSA as the upper limit of normal) in serum is suggestive of PCa; however, for confirmational diagnosis a transrectal prostatic needle biopsy is required. Biopsies themselves carry significant side effects such as risk of subsequent erectile dysfunction, serious infections and urinary conditions.

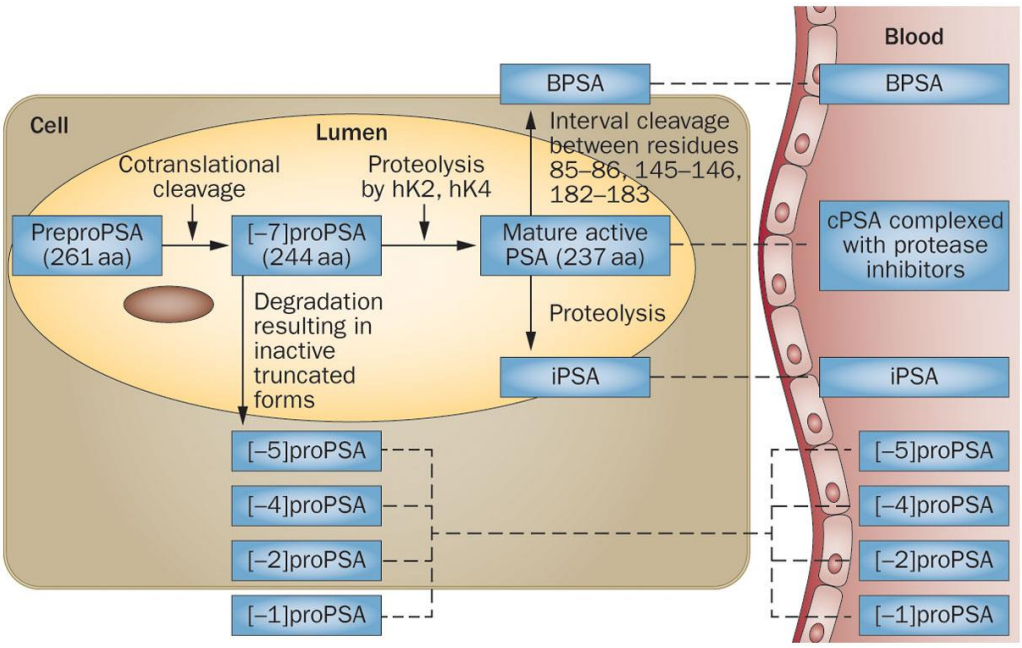

Figure 1.3. Schematic representation of the processing of PSA in the cell.

PSA is synthesized as a 261 amino acid pre-propeptide, which is co-translationally cleaved in the cell to generate [−7]proPSA (244 amino acids in size), an inactive precursor protein. [−7]proPSA is converted to mature active PSA (237 amino acids in size) by human kallikrein-2 (hK2). As a result of partial degradation of [−7]proPSA, different forms of proPSA such as [-1], [-2], [-4], and [-5]proPSA are developed. The majority of serum PSA that leaks into the serum from the prostate is complexed with serum protease inhibitors, primarily α_1-antichymotrypsin, and is termed 'complexed PSA' (cPSA). Ten to thirty percent of PSA is 'free' (fPSA) in the serum and is composed of various isoforms. Free PSA has three distinct isoforms: proPSA, which comprises 33% of fPSA, benign PSA (BPSA), which is regarded as a nicked form of PSA and makes up ~28% of fPSA, and 'inactive' or 'intact PSA' (iPSA), which decreases in concentration with cancer. Black arrows depict cellular processing of PSA. Dotted black arrows depict cellular transport of PSA isoforms. Abbreviations: BPSA, benign PSA; cPSA, complexed PSA; iPSA, inactive PSA. (Gilgunn et al., 2013).

There is considerable controversy as to the value of PSA as a marker of PCa despite its ongoing use. Initial arguments against the PSA diagnostic test stated that it was not clear whether the benefits of PSA screening outweighed the risks associated with follow-up diagnostic tests and cancer treatment (Thompson *et al.*, 2005). PSA screening could detect cancer that would not have become life-threatening (indolent cancer). This 'over-diagnosis' situation places men at risk of complications from unnecessary treatment such as, surgery or radiation therapy (40-50% of cases are unnecessarily treated) (Smith *et al.*, 2005a). PSA is not a cancer-specific protein and, therefore, its presence is not unique to the presence of cancerous cells (Jung *et al.*,

2000). PSA may be sufficient to use in the detection of residual cancer, recurrence and cancer regression following treatment (Dabbs, 2006). It was observed that a PSA level above 2.0 ng/mL following radical prostatectomy is often considered evidence of biochemical recurrence. The poor sensitivity associated with the PSA test has led to unsuccessful early diagnosis of PCa and failure to distinguish between aggressive versus non-aggressive disease. Additionally, other non-cancerous forms of prostate disease such as BPH and prostatitis can result in an increased PSA level, limiting the specificity of PSA elevation for cancer detection (Makarov *et al.*, 2009).

Statistics show that only one in four men with a PSA level greater than 4.0 μg/L have biopsy-proven prostate cancer. Therefore, determining which patients require treatment and patients to treat aggressively remains a dilemma. Lowering the PSA threshold has been suggested as an alternative to satisfy the current problems associated with the PSA test. However, when the PSA threshold is decreased there is an increased risk of identifying and unnecessarily treating indolent disease (Velonas *et al.*, 2013). There is growing evidence that the use of the distinct isoforms of PSA in addition to total PSA may significantly increase the diagnostic utility of PSA for PCa. The suggested need for multiple markers for the detection of PCa reflects not only the lack of specificity of the current PSA test but also the multidimensional nature of this disease which ranges from metastatic cancer to benign conditions and inflammation. For this reason, more specific and clinically relevant markers for PCa detection are highly warranted. This will allow clinicians to reduce the number of unnecessary surgical interventions and will help select patients suitable for appropriate treatment.

In 2012 the FDA approved the Beckman Coulter Prostate Health Index (PHI) test to evaluate the probability of a prostate cancer diagnosis. PHI is a mathematical combination of total PSA, free PSA and a PSA precursor protein known as [-2] proPSA according to the formula ([-2] proPSA/fPSA)x√tPSA (Filella & Giménez, 2013). The PHI test has not only demonstrated superior accuracy versus PSA and %fPSA for predicting the presence of prostate cancer, but also outperformed PSA testing for prediction of aggressive prostate cancer (Catalona *et al.*, 2011; Filella & Giménez, 2013; Nichol *et al.*, 2011). At a 90% threshold of sensitivity for prostate cancer detection, the PHI had a specificity of 31.6% compared with 19.8% and 10.8% for fPSA and PSA, respectively (Filella & Giménez, 2013). Corresponding values for

histopathologically aggressive prostate cancer were 30.1%, 21.7%, and 9.6% for PHI, fPSA, and PSA, respectively (Filella & Giménez, 2013). Using this test it may be possible to reduce the number of unnecessary biopsies, maintaining a high cancer detection rate whilst reducing the risk of over-diagnosis and over-treatment, particularly in the group of patients with a PSA level between 2 and 10 μg/L.

1.6 Prognosis and treatment of PCa

PCa is clinically diagnosed as localized or advanced cancer. There is marked disease heterogeneity associated with the disease. Some men have forms of PCa that progress very rapidly into metastatic disease while others may live relatively asymptomatically for many years. Subsequently, a large percentage of men die with the disease rather than from the disease. A patient's outcome is principally determined by metastases. According to the American Cancer Society (ACS) the most recent data suggest that relative 5 (Table 4) and 10 year survival rates for those diagnosed with early stage PCa are 100% and 98%, respectively, (based on patients diagnosed and first treated 5 or 10 years previously). These statistics infer early diagnosis is critical to improve and extend the quality of life of those diagnosed.

Table 4. Five-year relative survival rates at the time of diagnosis depending on the location of the cancer. (Adapted from http://www.cancer.org)

Stage of the disease	Five-year relative survival rate
Local – no sign that the cancer has spread outside of the prostate	~100%
Regional – cancer has spread in to the lymph nodes and tissue located in the vicinity of the original cancer	~100%
Distant – cancer has spread to distant lymph nodes, bones, or other organs	~28%

Treatment options for PCa are dependent on the health status of the patient, life-expectancy and tumour characteristics (Damber & Aus, 2008) including the stage of the tumour, aggressiveness and PSA level. In addition to these characteristics various patterns of tumour proliferation are associated with tumour aggressiveness and patient outcome. This is the basis of the Gleason grading system. Tumour grading (Gleason grading) determines how closely the tumour cells resemble their cell of origin. This

form of grading is extremely valuable as it aids the prediction of the extent of the disease, correlates well with patient survival, and helps in determining appropriate treatment options. The Gleason grading system was created by Donald F. Gleason in 1966. It is a system that categorizes cancerous tissue into five grades, 1 to 5 based on tumour differentiation (the degree of tumour resemblance to normal tissue). A Gleason grade associated with a tumour increases with increasing malignancy and cancer aggressiveness. Grade 1 corresponds to a well-differentiated tumour with the highest degree of resemblance to normal tissue and indicates a high chance of survival. Grade 5 is associated with poorly differentiated tumours and thus a low survival rate. PCa prognosis is associated with the overall Gleason score, which ranges from 2 to 10. The Gleason score represents the sum of the most prominent and second most prominent Gleason grades present in the tissue. Gleason grading has the ability to predict pathological stage, margin status, biochemical failure, local recurrences, lymph node involvement, and disease progression (Lopez-Beltran *et al.*, 2006).

The only issue associated with this form of tumour grading is the limited intra and inter-pathologist reproducibility. Difficulty can occur when attempting to distinguish between Gleason grade 3 and 4 or 4 and 5 tumours. The significance of this problem has led to the introduction of additional Gleason grades termed Gleason grade 4/5. Over/under grading a tumour is a major issue as therapy and overall prognosis of the disease are initially based on the Gleason grading system. Therefore, more specific molecular markers that can aid in the distinction between Gleason grades are urgently required.

The five types of standard treatment used for PCa are watchful waiting/active surveillance, surgery, radiation therapy, hormone therapy, and chemotherapy. Watchful waiting involves closely monitoring a patient's condition without the use of biochemical tests or treatment until symptoms appear or there is a change/ progression in the cancer. Active surveillance involves closely following a patient's condition through the use of tests including DRE, PSA test, transrectal ultrasound or transrectal needle biopsy in order to determine whether or not the cancer is developing. Watchful waiting or active surveillance are usually the preferred treatment for elderly men with early stage PCa.

Patients with tumours localized to the prostate gland may be treated with surgery to remove the tumour. The three types of surgery used are radical prostatectomy, pelvic lymphadenectomy, and transurethral resection of the prostate (TURP). Despite the benefits of surgery side effects can include impotence and leakage of urine from the bladder or stool from the rectum. This form of treatment is an option for patients in good health and who have confined, localized disease. Radiation therapy uses high energy x-rays or other forms of radiation to kill cancer cells and there are two forms of radiation therapy administered to cancer patients. The first is called external radiation therapy (machine outside the body which sends radiation towards the cancer). Conformational radiation is a type of external radiation that uses a computer-based system to generate a 3-dimensional (3-D) image of the tumour. The radiation beams are then shaped to fit the tumour size. This form of radiation therapy avoids damaging healthy cells, as the radiation is solely directed towards the tumour. Internal radiation is the second form of radiation therapy in which a radioactive substance sealed within needles, seeds, wires, or catheters is placed directly into or near the cancer. The type of radiation therapy administered is dependent on the type or stage of the cancer in question.

Hormone therapy is a form of cancer treatment that removes/blocks the action of certain hormones. In PCa, male sex hormones may cause the cancer to grow. The four types of hormone therapy available are luteinizing hormone therapy (releasing hormone agonists which stops the testicles from producing testosterone), anti-androgen therapy (block the action of androgens), orchiectomy (removal of the testicles), and estrogen therapy (administering female sex hormone). Chemotherapy uses drugs to stop the growth of cancer cells, either by killing the cells or preventing them from dividing. There are two forms of chemotherapy available for PCa treatment. Systemic chemotherapy is administered orally or injected directly into a vein or muscle whereas regional chemotherapy is placed directly into the cerebrospinal fluid, an organ, or body cavity. The form of chemotherapy administered is dependent on the type, health of the patient, and stage of the cancer being treated.

1.7 Biomarkers of PCa

1.7.1 Biomarkers of disease

The term 'biomarker' is defined by the National Institute of Health as "*a characteristic that is objectively measured and evaluated as an indicator of normal biological processes, pathogenic processes or pharmacological response to a therapeutic intervention or other health care intervention*". A biomarker can be produced by a diseased organ or from another location in the body in response to the disease. They can be found in biological fluids or in tissues in increased concentrations in patients with a certain disease. There are three main types of biomarkers; Type 0, type I and type II. Type 0 biomarkers are associated with disease and its progression independent of drug therapy (Vasan, 2006). Type I biomarkers reflect the effect of a therapeutic intervention and the mechanism of action of that intervention (Vasan, 2006). Type II biomarkers are associated with predicting the clinical outcome of a therapeutic intervention.

Molecular biomarkers are used in cancer research and refer to substances that are indicative of the presence of cancer in the body (Maruvada *et al.*, 2005). They can include changes in mRNA, DNA methylation, patterns of single-nucleotide polymorphisms (SNPs), protein or metabolite abundances providing that these patterns of change can be shown to correlate with the characteristics of the disease, and are preferably produced only by malignant tissue (Issaq *et al.*, 2010). The three types of cancer biomarkers are prognostic, predictive and pharmacodynamic markers. Prognostic markers assess the natural course of the cancer and aid in identifying the outcome of the disease. Predictive biomarkers evaluate how beneficial a particular cancer treatment is to the disease. Pharmacodynamic biomarkers can allow clinicians to determine the appropriate dose of drug therapy to administer as well as the effects of treatment on the tumour. Biomarkers are extremely valuable clinical tools, which can be used to detect cancer, examine biological behavior, predict the clinical outcome of the disease and monitor the therapeutic response and disease progression. The characteristics of a good biomarker are: high sensitivity and specificity, the ability to produce a high predictive value (for clinical relevance), accuracy, reproducibility, 'ease-of-use', and measured within a non-invasive or semi-invasive collected specimen (Issaq *et al.*, 2010). The FDA has approved a number of

biomarkers for monitoring specific cancers (including PCa); however, the majority of biomarkers identified are not sufficiently sensitive or specific.

1.7.2 Improving PCa diagnosis through the introduction of novel biomarkers

The shortcomings associated with PSA and its derivatives highlight the urgent need for novel, more specific and sensitive biomarkers for PCa diagnosis. Ideally, these novel biomarkers should be capable of detecting the presence of PCa cells, monitoring the progression of the disease and its response to therapy, predicting the possibility of recurrence and prognosticating the outcome of the disease. Advancements in biomedical research have significantly increased the rate at which novel PCa-specific biomarkers are being identified and subsequently developed. There are several new biomarkers (Pro-PSA, PCA-3 test, and TMPRSS2-ERG) available on the market but new ones are required in order to improve specificity and sensitivity. The following section discusses some of the more promising biomarkers, with particular focus on prostate-specific membrane antigen (PSMA) and secreted frizzled related protein-2 (SFRP-2), which may lead to an improvement in the diagnosis of PCa. These two markers are the focus of much of the research in this thesis.

1.7.2.1 Six-transmembrane epithelial antigen of the prostate (STEAP)

The STEAP gene family, are predominantly expressed in epithelial tissues and are thought to function as a channel in tight junctions, gap junctions or in cell adhesion (Hubert *et al.*, 1999; Ihlaseh-Catalano *et al.*, 2013). STEAP belongs to a small 'family' of cell-surface antigens that are expressed in PCa and could be potential targets for improving PCa diagnosis. These cell-surface antigens include prostate-specific membrane antigen (PSMA), prostate cancer tumour antigen 1 (PCTA-1), and prostate stem cell antigen (PSCA). PCTA-1 is a promising serum marker due to its high expression levels in PCa, and its high secretion levels (Hubert *et al.*, 1999). PSCA, which is expressed primarily in basal cells of normal prostate tissue, is detected in 80% of PCa cases analysed. STEAP is unique among this 'family' of cell-surface antigens due to its putative secondary structure and its potential function as a channel or transport protein. Immunohistochemical analysis of clinical specimens showed STEAP expression at all stages of PCa (Hubert *et al.*, 1999). Significant

expression was noted at the cell-cell junctions of the secretory epithelium of PCa cells.

Six-transmembrane epithelial antigen of the prostate 1 (STEAP1) is overexpressed in a number of different cancer tissues, particularly in the prostate, where its expression was found to be significantly higher than in normal prostate tissue (Hubert *et al.*, 1999; Yang *et al.*, 2001; Maia *et al.*, 2008, Gomes *et al.*, 2014). STEAP1 is primarily localized at the plasma membrane of the prostate secretory epithelium and is thought to play an important role in intracellular and intercellular communication (Gomes *et al.*, 2014). The localization of this protein at the cell-surface, its low expression levels in normal prostate tissue and high expression levels in prostate disease suggest that STEAP may be an ideal target for improving PCa diagnosis/prognosis. STEAP1 overexpression has been linked to poor prognosis in PCa, such as high-grade tumours, seminal vesicle invasion and biochemical recurrence (BCR) (Ihlaseh-Catalano *et al.*, 2013). A number of studies have been carried out to assess the ability of STEAP1 to distinguish malignant prostate tissues from BPH. The results from one particular study showed that STEAP1 presented high sensitivity (100%) and specificity (95.1%) to distinguish malignant tissue from BPH, suggesting that STEAP1 has the potential to detect early malignant prostate tissue. It has been observed that, in addition to PCa, STEAP1 is also overexpressed in PIN lesions, which could suggest that STEAP1 overexpression occurs before tumour initiation (Ihlaseh-Catalano *et al.*, 2013). Although further research is needed, STEAP1 is an interesting protein that could be used to improve the early diagnosis of PCa and assist in predicting treatment outcome.

1.7.2.2 Prostate-specific membrane antigen (PSMA)

Prostate-specific membrane antigen (PSMA), also known as glutamate carboxypeptidase II, N-acetyl-α-linked acidic dipeptidase I (NLD I), or folate hydrolase (FOHL), is a well-established type II integral membrane protein that was discovered in 1987 (Madu and Lu, 2010). PSMA is a 750 amino acid protein with a molecular weight of approximately 84 kDa. The PSMA gene is composed of 19 exons that span approximately 60kb of genomic DNA. This type II transmembrane protein contains a short NH_2-terminal cytoplasmic tail, which is ~ 19 amino acids in length, a single hydrophobic transmembrane domain (24 amino acids in length) and a large

extracellular domain (707 amino acids in length), at the COOH terminus of the protein (Rajasekaran *et al.*, 2005). The expression of PSMA has been noted at four consensus sites: the prostate (secretory acinar epithelium), the kidney (proximal tubules), nervous system glia (astrocytes and Schwann cells), and the small bowel (jejunal brush border) (Ristau *et al.*, 2013). Despite accepted expression in these tissues, the function of PSMA is only well defined in nervous system glia and small bowel (Ristau *et al.*, 2013). The reason for the presence of PSMA in the prostate remains undefined but research to date has shown that PSMA could act as a potential marker for analyzing carcinogenesis and progression of PCa. Studies carried out to compare the expression of PSMA in primary prostate tumours and metastatic lesions with benign tissue discovered that PSMA expression was significantly higher in malignant tissue and is positively associated with tumour grade and stage (Sweat *et al.*, 1998; Bostwick *et al.*, 1998; Ross *et al.*, 2003; Perner *et al.*, 2007; Minner *et al.*, 2011). Additionally, it has been shown that PSMA expression increases with higher-grade, aggressive forms of PCa, implying a functional role in PCa progression (Israeli *et al.*, 1994; Wright *et al.*, 1995; Wright *et al.*, 1996; Sweat *et al.*, 1998). PSMA has been used in immunoscintigraphy to monitor the progression of metastatic disease as a result of its high expression levels in cancerous prostate tissue (Gregorakis *et al.*, 1998). Three studies carried out on surgically treated prostate cancer patients showed that a high expression level of PSMA in tumour tissue was associated with biochemical recurrence (BCR) (Ross *et al.*, 2003; Perner *et al.*, 2007; Minner *et al.*, 2011). The results from this study highlight the possible prognostic utility of PSMA.

1.7.2.3 Glutathione S-transferase P I (GSTP I)

GSTP1 is a member of a ubiquitous family of multifunctional enzymes that conjugate reactive substrates with reduced glutathione (GSH) and play a role in detoxification (Madu and Lu, 2010). GSTs function to protect cells from cytotoxic and carcinogenic agents (Hayes and Pulford, 1995) and are expressed in normal tissues at variable levels in different cell types. In the absence of cancer the GSTP1 gene has been observed to be unmethylated, but during carcinogenesis hypermethylation of the GSTP1 promoter occurs. This hypermethylation is regarded to be a main characteristic of PCa. GSTP1 has shown excellent sensitivity in the detection of PIN and PCa. Therefore, patients with benign conditions or disease free can be distinguished from those with malignant conditions (Lee *et al.*, 1994; Brooks *et al.*,

1998; Cairns *et al.*, 2001; Jeronimo *et al.*, 2001; Lin *et al.*, 2001; Chu *et al.*, 2002). Furthermore, the hypermethylation of the GSTP1 gene during carcinogenesis can aid in distinguishing between PCa and BPH. A study carried out on urine samples of men who had undergone prostate biopsies showed the presence of the methylated GSTP1 gene through the use of PCR (Gonzalgo *et al.*, 2003). The results obtained from this investigation highlight the potential use of this marker in identifying the risks associated with men undergoing prostate biopsy (Gonzalgo *et al.*, 2003; Madu and Lu, 2010). Overall, the GSTP1 gene displays some exciting characteristics that make it a viable marker for improving PCa diagnosis. It is highly prevalent in disease states and its methylation status can be easily measured and analysed in biopsy tissue or from cells derived from samples of serum and urine. Once further research and validation studies are completed this biomarker could significantly enhance early PCa diagnosis as well as allowing post-treatment monitoring of the disease.

1.7.2.4 α-Methylacyl Coenzyme A Racemase (AMACR)

AMACR is a peroxisomal and mitochondrial enzyme involved in bile acid biosynthesis and β-oxidation of branched-chain fatty acids. In mammalian cells, this enzyme mediates the interconversion of (R)- and (S)-2-methyl-branched-chain fatty acyl coenzyme As (Rubin *et al.*, 2002). AMACR, also known as p504s, is a gene shown to be overexpressed in the majority of prostate adenocarcinomas and in high-grade PIN, but only weakly expressed in benign glands as identified by cDNA expression microarray- and immunohistochemical-based methods (Yamada *et al.*, 2013). This suggests that AMACR could be a specific marker for premalignant lesions and cancer cells within the prostate gland (Jiang *et al.*, 2001; Luo *et al.*, 2002; Rubin *et al.*, 2002). In comparisons between PCa tissues and non-malignant controls a 9-fold increase in mRNA levels of AMACR in 88% of the sample PCa tissues was demonstrated (Rogers *et al.*, 2004). Follow-up immunohistochemical studies and western blot analysis confirmed up-regulation at the protein level (Hessels and Schalken, 2013). In addition, AMACR expression in needle biopsies had 97% sensitivity and 100% specificity for PCa detection (Rubin *et al.*, 2002). AMACR shows potential for enhancing PCa diagnosis, although additional investigation is needed to validate the clinical usefulness of this marker.

1.7.2.5 Secreted Frizzled Related Protein-2 (SFRP-2)

Secreted-frizzled related proteins (SFRPs) are modular proteins, which fold into two separate domains (Bovolenta *et al.*, 2008). Their N-terminus contains a secretion signal peptide followed by a cysteine rich domain (CRD), which is composed of ten cysteine residues at conserved positions (Bovolenta *et al.*, 2008). These cysteine residues form a pattern of disulphide bridges. The C-terminal of SFRPs contains segments of positively charged residues, which confer heparin-binding capacity and six cysteine residues that form three disulphide bridges (Bovolenta *et al.*, 2008). SFRP-2, a member of the SFRP protein family, plays a regulatory role in the WNT (wingless) signaling pathway regulating cellular proliferation and differentiation. SFRP-2 has been identified as a possible biomarker in many cancers, such as colon cancer, liver cancer, breast cancer and lung cancer.

Methylation analysis carried out on WNT molecules and their antagonists by the epigenetic biomarker discovery group (Prostate Molecular Oncology, Institute of Molecular Medicine, Trinity College Dublin) within the Prostate Cancer Research Consortium (PCRC) using Quantitative Methylation-Specific PCR (QMSP) revealed hypermethylation of SFRP-2 (WNT antagonist) in 65% (48/74) of pooled tumours, 30% (6/20) of high-grade prostatic intraepithelial neoplasia, 11% of BPH glands from prostate cancer patients and 9% (7/69) of histologically benign tissue from patients with no evidence of PCa (Perry *et al.*, 2013).

Further studies carried out by Dr. Gillian O' Hurley (Department of Pathology, RCSI Education & Research Centre, Beaumont Hospital, & School of Biotechnology, DCU, Dublin 9) provided more insight into the expression of SFRP-2 in the cytoplasm of benign prostate epithelium, its loss in low-grade prostate tumours and that differential SFRP-2 expression identified sub-categories of Gleason grade 5 tumours. Dr. O' Hurley performed immunohistochemical (IHC) analysis on prostate cancer tissue microarrays with samples from 216 patients. Confirmatory gene expression profiling for SFRP-2 was carried out on 8 cases using Laser Capture Microdissection and TaqMan® Real-Time PCR. Strong to moderate SFRP-2 expression was observed in BPH epithelial cells and negative to weak SFRP-2 expression observed in tumour epithelium, particularly Gleason grade 3 and 4. However, in Gleason grade 5 carcinoma there was a 40:60 split in the immunoexpression of SFRP-2, where 40%

displayed strong to moderate SFRP-2 expression and 60% displayed negative SFRP-2 expression in epithelial cells. A morphological difference was noted in the Gleason grade 5 tumours that had strong to moderate SFRP-2 expression (Type A) and the Gleason grade 5 tumours that had no SFRP-2 expression (Type B). It was also noted that biochemical recurrence occurred after 5 years in patients that had strong to moderate SFRP-2 expression in Gleason grade 5 tumours with "Type A" morphology. There was no evidence that biochemical recurrence occurred in patients with negative SFRP-2 expression in Gleason grade 5 tumours with "Type B" morphology. From the results obtained from Dr. O' Hurley, SFRP-2 has been proposed as a possible marker of histologically benign glands and a possible subgroup of Gleason grade 5 tumours that may predict prognosis and biochemical recurrence (O' Hurley *et al.*, 2011).

1.7.3 Improving prostate cancer diagnosis through the generation of anti-prostate cancer-specific antibodies

Effective, accurate and specific methods of prostate cancer detection and clinical diagnosis are urgently warranted. The recent emphasis on the need for point-of-care patient management has led to the development of novel biosensor detection strategies that are suitable for miniaturization of assays for various targets including novel PCa-specific markers. These biosensors could provide rapid and reliable quantitative results 'anytime', 'anywhere'. A biosensor is an analytical device incorporating a biological or biologically derived sensitive 'recognition' element integrated or associated with a physio-chemical transducer (Turner, 2013). Biosensors are typically composed of three parts: the sensitive 'recognition element' (e.g. biological material such as tissue, microorganisms, organelles, cell receptors, enzymes, antibodies, nucleic acids etc., or biologically derived material), the 'transducer' or 'detector element' which functions in a physiochemical way (optical, piezoelectric, electrochemical etc.) and transforms the outcome resulting from the interaction of the analyte with the biological element into a signal that can be easily measured and quantified, and the associated signal processor that delivers and displays the results (Healy *et al.*, 2007).

Antibody-based biosensors or immunosensors have revolutionalised diagnostics for the detection of a plethora of analytes such as disease markers, food and

environmental contaminants, biological warfare agents and illicit drugs. Antibodies are ideal bio-recognition elements that provide sensors with high specificity and sensitivity. A major challenge facing researchers and clinicians in cancer research is the lack of high quality, well-characterised antibodies to target proteins. Although commercial production of antibodies is well established, the market has been driven so far by popularity of particular antibody targets, due to the fact that antibody companies are likely to make more profit on more popular targets. In consequence, antibodies do not exist for the majority of proteins in the human genome, and those that do are often very expensive and of highly variable quality.

Biomarker discovery, particularly in cancer research, requires the rapid validation of markers identified in studies to allow these markers to be quickly moved towards clinical utilization. However, the lack in availability of high quality antibodies to novel markers/proteins makes validation of potential biomarkers identified in cancer research extremely difficult. Therefore, there is an urgent requirement for well-characterised antibodies to be generated against novel target proteins. A major component of this research project is antibody development and characterisation to key markers of prostate cancer. The following section gives an introduction to the immune system and a background into monoclonal, polyclonal and recombinant antibodies.

1.7.4 Introduction to the immune system and antibodies

1.7.4.1 The immune system

The immune system functions to protect the body against infectious organisms, which are potentially harmful to the host. It is divided into two main sub-systems; non-adaptive (innate) and adaptive (acquired) immunity. Innate immunity is a non-specific defense mechanism to foreign molecules or antigens (Ag) (Conroy *et al.*, 2009). The innate immune response includes, physical barriers such as the skin, in addition to groups of proteins and phagocytic cells, (such as neutrophils, monocytes, macrophages, mast cells, and dendritic cells) that recognize specific features of foreign molecules and quickly become activated to remove/destroy the invaders. In contrast, the acquired immune system is highly specific to a particular pathogen. Acquired immunity is controlled by lymphocytes, which are responsible for the secretion of immunoglobulins (Igs). Adaptive immunity creates immunological

memory after an initial response to a specific pathogen, which leads to an enhanced response to subsequent encounters with that pathogen.

1.7.4.2 Antibody structure

Antibodies (Abs) or immunoglobulins (Igs) are highly soluble serum glycoproteins involved in the defence mechanisms of the immune system. They can be divided into five classes based on the sequence of their heavy chain constant regions i.e. IgM, IgD, IgG, IgE and IgA (Weiner *et al.*, 2010). IgG antibodies are found in all bodily fluids and are the most common antibody in the body, accounting for approximately 75 – 80% of all antibodies. The basic structure of an Ab is outlined in Figure 1.4. Igs can be subdivided into two distinct building blocks: the fragment of antigen binding (Fab) and the constant fragment (Fc) (Weiner *et al.*, 2010). An Ab has four polypeptide chains, two heavy chains and two light chains (either κ (kappa) or λ (lambda)), which are joined together by disulphide bonds (Conroy *et al.*, 2009). The heavy chain is composed of one variable region (variable heavy or V_H) and three constant regions (CH_1, CH_2 and CH_3). The light chain has one variable region (variable light or V_L) and one constant region (constant light or C_L).

The Fab component of the antibody contains the fragment variable (Fv) region, where the complementarity determining regions (CDRs) can be located (Weiner *et al.*, 2010). The CDRs form the antigen binding sites of the antibody and confer antigen specificity. There are three CDRs (CDR1, CDR2 and CDR3), arranged non-consecutively, on the amino acid sequence of a variable domain of an antigen receptor. Since the antigen receptors are typically composed of two variable domains (on two different polypeptide chains, heavy and light chain), there are six CDRs for each antigen receptor that can collectively come into contact with the antigen. A single antibody molecule has two antigen receptors and therefore contains twelve CDRs. The Fc region is essential for mediating effector functions such as antibody-dependent cell-mediated cytotoxicity (ADCC), antibody-dependent cellular phagocytosis, antigen presentation to the immune system, degranulation, complement-mediated lysis, and regulation of cell activation and proliferation.

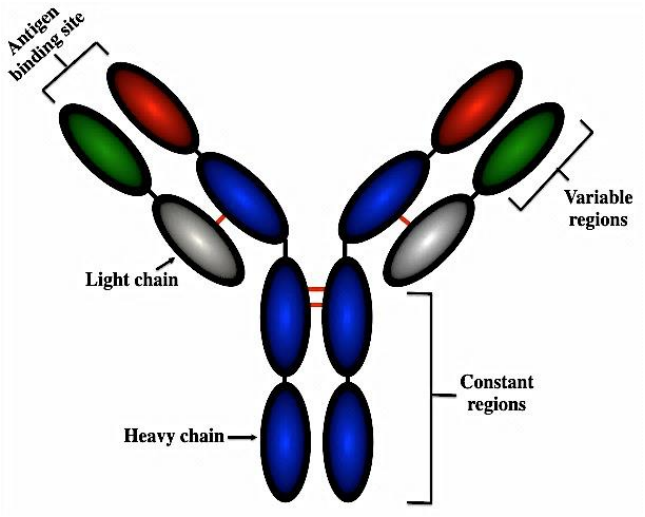

Figure 1.4. Structure of an IgG antibody (Ab).

A typical Ab is a large molecule of about 150 kDa made of four peptide chains. It contains two identical class γ heavy chains of about 50 kDa and two identical light chains of about 25 kDa, and thus has a tetrameric quaternary structure. The two heavy chains are linked to each other and to a light chain by disulfide bonds. The resulting tetramer has two identical halves, which together form the Y-like shape. Each end of the fork contains an identical antigen-binding site. (Adapted from Conroy et al., 2009).

The generation of antibodies for use in a diagnostic or therapeutic setting traditionally makes use of mice or rabbits, although the use of chickens has gained increasing popularity since chicken IgY was first described in 1969. Phylogenetic separation between birds and mammals makes possible the production of highly specific antibodies in chickens against highly conserved mammalian proteins. Chicken IgY is often referred to as chicken IgG due to its similarity in structure (see Figure 1.5) to mammalian IgG with 2 heavy ("nu" chains, ~67 - 70 kDa) and 2 light chains (~22 - 30 kDa) (Bird and Thorpe, 2002). Despite the similarities, there are some distinct differences between these immunoglobulins. Chickens have three different immunoglobulin classes: IgY, IgA and IgM, of which IgY constitutes approximately 75% of the total chicken immunoglobulin population. Similar to IgG, the Fc region of IgY mediates most of the biological effector functions, such as complement fixation and opsonisation (Tizard, 2002). However, unlike IgG, IgY can also mediate anaphylactic reactions, a function that is attributed to IgE in mammals (Mine & Kovacs-Nolan, 2002; Karlsson & Larsson, 2004; Mine & Yang, 2008). The DNA sequence of IgY shares a greater similarity to human IgE than that of IgG (Tizard,

2002). Interestingly, the most hydrophobic part of IgY is the Fc fragment. As the Fc fragment is larger in IgY than in IgG, the IgY molecule is more hydrophobic than IgG (Schade *et al.*, 2005). Additionally, the Fc region of IgY contains two carbohydrate chains as opposed to the one found in human IgG (Karlsson & Larsson, 2004; Jefferis, 2005).

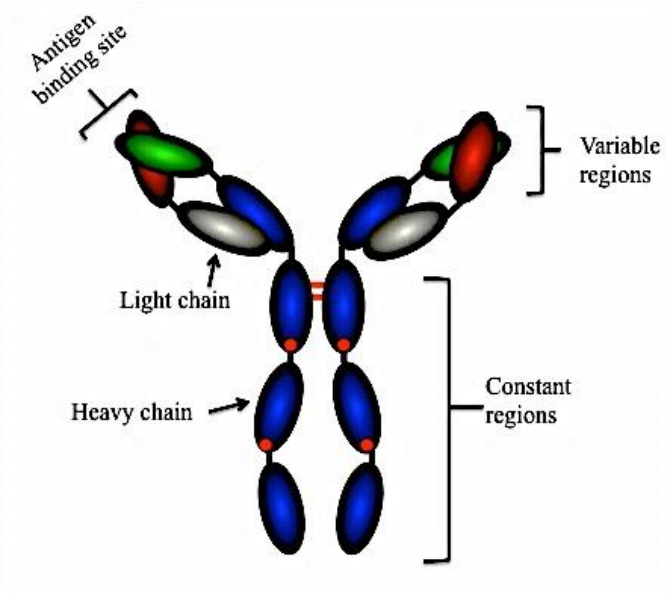

Figure 1.5. Structure of chicken IgY.

In chickens, immunoglobulin Y is the functional equivalent to Immunoglobulin G (IgG). It is composed of two light and two heavy chains. Structurally, IgG and IgY differ primarily in the heavy chains, which in IgY have a molecular mass of about 65 kDa, and are thus larger than in IgG. The light chains in IgY, with a molar mass of about 18 kDa, are somewhat smaller than the light chains in IgG. The molar mass of IgY thus amounts to about 166 kDa. The steric flexibility of the IgY molecule is less than that of IgG.

Human IgG contains only complex type oligosaccharides, whereas IgY contains three different types of *N*-linked oligosaccharides: oligomannose type (Man_{5-9} $GlcNAc_2$), monoglucosylated oligomannose type (Gly_1Man_{7-9} $GlcNAc_2$) and biantennary complex type (Ohta *et al.*, 1991; Jefferis, 2005). The greater carbohydrate content on IgY allows for the conjugation of larger amounts of enzyme or hapten. Similar to other full-length immunoglobulins with an antigen valency of 2, the IgY structural unit is a tetramer that is composed of two identical pairs of polypeptide chains. These are designated as “light” (L) and “heavy” (H), in reference to their molecular weight. The *N*-terminal portion of each chain defines a variable (V) region that is primarily responsible for antigen recognition. The C-terminal portion of each chain defines a

constant (C) region. Although IgY is similar in structure to IgG it is not identical. IgY contains two heavy chains with a molecular mass of 67 – 70 kDa each, and two light chains with a molecular mass of 25 kDa each. The IgY heavy chain is called upsilon (υ) and has one variable region and four constant regions (Cυ1 – Cυ4). In contrast, the gamma (γ) IgG heavy chain, which has only three constant regions (Cγ1 – Cγ3). Thus, IgY with the extra constant region has a greater molecular mass, 180 kDa, compared to that of IgG (150 kDa) (Narat, 2003).

IgY is also less flexible than IgG due to the absence of the hinge region. In IgG, the hinge region is located in the heavy chains between C_H1 and C_H2 domains and permits flexibility between the two Fab arms of the Y-shaped antibody molecule. The extra constant domain of IgY may be an evolutionary predecessor to the mammalian IgG hinge region. In addition, an IgY-like molecule is believed to be the evolutionary ancestor for both mammalian IgG and IgE (Tizard, 2002; Narat, 2003; Karlsson & Larsson, 2004; Mine & Yang, 2008). The pI range of IgY (5.7 – 7.6) is lower than that of IgG (6.1 – 8.5) (Schade *et al.*, 2005). IgY is more acidic than IgG and hence this may account for its greater stability in conditions of low pH (Hodek and Stiborova, 2003). IgY antibodies are resistant to high temperature and ionic strength and can be stored for over ten years at 4 °C without any significant loss in antibody activity. Chapter 4 and 5 of this thesis describe in detail the use of chickens for the generation of anti-SFRP-2 and anti-PSMA antibodies for use in immunohistochemistry for the detection of prostate cancer.

1.7.4.3 Monoclonal antibodies

Antibodies have been used extensively throughout the past number of decades as diagnostic tools in many different formats due to their exquisite specificity for their cognate antigen. Ab-based immunoassays are the most commonly used diagnostic assays and remain as one of the fastest growing technologies for the analysis of biomolecules (Borrebaeck, 2000). Conventional techniques for the preparation of antibodies in antiserum against a specific target consistently result in the production of non-homogenous antibodies with varying specificity and affinity, referred to as polyclonal antibodies (Morgan and Levinsky, 1985). Monoclonal antibody technology or hybridoma technology revolutionalised our vision for antibodies as tools for research for prevention, detection and treatment of diseases. In hybridoma

technology, a myeloma cell rendered drug sensitive through mutation in a growth-essential gene hypoxanthine guanine phosphoribosyl transferase (HGPRT) is chemically fused with immune cells from a host immunised with the target antigen of interest and the resulting cells are grown in medium containing the selective drug. Since the immune cells have a short life-span in tissue culture and the myeloma cells are drug sensitive, the only cells that will survive are those myeloma cells which obtained a normal HGPRT gene from the immune cells. Such cells also have a high chance of carrying the immune cell's Ab gene resulting in the generation of a hybridoma that can grow continuously *in vitro* and secrete a single monoclonal Ab (Skerra and Pluckthun, 1988). This approach has provided a number of advantages over the original art of polyclonal Ab generation. These advantages include (i) there is an unlimited source of homogenous mAb, since the hybridoma cell line is immortal (ii) large amounts of specific antibodies can be easily produced (iii) there is no or very low batch-to-batch variability.

Over the past 40 years, monoclonal Abs generated using hybridoma technology have provided the means for developing a number of highly specific and reproducible immunological assays for rapid and accurate diagnosis of many diseases. Despite this, adverse clinical outcomes and animal studies have highlighted underlying limitations of mAbs for use as therapeutics. Accordingly, many strategies have been developed in order to improve the specificity, and control the functions, of antibodies. Two such important approaches are the development of bispecific antibodies (bsAbs) and the introduction of recombinant antibody technology.

1.7.4.4 An introduction to recombinant antibody technology

Recombinant Ab technology allows the generation of Ab fragments that retain their stability and specificity (Conroy *et al.*, 2009). In comparison to the parental Abs, these minimized Abs have several advantages in, for example clinical practice, including better tumour penetration, lower retention times in non-target tissue and also the potential to reduce immunogenicity.

In the past, Ab fragments could only be generated by proteolytic cleavage which led to the production of $F(ab)_2$ and Fab antibodies (Conroy *et al.*, 2009). Two decades ago, Skerra *et al.* and Plukthun *et al.* described the use of vectors in bacterial systems

that could generate fully functional, correctly folded Fv and Fab Ab fragments (Pluckthun & Skerra, 1989). These vectors could offer soluble Ab secretion directly into the periplasm space by means of its oxidizing environment that contributes to the correct formation of disulphide bonds between the Ab domains (Ahmad *et al.*, 2012). Since then, Ab fragments have been produced in a variety of hosts such as, mammalian (Ho *et al.*, 2006), insect (Choo *et al.*, 2002), yeast (Ho *et al.*, 2006), plant (Galeffi *et al.*, 2006) and 'cell-free' systems.

Fv fragments, composed of the variable heavy (V_H) and variable light (V_L) domains linked via a disulphide bond, are the smallest antibody fragments with function in antigen binding activities. Stability issues associated with Fv antibodies were overcome by introducing a flexible $(Gly_4Ser)_3$ peptide linker into the Fv fragment resulting in the generation of a single chain Fv or scFv. By incorporating a human constant κ light chain to the terminal of the VL region of an scFv, a scAb fragment can be produced, which can improve the stability and expression of scFv antibodies. An additional extension to the scFv family is the Diabody (see Figure 1.6 for more detail). Here, the variable domains from two scFv antibodies are expressed as two polypeptide chains with the domains connected by a short polypeptide linker, forcing heterodimerization of the two chains. Dimeric scFv are composed of two scFv linked via a naturally dimeric protein (Conroy *et al.*, 2009).

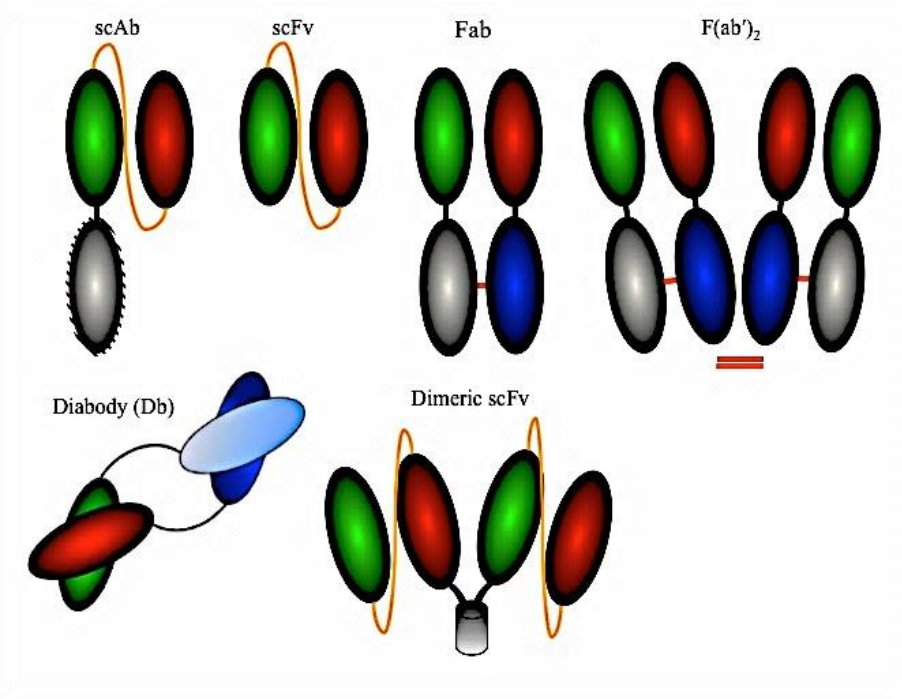

Figure 1.6. Recombinant antibody formats.

A scFv consists of the Variable heavy (V_H) and Variable light (V_L) regions of an antibody joined via a peptide linker. A scAb is composed of one variable heavy and variable light region and a constant light region. The Fab fragment is composed of the V_H and V_L domains with one constant heavy and light chain. F(ab')$_2$ involves linking two Fab antibodies by disulphide bonds. A Diabody is generated when the variable domains from two scFv antibodies are expressed as two polypeptide chains with the domains connected by a short polypeptide linker. A dimeric scFv is generated by the fusion of two scFv antibodies via a naturally occurring dimeric protein.

1.7.4.5 An introduction to bispecific antibodies

Bispecific antibodies combine two or more antigen-recognizing elements into a single construct and simultaneously address different antigens and epitopes (Byrne *et al.*, 2013). Bispecific antibodies were first introduced for potential clinical application over 30 years ago. Despite some significant biological effects elicited by these first generation bispecific antibodies, there was little significant impact on the clinical course of a disease state (Kufer *et al.*, 2004; Chames & Baty, 2009).

Issues associated with these antibodies included difficulty in large-scale production of homogenous batches and a lack of efficacy of murine antibody fragments. Human anti-mouse antibody (HAMA) responses were observed in the majority of treated patients (Byrne *et al.*, 2013) in addition to Fc-mediated side effects. Subsequently,

research has focused on approaches to overcome these limitations through the introduction of novel antibody formats.

With the advent of recombinant DNA technology, it is possible to overcome the shortcomings associated with traditional approaches for bispecific antibody production (Byrne *et al.*, 2013). Over 50 different bispecific antibody formats now exist, ranging from whole IgG-like molecules to small recombinant formats. Figure 1.7 shows a schematic overview of the most popular bispecific antibody formats in current use by different groups in academia, and the biotech and pharmaceutical industries. Bispecific antibodies and their clinical applications, and a novel approach to generate a bispecific antibody, will be discussed in further detail in chapter 3 of this thesis.

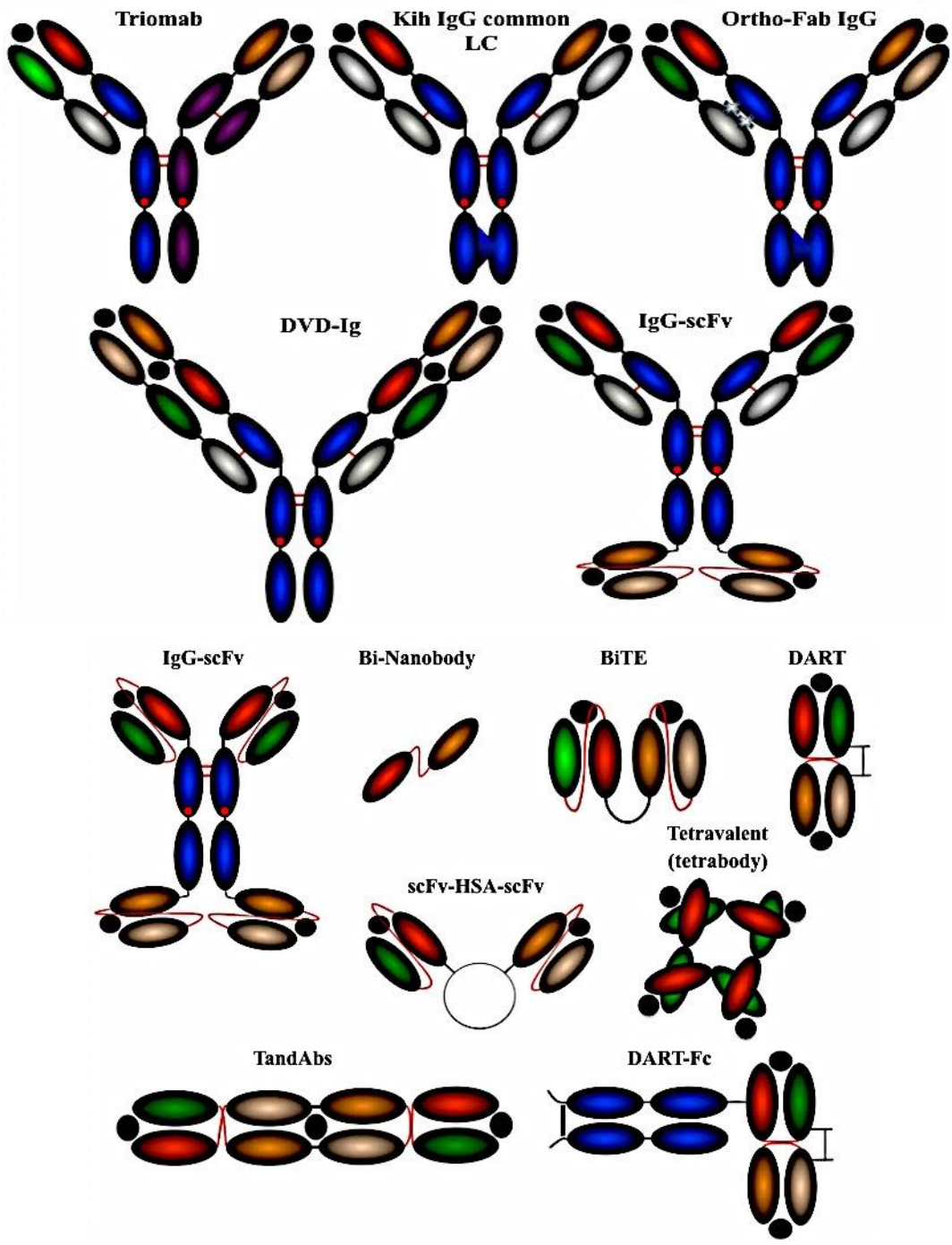

Figure 1.7. Various bispecific antibodies that are currently in clinical development/ already approved for cancer therapy.

The upper two lines including the IgG-scFv format depict immunoglobulin (Ig)-like bispecific antibodies comprising an Fc region, either bivalent or tetravalent molecules. Furthermore, several small bispecific and bispecific antibody fusion proteins have entered clinical trials. Abbreviations: BiTE; Bispecific T cell Engager, DART; Dual Affinity Retargeting, DVD-Ig; Dual-Variable-Domain Immunoglobulins, HSA; Human Serum Albumin, kih; knobs into holes, scFv; single chain fragment variable. (Adapted from Byrne et al., 2013)

1.8 Screening an antibody library through phage display

When generating an antibody to a specific target there are a number of things to consider. Firstly, the target biomarker needs to be identified, which in the case of this project was SFRP-2 and PSMA. Secondly, the animal model used to raise the antibodies of interest needs to be chosen. Thirdly, the format of antibody required needs to be identified, followed by the development of an immunisation schedule. Once the desired antibody fragment is generated an appropriate selection or screening method, such as phage display, is used in order to isolate target Abs from a vast library and to tailor them for their application (Conroy *et al.*, 2009).

Phage display is a molecular diversity technology for the study of protein-protein or protein-peptide interactions that allows the presentation of large peptide or protein libraries on the surface of filamentous phage. Filamentous bacteriophages are a group of viruses containing a circular single-stranded DNA (ssDNA) genome encapsulated in a long flexible protein capsid cylinder (Barbas *et al*., 2001). The Ff class of filamentous phages, namely f1, fd and M13, use the tip of the F conjugative pilus as a receptor and are, therefore, specific for *E. coli* containing the F plasmid. Filamentous phage does not produce a lytic infection in *E. coli*, but rather induces a state in which the infected bacteria produce and secrete particles without undergoing lysis. Filamentous phage are covered by approximately 3000 copies of small major coat protein (pVIII), with few copies of the minor coat proteins pIII (the product of gene III) and pVI displayed at one extremity of the phage particle, while pVII and pIX are present at the other extremity (Nilsson *et al.*, 2000). The principle of phage display involves displaying certain ligands, typically an antibody, fused with the carboxy terminal to a phage coat protein (pIII or pVIII). Traditionally, complete phage vectors or bacteriophage, which contained all the genetic information necessary for the phage life-cycle were utilized as display vectors, but advancements in recombinant antibody display technology have led to the development of small plasmid vectors and phagemids, which have become more popular vectors for display (Barbas *et al*., 2001). Phagemids contain the origins of replication for both the M13 phage and *E. coli* in addition to gene III. Additionally they contain the appropriate multiple cloning sites, and an antibiotic-resistance gene, but lack all other structural and non-structural gene products required for generating a complete phage (Barbas *et al*., 2001). The phagemid encoding the scFv-pIII fusion product is preferentially packaged into phage

particles using helper phage such as M13K07, which supplies all the structural proteins required for generating a complete phage.

Phage display libraries are typically generated from the cDNA obtained from an immunised animal model. The cDNA is prepared from the mRNA of the rearranged immunoglobulin B-cell genes. This cDNA is then used as a template for the polymerase chain reaction (PCR) amplification of the variable heavy and variable light chain genes encoding a restriction site for cutting with S*fi*I. Subsequently, these antibody gene segments are incorporated into a splice-by-overlap (SOE) PCR to join together the two variable domains. The SOE product is then purified and digested along with the pComb3XSS phagemid vector with the SfiI restriction enzyme. The scFv genes are then ligated into the digested vector using T4 DNA ligase and transformed into *E. coli*.

In a process known as panning (see Figure 1.8), the phage library is incubated with an immobilised target antigen. Weakly bound phage or phage that have a low affinity for their target antigen are removed by stringent washing steps during the panning process. The high-affinity bound phage are removed from the surface of a maxisorb plate by the addition of trypsin and re-amplified through infection of mid-logarithmic growth-phase *E. coli* cells. Affinity is enriched through multiple rounds of panning, a process that involves binding to reduced concentrations of the immobilised target and increasing the number of wash steps carried out in each round. Typically 4 to 6 rounds of panning and amplification are sufficient to select for phage displaying high-affinity antibody fragments.

Post panning, further screening and characterisation is carried out in order to identify the appropriate antibody clone specific for the application required. In the case of this project, it was necessary to identify antibodies for use in immunohistochemistry. The screening and characterisation techniques applied in this work were ELISA, Biacore, SDS-PAGE, Western Blotting, Dot Blotting, Fluorescent Microscopy, and Immunohistochemistry. All of these techniques will be described in more detail in the forthcoming chapters. The following section discusses the use of SPR technology and Biacore for screening antibody libraries.

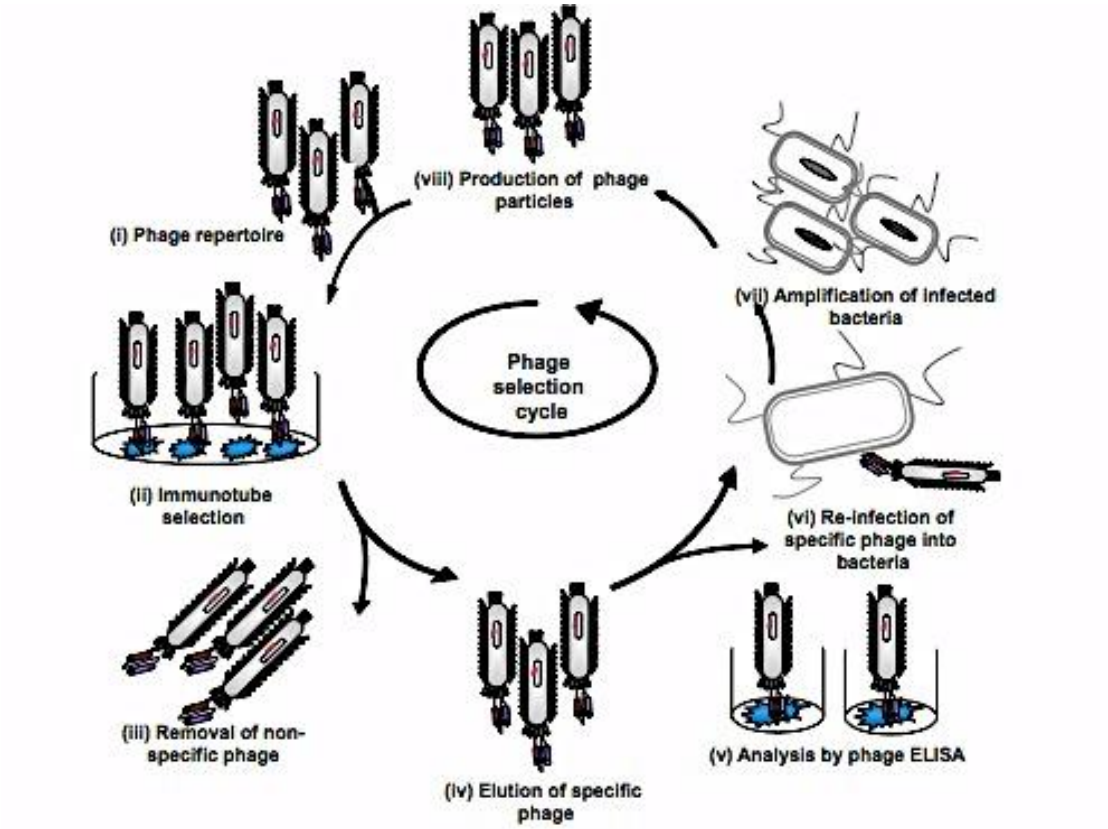

Figure 1.8. Overview of phage selection cycle i.e. panning.

The phage library is incubated with the target protein for an optimised length of time. Post incubation non-specific phage, are removed through washing. Target specific phage, are eluted using trypsin. The eluted phage can then be used to infect Gram-negative bacteria once again to produce a target-specific phage library. This cycle can be repeated a number of times resulting with high affinity target-specific antibodies.

1.9 Surface Plasmon resonance (SPR)

Surface plasmon resonance (SPR) has emerged as the most favoured technology for monitoring molecular interactions, due primarily to the fact that binding events can be monitored in 'real-time' and without the requirement for ancillary labels. These important characteristics facilitate accurate measurements, rapid analysis times, reduced additional costs and possible heterogeneities or other known complications associated with labeling of interactions.

SPR is an optical phenomenon as a result of the interaction of light with free electrons at a metal-dielectric interface (surface plasmon). The majority of SPR-based instruments are designed using a prism coupled to a dielectric metal for example gold. In this arrangement, a metal film is placed directly on top of a prism. Plane polarised

(P-polarised) light from a light source (LED at 760nm in Biacore^{TM} instruments) is incident on the surface at a specific angle, which allows total internal reflection (TIR) to occur. When the light hits the gold at the critical angle, not only does it internally reflect but it also leaks an electromagnetic energy called an evanescent wave, which moves exponentially across the gold interface exciting plasmons (electron charge density waves). This is seen as a drop in the intensity in the reflected light measured by the photo diode array detector. When analyte binds to the sensor surface a mass change occurs near the surface of the sensor chip. The refractive index near the sensor chip surface then changes, and this in turn changes the angle at which SPR occurs. The photo diode array detector detects the change in SPR angle and displays the change in real-time on a sensorgram.

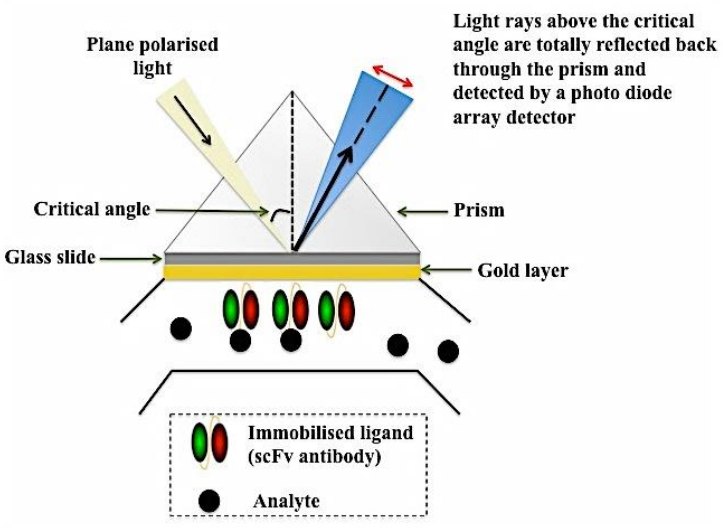

Figure 1.9. Schematic representation of the flow through mechanism of a SPR-based system.

SPR occurs on a thin layer of gold, which is sandwiched between a glass slide and the sample solution flowing through a specially designed microfluidic cartridge. Plane polarised light is directed onto the back of the gold sensor chip at a specific angle, which allows total internal reflection (TIR) to occur. When the light hits the gold at the critical angle, not only does it internally reflect but it also leaks an electromagnetic energy called an evanescent wave, which moves exponentially across the gold interface exciting plasmons (electron charge density waves). This is seen as a drop in the intensity in the reflected light measured by the photo diode array detector. When analyte binds to the sensor surface a mass change occurs near the surface of the sensor chip. The refractive index near the sensor chip surface then changes, and this in turn changes the angle at which SPR occurs. The photo diode array detector detects the change in SPR angle and displays the change in real-time on a sensorgram. (Adapted from Hodnik, & Anderluh, 2009).

Biacore™ (GE Healthcare) is the predominant manufacturer of the SPR systems found in many research laboratories, due to the range of instruments they have developed since the first SPR system in 1990. For this reason, Prof. O' Kennedy's research group, has three Biacore™ instruments: 1000, 3000 and 4000. The 1000 and 3000 systems are low volume analysis systems and are typically used to evaluate a maximum of 20 clones. The high-throughput and diverse nature of the 4,000 made it the predominant instrument used for screening and characterising the recombinant antibody libraries generated in this work. Method building on the Biacore™ 4000 and screening the recombinant anti-SFRP-2 and anti-PSMA libraries is described in more detail in chapter 2, 4 and 5 of this thesis.

1.10 Thesis aims and objectives

The principal aims of this research are the production and characterisation of prostate cancer-specific antibodies that may aid or improve prostate cancer diagnosis.

To achieve this several key objectives need to be realized:

1. Production of a biologically relevant recombinant secreted frizzled related protein-2 (SFRP-2) using a novel expression system.
2. Utilization of this protein to generate, select and characterise a recombinant anti-SFRP-2 antibody.
3. Generation, selection and characterisation of a recombinant antibody to prostate-specific membrane antigen.
4. Investigation of the utility of these scFv antibodies and derivatives (e.g. scAbs) as potential diagnostic reagents in ELISA, blotting and histochemical systems
5. Development of a unique theoretical approach for the generation of a novel bispecific antibody and initial studies on its practical feasibility, with a long term view of potential diagnostic/therapeutic applications

Chapter 2

Materials and Methods

2.1 Materials and Equipment

2.1.1 Reagents

All reagents used were of analytical grade and purchased from Sigma-Aldrich Ireland Ltd (Wicklow, Ireland) unless otherwise specified.

Reagent	Supplier
Acetic acid Agarose Molecular grade water Precept tablets Fermentas FastDigest® Enzymes Sodium Chloride (NaCl) PageRuler plus pre-stained protein ladder	Fisher Scientific Ireland, Suite 3, Plaza 212, Blanchardstown Corporate Park 2, Ballycoolin, Dublin 15, Ireland.
Antarctic phosphatase buffer Antarctic phosphatase enzyme	Brennan & Co., 61 Birch Avenue, Stillorgan Industrial Park, Stillorgan, Co. Dublin, Ireland.
Bacteriological Agar Tryptone Yeast extract	Cruinn Diagnostics Ltd., Hume Centre, Parkwest Business Park, Nangor Road, Dublin 12, Ireland.
Deoxynucleotide (dNTP)	Medical Supply Company Ltd., Damastown, Mulhuddart, Dublin 15, Ireland.
Glycogen New England restriction digest enzymes T4 DNA ligase enzyme and buffer Sodium acetate (NaOAc)	Bio-sciences Ltd., 3 Charlemont Terrace, Crofton Road, Dun Laoghaire,

Trizol RNAlater™	Dublin, Ireland.
PCR Primers	Integrated DNA Technologies, Interleuvenlaan 12A B-3001, Leuven, Belgium.
DNA Hyperladder (1kb) Instant*Blue*™	MyBio Ltd., Hebron Road Business Park, Co. Kilkenny, Ireland.
Virkon	Lennox Laboratory Supplies Ltd., John F. Kennedy Drive, Naas Road, Dublin 12, Ireland.
SureBlue TMB Microwell Peroxidase Substrate	Insight Biotechnology Ltd., P O Box 520, Wembley, Middlesex, HA9 7YN, United Kingdom.

2.1.2 Equipment

The equipment used throughout the course of this work and their suppliers are listed below.

Instrument	Manufacturer
NanoDrop™ ND-1000	NanoDrop Technologies, Inc., 3411 Silverside Rd 100BC, Wilmington, DE19810-4803, USA.
Trans-Blot® Semi-dry transfer cell	Bio-Rad Laboratories, Inc., 2000 Alfred Nobel Drive,

Bio-Rad PowerPac HC: 250V/3.0A/300W	Hercules, California 94547, USA.
Tecan® Safire 2™ plate reader	Tecan Group Ltd., Seestrasse 103, CH-8708 Männedorf, Switzerland.
PX2 thermal cycler	Thermo Electron Corporation, 81 Wyman Street, Waltham, MA 02454, USA.
Clifton stirred water bath	Nickel-Electro Ltd., Oldmixon Crescent, Weston-super-Mare, North Somerset BS24 9BL, United Kingdom.
Ohaus Explorer balance	Ohaus Europe GmbH, Heuwinkelstrasse 3, CH-8606 Nänikon, Switzerland.
Stuart Scientific See-saw rocker SSL4	Lennox Laboratory Supplies Ltd., John F. Kennedy Drive, Naas Road, Dublin 12, Ireland.
Priorclave tactrol 2 autoclave	Priorclave Ltd., 129/131 Nathan Way, West Thamesmead Business Park, London SE28 OAB, United Kingdom.
Eppendorf™ Centrifuge with swing-bucket rotor (A-4-62) and fixed-angle	Eppendorf UK Ltd., Endurance House,

rotor (F-45-30-11) New Brunswick Scientific U725 (-80 °C)	Vision Park Histon, Cambridge CB24 9ZR, United Kingdom.
37 °C static incubator	Sanyo Europe Ltd., 18 Colonial Way, Watford WD24 4PT, United Kingdom.
Heraeus Hera-safe Laminar flow cabinet	Thermo Scientific, 12-16 Sedgeway Business Park, Witchford, Cambridgeshire CB6 2HY, United Kingdom.

2.1.3 Cells

Cell lines

Cell Line	Derived from	Supplier
22RV1	CWR22R xenograft line	Supplied by Applied Biochemistry Group stocks
LNCaP	Left supraclavicular lymph node metastasis from a 50-year-old caucasian male in 1977	Supplied by Applied Biochemistry Group stocks

***E. coli* cells and genotypes**

Cell Line	Genotype	Catalogue number	Brand
One Shot® Top10 chemically competent cells	F- *mcrA* Δ(*mrr-hsd*RMS-*mcr*BC) Φ80*lacZ*ΔM15 Δ *lac*X74 *rec*A1 *ara*D139 Δ(*araleu*)7697 *gal*U *gal*K *rps*L (StrR) *end*A1 *nup*G	C4040-10	Invitrogen
One Shot®	F- *ompT hsdS*B (rB-mB-) *gal dcm*	C6010-03	Invitrogen

Star^{TM} BL21 (DE3) chemically competent cells	*rne131* (DE3)		
XL1 Blue	recA1 endA1 gyrA96 thi-1 hsdR17 supE44 relA1 lac *[F′* proAB lacI^{q}ZΔM15 *Tn*10 (*Tet*^{R})*]*	200249	Stratagene

2.1.4 Medium used for the growth of bacterial cells

Medium	Component	Composition
Luria Broth (LB)	Tryptone	10g/L
	Yeast Extract	5g/L
	NaCl	10g/L
	Agar (if required)	15g/L
Super Broth (SB)	MOPS	10g/L
	Tryptone	30g/L
	Yeast extract	20g/L

2.1.4.1 Medium additives used for the growth of bacterial cells

Antibiotics

Antibiotics used for bacterial cell culture were prepared as described below and sterile filtered (0.2μM) before use. Antibiotic stocks were retained in aliquots to reduce the instances of contamination.

Antibiotic	Component	Composition
100mg/mL (w/v) Carbenicillin	Carbenicillin salt	500mg
	Molecular grade water	5mL
70mg/mL (w/v) Kanamycin	Kanamycin	700mg
	Molecular grade water	10mL
5mg/mL (w/v) Tetracycline	Tetracycline	50mg
	Molecular grade water	10mL

2.1.5 Buffers

Buffer	Component	Composition
Phosphate Buffered Saline (PBS) (pH 7.4)	NaCl KCl Na_2PO_4 KH_2PO_4	0.15M 2.5mM 10mM 18mM Reagents are dissolved in 800mL ultra pure H_2O, pH is adjusted to 7.4, by titration with appropriate acid or base and made up to 1 litre with ultra pure H_2O.
5% (w/v) PBS-Milk (PBSM) (pH 7.4)	PBS Milk Marvel	1X 5% (v/v)
0.05% (v/v) PBS-Tween (PBST) (pH 7.4)	PBS Tween 20	1X 0.05% (v/v)
1% (w/v) PBST-Milk Marvel (MM) (PBSTM) (pH 7.4)	PBST Milk Marvel	1X 1% (w/v)

2.1.5.1 Sodium dodecyl sulfate polyacrylamide gel electrophoresis (SDS-PAGE) and Western Blotting (WB)

	Components	Volume
12.5% (w/v) Separation gel (1 gel: 6mL)	1M TrisHCl pH 8.8 30% Acrylagel 2% Bis-Acrylagel Water Deionized 10% SDS 10% APS (50mg in 500uL) TEMED	1.5mL 2.5mL 1.0mL 934µL 30µL 30µL 6µL

4.5% (w/v) Stacking gel (1 gel: 2.5mL)	1M TrisHCl pH 6.8 30% Acrylagel 2% Bis-Acrylagel Water Deionized 10% SDS 10% APS (50mg in 500uL) TEMED	300µL 375µL 150µL 1.74µL 24µL 24µL 2.5µL
10X electrophoresis buffer	50mM Tris, pH 8.3 196mM Glycine 0.1% (w/v) SDS dH_2O	30g 144g 10g to 1L
Loading buffer (4X)	0.5M Tris, pH 6.8 Glycerol 1-mercaptoethanol 20% (w/v) SDS Bromophenol blue dH_2O	2.5mL 2.0mL 0.5mL 2.5mL 20ppm 1.25mL
Transfer Buffer (500mL)	Trizma Base Glycine Methanol dH_2O	2.4g 7.2g 100mL 400mL

2.1.5.2 Protein purification buffers

2.1.5.2.1 PBS-based buffers

Buffer	Components
Equilibration buffer	1X PBS + 150mM NaCl + 10mM Imidazole, pH 8.0
Wash buffer	Equilibration buffer + 0.5% Tween®20, pH 8.0
Elution buffer	100mM NaOAc, pH 4.2
Neutralisation buffer	10X PBS + 100mM NaOH (1:1)

2.1.5.2.2 NaH_2PO_4-based buffers

Buffer	Components
Lysis buffer	50mM NaH_2PO_4 + 300mM NaCl + 10mM Imidazole, pH 7.5
Wash buffer A	50mM NaH_2PO_4 + 1M NaCl + 10% glycerol + 15mM Imidazole + 1% Triton X-100, pH 7.5
Wash buffer B	50mM NaH_2PO_4 + 1M NaCl + 10% glycerol + 20mM Imidazole + 1% Triton^{TM} X-100, pH 7.5
Elution buffer	50mM NaH_2PO_4 + 300mM NaCl + 250mM Imidazole, pH 7.5

2.1.5.2.3 Osmotic shock buffers

Buffer	Composition
Equilibration buffer	50mM NaH_2PO_4 + 100mM NaCl + 490mL dH_2O (500mL total) pH 8.0
Osmotic shock buffer A (OSB-A)	1XPBS + 150mM NaCl (200mL total) pH 8.0
Osmotic shock buffer B (OSB-B)	1XPBS +150mM NaCl + 1M Sucrose + 2mM EDTA (200mL total) pH 8.0
Periplasmic buffer	5mM $MgSO_4$ prepared in dH_2O (200mL total) pH 8.0
Wash buffer A	10mM Imidazole prepared in equilibration buffer (200mLtotal) pH 8.0
Wash buffer B	20mM Imidazole prepared in equilibration buffer (200mL total) pH 8.0
Elution buffer	300mM Imidazole prepared in dH_2O (4mL total) pH 8.0

2.1.6 Commercially sourced kits and solutions

Kit	Supplier
Superscript III® Reverse Transcriptase Kit (18080-051) Platinum® Taq DNA Polymerase High Fidelity (11304011)	Biosciences, 3 Charlemont Terrace, Crofton Road, Dun Laoghaire, Dublin, Ireland.
Phusion® Taq DNA Polymerase High Fidelity (M0530S)	Brennan & Co., 61 Birch Avenue, Stillorgan Industrial Park, Stillorgan, Co. Dublin, Ireland.
NucleoSpin® Gel and PCR Clean up Kit (NZ74060950) NucleoSpin® Plasmid mini prep (NZ74058850) NucleoBind® Xtra midi plasmid kit (NZ74041050) DreamTaq® DNA Polymerase High Fidelity (EP0703)	Fisher Scientific Ireland, Suite 3, Plaza 212, Blanchardstown Corporate Park 2, Ballycoolin, Dublin 15, Ireland.
Ni-NTA His•Bind® Resin (ANN0025)	MyBio Ltd., Hebron Road Business Park, Co. Kilkenny, Ireland.
GoTaq® Flexi DNA Polymerase (M8301)	Medical Supply Company Ltd., Damastown, Mulhuddart, Dublin 15,

	Ireland.

2.1.7 Commercially sourced antibodies

Antibody	Species	Supplier
Anti-polyhistidine (HIS) HRP Anti-Chicken IgY (IgG) whole molecule-HRP Anti-Rabbit IgG whole molecule-HRP	Mouse Rabbit Goat	Sigma-Aldrich Ireland Ltd., Vale Road, Arklow, Wicklow, Ireland.
Anti-SFRP-2 (ab77618) Anti-SFRP-2 (ab92667) Anti-PSMA (ab133579) Anti-HIS-DyLight®488 (ab117512) Anti-Chicken IgY H/L (HRP)	Goat Rabbit Rabbit Mouse Rabbit	Abcam, 330 Cambridge Science Park, Cambridge, CB4 0FL, United Kingdom.
Anti-Hemagglutinin (HA)-Peroxidase	Rat	Roche Diagnostics Corporation, Roche Applied Science, 9115 Hague Road, P.O. Box 50414, Indianapolis IN 46250-0414, USA.

2.1.8 Commercially sourced protein and peptides

Protein/Peptide	Species/Source	Catalogue number	Supplier
Folate Hydrolase (FOLH1) (Prostate-Specific Membrane Antigen) (PSMA) (750AA)	Human	ABIN1462478	Antibodies-online GmbH, Schloss-Rahe Strasse 15, 52072 Aachen,

			Germany.
SFRP-2 protein	Mouse	50028-M08H	Suite B-310 (also Suite B-209, B-203), 14 Zhong He Street, BDA, Beijing 100176, P. R. China.
Bovine serum albumin (BSA)	Animal derived	BPE1600	Fisher Scientific Ireland, Suite 3, Plaza 212, Blanchardstown Corporate Park 2, Ballycoolin, Dublin 15, Ireland.

2.1.9 Vectors

Vector	Resistance	Catalogue	Supplier
pET 26b(+) pET 28b(+)	Kanamycin Kanamycin	69862 69865	Novagen, Merck KGaA, Darmstadt, Germany.
pComb3XSS	Ampicillin	N/A	Prof. C. Barbas III, The Scripps Institute, La Jolla, San Diego, California, USA.
pMoPAC16	Ampicillin	N/A	Andrew Hayhurst, University of Texas at Austin, Austin, TX 78712 – 1095, USA.

2.2 Methods

2.3 Expression and purification of recombinant Secreted Frizzled Related Protein-2 (SFRP-2) using a novel approach

The following section outlines the methods applied for the production of recombinant SFRP-2 protein using a novel expression system.

A wide variety of factors can regulate and influence gene expression levels in *E. coli*, including synonymous codon bias. Synonymous codon bias refers to differences in the frequency of occurrence of synonymous codons in coding DNA. Different organisms can demonstrate particular preferences for one of the several codons that encode the same amino acid. In fast growing organisms such as *E. coli* it is thought that the codon preference reflects the composition of their tRNA pool and helps to achieve faster translation rates and high accuracy.

The native DNA sequence of the SFRP-2 gene employs tandem rare codons that can reduce the efficiency of translation or even disengage the translational machinery due to synonymous codon bias in *E. coli*. Codon optimisation was performed by Dr. Gillian O' Hurley using Genscript software for the SFRP-2 gene to allow for synonymous codon bias in *E. coli* to improve translation efficiency.

The optimised DNA sequence corresponding to amino acids 165-295 on the human SFRP-2 protein, including the *Nco* I and *Hind* III restriction sites, was cloned into a pUC57 vector using EcoRV restriction enzyme by Genscript USA Inc. (USA) (see Figure 2.10 below). This is the most immunogenic proportion of the SFRP-2 and was successfully used by Atlas antibodies to produce their fusion protein, which generated their SFRP-2 polyclonal antibody.

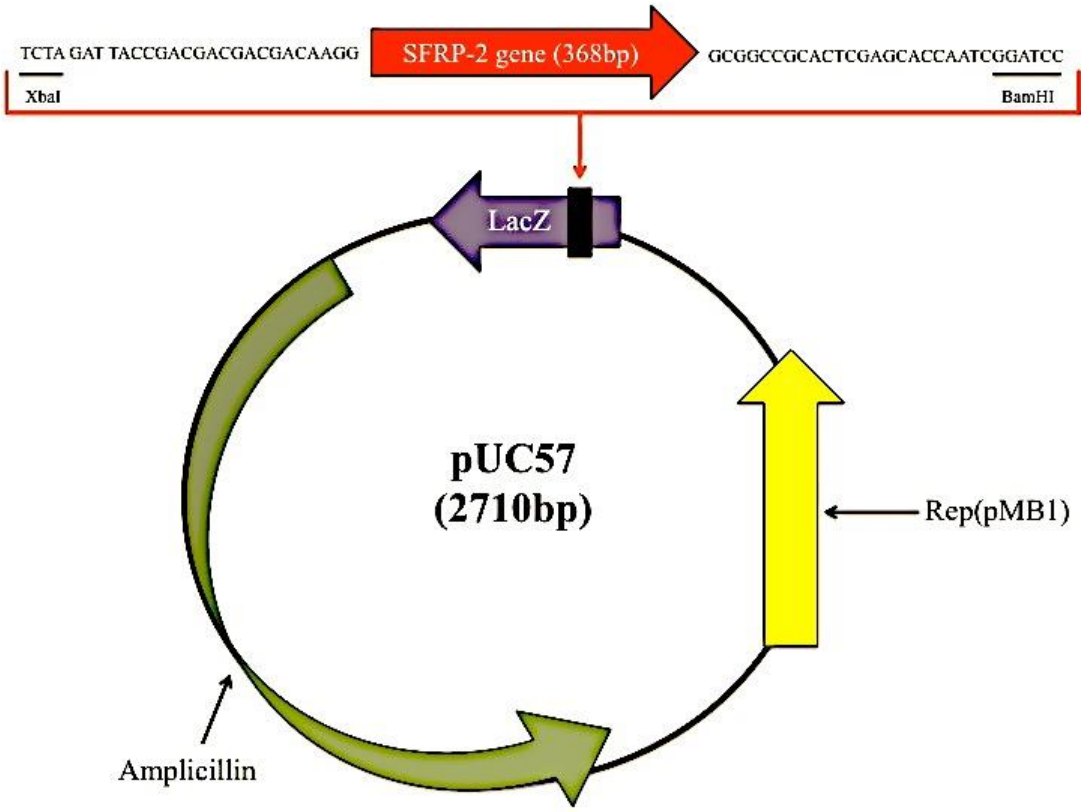

Figure 2.10. Map of pUC57 vector.

The *pUC57 vector map designed by Genscript USA Inc. (USA). The map locates where the optimised DNA sequence corresponding to the amino acids 165-295 on the human SFRP-2 protein was cloned into the pUC57 vector. The map also locates the pMB 1 replication origin, the amplicillin resistant gene and the Lac Z gene.*

Additionally, a novel expression system was developed, that takes advantage of the favourable expression and solubility profile of fatty acid binding protein (FABP), and employed in the expression of the SFRP-2 protein. The following section covers the methods applied to demonstrate the 'proof-of-concept', for this novel expression strategy, for the improved expression of a 'difficult-to-express' protein, SFRP-2. The SFRP-2 protein was fused C-terminally, downstream of a standard GS-rich linker sequence, to the human heart-type fatty acid protein (hFABP), in a pET28b (+) vector system, and yielded highly soluble chimeric fusion protein. The chimeric protein was successfully used to immunise an animal with a clearly measurable titre achieved.

2.3.1 PCR primers for amplification of SFRP-2 gene

Table 5. PCR primers for the amplification of the SFRP-2 gene.

Primer name	Sequence 5' – 3'
SFRP-2_F1.1	gaggaggaggagcgGAGCTCgcaaccgaagaagcaccgaaagtg
SFRP-2_R1.1	aggagtccttttGCGGCCGCttcgcgttgacctttttgcC

2.3.2 PCR amplification of SFRP-2 gene

The optimised SFRP-2 gene, designed by Dr. Gillian O' Hurley and provided by Genscript USA Inc. (USA) was amplified on a large scale using MyTaq™ Red Mix. The components, volumes, and conditions used for this PCR reaction are displayed in Tables 7 and 8. Once amplified large-scale, this sample was ethanol precipitated overnight and purified through gel extraction as described previously in section 8.1.3.

Table 6. The components and volumes used for the amplification of the SFRP-2 gene large-scale using MyTaq Red Mix.

Component	Volume for a small-scale reaction (µL) (1X)	Volume for a large-scale reaction (µL) (20X)
MyTaq™ Red Mix Buffer	25	500
Forward primer - SFRP-2_F1.1	0.5	10
Reverse primer - SFRP-2_R1.1	0.5	10
Template DNA – SFRP-2 gene	1	20
Molecular Grade H_2O (sterile)	to 50	to 1000
Total volume	50	1000

Table 7. The conditions used for the amplification of the SFRP-2 gene large-scale using MyTaq Red Mix.

Step	Temperature (°C)	Time (s)	Cycle
Initial denature	94	120	1 cycle
Denature	94	30	30 cycles
Anneal	56	30	
Extend	72	30	
Final extension	72	300	1 cycle
Hold	4	-----	-------

2.3.3 pET28b (+)-hFABP vector preparation

The pET28b (+)-hFABP vector stock was kindly provided by Dr. Stephen Hearty. An overnight culture (10mL SB supplemented with 25µg/mL Kanamycin) was prepared using 1-2µL of pET28b (+)-hFABP stock and incubated at 37°C shaking at 220rpm. This overnight culture was then used to inoculate 100mL SB (25µg/mL Kanamycin) and grown overnight at 37 °C shaking at 220rpm. Bacteria were collected by centrifugation at 4000 x g at 4°C for 30 minutes and the plasmid purified using NucleoBond® Xtra Midi as per the manufacturers' guidelines. Purified plasmid was resuspended in a final volume of 200µL molecular grade H_2O and quantified using the NanoDrop ND^{TM} 1000 nucleic acid DNA-50 setting.

2.3.4 Restriction digestion of pET28b (+)-hFABP vector and the amplified SFRP-2 gene using Sac1 and Not1 fast digest enzymes

Post amplification of the SFRP-2 gene and preparation of the pET28b (+)-hFABP plasmid a restriction digest using *Sac*I and *Not*I was performed. Table 9 outlines the components used for the restriction digest of the amplified SFRP-2 gene (insert) using *Sac*I and *Not*I FastDigest® enzymes. Table 10 outlines the components used for the restriction digest of pET28b (+)-hFABP (vector) using *Sac*I and *Not*I FastDigest® enzymes.

Table 8. Components and volumes required for the restriction digest of the amplified SFRP-2 gene using SacI and NotI FastDigest enzymes.

Component	Final concentration
SFRP-2 template DNA	5µg
10X Fermentas FastDigest (FD) Buffer	1X
*Sac*1	Variable*
*Not*1	Variable*
Molecular grade H_2O	to 100µL
* 1 µL of Fast Digest *Sac*I and *Not*I restriction enzyme digests 1 µg of plasmid DNA and 0.2 µg of PCR product in 5 minutes at 37 °C.	

The SFRP-2 gene digest was incubated in the PCR cycler for 1 hour at 37°C and then transferred from the PCR tube to a sterile 1.5mL tube. Ethanol precipitation, gel extraction and purification were carried out as previously described in section 8.1.2 and 8.1.3.

Table 9. The components required for the digestion of the pET28b(+)-hFABP vector using FastDigest NotI and SacI enzymes.

Component	Final concentration
pET28b(+)-hFABP Vector (10 µg)	10µg
10x Fermentas fast digest (FD) buffer	1X
*Sac*1	Variable*
*Not*1	Variable*
Molecular grade H_2O	to 100µL
* 1 µL of Fast Digest SacI and NotI restriction enzyme will digest 1 µg of plasmid DNA and 0.2 µg of PCR product in 5 minutes at 37 °C.	

The restriction digest of the pet28b (+)-hFABP vector was incubated in the PCR cycler for 1 hour at 37°C followed by an inactivation step for 20 minutes at 65°C. 1X antarctic phosphatase buffer and 5 µL of antarctic phosphatase enzyme was then added to the sample. Antarctic phosphatase catalyzes the removal of 5´phosphate from DNA and RNA. Since phosphatase-treated fragments lack the 5´phosphoryl

termini required by ligases, they cannot self-ligate. Thus antarctic phosphatase treatment of the vector increases ligation efficiency post digestion. The sample was then incubated at 37°C for 30 minutes followed by a deactivation step for 20 minutes at 65°C. Ethanol precipitation, gel extraction and purification was then carried out as previously described in section 8.1.2 and 8.1.3.

2.3.5 Ligation of SFRP-2 gene into pET28b (+)-hFABP and transformation in to TOP10F' chemically competent cells

The purified SFRP-2 digested sample was then ligated into the purified digested pET28b (+)-hFABP vector using T4 ligase (NEB) under the reaction conditions outlined in Table 11. The reaction was carried out overnight at room temperature. The ligations were then deactivated at 65°C for 20 minutes and ethanol precipitated overnight at -20°C.

Table 10. The components required for the ligation of SFRP-2 into the pET28B(+)-hFABP vector.

Component	Ligation	Control (digested pET28b(+)-hFABP vector
Molecular grade H_2O	To 100µL	To 100µL
T4 DNA ligase buffer (10X)	1X	1X
SFRP-2 gene (insert)	300ng	-----
pET28b(+)-hFABP (vector)	100ng	100ng
T4 DNA ligase	10U/µg	10U/µg

Once the samples were efficiently precipitated, the ligation reactions were centrifuged at 12,000 x g for 30 minutes at 4°C and the pellets were resuspended in 15µL molecular grade H_2O (preheated to 50°C) for transformation. Heat shock transformation was carried out as described in section 8.1.13. TOP10F' chemically competent cells were used for this transformation.

2.3.6 'Colony-pick' PCR analysis of transformed pET28b(+)-hFABP vector containing the SFRP-2 gene

Ten single colonies were randomly picked from an LB agar plate containing the transformed pET28b (+)-hFABP vector and incorporated into a 'colony-pick' PCR to ensure the vector was harboring the SFRP-2 gene. A sterile tip was used to pick a single colony into the following mixture, which was then placed in a PCR machine. The amplified samples were subsequently analysed via gel electrophoresis on a 1% (w/v) agarose gel.

Table 11. The components required for colony pick PCR analysis of transformed pET28b(+)-hFABP vector.

Component	Volume (µL)/reaction
Molecular grade water	to 50
MyTaq™ Red Mix Buffer	25
Forward primer - SFRP-2_F1.1	0.5
Reverse primer - SFRP-2_R1.1	0.5
Total	50

The colony pick PCR reaction was carried out in a PCR cycler. The conditions used for this PCR are displayed in Table 13.

Table 12. Conditions used for colony pick PCR of pET28b(+)-hFABP vector.

Step	Temp (°C)	Time (s)	Number of cycles
Initial denature	94	30	1 cycle
Denature	94	30	30 cycles
Anneal	56	30	
Extend	72	30	
Extend	72	300	1 cycle
Hold	4	-----	-----

2.3.7 Positive expression of SFRP-2 colony picked clones

The positive pET28b(+)-hFABP-SFRP-2 clones obtained from the colony pick PCR were inoculated in 10mLs of SB (containing 25µg/mL kanamycin) and incubated overnight at 37°C at 220rpm. The following day an aliquot of the overnight cultures was subcultured into 10mLs of fresh SB medium (containing 25µg/mL of kanamycin). The samples were then incubated at 37°C until an optical density at 600nm (OD_{600nm}) of ~0.7 was obtained. The remainder of the cultures were centrifuged and glycerol stocks were prepared as described in section 8.1.8. When an OD_{600nm} of ~0.7 was obtained 5mL of each culture was removed and added to a fresh 50mL tube. Zero point one mM IPTG was added to one tube only and the temperature was turned down to 25°C. This provided an uninduced and induced set of samples for each clone. After 4 hours of induction a 1mL sample was taken from each clone and added to a sterile 1.5mL tube, centrifuged at 12,000 x g, and the supentant was discarded. The pellets were resuspended in 100µL of 1X sterile PBS and 4XSDS-PAGE loading dye. The samples were boiled for 2 minutes at 98°C and then centrifuged at 12,000 x g at 4°C for 30 minutes. The samples were then analysed through SDS-PAGE and Western blot as described in sections 8.1.16 and 8.1.17. The Western blot was initially probed with a 1 in 2000 dilution of a commercial anti-SFRP-2 polyclonal antibody (Abcam) raised in goat, followed by incubation with a commercial anti-goat-HRP secondary antibody (Abcam).

2.3.8 Optimisation of expression of SFRP-2

To assess the impact of culture time, temperature and IPTG concentration a time course (2 hours, 3 hours and 4 hours) at 25°C and 30°C with shaking at 220rpm was undertaken with a range of IPTG concentrations (0.05mM, 0.1mM and 0.2mM) as described in the generic expression optimisation method (section 8.1.14) and analysed by SDS-PAGE (section 8.1.16) and WB (section 8.1.17). For WB analysis the lysates were probed with a commercial anti-SFRP-2 polyclonal antibody (Abcam) raised in goat, followed by incubation with a commercial anti-goat-HRP secondary antibody (Abcam) both at a 1 in 2,000 dilution in 1% (w/v) PBSTM.

2.3.9 Optimisation of purification of SFRP-2

A 10mL overnight culture of SFRP-2 (SB with 25µg/mL kanamycin) was used to inoculate a 400mL culture which was allowed to grow at 37°C shaking at 220rpm until an OD_{600nm} of ~0.7 was reached. At this point, the culture was induced with

0.05mM IPTG (optimised in section 2.3.8) for four hours at 25°C (optimised in section 2.3.8). The culture was then decanted into 2 x 250mL Oak Ridge tubes and centrifuged at 4,000 x g at 4°C for 40 minutes. The collected cell pellet was then lysed (using either the method described in section 8.1.9 or 8.1.10). PBS and NaH_2PO_4-based buffers were used throughout the optimisation of purification for SFRP-2.

2.3.10 Purification and concentration of produced proteins using IMAC column

Purification and concentration of SFRP-2 was carried out using the IMAC column purification and concentration generic methodology delineated in section 8.1.15.

2.4 The generation of a chicken anti-SFRP-2 scFv library

The following section outlines the methods implemented to generate an anti-SFRP-2 scFv and an anti-SFRP-2 scAb. The purified SFRP-2 protein obtained using a novel expression system described in section 2.3 was utilised as the primary antigen to induce a SFRP-2-specific immune response in an avian host. Following a full immunisation schedule, a serum titre was performed in order to ensure that high anti-SFRP2 antibody titre responses were observed. RNA extraction and cDNA synthesis was performed and an anti-SFRP-2 scFv library was constructed. In order to ensure native protein reactivity, mammalian-based expression of the full-length SFRP-2 protein was initiated in collaboration with Dr. P.J. Conroy and Prof. James C. Whisstock in Monash University, Melbourne. The screening strategy for the anti-SFRP-2 scFv library was based on the full-length SFRP-2 protein, in addition to antibody characterisation.

2.4.1 Immunisation schedule of a white leghorn chicken with purified SFRP-2 antigen

A female leghorn chicken was initially immunised sub-cutaneously with a mixture of equal parts of purified SFRP-2 antigen (method for the expression and purification of this antigen was described in section 2.3) in sterile PBS (1X) and Freund's complete adjuvant. The final concentration of the initial immunisation was 100 μg/mL. The first boost (day 14) was then administered using 75 μg/mL of purified SFRP-2 in PBS, mixed in a 1:1 ratio with Freund's incomplete adjuvant, in a final volume of 1mL. The 3 boosts that followed (days 36, 52 and 66) all contained a reduced

concentration of SFRP-2 in PBS (50µg/mL, 25µg/mL and 10µg/mL) and were administered in the same manner as the first boost.

2.4.2 Chicken anti-serum titre analysis of immune response to SFRP-2

Nunc Maxisorb™ immunoplates were coated with 100µL per well of purified SFRP-2 antigen (expressed and purified as described in section 2.3) in PBS (1X) at a concentration of 1µg/mL and incubated overnight at 4°C. The plate was then blocked with PBS (1X) containing 5 % (w/v) Milk Marvel for 1 hour at 37°C. The plate was washed three times with PBST and three times with PBS. Doubling dilutions of serum were prepared in 1% (w/v) PBSTM. The prepared dilutions were applied in duplicate (100µL) across the SFRP-2 coated wells. The plate was incubated and washed as described in the previous step and 100µL of a 1 in 2000 dilution of an anti-chicken-HRP-labeled antibody (Sigma) in PBST containing 1 % (w/v) Milk Marvel was applied to each well. The plate was incubated for 1 hour at 37°C, washed as before, and TMB substrate was added (100µL/well). Following incubation for 10-15 minutes at room temperature, the reaction was stopped by the addition of 10% (v/v) HCl and the absorbance read at 450nm on a Tecan Safire2™ plate-reader.

2.4.3 Extraction and isolation of total RNA from chicken spleen and bone-marrow

Once a sufficient immune response was obtained isolation of total RNA from chicken spleen and bone-marrow was carried out. 24 hours prior to sacrifice, centrifuge tubes were prepared (Oakridge Centrifuge Tubes) by rinsing thoroughly with freshly prepared bleach and allowed to soak for 30 minutes. The tubes were then RNase Zapped and covered in tinfoil overnight. The homogenizer and probe were then washed in bleach for 30 minutes and rinsed with tap water followed by RNase Zap for 30 minutes. They were then rinsed with molecular grade water, wrapped in tinfoil and autoclaved. The homogeniser and probe were then placed in an 80°C drying oven overnight.

The laminar flow hood was switched on and cleaned thoroughly with 70% (v/v) IPA followed by RNase Zap. The centrifuges and rotors were switched on and pre-chilled to 4°C. The centrifuge tubes were rinsed with molecular grade water into an “RNase

Zapped" beaker. The tubes were left filled with water in the laminar until ready for use. Seventy five percent molecular grade ethanol was prepared with molecular grade water under sterile conditions and placed at -20°C. An appropriate aliquot of Trizol was then placed on ice and left on ice until ready for use.

The spleen and bone marrow were removed as directed and placed in a 50mL RNase-free tube. The homogeniser probe and parts were rinsed with molecular grade water and assembled. Ten mL of ice cold Trizol was added immediately to the spleen/bone marrow and the spleen was homogenised. When completely homogenised, a further 20mL of ice cold Trizol was added to the sample. This was then allowed to stand for 10 minutes at room temperature (RT). The B-cells were extracted from the bone marrow by flushing the bone marrow with Trizol into a 50mL tube. The samples were then centrifuged at 3,525 x g for 15-20 minutes at 4ºC. The supernatant was carefully removed to a 50mL Oakridge tube and 6mL of molecular grade chloroform was added. The samples were shaken vigorously for 15 seconds, allowed to stand at RT for 15 minutes, and centrifuged at 11,000 x g for 30 minutes at 4ºC. The upper aqueous layer was removed. It is important to ensure that no organic layer of the protein is transferred from the interphase. The aqueous upper layer was transferred to a 85mL Oakridge tube and 15mL of molecular grade isopropanol (IPA) was added. The samples were shaken vigorously for 15 seconds and allowed to stand at RT for 10 minutes, followed by centrifugation at 11,000 x g for 30 minutes at 4ºC. The supernatant was carefully removed (to waste) without disturbing the pellets. Thirty mL of 75% v/v molecular grade ethanol (EtOH) was added and the sample was centrifuged at 11,000 x g for 30 minutes at 4ºC. The supernatant was removed to waste and the RNA pellets were allowed to air dry. Five hundred µL of molecular grade water was then added. The RNA pellets were resuspended by gently pipetting up and down the molecular grade water along the side of the tubes. The RNA was then stored on ice. It is critical at this stage to immediately proceed to cDNA synthesis due to the unstable nature of RNA.

2.4.4 RNA Quantification/Storage

The RNA was quantified using a NanoDrop spectrophotometer. Undiluted samples were prepared with molecular grade water with concentrations ranging from a 1 in 50

dilution to a 1 in 400 dilution. Three readings were obtained in order to ensure accuracy and consistency between dilutions. Typical yields obtained from a chicken spleen are between 5-10µg/µL RNA and for chicken bone marrow are between 1-4µg/µL RNA. The $A_{260:\ 280}$ ratio should be in the range of 1.6 – 1.9 for acceptable quality of RNA to proceed with cDNA synthesis. Remaining RNA that is not needed for cDNA synthesis can be ethanol precipitated by adding the components outlined in Table 14.

Table 13. Components required for ethanol precipitation of RNA.

Component	Volume
RNase Free NaOAC pH 5.2	0.1X Vol.
Ice cold 100% EtOH	2 X Vol.
Glycogen	1µL

2.4.5 Reverse transcription of total RNA to cDNA

A PCR was performed to convert total RNA to cDNA by reverse transcription. This reaction was carried out using a Superscript ™ III first strand cDNA synthesis kit, which is obtained from Invitrogen. The cDNA serves as a template for the amplification of the variable light and variable heavy chain gene fragments.

2.4.5.1 cDNA Synthesis

Total RNA was transcribed to cDNA by reverse transcriptase PCR. The cDNA served as a template for the amplification of the variable heavy and variable light chain gene fragments.

A total quantity of 5µg of RNA is required for each reaction. A 20X reaction was prepared as described in Table 15.

Table 14. Components and volumes required for the initial stage of cDNA synthesis from RNA.

Mixture 1 components	1x	20x
Total RNA	1µL	20µL
Oligo (dT) 50µM	1µL	20µL
dNTPs 10mM	1µL	20µL
Molecular grade H_2O	to 20µL	to 200µL
Total volume	20µL	200µL

Mixture 1 was dispensed into 8 x 25µl aliquots and briefly centrifuged at 11,000 x g before being placed in to the PCR machine. Step 1 outlined in Table 17 was allowed to run. Mixture 2 was then prepared as described in Table 16.

Table 15. Components and volumes required for the final stage of cDNA synthesis from RNA..

Mixture 2	1x	20x
10x RT Buffer	2µL	40µL
$MgCl_2$ 25mM	4µL	80µL
DTT 0.1M	2µL	40µL
RNase Out (40U/µL)	1µL	20µL
Superscript III RT (200U/µL)	1µL	20µL
Total	20µL	200µL

Once step 1 was complete the PCR tubes were placed on ice for 1-3 minutes, which allowed them to cool. Twenty-five µL of mixture 2 was then added to each of the 8 PCR tubes. Step 2 of the programme outlined in Table 17 was then run. After step two was complete the tubes were placed on ice for a further 1-3minutes. Two µL of RNase H was added to each tube, and the tubes were then placed back in the PCR machine and Step 3 of the cycle (outlined in Table 17) was allowed to run. The samples were then pooled together into a fresh, sterile, clearly labelled 1.5mL tube.

The DNA was quantified using the NanoDrop spectrophotometer. Ten µL aliquots of cDNA were prepared and stored at -80^{o}C.

Table 16. Thermo cycler conditions used throughout cDNA synthesis.

Step	Time (minutes)	Temperature (^{o}C)
1	5	65
Pause		4
2	50	50
	5	85
Pause		4
3	20	37
Pause	-----	4

2.4.6 Anti-SFRP-2 scFv library construction

Antibody construction was carried out as described by Andris-Winhopf and co-workers (Andris-Winhopf *et al.*, 2000). The initial steps involved in generating the library require the amplification of the antibody variable domains for the synthesised cDNA isolated from both the spleen (SP) and the bone marrow (BM) of the chicken immunised with the purified SFRP-2 protein.

The primers used for library building are those published in Chapter 9 of Phage Display: a laboratory manual and host specific sub chapters (Barbas *et al.*, 2001). All primers used were those to clone antibody fragments into the pComb3x vector series. The list of primers used to construct avian scFv fragments from immune libraries introducing the long linker (GGSSRSSSSGGGGSGGGG) between the variable heavy and light chains is shown in Table 18. All primers were commercially synthesised by Integrated DNA Technologies (Interleuvenlaan 12A B-3001 Leuven, Belgium).

Table 17. Avian scFv library PCR primer list.

Primer Name	**Sequence 5' – 3'**
Primers for the amplification of the variable heavy gene	
CSCVHo-FL: (sense - Long linker)	GGT CAG TCC TCT AGA TCT TCC GGC GGT GGT GGC AGC TCC GGT GGT GGC GGT TCC GCC GTC ACG TTG GAC GAG
CSCG-B (reverse)	CTG GCC GGC CTG GCC ACT AGT GGA GGA GAC GAT GAC TTC GGT CC
Primers for the amplification of the variable light (Vλ)	
CSCVK (sense)	GTG GCC CAG GCG GCC CTG ACT CAG CCG TCC TCG GTG TC
CKJo-B (reverse)	GGA AGA TCT AGA GGA CTG ACC TAG GAC GGT CAG G
Primers for use in the splice-by-overlap extension (SOE) PCR	
CSC-F (sense)	GAG GAG GAG GAG GAG GAG GTG GCC CAG GCG GCC CTG ACT CAG
CSC-B (reverse)	GAG GAG GAG GAG GAG GAG GAG CTG GCC GGC CTG GCC ACT AGT GGA GG

2.4.7 Variable domain amplification

The first round of PCR involved separate amplification of variable heavy and light chains. Initially, the $MgCl_2$ concentration for the reaction was optimised to ensure high-yield specific-bands by titration in the concentration range (from 1.5mM to 4mM) followed by large-scale synthesis at the optimised 2.0mM $MgCl_2$ for variable heavy (V_H) (spleen), 4.0mM $MgCl_2$ for variable light (V_L) (spleen), 4.0mM $MgCl_2$ for variable heavy (V_H) (bone marrow) and 2.0mM $MgCl_2$ for variable light (V_L) (bone marrow). GoTaq® Flexi Buffer was used for this PCR optimisation.

The PCRs were carried out using the parameters outlined in Table 19.

Table 18. Variable domain amplification PCR cycler parameters.

Stage	Step	Temperature (°C)	Time (s)	No. of cycles
1	Initial denature	94	120	1
2	Denature	94	15	30
	Annealing	56	30	
	Extension	72	60	
3	Final extension	72	600	1

Large-scale variable PCR products were resolved on 1.5% agarose gels and purified through gel extraction as described in section 8.1.3. Purified products were quantified using the NanoDrop ND 1000TM using DNA-50 setting. Note: All PCR products were eluted from the column in 15µL of preheated (~70 °C) molecular grade water.

2.4.8 Splice-by-overlap extension (SOE) PCR

The second round of PCR joined together the variable domains into a single scFv construct in the V_L-V_H orientation. The overlap of V_L-V_H was possible due to the overlapping 'tails' in the light chain reverse (CKJo-B) and heavy chain forward primers (CSCVHo-FL). This was carried out using the overlap primer pair (CSC-F and CSC-B) to complete the construct and introduce upstream and downstream Sfi*I* sites for easy transition into the PComb3X vector series. In addition 'clamp' sequences $(GAG)_6$ on these primers allowed efficient digestion of the PCR products. MyTaq™ Red Mix was employed at this stage of library construction. Table 20 details the components used for the large-scale SOE amplification reaction used for both spleen and bone marrow.

Table 19. Splice-by-overlap extension PCR components for spleen and bone-marrow.

Component	Volume (µL) added for overlap of spleen V_H and V_L chain genes	Volume (µL) added for overlap of bone-marrow V_H and V_L chain genes
MyTaq™ Red Mix	500	500
Molecular grade H_2O	to final volume of 1000	to final volume of 1000
CSC-F (60nMol)	10	10
CSC-B (60nMol)	10	10
V_L	100 ng/50µL reaction	100 ng/50µL reaction
V_H	100 ng/50µL reaction	100 ng/50µL reaction
Total Volume	1000	1000

Both SOE PCR reactions were carried out under the cycling parameters outlined in Table 21.

Table 20. SOE PCR cycling conditions.

Stage	Step	Temperature (°C)	Time (s)	No. of cycles
1	Initial denature	94	120	1
2	Denature	94	15	30
	Annealing	55	30	
	Extension	68	60	
3	Final extension	68	600	1

SOE-PCR products were purified through gel extraction as described in section 8.1.3. The purified products were eluted in 50µL of preheated (~70°C) molecular grade water and stored at – 20°C until ready to proceed to restriction digest.

2.4.9 pComb3XSS vector preparation for digestion

The pComb3XSS vector stock was kindly provided by Dr. Paul Conroy. An overnight culture (10mL SB supplemented with 100µg/mL Carbenecillin) was prepared using 1-2µL of the pComb3XSS vector stock and incubated at 37°C shaking at 220rpm. This overnight culture was then used to inoculate 100mL SB (100µg/mL Carbenecillin) and grown overnight at 37°C shaking at 220rpm. Bacteria were collected by centrifugation at 4,000 x g at 4°C for 30 minutes and the plasmid purified using NucleoBond® Xtra Midi as per the manufacturers' guidelines. Purified plasmid was resuspended in a final volume of 200µL molecular grade H_2O and quantified using the NanoDrop ND^{TM} 1000 nucleic acid DNA-50 setting.

2.4.10 Restriction-digest of the purified overlap PCR product and vector DNA

Both the purified pComb3XSS and SOE-PCR products from the BM and SP were digested in large-scale for ligation of both libraries into the pComb3XSS vector.

Table 21. Components and volumes required for restriction digest of anti-SFRP-2 spleen and bone marrow scFv libraries.

Component	**Concentration/Volume (**µL)/ reaction for restriction digest of bone-marrow SOE	**Concentration/Volume (**µL)/ reaction for restriction digest of spleen SOE
Fermentas fast digest buffer	20	20
Fermentas Fast digest *Sfi*I (36U per µg of DNA)	360 U	360 U
Purified overlap SOE-PCR product	10 µg	10 µg
Molecular grade water	to 200 µL	to 200 µL

The digests were incubated for 5 hours at 50ºC, followed by a denaturation step at 65ºC for 20 minutes. The BM and SP were then stored as an ethanol precipitation

until required (see section 8.1.1 for ethanol precipitation).

Table 22. Components and volumes required for restriction digest of the purified pComb3xSS plasmid.

Component	**Concentration/Volume (**µL)/ reaction for restriction digest of pComb3xSS vector for spleen	**Concentration/Volume (**µL)/ reaction for restriction digest of pComb3xSS vector for bone-marrow
Fermentas fast digest buffer	20	20
Fermentas Fast digest *Sfi*I (36U per µg of DNA)	360 U	360 U
Purified pComb3XSS vector	10 µg	10 µg
Molecular grade water	to 200 µL	to 200 µL

The pComb3xSS vector digests were incubated for 5 hours at 50ºC, followed by a denaturation step at 65ºC. The S*fi*I digested vector samples were then triple digested and antarctic phosphatase treated (Table 24).

Table 23. Triple digest and antarctic phosphatase treatment of SfiI digested pComb3xSS vector.

Component	**pComb3xSS vector**	**Temperature (**ºC) **and time (minutes)**
Xho*I* [20U/ µL]	3 U/µg	37 ºC for 60 minutes followed by 65 ºC for 20 minutes
Xba*I* [20U/ µL]	3 U/µg	
Antarctic Phosphatase buffer (10X)	1X	37 ºC for 30 minutes followed by 65 ºC for 20 minutes
Antarctic Phosphatase [5U/ µL]	1 U/µg	

Post-triple digestion and antarctic phosphatase treatment, the vector was stored as an ethanol precipitation until required. All the digested product precipitations were completed, as described in section 8.1.1. The products were purified by resolution on 0.5% (w/v) (pComb3xSS) or 2% (w/v) (BM and SP) agarose gels, the relevant bands excised and extracted using NucleoSpin® gel extraction kit as per the manufacturers' instructions (eluted in 50µL molecular grade H_2O).

2.4.11 Ligation of the digested overlap PCR product with pComb3xSS vector DNA

The purified S*fi*I digested scFv inserts were then ligated into the prepared pComb3X vector using T4 ligase (NEB) under the reaction conditions outlined in Table 25. The reaction was carried out overnight at room temperature. The ligations were then deactivated at 65ºC for 20 minutes and ethanol precipitated overnight at -20ºC as described in section 8.1.1. The ligation pellet was resuspended in 20µL of molecular grade water and transformed into *E. coli* XL1-Blue electrocompetent cells (Stratagene) by electroporation.

Table 24. Ligation reaction conditions used for ligation of spleen and bone marrow libraries into pComb3xSS vector.

Component	Spleen/ pComb3xSS	Bone-marrow/ pComb3xSS	pComb3xSS vector control
pComb3xSS (digested and purified)	1.4 µg	1.4	1.4
Overlap PCR product (digested and purified)	700 ng	700	0
T4 DNA ligase buffer	20 µL	20 µL	20 µL
T4 DNA ligase	10 µL	10 µL	10 µL
Total	200 µL	200 µL	200 µL

2.4.12 Transformation of E.coli XL1-Blue electrocompetent cells with pComb3XSS vector containing light and heavy chain genes and measurement of transformation efficiencies

Ligations and electroporation cuvettes (0.2cm, Bio-Rad) were incubated on ice for 5 minutes. At the same time the electrocompetent *E.coli* XL1-Blue cells were thawed on ice. Seven and a half µL of the library ligation was added to each 150µL *E.coli* XL1-Blue cell aliquots. The cells and DNA were left to stand for 1 minute after gentle mixing. DNA was electroporated into the cells using the Gene Pulser xCell Electroporation system (Bio-Rad) with the following parameters; 2.5kV, 25µF and 200Ω ($\tau = 4.0$msec). Once electroporation was completed each cuvette was immediately flushed with 1mL SOC medium and transferred to a 50mL pre-warmed tube. This was followed by a further 1mL wash with SOC. All the electroporated samples (both BM and SP ~ 8mLs) were combined into the one 50mL tube and placed at 37°C ,shaking at 230rpm for 1 hour. The control ligation (2 x 7.5µL ligation) was also electroporated and treated in the same fashion. To both the library and the control 10mL of pre-warmed SB (with 3µL of 100mg/mL Carbenicillin and 30µL of 5mg/mL Tetracycline) was added. A 20µL sample of the library was removed into 180µL SB for titre determination by plating a 10-fold serial dilution range (plated 100µL of 10^{-3} to 10^{-6} inclusive on LB-Carbenicillin (50µg/mL) agar plates).

A 2µL sample was removed from the control library and diluted into 200µL SB followed by plating 10µL and 100µL of this 1 in 100 dilution onto LB-Carbenicillin (50µg/mL) agar plates. The control was then discarded. The library was then incubated at 37°C shaking at 230rpm for a further hour after which 4µL of Carbenicillin (100µg/mL) was added. After incubation for 1 hour at 37°C with shaking at 230rpm, 2mL of helper-phage (VCSM13: 1.0 x 10^{13} cfu/mL) was added and the library transferred to a 500mL baffled flask containing 183mL SB (pre-warmed to 37°C) with 92.5µL Carbenicillin (100mg/mL) and 370µL Tetracycline (5µg/mL). The culture was left static for 15 minutes followed by incubation for 2 hours as described in the previous incubation step. Two hundred and eighty µL of Kanamycin (70µg/mL) was added and the cultures were allowed to grow at 37°C with shaking at 230rpm overnight. At this stage the anti-SFRP-2

library is displayed on the phage particle and is ready for panning.

2.4.13 Rescue and subsequent precipitation of scFv-displaying phage

Phage rescue is the process carried out at each round of panning to recover the selected antibody-displaying phage from culture supernatant. After incubation of the transformed library overnight (section 2.4.12) the phage were isolated by PEG8000 precipitation. This was carried out after each round of panning e.g. R0 = transformed library recovery, R1 = recovered phage after 1st round of panning and so on. The phage-anti-SFRP-2 scFv library culture was placed in 2 x 250mL or 2 x 85mL (depending on culture volume) centrifuge bottles. A 1mL sample was removed, centrifuged at 9,000 x g for 5 minutes at RT. The cells and supernatant were retained for DNA/soluble antibody analysis if required. The centrifuge bottles were centrifuged at 9,000 x g for 15 minutes at 4°C (Eppendorf 5810R) after which 4% (w/v) PEG8000 and 3% (w/v) NaCl was added to each supernatant after transfer to a set of clean centrifuge bottles. The phage rich supernatant was shaken at 230rpm for 5 minutes at 37°C. The precipitating phage was then put on ice for 30 minutes before centrifuging at 9,000 x g for 15 minutes at 4°C. The supernatant was discarded and the tubes dried by inversion for 10 minutes. The phage pellet was then resuspended in 2 x 1mL of 1 mg/mL BSA with 0.02% (w/v) NaN_3 in PBS. The phage preparation was then transferred to a 2mL micro-centrifuge tube and any residual cellular debris removed by centrifugation (full speed for 5 minutes at 4°C).

2.4.14 Enrichment of phage library via panning against immobilised antigens

To a previously coated (100µL x 8 wells of SFRP-2 full-length protein at 4°C overnight (O/N)) and blocked (200µL of 5% (w/v) PBSM for 2 hours at 37°C) ELISA plate, 100µL of the rescued phage was added to each coated and blocked well and incubated with the antigen for 2 hours at 37°C. Non-specific phage were removed with sequential PBST (200µL/well x 5) and PBS (200µL/well x 5) washes. Anti-SFRP-2-specific bound phage were eluted by incubation with 100µL/well of 10mg/mL trypsin in PBS at 37°C for 30 minutes. The eluted phage (~800µL) was then used to infect 5mL of mid-exponential ($O.D_{600}$ ~0.4) *E. coli* XL-1 blue cells for 15 minutes, static at RT. Pre-warmed SB medium (6mL) containing 1.6µL of Carbenicillin (100mg/mL) was added to the infected cells. A 2µL sample was

removed and diluted in 200µL SB for output titre determination by plating 10µL and 100µL of this onto LB-Carbenicillin (50µg/mL) agar plates. The 8mL output library was placed at 37°C shaking at 230rpm for 1 hour followed by the addition of 2.4µL of Carbenicillin (100mg/mL) and incubation at 37°C shaking at 230rpm for 1 hour. Helper-phage (1mL of VCSM13: 1.0 x 10^{13} cfu/mL) was added and the culture transferred to a 250mL baffled flask containing 92mL SB with 46µL of Carbenicillin (100 mg/mL) plus 184µL of Tetracycline (5mg/mL) and incubated at 37°C with shaking at 230rpm for 2 hours. In the final step 140µL of Kanamycin (70mg/mL) was added and the culture incubated as above overnight. An input titre was performed during these incubation steps by the addition of 10µL of the rescued phage to 90µL of SB medium and 10-fold serially diluting to 10^{-9}. A 2µL sample of the 10^{-7}, 10^{-8} and 10^{-9} dilutions were infected into mid-exponential phase *E. coli* XL-1 blue (100µL) and plated (50µL) onto LB-Carbenicillin plates (50µg/mL) after static incubation at RT for 15 minutes. This panning procedure was repeated on successive days (referred to as rounds), employing the stringency conditions delineated in Table 26 to exert selective pressure on the library to isolate high-affinity clones.

Table 25. Panning conditions for the generation of the SFRP-2-specific chicken scFv library using varying concentrations of SFRP-2 coated on the wells of an ELISA plate. The stringency of each consecutive round of panning was altered by increasing the number of washes with PBST and PBS and decreasing the antigen coating concentration.

Panning round	SFRP-2 antigen coating conc. (µg/mL)	Washing frequency
1	100	3 X PBS, 3 X PBST
2	50	5 X PBS, 5 X PBST
3	25	7 X PBS, 7 X PBST
4	10	10 X PBS,10 X PBST

2.4.15 Library titre estimation for anti-SFRP-2 scFv library

For estimation of input and output titre, infected eluted phage (10µL) was diluted in 1mL of SB medium and plated out (in 10 and 100µL volumes) on SB agar

containing 100µg/mL Carbenicillin. The plates were incubated overnight at 37°C and the total number of transformants calculated. The library size was calculated by counting the number of ampicillin-resistant colonies.

2.4.16 Anti-SFRP-2 polyclonal phage pool ELISA and colony pick PCR

After completion of the panning experiments a polyclonal-phage ELISA was carried out to assess the success of the panning conditions and to identify the round in which enrichment of phage displaying SFRP-2-specific antibodies had occurred. A Nunc Maxisorb™ plate was coated with 100µL per well of 1µg/mL full-length SFRP-2 protein and incubated overnight at 4°C. The excess antigen was discarded and the plate was subsequently blocked with 200µL 5% (w/v) PBSM at 37°C for 1 hour. Phage (from each round of panning), diluted 3 -fold 1% (w/v) PBSM, was added to the plate in triplicate at 100µL per well. Negative (M13 helper phage) controls were also added to the plate in triplicate. The plate was incubated for 2 hours at 37°C and then washed 3 times with PBST and 3 times with PBS. Bound antibodies were detected following the addition of 100µL of a HRP-labelled anti-M13 secondary antibody in PBS containing 1% (w/v) PBSM. The plate was incubated for 1 hour at 37°C, washed 3 times with PBST and 3 times with PBS, and TMB substrate (Sigma) was added (100µL/well). Following incubation for 30 minutes at 37°C, the reaction was stopped by the addition of 10% (v/v) HCl and the absorbance read at 450nm on a Tecan Safire2™ plate-reader.

2.4.17 Screening and ranking of avian scFv clones by monoclonal phage ELISA and Biacore 4000

Three hundred and eighty four avian scFv clones from round 4 of panning were screened by ELISA and through the use of the Biacore 4000 in order to identify anti-SFRP-2-specific scFv antibodies. Biacore evaluation software was used to rank the scFv clones based on stability early and late. Six anti-SFRP-2 scFv clones were brought forward from screening and ranking studies into expression studies.

2.4.18 Monoclonal soluble scFv ELISA for the detection of SFRP-2-specific scFv clones

Once the round corresponding to selective enrichment of the library was identified by the polyclonal-phage ELISA, the phage were infected into mid-exponential *E. coli* TOP10F'. A small amount of phage (1-20µL) was added to a growing culture of *E. coli*

TOP10F' and incubated for 1 hour at 37°C, while shaking at 230rpm. The cells were then diluted serially from 10^{-1} to 10^{-7} in SB medium and plated onto LB-Carbenicillin (50µg/mL) agar plates to isolate single colonies. Individual colonies (384 in total) were picked and grown overnight at 200rpm, 37°C in single wells containing 100µL SB medium with 100µg/mL Carbenicillin (stock plates). The following day the stock plates were then sub-cultured into fresh SB medium (180µL) containing 1 x 505 (0.5% (v/v) glycerol, 0.05% (v/v) glucose final concentration), 1 mM $MgSO_4$ and 100µg/mL Carbenicillin. Glycerol was added to the overnight stock plates to a final concentration of 15% (v/v) and then transferred to the -80°C freezer for long-term storage. The sub-cultured plates were incubated at 37°C, while shaking at 200rpm until cells reached an optical density at 600 nm (OD_{600nm}) of ~0.7. Expression was then induced by addition of IPTG to a final concentration of 1mM and incubating at 30°C (180rpm) overnight. Four Nunc Maxisorb™ plates were coated with 100µL of 1µg/mL SFRP-2 full-length protein and incubated overnight at 4°C. The excess antigen was discarded and the plates were blocked with 200µL per well of PBS containing 5% (w/v) MM for 1 hour at 37°C. Meanwhile, the overnight plates of expressed clones were removed from the 30°C incubator and subjected to a freeze-thaw protocol for the production of scFv-enriched lysate. The plates were placed at -80°C until frozen and then thawed at 37°C (this step was repeated a total of 3 times). The plates were then centrifuged at 4,000 x g for 15 minutes in an Eppendorf 5810r centrifuge, to obtain the scFv-enriched lysate supernatant. The lysate supernatant (100µL) was added to the corresponding well in each ELISA plate, mixed gently and incubated for 1 hour at 37°C. The plates were washed three times with PBST and three times with PBS, followed by the addition of 100µL per well of a HRP-labelled anti-HA antibody, at a 1 in 2,000 dilution in PBST containing 1% (w/v) MM. The plate was incubated for 1 hour at 37°C, washed as previously stated, and 100µL TMB substrate was added per well. Following incubation for 30 minutes at 37°C, the reaction was stopped by the addition of 10% (v/v) HCl and the absorbance read at 450 nm on a Tecan Safire2™ plate-reader.

2.4.19 CM5 series S immobilization conditions

Post hydrodynamic addressing and normalization, the SFRP-2 full-length protein was immobilised onto the surface of the CM5 dextran chip. The CM5 dextran

surface is a three dimensional surface containing carboxyl groups (COOH) attached to the gold surface layer. The chip surface was activated by mixing equal volumes of 400mM EDC (N-ethyl-N-(dimethyl-minopropyl) carbodiimide hydrochloride) and 100mM NHS (N-hydroxysuccinimide) and injecting the mixture over the surface for 7 minutes at a flow rate of 10µL/min. The EDC solution strips a H^+ ion from the carboxyl group resulting in a negatively charged sensor surface. The NHS solution encourages binding of the amine groups in the protein of interest to the COO^--rich (negatively charged) sensor surface. The SFRP-2 full-length protein was injected over the activated surface for 30 minutes at 10µL/min flow rate. Unreactive NHS groups were capped, and deactivated and non-covalently bound proteins removed using 1M ethanolamine hydrochloride, pH 8.5, for 10 minutes at 10µL/min. After capping, the surface was regenerated using 10µL of a 10mM NaOH solution.

2.4.20 High-throughput screening and ranking of scFv clones using Biacore 4000 by immobilizing SFRP-2 on the chip surface

A surface of ~12,000RU was prepared by amine-coupling of SFRP-2 full-length protein as described in section 2.4.19. Three hundred and eighty four clones were involved in the analysis and the clones were expressed and prepared as described in section 2.4.18 followed by dilution in 1X HBS-EP^+ (1 in 5). Data were evaluated using the dedicated Bia-Evaluation software. Data based on stability early and late was generated allowing clones to be ranked based on percentage remaining.

2.4.21 Small-scale expression of top anti-SFRP-2-specific scFv binders identified from monoclonal ELISA and Biacore 4000 screening

Six anti-SFRP-2 scFv clones identified from ELISA and Biacore screening were brought forward into small-scale expression studies. Six overnight cultures were prepared containing 10mL SB, 100µg/mL Carbenecillin, and 1-2µL of a glycerol stock corresponding to the appropriate clones. The overnight cultures were incubated at 37°C, 220rpm. The following morning, 6 x 200mL cultures were inoculated with 20µL of the overnight cultures from each clone. The cultures were incubated at 37°C, 220rpm until an OD_{600nm} of ~0.7 was obtained. One mM IPTG was added to each culture and the samples were incubated at 30°C overnight at 220rpm. The following day the cultures were centrifuged at 12,000 x g, 4°C for 30 minutes. The pellets were stored at -80°C for fifteen

minutes followed by a brief thaw at 37°C for 10 minutes. Each pellet was resuspended in 2mL 1mg/mL lysozyme and stored at RT with gentle agitation for 30 minutes. Two more freeze thaw cycles were completed followed by centrifugation at 12,000 x g at 4°C for 20 minutes. Thirty µL of lysate was taken from each sample and mixed with 4XSDS-PAGE loading dye. The samples were boiled at 95°C for 5 minutes and protein fractions were visualised via SDS and WB as described in sections 8.1.16 and 8.1.17.

2.4.22 Large-scale expression of anti-SFRP-2 scFv clones F3 and C4

A 10mL overnight culture was prepared containing SB, 100µg/mL Carbenecillin, and 1-2µL of a glycerol stock corresponding to the appropriate clones (C4 and F3). Five 200mL cultures were inoculated with 200µL of the overnight culture and incubated at 37°C, 200rpm until an OD_{600nm} of ~0.7 was obtained. The optimum concentration of IPTG was added (previously optimised as described in section 8.1.14) and the culture flasks were incubated at the optimum (previously optimised as described in section 8.1.14) induction temperature overnight at 220rpm. The following day the cultures were centrifuged at 4,000 x g, 4°C for 30 minutes (4 x 250mL bottles) and the antibody was purified by osmotic shock (described in section 2.4.24) and IMAC (8.1.15).

2.2.23 Purification of the expressed anti-SFRP-2 scFv clones using osmotic shock buffers and immobilised metal affinity chromatography (IMAC)

Post centrifugation at 4,000 x g, 4°C for 30 minutes, the supernatant was discarded and the pellets were dried on tissue for 2 minutes. Each pellet was resuspended in 7.5mL OSB-A (30mL in total) and transferred into 2 x 85mL oak-ridge tubes (i.e. 15mL in each bottle). 15 mL of OSB-B buffer was added to each tube. The tubes were then incubated for 10 minutes at room temperature. Shocked cells were collected at 10,000 x g (4°C) for 20 minutes and the supernatant was discarded. The pellets were resuspended in 15mL periplasmic buffer per tube – so should have ~30mL at the end of this. Samples were then placed on ice for 10 minutes and inverted every 2 minutes. The tubes were then centrifuged at 10,000 x g (4°C) for 20 minutes to collect the supernatant. The supernatant was transferred to 1 x 50mL tube (~30mLs). Using a 50mL syringe the protein preparation was sequentially filtered through 0.45µm and 0.2µm filters. One hundred µL of the filtered lysate (FL) was removed for SDS and WB analysis.

Two mL Nickel Resin Slurry (~1mL column) was added to a 20mL column. The settled resin was washed with 30mL equilibration buffer followed by 10mL OSB-A buffer. The resin was then incubated with the filtered lysate for 1 hour at 4°C on the roller. The resin/lysate mix was then applied to the column and the resin allowed to settle. The flow through was collected in a 50mL tube and 10mL of wash A was applied to the column. Wash A was collected in a 50mL tube and 10mL of wash B was applied to the column. One hundred µL of the flow through (FT), wash A (WA) and wash B (WB) were removed for SDS and WB analysis. Four mL of the elution buffer was applied to the column and collected in a 50mL tube. One hundred µL of the eluted protein was removed for SDS and WB analysis. The protein sample was then concentrated as normal following the protocol described in section 8.1.15.

2.4.24 ELISA analysis of purified anti-SFRP-2 scFv clones F3 and C4 to identify antibody working dilution in ELISA

Zero point five µg/mL of SFRP-2 full-length protein was used to coat the required number of wells of an ELISA plate overnight at 4°C. The excess antigen was discarded and the plate was subsequently blocked with 200µL 5% (w/v) PBSM at 37°C for 1 hour. The blocking solution was poured off to waste and 100µL of varying dilutions of the anti-SFRP-2 svFv clones were prepared in 1% (w/v) PBSTM in triplicate and applied to the wells. An anti-SFRP-2 commercial polyclonal antibody (positive control) was prepared in the same manner and applied to the plate in duplicate. An anti-PSMA commercial polyclonal antibody (negative control) was prepared in the same manner and applied to the plate in duplicate. The plate was incubated for 2 hours at 37°C, washed 3 times with PBST and 3 times with PBS. The anti-SFRP-2 scFv antibody was detected following the addition of 100µL of a HRP-labelled anti-HA secondary antibody in PBS containing 1% (w/v) MM. The plate was incubated for 1 hour at 37ºC, washed 3 times with PBST and 3 times with PBS, and TMB substrate (Sigma) was added (100µL/well). Following incubation for 30 minutes at 37ºC, the reaction was stopped by the addition of 10% (v/v) HCl and the absorbance read at 450nm on a Tecan Safire2^{TM} plate-reader.

2.4.25 Western Blotting analysis of anti-SFRP-2 scFv clones F3 and C4

One µg of the SFRP-2 full-length protein was prepared for SDS-PAGE and WB analysis in molecular grade H_2O and 4XSDS-PAGE loading dye. The sample was

boiled at 95°C for 5 minutes to denature the protein and loaded to separate wells in the SDS gel. The gel was resolved at 120V for 60 minutes. The SDS gel was transferred to WB and the blot was blocked for 1 hour at RT. Varying dilutions (1 in 100, 1 in 500, 1 in 1,000, 1 in 2,000, and 1 in 5,000) of the anti-SFRP-2 scFv clones F3 and C4 were prepared in 1% (w/v) PBSTM and used to probe the SFRP-2 western blots. The primary antibodies were incubated with the western blots for 1 hour at RT. The blots were washed 3 times with PBST and 3 times with PBS. A 1 in 2,000 dilution of anti-chicken IgY (IgG)-HRP was used to probe the anti-SFRP-2 scFv antibody clones at RT for 1 hour. The blots were washed 3 times with PBST and 3 times with PBS and developed with the addition of 500 µL of TMB substrate for membranes.

2.4.26 Dot blot analysis of anti-SFRP-2 scFv clones F3 and C4

A dot blot is a technique used to identify the presence of proteins much like a western blot. It represents a simplification of the western blot method. In a dot blot the protein to be detected is not denatured prior to analysis or separated by electrophoresis. Instead, a mixture containing the protein to be detected is applied directly on a membrane as a dot, and then is spotted through circular templates directly onto the membrane or paper substrate. This technique was carried out in order to determine if the anti-SFRP-2 scFv could detect the SFRP-2 protein in its native state (i.e. non-denatured). PVDF membrane was used for this analysis. Due to the hydrophobic nature of the PVDF membrane it was necessary to prime the membrane prior to use. The membrane was submerged in 100% ethanol for 3 minutes, followed by 75% ethanol for 5 minutes. The membrane was then equilibrated in distilled H_2O for 20 minutes and air dried for 10 minutes. The SFRP-2 protein was applied in a dot format to the membrane, diluted in molecular grade water to a final concentration of 2µg/mL, and allowed to soak into the membrane. The dot blots were blocked in 5% (w/v) PBSM for 1 hour at RT followed by washing x 3 PBST and x 3 PBS. Varying dilutions (1 in 100, 1 in 500, 1 in 1,000, 1 in 2,000, and 1 in 5,000) of the anti-SFRP-2 scFv clone were prepared in 1% (w/v) PBSTM and used to probe the SFRP-2 dot blots. The primary antibody was incubated with the blots for 1 hour at RT. The blots were washed 3 times with PBST and 3 times with PBS. A 1 in 2,000 dilution of anti-chicken IgY (IgG)-HRP was used to probe the anti-SFRP-2 scFv at RT for 1 hour. The blot was

washed 3 times with PBST and 3 times with PBS and developed with the addition of 500µL of TMB substrate for membrane.

2.4.27 Reformatting anti-SFRP-2 scFv clone F3 to scAb

In order to attempt to overcome weak expression issues associated with the scFv antibody format, the anti-SFRP-2 scFv clone F3 was reformatted to a scAb. The addition of a constant domain can allow ease of expression and purification and improve protein folding issues which could be interfering with antibody/antigen interaction.

2.4.27.1 Preparation of anti-SFRP-2 scFv clone F3 for reformatting to scAb

An overnight culture of the anti-SFRP-2 scFv clone F3 was prepared in SB and carb (100µg/mL) at 37°C, 220rpm. The culture was centrifuged at 4,000 x g at 4°C. A plasmid prep of this clone was prepared using a NucleoSpin® Plasmid kit according to the manufacturers' guidelines. Using the primers outlined in Table 27 a PCR reaction was set up with the plasmid DNA of clone F3 in order to prime the DNA to allow this insert to be cloned into the pMoPAC vector. MyTaq™ Red Mix was used for this PCR. A large-scale reaction was set up using the components and volumes outlined in Table 28. The PCR was run under the conditions outlined in Table 29.

Table 26. PCR primers for reformatting a scFv to a scAb.

Primer Name	**Sequence 5' – 3'**
Primers for reformatting scFv to scAb	
ChiVL-VHPac-F	GGA AAT CGC GGC GGC CCA GCC GGC CAT GGC GCT GAC TCA G
ChiVL-VHPac-R	TTA CTC GCG GCC CCC GAG GCC GCA CTA GTG GA

Table 27. The components and volumes applied in the amplification of the anti-SFRP-2 scFv F3 plasmid using the primers outlined in Table 27.

Component	Volume (µL)/ concentration (ng)
MyTaq^{TM} ready mix buffer	250
Forward primer: ChiVL-VHPac-F	5
Reverse primer: ChiVL-VHPac-R	5uL
Anti-SFRP-2 scFv F3 plasmid DNA	1000 ng total
Molecular grade H_2O	235uL
Total	500uL

Table 28. Cycling conditions used for the amplification of anti-SFRP-2 scFv clone F3 plasmid using the primers outlined in Table 27.

Step	Temperature (°C)	Time (seconds)	Cycle number
Initial denature	95	60	1 cycle
Denature	95	15 seconds	30 cycles
Anneal	56	15 seconds	
Extend	72	15 seconds	
Extend	72	600	1 cycle
Hold	4	Indefinitely	N/A

Once completed the PCR product was run on a 1.5% agarose gel and the bands were excised for purification using a NucleoSpin® gel and PCR clean up kit.

2.4.27.2 pMoPAC vector preparation for digestion

The pMoPAC vector stock was kindly provided by Dr. Stephen Hearty. An overnight culture (10mL SB supplemented with 100µg/mL Carbenicillin) was prepared using 1-2µL of the pMoPAC vector stock and incubated at 37°C shaking at 220rpm. This overnight culture was then used to inoculate 100mL SB (100µg/mL Carbenicillin) and grown overnight at 37°C shaking at 220rpm. Bacteria were collected by centrifugation at 4,000 x g at 4°C for 30 minutes and the plasmid purified using NucleoBond® Xtra Midi as per the manufacturers' guidelines. Purified plasmid was

resuspended in a final volume of 200µL molecular grade H_2O and quantified using the NanoDrop ND^{TM} 1000 nucleic acid DNA-50 setting.

2.4.27.3 Restriction-digest of anti-SFRP-2 scFv F3 and pMoPAC purified plasmids

Both the purified pMoPAC and anti-SFRP-2 scFv F3 plasmids were S*fi*I digested large-scale (Table 30 and 31).

Table 29. Components and volumes required for restriction digest of anti-SFRP-2 scFv F3 plasmid.

Component	**Concentration/Volume (**µL)/ reaction for restriction digest of anti-SFRP-2 scFv F3 plasmid
Fermentas fast digest buffer	20
Fermentas Fast digest *Sfi*I (36U per µg of DNA)	180 U
Anti-SFRP-2 scFv F3 plasmid	5µg
Molecular grade water	to 200µL

The digest was incubated for 5 hours at 50ºC, followed by a denaturation step at 65ºC for 20 minutes. The digest was then stored as an ethanol precipitation until required.

Table 30. Components and volumes required for the restriction digest of the purified pMoPAC vector plasmid.

Component	**Concentration/Volume (**µL)
Fermentas fast digest buffer	20
Fermentas Fast digest *Sfi*I (36U per µg of DNA	360 U
Purified pMoPAC vector plasmid	10 µg
Molecular grade water	to 200 µL

The pMoPAC vector digest was incubated for 5 hours at 50ºC, followed by a denaturation step at 65ºC. The S*fi*I digested vector sample was then antarctic phosphatase treated (Table 32). Post antarctic phosphatase treatment the vector was stored as an ethanol precipitation until required. All the digested product precipitations were completed, as described in section 8.1.1. The products were purified by resolution on 0.5% (w/v) (pMoPAC) or 2% (w/v) (anti-SFRP-2 F3 clone) agarose gels, the relevant bands excised and extracted using a NucleoSpin® gel extraction kit as per the manufacturers' instructions (eluted in 50 µL molecular grade H_2O).

Table 31. Antarctic phosphatase treatment of S*fi*I digested pMoPAC vector.

Component	Concentration	Temperature (ºC) and time (minutes)
Antarctic Phosphatase buffer (10X)	1X	37 ºC for 30 minutes followed by 65 ºC for 20 minutes
Antarctic Phosphatase [5U/ µL]	1 U/µg	

2.4.27.4 Transformation of *E.coli* TOP10F' chemically competent cells with pMoPAC vector containing the anti-SFRP-2 F3 clone insert

A heat shock transformation was performed as described in section 8.1.13. A 2µL sample was removed from the transformed *E. coli* culture and diluted into 200µL SB followed by plating 10µL and 100µL of this 1 in 100 dilution onto LB-Carbenicillin (50µg/mL) agar plates.

2.4.27.5 'Colony-pick' PCR to identify the pMoPAC clones harboring the anti-SFRP-2 F3 clone insert

Ten single colonies were randomly picked from the titre plates from the pMoPAC/anti-SFRP-2 F3 transformation and incorporated into a 'colony-pick' PCR to ensure the vector was harboring the scFv fragment insert. A sterile tip was used to pick a single colony into the mixture outlined in Table 33, which was then placed in a Biometra $T_{gradient}$ PCR machine. The conditions used for this PCR reaction are outlined in Table 34. The amplified scFv fragments were subsequently analysed via gel electrophoresis on a 1% (w/v) agarose gel. Glycerol stocks were

prepared for the positive clones identified from the colony pick PCR. One positive clone was brought forward for expression studies.

Table 32. Components and volumes required for 'colony-pick' PCR analysis of scAb clones.

Component	Concentration per 50 µL reaction
MyTaq™ Red Mix	25 µL
H_2O	to 50 µL
Colony picked	variable
ChiVL-VHPac-F	0.5 µL
ChiVL-VHPac-R	0.5 µL
Total	50 µL

Table 33. Cycling conditions used for 'colony-pick' PCR.

Stage	Step	Temperature (°C)	Time (s)	No. of cycles
1	Initial denature	94	120	1
2	Denature	94	15	30
	Annealing	55	30	
	Extension	68	60	
3	Final extension	68	600	1

2.4.27.6 Small-scale expression optimisation of anti-SFRP-2 scAb F3

An overnight culture was prepared containing 10mL SB, 100µg/mL Carbenecillin, and 1-2µL of a glycerol stock of the anti-SFRP-2 scAb F3. The overnight culture was incubated at 37°C, 220rpm. The following morning a 4 x 10mL cultures were inoculated with 20µL of the overnight cultures. The culture was incubated at 37°C, 220rpm until an OD_{600nm} of ~0.7 was obtained. Varying dilutions of IPTG (0.25mM, 0.5mM, 0.8mM, 1mM) were added to the four different tubes and the temperature was turned down to 30°C. After 2 hours a 1mL sample was taken from each tube and centrifuged at 12,000 x g 4°C. The supernatant was removed and the pellet was frozen at -80°C until required. After 4 hours and after overnight incubation a 1mL sample was taken and treated in the same manner as described above

resulting in 12 samples, each representing a different IPTG concentration and induction time. The 12 pellets were thawed at 37°C and resuspended in 100µL of 1mg/mL lysozyme prepared in PBS. The samples were incubated at RT for 30 minutes with gentle agitation. Two additional freeze-thaw steps were carried out followed by a brief centrifugation at 12,000 x g, 4°C. Thirty µL of lysate from each sample was removed and mixed with 4XSDS-PAGE loading dye and boiled for 5 minutes at 95°C. The protein fractions were subsequently analysed by SDS and WB in order to determine the optimum induction time and IPTG concentration for the expression of the anti-SFRP-2 scAb clone F3.

2.4.27.7 Large-scale expression of anti-SFRP-2 scAb clone F3

Once the optimum conditions for expression were determined, the anti-SFRP-2 scAb F3 was expressed large-scale (1 L) and purified through osmotic shock as described in section 2.4.24. The antibody was concentrated as described in section 8.1.15 and the protein fractions were analysed by SDS-PAGE and WB (described in section 8.1.16 and 8.8.17).

2.4.27.8 ELISA analysis of anti-SFRP-2 scAb clone F3

Zero point five µg/mL of SFRP-2 full-length protein was used to coat the required number of wells of an ELISA plate overnight at 4°C. The excess antigen was discarded and the plate was subsequently blocked with 200µL 5% (w/v) PBSM at 37°C for 1 hour. The blocking solution was poured off to waste and 100 µL of varying dilution (1 in 10, 1 in 50, 1 in 100, 1 in 500, 1 in 1,000) of the anti-SFRP-2 scAb clone F3 was prepared in 1% (w/v) PBSTM in triplicate and applied to the wells. An anti-SFRP-2 commercial polyclonal antibody (positive control) was prepared in the same manner and applied to the plate in duplicate. An anti-PSMA commercial polyclonal antibody (negative control) was prepared in the same manner and applied to the plate in duplicate. The plate was incubated for 2 hours at 37°C, washed 3 times with PBST and 3 times with PBS. The anti-SFRP-2 scAb antibody was detected following the addition of 100µL of a HRP-labelled anti-HIS secondary antibody in PBS containing 1% (w/v) MM. The plate was incubated for 1 hour at 37ºC, washed 3 times with PBST and 3 times with PBS, and TMB substrate (Sigma) was added (100µL/well). Following incubation for 30 minutes at 37ºC, the reaction was stopped by the addition of 10% (v/v) HCl and the absorbance read at 450nm on a Tecan Safire2^{TM} plate-reader.

2.4.27.9 Western blotting analysis of anti-SFRP-2 scAb F3

One µg of the SFRP-2 full-length protein was prepared for SDS-PAGE and WB analysis in molecular grade H_2O and 4XSDS-PAGE loading dye. The sample was boiled at 95°C for 5 minutes to denature the protein and loaded to separate wells in the SDS gel. The gel was resolved at 120V for 60 minutes. The SDS gel was transferred to WB and the blot was blocked for 1 hour at RT. Varying dilutions (1 in 100, 1 in 500, 1 in 1,000, 1 in 2,000, and 1 in 5,000) of the anti-SFRP-2 scAb were prepared in 1% (w/v) PBSTM and used to probe the SFRP-2 western blots. The primary antibody was incubated for 1 hour at RT. The blot was washed 3 times with PBST and 3 times with PBS. A 1 in 2,000 dilution of anti-chicken IgY (IgG)-HRP was used to probe the anti-SFRP-2 scAb at RT for 1 hour. The blot was washed 3 times with PBST and 3 times with PBS and developed with the addition of 500 µL of TMB substrate for membranes.

2.4.27.10 Dot blot analysis of anti-SFRP-2 scAb

This technique was carried out in order to determine if the anti-SFRP-2 scAb could detect the SFRP-2 protein in its native state (i.e. non-denatured). The PVDF membrane was primed and equilibrated as described in section 2.4.27. The SFRP-2 protein was applied in a dot format to the membrane, diluted in molecular grade water to a final concentration of 2µg/mL, and allowed to soak into the membrane. The dot blots were blocked in 5% (w/v) PBSM for 1 hour at RT followed by washing x 3 PBST and x 3 PBS. Varying dilutions (1 in 100, 1 in 500, 1 in 1,000, 1 in 2,000, and 1 in 5,000) of the anti-SFRP-2 scAb were prepared in 1% (w/v) PBSTM and used to probe the SFRP-2 dot blots. The primary antibody was incubated with the blots for 1 hour at RT. The blots were washed 3 times with PBST and 3 times with PBS. A 1 in 2,000 dilution of anti-chicken IgY (IgG)-HRP was used to probe the anti-SFRP-2 scAb at RT for 1 hour. The blot was washed 3 times with PBST and 3 times with PBS and developed with the addition of 500 µL of TMB substrate for membranes.

2.4.28 Fluorescent microscopy analysis of the anti-SFRP-2 scAb F3 and scFv F3

Normal prostate tissue, benign prostatic hyperplasia prostate tissue, and malignant prostate tissue were ordered in from Abcam for fluorescent microscopy analysis. The

primary antibodies used to probe the tissue on each slide were the anti-SFRP-2 scFv F3 and anti-SFRP-2 scAb F3.

2.4.28.1 Deparaffinization of prostate tissue slides

On arrival the tissue was impregnated with wax in order to protect the prostate tissue prior to analysis. It was necessary to remove this wax to proceed with the analysis. The materials and reagents required for this step and incubation times are outlined in the Table 35. The slides were immersed in the solutions outlined in Table 35 for the appropriate time followed by submersion in water until ready to move on to the antigen retrieval step. At no time from this point onwards were the slides allowed to dry. Drying out could cause non-specific antibody binding and therefore high background staining.

Table 34. Reagents and incubation times required for deparaffinization of prostate tissue slides.

Reagent	Incubation time (minutes)
Xylene	2 x 3 minutes
Xylene 1:1 with 100% ethanol	1 x 3 minutes
100% Ethanol	2 x 3 minutes
95% Ethanol	3 minutes
70% Ethanol	3 minutes
50% Ethanol	3 minutes
H_2O	Running cold tap water to rinse
Distilled H_2O (dH_2O)	Constant

2.4.28.2 Antigen retrieval from formalin-fixed tissue

Most formalin-fixed tissue requires an antigen retrieval step before immunohistochemical staining can proceed. This is due to the formation of methylene bridges during fixation, which cross-link proteins and therefore mask antigenic sites. The two methods of antigen retrieval are heat-mediated (also known as heat-induced epitope retrieval, or HIER) and enzymatic. Both antigen retrieval methods serve to break the methylene bridges and expose the antigenic sites in order to allow the

antibodies to bind. Some antigens prefer enzymatic to heat mediated antigen retrieval and vice versa. Enzymatic retrieval can sometimes damage the morphology of the section, so the concentration and treatment time need to be tested. Antigen retrieval with Tris/EDTA pH 9.0 buffer is suitable for most antigens. Sodium citrate pH 6.0 is also widely used. Heat-induced epitope retrieval is most often performed using a pressure cooker, a microwave, or a vegetable steamer. Additionally, some labs will use a water bath set to 98°C and incubate the slides in retrieval solution for 20 minutes.

2.4.28.2.1 Antigen retrieval using Tris/EDTA buffer (pH 9.0) and a water bath heated to 98°C

Post deparaffinization, slides were immersed in antigen retrieval buffer and incubated at 98°C for twenty minutes in a water bath. After 20 minutes, the slides were stored in tap water until ready to block.

Table 35. Components and volumes required to prepare the antigen retrieval buffer for prostate tissue slides.

Component	Weight (g)/ Volume (mL)	pH
Tris	1.21g	pH buffer to 9.0
EDTA	0.37g	
H_2O	to 1000 mL	
Tween 20	0.5 mL	

2.4.28.3 Blocking the prostate tissue slides and preparation for probing with anti-SFRP-2 scFv and scAb antibodies

All incubations for this step were carried out in a humidified chamber to avoid drying of the tissue. Drying at any stage leads to non-specific binding and ultimately high background staining. A shallow, plastic box with a sealed lid and wet tissue paper in the bottom was the chamber used for this protocol. The slides were transferred from water into blocking solution. Slides were blocked in 10% (w/v) normal serum (dependent on the species used to raise the secondary antibody) with 1% (w/v) BSA in PBS for 2 hours at room temperature. After 2 hours the slides were drained and tissue was used to wipe away residual blocking solution.

2.4.28.4 Probing prostate tissue with primary and secondary antibody

To pre-blocked tissue an appropriate dilution of primary antibody, diluted in PBS with 1% (w/v) BSA, was applied and incubated with the tissue O/N at 4°C. If the concentration of the antibody is not provided, it is recommended to try 0.5µg/ml and 5µg/ml overnight at 4°C. If the antibody is unpurified, it is recommended to start with the dilutions outlined in Table 37, and also testing a 20-fold higher dilution.

Table 36. Recommended dilutions for unpurified/purified recombinant antibody.

Primary antibody	Dilution
Whole anti-serum	1: 50 – 1:100
Tissue culture supernatant	Neat
Bacterial lysate	Neat or optimised dilution
Purified recombinant antibody	Variable dependent on prior optimisation in WB and dot blot analysis

The following day the tissue slides were washed 2 x 5 minutes with PBS 0.025% TritonX100 with gentle agitation. The fluorophore-conjugated secondary antibodies (anti-HIS-Alexofluor488 for scFv and scAb and anti-rabbit Alexofluor488 for positive controls) were diluted to the concentration recommended by the manufacturer in TBS with 1% (w/v) BSA and applied to the slides. The tissue was incubated for 1 hour at room temperature with the secondary antibodies. This step is completed in the dark in order to avoid photo bleaching. The slides were washed 3 x 5 minutes with PBS. All slides were analysed using a fluorescent microscope.

2.5 Generation of a chicken anti-PSMA scFv library

The following section describes the methods applied for the generation of a recombinant anti-PSMA scFv and scAb and the characterisation of these antibodies.

2.5.1 Immunisation schedule of a white leghorn chicken with two prostate cancer cell lines LNCaP and 22RV1

A female leghorn chicken was initially immunised sub-cutaneously with a mixture of equal parts of 22RV1 and LNCaP prostate cancer cell lines and Freund's complete

adjuvant. The number of cells used for this immunisation was 4 x 10^7, which was split equally between each cell line. The first boost (day 28) was then administered as before, mixed in a 1:1 ratio with Freund's incomplete adjuvant, in a final volume of 1.5mL. The 3 boosts that followed (days 56, 84 and 112) all contained the same concentration of cells and were administered in the same manner as the first boost.

2.5.2 Chicken anti-serum titre analysis of immune response to PSMA

Nunc Maxisorb™ immunoplates were coated with 100µL per well of a commercial PSMA antigen (Antibodies-online GmBh) in PBS at a concentration of 1µg/mL and incubated overnight at 4°C. The plate was then blocked with PBS containing 5 % (w/v) Milk Marvel for 1 hour at 37°C. The plate was washed three times with PBST and three times with PBS. Doubling dilutions of serum were prepared in 1% (w/v) PBSTM. The prepared dilutions were applied in duplicate (100µL) across the PSMA coated wells. The plate was incubated and washed as described in the previous step and 100µL of a 1 in 2,000 dilution of an anti-chicken-HRP-labeled antibody (Sigma) in PBST containing 1 % (w/v) Milk Marvel was applied to each well. The plate was incubated for 1 hour at 37°C, washed as before, and TMB substrate was added (100µL/well). Following incubation for 10-15 minutes at room temperature (RT), the reaction was stopped by the addition of 10% (v/v) HCl and the absorbance read at 450nm on a Tecan Safire2™ plate-reader.

2.5.3 Extraction and isolation of total RNA from chicken spleen and bone-marrow

Once a sufficient immune response was obtained isolation of total RNA from chicken spleen and bone marrow was carried out as previously described in section 2.4.3.

2.5.4 RNA Quantification/Storage

The RNA was quantified using a NanoDrop spectrophotometer. Undiluted samples were prepared with molecular grade water with concentrations ranging from 1:50 to 1:400. Three readings were obtained in order to ensure accuracy and consistency between dilutions. Typical yields obtained from chicken spleen are between 5-10µg/µL RNA and for chicken bone marrow are between 1-4µg/µL RNA. The $A_{260:280}$ ratio should be in the range of 1.6 – 1.9 for acceptable quality of RNA to proceed

with cDNA synthesis. Remaining RNA that is not needed for cDNA synthesis can be ethanol precipitated by adding the components outlined in Table 38.

Table 37. Components required for ethanol precipitation of RNA.

Component	Volume
RNase Free NaOAC pH 5.2	0.1X Vol.
Ice cold 100% EtOH	2 X Vol.
Glycogen	1µL

2.5.5 Reverse transcription of total RNA to cDNA

A PCR is performed to convert total RNA to cDNA by reverse transcription. This reaction was carried out using a Superscript^{TM} III first strand cDNA synthesis kit, which is obtained from Invitrogen. The cDNA serves as a template for the amplification of the variable light and variable heavy chain gene fragments.

2.5.5.1 cDNA Synthesis

Total RNA was transcribed to cDNA by reverse transcriptase PCR. The cDNA served as a template for the amplification of the variable heavy and variable light chain gene fragments. cDNA synthesis was carried out as previously described in section 2.4.5.1.

2.5.6 Anti-PSMA scFv library construction

Antibody construction was carried out as described by Andris-Winhopf and co-workers (Andris-Winhopf *et al.*, 2000). The initial steps involved in generating the library require the amplification of the antibody variable domains for the synthesised cDNA isolated from both the spleen (SP) and the bone marrow (BM) of the chicken immunised with the prostate cancer cell lines (22RV1 and LNCaP). The primers used for library building are those published in Chapter 9 of Phage Display: a laboratory manual and host specific sub chapters. All primers used were those to clone antibody fragments into the pComb3x vector series. The list of primers used to construct avian scFv fragments from immune libraries by introducing the long linker (GGSSSSSSSGGGGSGGGG) between the variable heavy and light chain is shown in

Table 18 in section 2.4.6. All primers were commercially synthesised by Integrated DNA Technologies (Interleuvenlaan 12A B-3001 Leuven, Belgium).

2.5.7 Anti-PSMA variable domain amplification

The first round of PCR involved separate amplification of variable heavy and light chains. Initially, the $MgCl_2$ concentration for the reaction was optimised to ensure high-yield specific-bands by titration in the concentration range (from 1.5mM to 4mM) followed by large-scale synthesis at the optimised 3.0mM $MgCl_2$ for variable heavy (V_H) (spleen), 4.0mM $MgCl_2$ for variable light (V_L) (spleen), 1.5mM $MgCl_2$ for variable heavy (V_H) (bone marrow) and 3.0mM $MgCl_2$ for variable light (V_L) (bone marrow). GoTaq® Flexi Buffer was used for this PCR optimisation. The PCRs were carried out using the cycling parameters displayed in Table 19 in section 2.4.7.

Large-scale variable PCR products were resolved on 1.5% agarose gels and purified through gel extraction as described in section 8.1.3. Purified products were quantified using the NanoDrop ND 1000^{TM} using DNA-50 setting. Note: All PCR products were eluted from the column in 15µL of preheated (~70°C) molecular grade water.

2.5.8 Splice-by-overlap extension (SOE) PCR

The second round of PCR joined together the variable domains into a single scFv construct in the V_L-V_H orientation. The overlap of V_L-V_H is possible due to the overlapping 'tails' in the light chain reverse (CKJo-B) and heavy chain forward primers (CSCVHo-FL). This was carried out using the overlap primer pair (CSC-F and CSC-B) to complete the construct and introduce upstream and downstream Sfi*I* sites for easy transition into the PComb3x vector series. In addition 'clamp' sequences $(GAG)_6$ on these primers promote efficient digestion of the PCR products. MyTaq™ Red Mix was employed at this stage of library construction. Table 20 in section 2.4.8 details the components used for the large-scale SOE amplification reaction used for both spleen and bone marrow. Both SOE PCR reactions were carried out under the cycling parameters outlined in Table 21 in section 2.4.8. SOE-PCR products were purified through gel extraction as described in section 8.1.3. The purified products were eluted in 50µL of preheated (~70°C) molecular grade water and stored at – 20°C until ready to proceed to restriction digest.

2.5.9 pComb3xSS vector preparation for digestion

The pComb3xSS vector stock was kindly provided by Dr. Paul Conroy and prepared for restriction digest as previously described in section 2.4.9.

2.5.10 Restriction-digest of the purified overlap PCR product and vector DNA

Both the purified pComb3XSS and SOE-PCR products from the BM and SP were digested in large-scale for ligation of both libraries into the pComb3xSS vector following the protocol described in section 2.4.10.

2.5.11 Ligation of the digested overlap PCR product with pComb3xSS vector DNA

The purified S*fi*I digested scFv inserts were then ligated into the prepared pComb3x vector using T4 ligase (NEB) under the reaction conditions outlined in Table 25 in section 2.4.11. The reaction was carried out overnight at room temperature. The ligations were then deactivated at 65ºC for 20 minutes and ethanol precipitated overnight at -20ºC as described in section 8.1.1. The ligation pellet was resuspended in 20µL of molecular grade water and transformed into *E. coli* XL1-Blue electrocompetent cells (Stratagene) by electroporation as described in section 2.4.12.

2.5.12 Rescue and subsequent precipitation of scFv-displaying phage

See section 2.4.13 for detailed protocol.

2.5.13 Enrichment of phage library via panning against immobilised antigens

To a previously coated (100µL x 8 wells of commercial full-length PSMA protein at 4°C O/N) and blocked (5% (w/v) PBSM, 2 hour at 37 °C) ELISA plate, 100µL of the rescued phage was added to each coated and blocked well and incubated with the antigen for 2 hours at 37°C. Non-specific phage were removed with sequential PBST (200µL/well x 5) and PBS (200µL/well x 5) washes. Anti-PSMA-specific bound phage were eluted by incubation with 100µL/well of 10mg/mL trypsin in PBS at 37°C for 30 minutes. The eluted phage (~800µL) was then used to infect 5mL of mid-exponential ($O.D_{600nm}$ ~0.4) *E. coli* XL-1 blue cells for 15 minutes, static at RT. Pre-warmed SB medium (6mL) containing 1.6µL of Carbenicillin (100mg/mL) was added to the infected cells. A 2µL sample was removed and diluted in 200µL SB for output titre determination by plating 10µL and 100µL of this onto LB-Carbenicillin (50µg/mL) agar plates. The 8mL output library was placed at 37°C

shaking at 230rpm for 1 hour followed by the addition of 2.4µL of Carbenicillin (100mg/mL) and incubation at 37°C shaking at 230rpm for 1 hour. Helper-phage (1mL of VCSM13: 1.0 x 10^{13} cfu/mL) was added and the culture transferred to a 250mL baffled flask containing 92mL SB with 46µL of Carbenecillin (100mg/mL) plus 184µL of Tetracycline (5mg/mL) and incubated at 37°C with shaking at 230rpm for 2 hours. In the final step 140µL of Kanamycin (70mg/mL) was added and the culture incubated as above overnight. An input titre was performed during these incubation steps by the addition of 10µL of the rescued phage to 90µL of SB medium and 10-fold serially diluting to 10^{-9}. A 2µL sample of the 10^{-7}, 10^{-8} and 10^{-9} dilutions were infected into mid-exponential phase *E. coli* XL-1 blue (100µL) and plated (50µL) onto LB-Carbenicillin plates (50 µg/mL) after static incubation at RT for 15 minutes. This panning procedure was repeated on successive days (referred to as rounds), employing the stringency conditions delineated in Table 39 to exert selective pressure on the library to isolate high-affinity clones.

Table 38. Panning conditions for the generation of the PSMA-specific chicken scFv library using varying concentrations of PSMA coated on the wells of an ELISA plate. The stringency of each consecutive round of panning was altered by increasing the number of washes and decreasing the antigen coating concentration.

Panning round	PSMA antigen coating conc. (µg/mL)	Washing frequency
1	100	3 X PBS, 3 X PBST
2	50	5 X PBS, 5 X PBST
3	25	7 X PBS, 7 X PBST
4	10	10 X PBS,10 X PBST

2.5.14 Library titre estimation for anti-PSMA scFv library

Library titre estimation for the anti-PSMA scFv library was carried out as described in section 2.4.15.

2.5.15 Anti-PSMA polyclonal phage pool ELISA and colony pick PCR

After completion of the panning experiments, a polyclonal-phage ELISA was carried out to assess the success of the panning conditions and to identify the round in which

enrichment of phage displaying PSMA-specific antibodies had occurred. A Nunc Maxisorb™ plate was coated with 100µL per well of 1µg/mL full-length PSMA protein and incubated overnight at 4°C. The excess antigen was discarded and the plate was subsequently blocked with 200µL 5% (w/v) PBSM at 37°C for 1 hour. Phage (from each round of panning), diluted 3-fold 1% (w/v) PBSM, was added to the plate in triplicate at 100µL per well. Negative (M13 helper phage) controls were also added to the plate in triplicate. The plate was incubated for 2 hours at 37°C and then washed 3 times with PBST and 3 times with PBS. Bound antibodies were detected following the addition of 100µL of a HRP-labelled anti-M13 secondary antibody in PBS containing 1% (w/v) PBSM. The plate was incubated for 1 hour at 37°C, washed 3 times with PBST and 3 times with PBS, and TMB substrate (Sigma) was added (100µL/well). Following incubation for 30 minutes at 37°C, the reaction was stopped by the addition of 10% (v/v) HCl and the absorbance read at 450nm on a Tecan Safire2™ plate reader.

2.5.16 Screening and ranking of avian anti-PSMA scFv clones by monoclonal phage ELISA and Biacore 4000

Three hundred and eighty four anti-PSMA avian scFv clones from round 3 and 4 of panning were screened by ELISA and through the use of the Biacore 4000 in order to identify anti-PSMA-specific scFv antibodies. Biacore evaluation software was used to rank the scFv clones based on stability early and late.

2.5.17 Monoclonal soluble scFv ELISA for the detection of PSMA-specific scFv clones

Once the round corresponding to selective enrichment of the library was identified by the polyclonal-phage ELISA, the phage were infected into mid-exponential *E. coli* TOP10F'. A small amount of phage (1-20µL) was added to a growing culture of *E. coli* TOP10F' and incubated for 1 hour at 37°C, while shaking at 230rpm. The cells were then diluted serially from 10^{-1} to 10^{-7} in SB medium and plated onto LB-Carbenicillin (50mg/mL) agar plates to isolate single colonies. Individual colonies (384 in total) were picked and grown overnight at 200 rpm and 37°C in single wells containing 100µL SB medium with 100µg/mL Carbenicillin (stock plates). The stock plates were then sub-cultured into fresh SB medium (180µL) containing 1 x 505 (0.5% (v/v) glycerol, 0.05% (v/v) glucose final concentration), 1 mM $MgSO_4$ and

100µg/mL Carbenicillin. Glycerol was added to the overnight stock plates to a final concentration of 15% (v/v) and then transferred to the -80°C freezer for long-term storage. The sub-cultured plates were incubated at 37°C, while shaking at 200rpm until cells reached an optical density at 600nm (OD_{600nm}) of ~0.7. Expression was then induced by addition of IPTG to a final concentration of 1mM and incubating at 30°C (180 rpm) overnight. Four Nunc Maxisorb™ plates were coated with 100µL of 1µg/mL PSMA full-length protein and incubated overnight at 4°C. The excess antigen was discarded and the plates were blocked with 200µL per well of PBS containing 5% (w/v) MM for 1 hour at 37°C. Meanwhile, the overnight plates of expressed clones were removed from the 30°C incubator and subjected to a freeze-thaw protocol for the production of scFv-enriched lysate. The plates were placed at -80°C until frozen and then thawed at 37°C (this step was repeated a total of 3 times). The plates were then centrifuged at 4,000 x g for 15 minutes in an Eppendorf 5810r centrifuge, to obtain the scFv-enriched lysate supernatant. The lysate supernatant (100µL) was added to the corresponding well in each ELISA plate, mixed gently and incubated for 1 hour at 37°C. The plates were washed three times with PBST and three times with PBS, followed by the addition of 100µL per well of HRP-labelled anti-HA antibody, at a 1 in 2,000 dilution in PBST containing 1% (w/v) MM. The plate was incubated for 1 hour at 37°C, washed as previously stated, and 100µL TMB substrate was added per well. Following incubation for 30 minutes at 37°C, the reaction was stopped by the addition of 10% (v/v) HCl and the absorbance read at 450 nm on a Tecan Safire2™ plate reader.

2.5.18 CM5 series S immobilization conditions for PSMA screening

Post hydrodynamic addressing and normalization, the commercial PSMA full-length protein was immobilised onto the surface of the CM5 dextran chip. The chip surface was activated by mixing equal volumes of 400mM EDC and 100mM NHS and injecting the mixture over the surface for 7 minutes at a flow rate of 10µL/min. The PSMA full-length protein was injected over the activated surface for 30 minutes at 10µL/min flow rate. Unreactive NHS groups were capped, and deactivated and non-covalently bound proteins removed using 1M ethanolamine hydrochloride, pH 8.5, for 10 minutes at 10µL/min. After capping, the surface was regenerated using of 20mM NaOH solution.

2.5.19 High-throughput screening and ranking of scFv clones using Biacore 4000 by immobilizing PSMA on the chip surface

A surface of ~7,000 response units (RU) was prepared by amine-coupling of the full-length PSMA protein as described in section 2.5.18. Three hundred and eighty four clones were involved in the analysis and the clones were expressed and prepared as described in section 2.4.17 followed by dilution in 1XHBS-EP+ (1 in 5). Bia-Evaluation software was used to analyse the data. Data based on stability early and late was generated allowing clones to be ranked based on percentage remaining.

2.5.20 Small-scale expression of top anti-PSMA-specific scFv binders identified from monoclonal ELISA and Biacore 4000 screening

Small-scale expression of the top anti-PSMA scFv clones was carried out as described in section 2.4.22.

2.5.21 Large-scale expression of anti-PSMA scFv clones B8

Large-scale expression of anti-PSMA scFv clones B8 was carried our as previously described in section 2.4.27.7.

2.5.22 Purification of the expressed anti-PSMA scFv clones using osmotic shock buffers and immobilised metal affinity chromatography (IMAC)

The expressed anti-PSMA scFv clones were purified by osmotic shock as described in section 2.4.24.

2.5.23 ELISA analysis of purified anti-PSMA scFv clones B8 to identify antibody working dilution in ELISA

See section 2.4.25.

2.5.24 Western Blotting analysis of anti-PSMA scFv clones B8 and D6

See section 2.4.26.

2.5.25 Dot blot analysis of anti-PSMA scFv clones B8

A dot blot analysis of the anti-PSMA scFv clones was carried out as described in section 2.4.27.

2.5.26 Reformatting anti-PSMA scFv clone B8 to scAb

In order to attempt to overcome weak expression issues associated with the scFv, the anti-PSMA scFv clone B8 was reformated to a scAb, expressed and purified following the protocol described in section 2.4.27.1 – 2.4.27.7.

2.5.27 ELISA analysis of anti-PSMA scAb clone B8

Zero point five µg/mL (100µL) of PSMA full-length protein was used to coat the required number of wells of an ELISA plate overnight at 4°C. The excess antigen was discarded and the plate was subsequently blocked with 200 µL 5% (w/v) PBSM at 37°C for 1 hour. The blocking solution was poured off to waste and 100µL of varying dilution (1 in 10, 1 in 50, 1 in 100, 1 in 500, 1 in 1000) of the anti-PSMA scAb clone B8 was prepared in 1% (w/v) PBSTM in triplicate and applied to the wells. An anti-PSMA commercial polyclonal antibody positive control was prepared in the same manner and applied to the plate in duplicate. A anti-SFRP-2 commercial polyclonal antibody (negative control) was prepared in the same manner and applied to the plate in duplicate. The plate was incubated for 2 hours at 37°C, washed 3 times with PBST and 3 times with PBS. The anti-PSMA scAb antibody was detected following the addition of 100µL of a HRP-labelled anti-His secondary antibody in PBS containing 1% (w/v) MM. The plate was incubated for 1 hour at 37ºC, washed 3 times with PBST and 3 times with PBS, and TMB substrate (Sigma) was added (100µL/well). Following incubation for 30 minutes at 37ºC, the reaction was stopped by the addition of 10% (v/v) HCl and the absorbance read at 450nm on a Tecan Safire2^{TM} plate-reader.

2.5.28 Western blotting analysis of anti-PSMA scAb B8

One µg of the PSMA full-length protein was prepared for SDS-PAGE and WB analysis in molecular grade H_2O and 4XSDS-PAGE loading dye. The sample was boiled at 95°C for 5 minutes to denature the protein and loaded to separate wells in the SDS gel. The gel was resolved at 120V for 60 minutes. The SDS gel was transferred to WB and the blot was blocked for 1 hour at RT. Varying dilutions (1 in 100, 1 in 500, 1 in 1000, 1 in 2000, and 1 in 5000) of the anti-PSMA scAb were prepared in 1% (w/v) PBSTM and used to probe the PSMA western blots. The primary antibody was incubated for 1 hour at RT. The blot was washed 3 times with PBST and 3 times with PBS. A 1 in 2000 dilution of anti-chicken IgY (IgG)-HRP was used to probe the anti-PSMA scAb at RT for 1 hour. The blot was washed 3 times

with PBST and 3 times with PBS and developed with the addition of 500µL of TMB substrate for membranes.

2.5.29 Dot blot analysis of anti-PSMA scAb

This technique was carried out in order to determine if the anti-PSMA scAb could detect the PSMA protein in its native state (i.e. non-denatured). This experiment was carried out as previously described in section 2.4.28.10.

2.5.30 Fluorescent microscopy analysis of the anti-PSMA scAb B8

Normal prostate tissue, benign prostatic hyperplasia prostate tissue, and malignant prostate tissue were ordered in from Abcam for fluorescent microscopy analysis. The anti-PSMA scAb B8 was used as the primary antibody to probe varying types of prostate tissue as described previously in section 2.4.29.1 – 2.4.29.4.

2.6 Development of a bispecific antibody generation strategy

In addition to the development of a novel expression system (section 2.3) and the generation of two prostate cancer-specific antibodies (section 2.4/2.5) this project explored the concept of bispecific antibody generation through a novel approach. Bispecific antibodies (bsAb) are antibody-derived proteins with the ability to bind to two different epitopes on the same or different antigens. The following section presents the methodology involved in the 'proof-of-concept' experiments for this novel bispecific antibody generation strategy. In future projects this strategy could be applied for the generation of a bispecific anti-prostate cancer-specific antibody, which could then be applied in a diagnostic setting. The ability of bispecific antibodies to simultaneously bind to a specific antigen and a given detection moiety enables them to function as excellent bifunctional immunoprobe in diagnostic assays. This approach to bispecific antibody generation could be applied to any antibody once the primer design is altered to suit the antibody of interest. Anti-cTnI and anti-MPO antibodies were applied in the 'proof-of-concept' studies as both of these antibodies were readily avaible in the lab and showed high specificity to their target antigen.

2.6.1 Primer list for bispecific antibody strategy

All primers were commercially synthesised by Integrated DNA Technologies (Interleuvenlaan 12A B-3001 Leuven, Belgium). The primers applied in the 'proof-of-concept' studies to generate the anti-cTnI x anti-MPO bispecific antibody are outlined in Table 40.

Table 39. Bispecific antibody construction primer list.

Name	Sequence 5' – 3'
Anti-cTnI scFv generation (~ 800bp)	
Bi_C_(VL-VH)-F	ACG GCA GCC GCT GCA TTG TTA TTA CTC GCT GCC CAA CCA GCC ATG GGA TCC CTG ACT CAG CCG TCC TCG G
C_FAB_VH-R	GG CGA TGT GGG GCT CGC GGA GGA GAC GAT GAC TTC GGT CC
Anti-cTnI constant heavy region (C_H) amplification (~ 400bp)	
C_FAB_CH-F	C GCG AGC CCC ACA TCG CCC CCC CG
HUC2-CH1-R-1	CTG GCC GGC CTG GCC ACT AGT GAC CTG CAC CTC TGG GGC TAC AGG
Anti-cTnI scAb amplification – PCR to overlap the anti-cTnI scFv with the anti-cTnI constant heavy region (~ 1200bp)	
Bi_C_(VL-VH)-F	ACG GCA GCC GCT GCA TTG TTA TTA CTC GCT GCC CAA CCA GCC ATG GGA TCC CTG ACT CAG CCG TCC TCG G
HUC2-CH1-R-1	CTG GCC GGC CTG GCC ACT AGT GAC CTG CAC CTC TGG GGC TAC AGG
Anti-MPO variable heavy (V_H) region amplification (~400bp)	
Bi_C_(VH-VL)_VH-F	GTG GCC CAG GCG GCC GAG CTC TCC GCC GTG ACG TTG GAC GAG
C_(VH-VL)_VH-R	GGAAGATCTAGAGGAACCACCGGAGGAGACGATGACTTCGGTCC
Anti-MPO variable light (V_L) region amplification (~350bp)	
C_(VH-VL)_VK-F	GGT GGT TCC TCT AGA TCT TCC GGC GGT GGT GGC AGC TCC GGT GGT GGC GGT CTG ACT CAG CCG TCC TCG GTG TC
C_FAB_VK-R	TCT AGA TCT TCC GGC GGT GGT GGC AGC TCC GGT GGT GGC GGT CTG ACT CAG
Anti-MPO scFv amplification – PCR overlap of V_H and V_L region (~ 800bp)	
Bi_C_(VH-VL)_VH-F	GTG GCC CAG GCG GCC GAG CTC TCC GCC GTG ACG TTG GAC GAG
C_FAB_VK	GGG GGC CAC CTT GGG CTG TAG GAC GGT CAG G

-R	
Anti-MPO constant light region (C_L) amplification (~ 350-400bp)	
C_FAB_CL-F	CAG CCC AAG GTG GCC CCC ACC ATC ACC
C_FAB_CL-R	TCCAGCGGCTGCGCTAGGCAATAGGTATTTCATTTTAAATTCCTC CTAATTAATTATCTAGAATTAGCACTCGGACCTCTTCAG
Anti-MPO scAb amplification - PCR to overlap the anti-MPO scFv with the anti-MPO constant heavy domain (~ 1200bp)	
Bi_C_(VH-VL)_VH-F	GTG GCC CAG GCG GCC GAG CTC TCC GCC GTG ACG TTG GAC GAG
C_FAB_CL-R	TCCAGCGGCTGCGCTAGGCAATAGGTATTTCATTTTAAATTCCTC CTAATTAATTATCTAGAATTAGCACTCGGACCTCTTCAG
Bispecific antibody generation (bsAb) - PCR to overlap the anti-MPO scAb with the anti-cTnI scAb to generate a anti-MPO x anti-cTnI bsAb (~ 2400bp)	
Bi_C_(VH-VL)_VH-F	GTG GCC CAG GCG GCC GAG CTC TCC GCC GTG ACG TTG GAC GAG
HUC2-CH1-R-1	CTG GCC GGC CTG GCC ACT AGT GAC CTG CAC CTC TGG GGC TAC AGG

2.6.2 PCR amplification of the anti-cTnI antibody construct

2.6.2.1 anti-cTnI scFv antibody generation

Optimisation of the $MgSO_4$ concentration was carried out according to Table 41 for the amplification of the V_L-V_H (scFv) region using a cTnI antibody clone number 270 donated by Dr. Paul Conroy. Platinum® *Taq* DNA polymerase High Fidelity was applied in this PCR. Table 42 outlines conditions that were used throughout this optimisation experiment. Once optimised, the anti-cTnI scFv region was amplified large-scale using the primers outlined in Table 40 (Bi_C_(VL-VH)-F and

Table 40. Reagents and volumes used for the amplification of the anti-cTnI scFv using Platinum Taq DNA polymerase High Fidelity buffer.

Components	**1.5mM (µL)**	**2.0mM (µL)**	**3.0mM (µL)**	**4.0mM (µL)**	**Negative control**	**Final Conc.**
Molecular grade H_2O	to 50	to 50	to 50	to 50	to 50	N/A
10X High fidelity Platinum® PCR buffer	5	5	5	5	5	1X
$MgSO_4$ (50mM stock)	1.5	2	3	4	1.5	Variable
dNTP mix (10mM stock)	1	1	1	1	1	0.2mM
Forward primer - Bi_C_(VL-VH)-F	1-2	1-2	1-2	1-2	1-2	0.2-0.4µM
Reverse primer - C_FAB_VH-R	1-2	1-2	1-2	1-2	1-2	0.2-0.4µM
Template DNA – anti-cTnI scFv template	Variable	Variable	Variable	Variable	N/A	<250ng*
Platinum® *Taq* DNA polymerase	0.2	0.2	0.2	0.2	0.2	1.0 unit**
Total volume	50	50	50	50	50	---------

* Use of high quality, purified DNA templates greatly enhances the success of PCR reactions. The amount of template DNA required per reaction varies depending on the quality of template DNA in addition to the initial concentration of the template.
** 1.0 unit is sufficient for amplifying the majority of targets. In some cases, an increase in the concentration of polymerase may be required (this increase should be optimised)

Table 41. Cycling conditions applied for the amplification of the anti-cTnI scFv using Platinum Taq DNA polymerase High Fidelity buffer.

Step	Temperature (°C)	Time (seconds)	No. of cycles
Initial denature	94	30 -120	1
Denature	94	15 – 30	25 – 35
Anneal	55	15 – 30	
Extension	68	60	
Final extension	68	300 - 600	1

2.6.2.2 Anti-cTnI constant heavy (C_H) region amplification

Optimisation of the $MgCl_2$ concentration was carried out for the amplification of the anti-cTnI constant heavy (C_H) region using chicken spleen cDNA (supplied by Dr. Paul Conroy) and GoTaq® Flexi DNA Polymerase. Table 43 and 44 outline the components and conditions that were used throughout this optimisation experiment. Once optimised, the C_H region was amplified large-scale using the primers outlined in Table 40 and purified through gel extraction (see section 8.1.3).

Table 42. Reagents and volumes used for the amplification of the anti-cTnI constant region using GoTaq Flexi DNA Polymerase.

Components	1.5mM (µL)	2.0mM (µL)	3.0mM (µL)	4.0mM (µL)	Negative control	Final Conc.
Molecular grade H_2O	to 50	to 50	to 50	to 50	to 50	N/A
5X Green GoTaq® Flexi buffer	10	10	10	10	10	1X
$MgCl_2$ (25mM stock)	3	4	6	8	3	Variable
dNTP mix (10mM stock)	1	1	1	1	1	0.2mM
Forward primer - C_FAB_CH-F	0.5	0.5	0.5	0.5	0.5	0.1-1.0µM
Reverse primer - HUC2-CH1-R-1	0.5	0.5	0.5	0.5	0.5	0.1-1.0µM
Template DNA – chicken spleen cDNA	Variable	Variable	Variable	Variable	N/A	<0.5µg/50 µL reaction
Platinum® *Taq* DNA polymerase	0.25	0.25	0.25	0.25	0.25	1.25 unit
Total volume	50	50	50	50	50	---------

Table 43. PCR cycling conditions for the amplification of the anti-cTnI constant heavy region using GoTaq Flexi DNA Polymerase.

Step	Temperature (°C)	Time (seconds)	No. of cycles
Initial denature	94	30 -120	1
Denature	94	15 – 30	25 – 35
Anneal	42 - 65	15 – 30	
Extension	72	60	
Final extension	72	300 - 600	1

2.6.2.3 PCR amplification of the anti-cTnI scAb

Optimisation of the $MgSO_4$ concentration was carried out according to section 2.6.2.1 for the amplification of the anti-cTnI scAb. Purified anti-cTnI scFv template DNA and the constant heavy (C_H) region were incorporated into the PCR. Platinum® *Taq* DNA polymerase High Fidelity was used. Table 41 and Table 42 outline the components and conditions that were used throughout this optimisation experiment. Once amplification was optimised the anti-cTnI scAb was amplified large scale using the primers outlined in Table 40 (Bi_C_(VL-VH)-F and HUC2-CH1-R-1) and purified through gel extraction (section 8.1.3).

2.6.3 PCR amplification and overlap of bispecific anti-MPO antibody construct

In order to construct the anti-MPO scAb it was necessary to re-orientate the anti-MPO scFv to the V_H-V_L format from the V_L-V_H format. This was achieved by amplifying the V_H and V_L regions of the anti-MPO scFv individually and then carrying out an overlap extension PCR in order to overlap the two regions.

2.6.3.1 Optimisation of the $MgSO_4$ concentration for the amplification of the variable heavy (V_H) region using a anti-MPO scFv (V_L-V_H format) as the template DNA

Optimisation of the $MgSO_4$ concentration was carried out according to section 2.6.2.1 for the amplification of the V_H region using an anti-MPO scFv clone (supplied by Dr. Stephen Hearty) and Platinum® *Taq* DNA Polymerase High Fidelity. Table 41 and Table 42 outline the components and conditions that were used throughout this optimisation experiment. Once optimised the V_H region was amplified large-scale using the primers outlined in Table 40 (Bi_C_(VH-VL)_VH-F and C_(VH-VL)_VH-R) and purified through gel extraction (section 8.1.3).

2.6.3.2 Optimisation of the $MgSO_4$ concentration for the amplification of the variable light (V_L) region using a anti-MPO scFv (V_L-V_H format) as the template DNA

Optimisation of the $MgSO_4$ concentration was carried out according to section 2.6.2.1 for the amplification of the V_L region using an anti-MPO scFv clone (supplied by Dr. Stephen Hearty) and Platinum® *Taq* DNA Polymerase. Table 41 and Table 42 outline the components and conditions that were used throughout this optimisation

experiment. Once optimised the V_L region was amplified large-scale using the primers outlined in Table 40 (C_(VH-VL)_VK-F and C_FAB_VK-R) and purified through gel extraction (section 8.1.3).

2.6.3.3 Optimisation of the $MgSO_4$ concentration for the amplification of the anti-MPO scFv (V_H-V_L format)

Optimisation of the $MgSO_4$ concentration was carried out according to section 2.6.2.1 for the amplification of the anti-MPO scFv region using Platinum® *Taq* DNA Polymerase High Fidelity. Table 41 and Table 42 outline the components and conditions that were used throughout this optimisation experiment. Once optimised the anti-MPO scFv (V_H-V_L format) was amplified large scale using the primers outlined in Table 40 (Bi_C_(VH-VL)_VH-F and C_FAB_VK-R) and purified through gel extraction (section 8.1.3).

2.6.3.4 Optimisation of the $MgCl_2$ concentration for the amplification of the anti-MPO constant light (C_L) region

Optimisation of the $MgCl_2$ concentration was carried out according to section 2.6.2.2 for the amplification of the constant light (C_L) region using chicken spleen cDNA and GoTaq® Flexi DNA Polymerase. Table 43 and Table 44 outline the components and conditions that were used throughout this optimisation experiment. Once optimised, the C_L region was amplified large-scale using the primers outlined in section 2.6.1 (C_FAB_CL-F and C_FAB_CL-R) and purified through gel extraction (section 8.1.3).

2.6.3.5 Optimisation of $MgSO_4$ concentration for the amplification of anti-MPO scAb

Optimisation of the $MgSO_4$ concentration was carried out according to section 2.6.2.2 for the amplification of the anti-MPO scAb using Platinum® *Taq* DNA Polymerase High Fidelity. Table 41 and Table 42 outline the components and conditions that were used throughout this optimisation experiment. Once amplification was optimised the anti-MPO scAb was amplified large-scale using the primers outlined in Table 40 (Bi_C_(VH-VL)_VH-F and C_FAB_CL-R) and purified through gel extraction (section 8.1.3).

2.6.3.6 Optimisation of $MgSO_4$ concentration for the PCR overlap of the anti-MPO scAb and the anti-cTnI scAb to generate an anti-MPO x anti-cTnI bsAb

Optimisation of the $MgSO_4$ concentration was carried out according to section 2.6.2.2 for the amplification of the anti-MPO x anti-cTnI bsAb using Platinum® *Taq* DNA Polymerase High Fidelity. Table 41 and Table 42 outline the components and conditions that were used throughout this optimisation experiment. Once optimised the anti-MPO x anti-cTnI bsAb construct was amplified large-scale using the primers outlined in section 2.6.1 (Bi_C_(VH-VL)_VH-F and HUC2-CH1-R-1) and purified through gel extraction (section 8.1.3).

Chapter 3

Production of an antigen grade SFRP-2 protein using a novel expression system

Chapter overview

Although management of PCa patients has improved significantly, early detection is a crucial parameter in contributing to increased survival. Thus it is important to have reliable ways to diagnose the disease, as aggressive therapies can lead to significant risk of treatment-related side effects, which will impact on the patient's quality of life. The widespread use of prostate specific antigen (PSA) as a screening tool for PCa has led to a decline in death rates due to the disease and a decrease in the prevalence of advanced stage disease diagnosis (Prensner *et al.*, 2012; Crawford *et al.*, 2014). However, there is continued debate over the efficacy of prostate specific antigen (PSA) as a diagnostic marker, as its poor specificity has led to PCa not being detected at an early stage. Additionally, PSA cannot decipher between aggressive and non-aggressive disease leading to over-treatment of the disease and associated morbidity. The discovery of novel biomarkers of prostate cancer with the ability to distinguish clinically indolent disease from aggressive forms of PCa would be extremely beneficial.

The use of well-characterised antibodies is vital for clinical diagnostics and protein studies. One of the major challenges that faces researchers and clinicians world-wide in the area of cancer research is the lack of high quality, well validated antibodies to novel target proteins that may aid in improving the diagnosis and treatment of the disease. The aim of this research is to combat such challenges by generating anti-PCa specific antibodies to aid in improving the diagnosis of the disease. Successful antibody generation depends on the use and availability of high quality antigen. However, like antibodies to novel proteins in cancer research, there is also a lack in availability of high quality, suitable commercially available antigens. The generation of antibodies to these proteins is not straightforward and often requires heterologous production of recombinant proteins. Secreted Frizzled Related Protein-2 (SFRP-2) is a novel marker in prostate cancer (as discussed in detail chapter 4 of this thesis) and paucity of high quality commercially available antigen and antibodies is an impediment to research on this marker. Previous work carried out by Dr. Gillian O' Hurley showed SFRP-2 as a very interesting immunohistochemical marker in PCa, displaying positivity in BPH tissue and negative expression in tumour epithelium

(mainly in Gleason grade 3 and 4). It is also suggested as a possible surrogate marker of a subgroup of Gleason grade 5 tumours.

This chapter presents the development of a novel expression system, which takes advantage of the favorable expression and solubility profile of fatty acid binding protein (FABP). This novel system was employed in the expression of a 'difficult-to-express' protein, namely, SFRP-2. The SFRP-2 protein was fused C-terminally, downstream of a standard GS-rich linker sequence, to the N-terminally positioned human heart-type fatty acid protein (hFABP), in a pET28b (+) vector system, and yielded highly soluble chimeric fusion protein. This fusion protein was utilised in an immunisation campaign in an avian model and allowed the production and generation of anti-SFRP-2 recombinant antibody formats, which are currently being utilized in an IHC study of prostate cancer tissue in Beaumont Hospital (described in detail in chapter 4).

In addition to SFRP-2, this novel fusion strategy was also applied successfully for the improved expression of a 'difficult-to-express' antibody to complete the 'proof-of-concept' studies.

3.1 Advances in recombinant protein expression technologies allow the enhancement of soluble protein expression in *E. coli*

The introduction of recombinant DNA technology in the 1970s prompted the expression of a variety of proteins in several host organisms. However, *E. coli* remains the dominant host for producing recombinant proteins owing to its fast, inexpensive, and high yield protein production, together with the well characterised genetics and variety of available molecular tools (Demain & Vaishnav, 2009). As a bacterial system, *E. coli* has, however, limitations in expressing more complex proteins due to the lack of sophisticated machinery to perform post-translational modifications, resulting in poor solubility of the protein of interest that are produced as inclusion bodies. Studies have demonstrated that up to 75% of human proteins can be successfully expressed in *E. coli* but only 25% are produced in an active soluble form using this host system (Bussow *et al.*, 2005; Pacheco *et al.*, 2012; Costa *et al.*, 2014). Other problems found with this host system include correct formation of disulphide bonds, absence of chaperones for the correct folding of proteins, and mis-match between the codon usage of the host cell and the protein of interest (Terpe, 2006; Demain & Vaishnav, 2009; Pacheco *et al.*, 2012).

Despite the above-mentioned issues of *E.coli* recombinant protein production, the benefits of cost, ease-of-use and scale make it essential to design new strategies directed for recombinant soluble protein production in this host cell. Recombinant proteins show large variability in terms of their expression, solubility, stability, and functionality, making them difficult targets for large-scale analyses and production. Secreted Frizzled-Related Protein 2 (SFRP-2) is known to be ‘difficult-to-express’ and the lack of reliable commercially available recombinant SFRP-2 protein reflects this issue. Advances in recombinant protein expression have allowed the development of technologies, which could be applied to aid in improving the expression of proteins such as SFRP-2. These advances include, better expression systems and host strains, improvement in mRNA stability, the ability to perform host-specific optimization, the use of secretory pathways, co-expression with chaperons, post-translational modifications and many more. However, the addition of fusion tags is quickly becoming the most effective technology in improving the expression, solubility, and production of biologically active proteins. The following section presents the most common fusion tags applied, in addition to, the introduction of a novel invention

comprising a fusion protein system to facilitate generic expression of target proteins.

3.2 Fusion tags for the improvement of protein expression and solubility

Genetically engineered fusion tags can improve the variable expression yield and poor solubility of many recombinant proteins, in addition to allowing the purification of virtually any protein without prior knowledge of its biochemical properties. Appropriate design and use of the right fusion tag can promote correct folding of the target of interest, leading to maximum recovery of functional protein. When designing a fusion strategy, the choice of the fusion partner depends on several aspects, such as: (i) the purpose of the fusion (is it for solubility improvement or affinity purification?), (ii) the amino acid composition and size of the fusion tag (target proteins may require larger or smaller tags depending on their application), (iii) the required production levels (the use of larger tags promotes larger production levels than smaller fusion tags), and, (iv) the location of the tag (fusion partners can promote different effects when located at the N-terminus or the C-terminus of the passenger protein). There are a number of fusion tags available for different applications. Table 45 outlines the most common fusion tags applied for enhancing the expression and solubility of proteins and their subsequent purification.

Table 44. Commonly used fusion tags for enhancing protein expression, solubility and purification. (Adapted from Costa *et al.*, 2014).

Affinity tags				
Tag	**Size (aa or kDa)**	**Tag placement**	**Application**	**Reference**
Polyhistidine (His)-tag	6 – 8 aa	N-, C-, or internal	Purification	(Gaberc-Porekar & Menart, 2001)
Strep II tag	8 aa		Purification	(Schmidt & Skerra, 1994)
FLAG-tag	8 aa	N-, C-	Purification	(Einhauer & Jungbauer, 2001)
Human influenza hemagglutinin (HA)-tag	9 aa	N-, C-	Purification	(Terpe, 2003)
c-Myc-tag	11 aa	N-, C-	Purification	(Terpe, 2003)
Calmodulin binding domain	26 aa	N-, C-	Purification	(Vaillancourt *et al.*, 2000)
Cellulose binding domain	27 – 129 aa	N-, C-	Purification	(Tomme *et al.*, 1998; Ramos *et al.*, 2010; Ramos et al., 2013)
Solubility-enhancing tags				
Tag	**Size (aa or kDa)**	**Tag placement**	**Application**	**Reference**
Glutathione-S-transferase (GST)	211 (kDa)	N-	Enhances solubility and purification	(Smith & Johnson, 1988)
Maltose-binding protein (MBP)	396 (kDa)	N-, C-	Enhances solubility and purification	(Pryor & Leiting, 1997; Di Guan *et al.*, 1988)
T7 gene10	260 aa	N-	Enhances solubility and purification	(Esposito &Chatterjee, 2006)
N-utilization substance (NusA)	495 aa	N-	Enhances solubility	(Davis et al., 1999)
Thioredoxin (Trx)	109 aa	N-, C-	Enhances solubility	(Lavallie *et al.*, 1993)
Small ubiquitin modified (SUMO)	100 aa	N-	Enhances solubility	(Butt *et al.*, 2005; Marblestone *et al.*, 2006)

Fusion tags are usually divided into two categories. The first are affinity tags, which aid in the purification of recombinant proteins (Costa *et al.*, 2014). The use of affinity tags for recombinant protein purification offers several advantages over conventional chromatographic techniques, such as, the target protein does not interact with the chromatographic resin (Waugh, 2005), pure target proteins can be obtained after one step purification (Terpe, 2003), affinity tags are economically favorable and time-saving, as they allow different proteins to be purified using a common method in contrast to highly customized procedures applied in traditional chromatographic purification (Arnau *et al.*, 2006). Unfortunately these tags do not improve the expression or enhance the solubility of the protein. Solubility-enhancing tags, the second form of affinity tags, specifically improve expression, solubility and recovery of functional proteins.

3.3 Solubility-enhancing tags

Solubility-enhancing tags are generally large peptides or proteins that increase the expression and solubility of recombinant proteins. Currently, no single fusion tag can increase the expression and solubility of all proteins. The mechanism by which fusion tags enhance the solubility of their partner protein is not fully understood, but several hypotheses have been suggested (Butt *et al.*, 2005; Nallamsetty & Waugh, 2007); (i) misfolded or unfolded proteins are sequestered and protected from the solvent and the soluble protein domains face outwards; (ii) the fusion tag drives its partner protein into a chaperone-mediated folding pathway (Huang & Chuang, 1999; Douette *et al.*, 2005); (iii) hydrophobic patches of the fusion tag interact with partially folded passenger proteins, preventing their self-aggregation, and prompting their proper folding (Waugh, 2005; Nallamsetty & Waugh, 2007); (iv) highly acidic fusion partners have been suggested to inhibit protein aggregation by electrostatic repulsion (Zhang *et al.*, 2004; Su *et al.*, 2007).

A large variety of solubility enhancing tags are commercially available (Table 45), including the well-established Maltose-binding protein (MBP), N-utilization substance (NusA), thioredoxin (Trx), Glutathione-S-transferase (GST), and small ubiquitin modified (SUMO), in addition to more novel fusion partners, such as, the *Fasciola hepatica* 8-kDa antigen (Fh8) tag (Costa *et al.*, 2014).

MBP, a large periplasmic, highly soluble protein of *E. coli*, acts as an excellent solubility enhancing tag, in addition to acting as an affinity tag that permits direct purification post expression. When applied in a fusion context, MBP promotes target protein solubility by displaying chaperone intrinsic activity (Kapust & Waugh, 1999; Bach *et al.*, 2001; Fox *et al.*, 2001). This fusion partner shows more efficient activity at the N-terminus of the target protein rather than the C-terminus (Costa *et al.*, 2014) and promotes correct folding of the target protein by interacting with the latter, and preventing its self-association.

NusA is a transcription termination protein that promotes/prevents RNA polymerase pausing. NusA is used as a fusion partner to promote the production of highly soluble active protein (De Marco *et al.*, 2004; Dummler *et al.*, 2005; Turner *et al.*, 2005). The ability of NusA to promote the soluble production of protein may be related to its solubility and biological activity in *E. coli*. NusA functions by slowing down translation at the transcriptional pauses, allowing more time for correct protein folding (Costa *et al.*, 2014). In contrast to MBP, NusA does not display intrinsic affinity properties and therefore requires the addition of an affinity tag, such as the His-tag, for efficient protein production (Davis *et al.*, 1999).

Trx is an intracellular protein of *E. coli* that is highly soluble and is expressed in its cytoplasm (Young *et al.*, 2012; Costa *et al.*, 2014). Co-expression of a target protein with the *E. coli* Trx leads to significant improvement in the solubility of the protein of interest. Trx is also employed during expression to prevent the formation of inclusion bodies, by taking advantage of its instrinsic oxido-reductase activity, which reduces the formation of disulphide bonds through thio-disulphide exchange (Stewart *et al.*, 1998; LaVallie *et al.*, 2000; Young *et al.*, 2012). Trx can be placed at either the N- or C-terminus, but this fusion partner is more effective at the N-terminal of the target protein (Terpe, 2003; Dyson *et al.*, 2004; Costa *et al.*, 2014). One drawback of this fusion tag is its lack of affinity properties and, like NusA, it requires an additional affinity tag in order to complete protein purification.

Small ubiquitin-modified (SUMO) tags are emerging as a viable alternative for increasing both the expression and solubility of otherwise ‘hard-to-express’ proteins (Butt *et al.*, 2005). It is hypothesized that SUMO tags promote the correct folding of their target protein by exerting chaperoning effects (Marblestone *et al.*, 2006).

Advantageously, the SUMO tag can be cleanly excised using SUMO protease, which recognizes the conformation of SUMO protein rather than a specific sequence within SUMO. Initially, the SUMO system was confined to *E. coli*, as highly conserved SUMO proteases are present in eukaryotes that cleaved the SUMO tag. However, the recently developed SUMOstar tag, a modified version of SUMO, is not recognized by the native eukaryotic protease and is specifically cleaved by the genetically engineered SUMOstar protease. Thus, the SUMOstar system can be used effectively in both prokaryotic and eukaryotic systems. Glutathione-S-transferase (GST) is one of the most popular affinity fusion partners for promoting the production of soluble protein, followed by a single step purification. This fusion partner can protect its target protein from proteolytic degradation, stabilizing it in its soluble fraction (Kaplan *et al.*, 1997; Hu *et al.*, 2008; Young *et al.*, 2012). In addition to *E. coli*, GST has been applied as a fusion partner in a number of hosts such as yeast (Mitchell *et al.*, 1993), insect (Beekman *et al.*, 1994) and mammalian cells (Rudert *et al.*, 1996) proving its flexibility as a fusion partner.

Despite the advantages that current fusion tags have to offer, there are disadvantages that require novel approaches to fusion protein technology in order to overcome them. Some fusion proteins, although advantageous for expression, have no intrinsic value as affinity handles for purification, as mentioned previously for tags such as NusA, Trx, and SUMO. Consequently, these systems routinely contain an additional 'second' tag for purification. Frequently this tag is a polyhistidine tag. This has demonstrated good generic performance and is widely validated but nonetheless, it is considered within the biopharmaceutical industry to be a cleanup rather than a *bona fide* purification method. Hence, additional secondary cleanup steps such as fast protein liquid chromatography (FPLC) are obligatory. Many common fusion protein systems require very expensive affinity purification resins, most of which are subject to restrictive and penal licensing arrangements.

The application of traditional fusion tags can also result in changes in protein conformation, poor yields, loss or alteration of biologically activity and toxicity of the target protein. Hence, it is desirable to remove the tag from the protein post expression. When designing a fusion tag, therefore, careful consideration must be given to how the tags will be removed to produce native proteins without any extraneous sequences. Proteases are routinely used for this purpose. The principlal

concerns with using a protease for removing a tag are (i) removing the protease following digestion, and (ii) non-specific digestion of the target protein by the protease. Resolving the first concern is relatively straightforward, although in most cases it involves an additional chromatography step.

The second concern is more difficult to resolve. Non-specific cleavage is influenced by a number of parameters, such as the enzyme-to-substrate ratio (lower is better), temperature, pH, salt concentration, and length of exposure. TEV protease, thrombin, FXa, and EK all have well defined recognition sequences, but all of them have been found to cause "nicking" of the target protein in some instances. TEV protease has been re-engineered to try to increase its specificity (and stability), resulting in AcTEV (Invitrogen, Carlsbad, CA) and ProTEV (Promega, Madison, WI). Whether or not such engineering has reduced non-specific proteolysis remains to be seen. In addition, other tricks must be used with the native enzymes. For instance, one supplier recommends using FXa at pH 6.5, well below its pH optimum, to minimize non-specific cleavage. Of course, this requires the use of higher enzyme-to-substrate ratios and longer digestion times to achieve complete cleavage.

Considering no other technology has been as effective in improving the expression, solubility and production of biologically relevant protein and considering the disadvantages associated with fusion tags most commonly applied, it is clear that novel fusion technology is warranted to improve this technology for ease-of -use. The following section introduces a novel expression system that allows improved expression and solubility followed by subsequent one-step purification.

3.4 A novel fusion protein system with diverse applications

This chapter presents the results obtained from the optimisation of expression of a known (from a previous study completed by Prof. O' Kennedy's research group) 'difficult-to-express' protein, SFRP-2, applying a novel expression system. Dr. Stephen Hearty, a senior research fellow, working under the supervision of Prof. Richard O' Kennedy, proposed this novel expression system for the improving *E. coli* expression of recombinant proteins. The 'proof-of-concept' study behind this novel system was completed as part of this research. Two expression cassettes were designed to determine if the position of the fusion tag, either on the N or C terminal, would affect the ability of this system to promote the production of soluble

recombinant protein. The expression cassette outlined in Figure 3.11 comprises a N-terminally positioned fusion protein, namely heart fatty acid binding protein, which is known to express well, to facilitate the expression of 'difficult-to-express' proteins. The protein of interest is cloned into a vector in frame with the novel fusion protein to potentiate improved expression and can also serve as an affinity tag for subsequent purification purposes, obliterating the need for multiple purification approaches post expression. The cassette is designed to include a cleavage site of choice (CSOC), which is useful if the protein of interest has to be presented without a fusion partner in the end application. A N-terminally positioned His-tag and C-terminally positioned 'tag-of-choice' (TOC) allow for ease of purification post expression. Additional advantages of this invention include the ability to perform direct immobilization with concomitant improved stability and solubility (e.g. to Fatty acid-coated surfaces – Biacore chips, beads etc.). This system is also readily quantifiable using previously produced anti-FABP antibodies, in quantitative immunoassays (e.g. ELISA or Biacore-based), or through reporter substrates such as 11-(5-dimethylaminonapthalenesulphonyl)-undecanoic acid (DAUDA) or any other suitable fatty acid analogue or labelled fatty acid (e.g. labelled oleic acid).

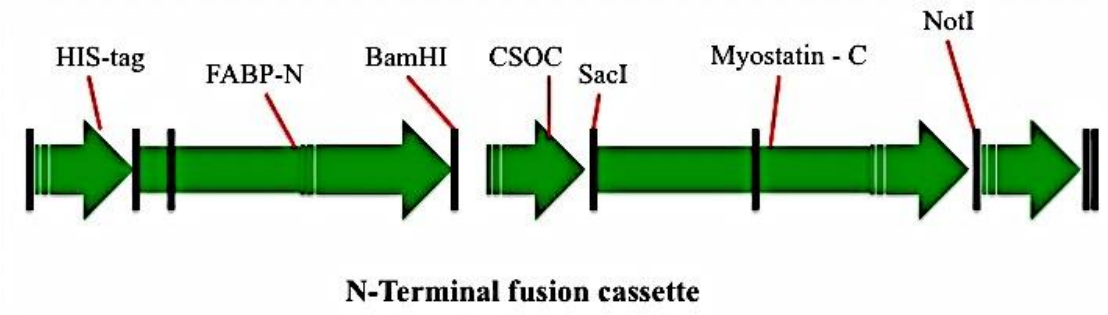

Figure 3.11. Representative N-terminal FABP fusion cassette.

Here we illustrate heart-type FABP (hFABP) as the fusion partner, although it could conceivable, be any of the broader FABP family of proteins. The incorporation of a proteolytic cleavage site of choice (CSOC) (e.g. TEV, factor Xa, thrombin etc.) is useful when the protein of interest (in this example, Myostatin) must be presented without a fusion partner in its end application. The incorporation of an N-terminal His-tag facilitates selective removal of the cleaved FABP fusion component and, likewise, the cleavage protease if it also has a His-tag. Incorporation of restriction enzyme sites such as NotI and SacI allow one to excise the myostatin stuffer molecule out of the cassette to replace it with the protein of interest.

Figure 3.12 represents a C-terminal fusion cassette version of this novel expression system. Some fusion partners can function as solubility enhancers when positioned at either terminal. This cassette was designed to test the flexibility of the FABP fusion strategy. Both cassettes are flexible as to the choice of leader sequence for expression (e.g. use of pelB for directing periplasmic expression).

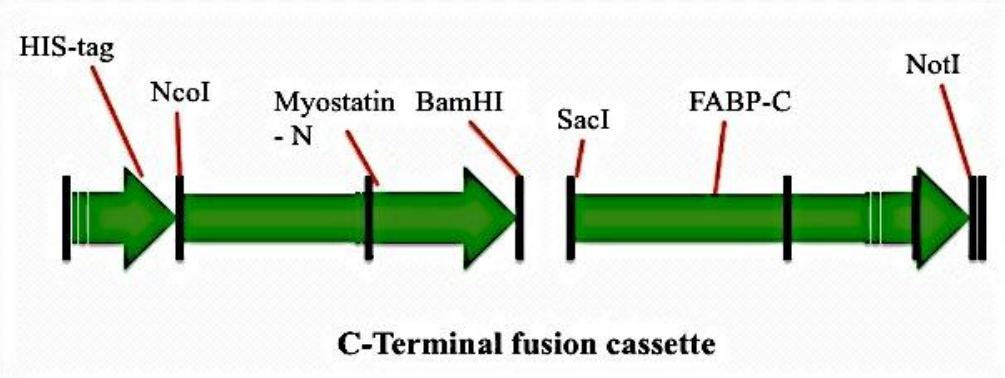

Figure 3.12. Representative C-terminal FABP fusion cassette.

The cassette can be shuttled into any compatible vector using available restriction enzyme (RE) sites, by introducing new RE sites or by any other standard cloning method. In this example, myostatin is the test 'difficult-to-express' protein. Incorporation of restriction enzyme sites such as BamHI and NcoI allow one to excise the myostatin stuffer molecule out of the cassette in order to replace it with the protein of interest.

3.5 Results

3.5.1 Codon optimisation of the SFRP-2 gene

A wide variety of factors can regulate and influence gene expression levels in *E. coli*, including synonymous codon bias. Synonymous codon bias refers to differences in the frequency of occurrence of synonymous codons in coding DNA. Different organisms can demonstrate particular preferences for one of the several codons that encode the same amino acid. In fast growing organisms such as *E. coli* it is thought that the codon preference reflects the composition of their tRNA pool and helps to achieve faster translation rates and high accuracy.

The native DNA sequence of the SFRP-2 gene employs tandem rare codons that can reduce the efficiency of translation or even disengage the translational machinery due to synonymous codon bias in *E. coli*. Codon optimisation was performed by Dr. Gillian O' Hurley using Genscript software for the SFRP-2 gene to allow for synonymous codon bias in *E. coli* to improve translation efficiency.

The optimised DNA sequence corresponding to amino acids 165-295 on the human SFRP-2 protein, including the *Nco* I and *Hind* III restriction sites, was cloned into a pUC57 vector using EcoRV restriction enzyme by Genscript USA Inc. (USA). This is the most immunogenic portion of the SFRP-2 and was successfully used by Atlas antibodies to produce their fusion protein, which generated their SFRP-2 polyclonal antibody. This particular anti-SFRP-2 antibody (Atlas antibodies) was important, as it was used in immunohisochemical study of prostate to assess the expression pattern of SFRP-2 in prostate cancer (O'Hurley *et al.*, 2011). However, prior to commencement of this project, this antibody was removed from the market for unknown reasons. Figure 3.13 outlines the original SFRP-2 gene and the optimised SFRP-2 gene, where the codon changes are highlighted in red.

Original SFRP-2 gene

ATGGCCACCGAGGAAGCTCCAAAGGTATGTGAAGCCTGCAAAAATAAAA
ATGATGATGACAACGACATAATGGAAACGCTTTGTAAAAATGATTTTGCA
CTGAAAATAAAAGTGAAGGAGATAACCTACATCAACCGAGATACCAAAA
TCATCCTGGAGACCAAGAGCAAGACCATTTACAAGCTGAACGGTGTGTCC
GAAAGGGACCTGAAGAAATCGGTGCTGTGGCTCAAAGACAGCTTGCAGT
GCACCTGTGAGGAGATGAACGACATCAACGCGCCCTATCTGGTCATGGGA
CAGAAACAGGGTGGGGAGCTGGTGATCACCTCGGTGAAGCGGTGGCAGA
AGGGGCAGAGAGAG

Codon optimised SFRP-2 gene

ATGGCGACCGAAGAAGCCCCGAAAGTTTGAGAAGCATGTAAAAACAAAA
ACGATGACGATAACGACATTATGGAAACGCTGTGCAAAAACGATTTCGCT
CTGAAAATCAAAGTCAAAGAAATCACCTACATCAACCGTGACACGAAAAT
TATCCTGGAAACCAAATCCAAAACGATTTACAAACTGAATGGCGTCAGCG
AACGCGACCTGAAAAAATCTGTGCTGTGGCTGAAAGATAGTCTGCAGTGC
ACCTGTGAAGAAATGAACGATATTAATGCCCCGTATCTGGTGATGGGCCA
GAAACAAGGCGGTGAACTGGTGATCACGAGCGTTAAACGTTGGCAGAAA
GGTCAACGCGAA

Figure 3.13. Codon optimisation of the SFRP-2 gene.

The original SFRP-2 gene was codon optimised to allow for synonymous codon bias in E. coli to improve translational efficiency using Genscript software.

3.5.1.1 Application of the N-terminal Fusion Cassette to promote soluble protein expression

3.5.1.1.1 SFRP-2-hFABP recombinant fusion protein expression in Tuner E. coli

The optimised SFRP-2 gene (shown in Figure 3.13) was cloned into a pET-28b (+) vector (Figure 3.14) which contained a heart fatty acid binding protein (hFABP) gene sequence (Figure 3.15), a *Sac* I and *Not* I restriction site and a lac operator spliced together with a T7 promotor. Heart fatty acid binding protein is a 15 kDa, hydrophilic protein involved in maintaining myocardial homeostasis via transporting long-chain fatty acids to different sites of oxidation and esterification in the cell. It has become an important early marker of acute myocardial infarction (Kleine *et al.*, 1992). Within

the BDI hFABP was found to be an excellent expressing protein in an *E. coli* expression system.

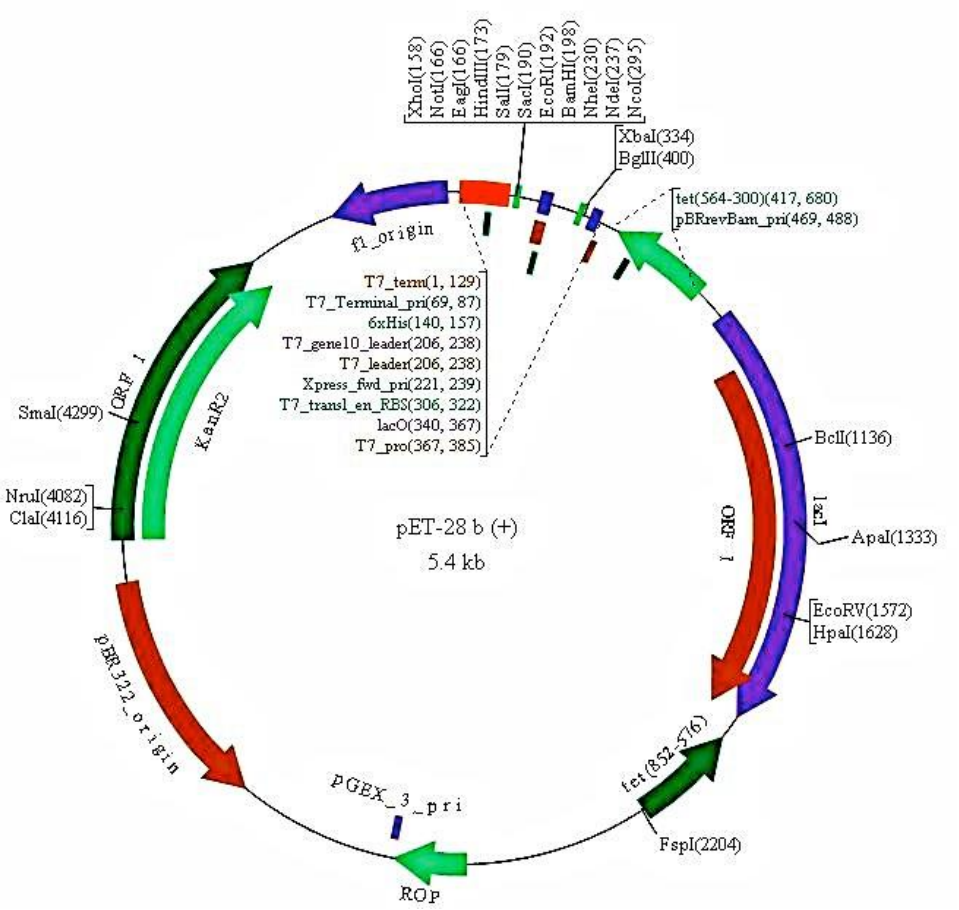

Figure 3.14. pET28b (+) vector map.

The pET28b (+) vector carries an N-terminal His-Tag, thrombin, and a T7-Tag configuration. Unique sites are shown on the vector map.

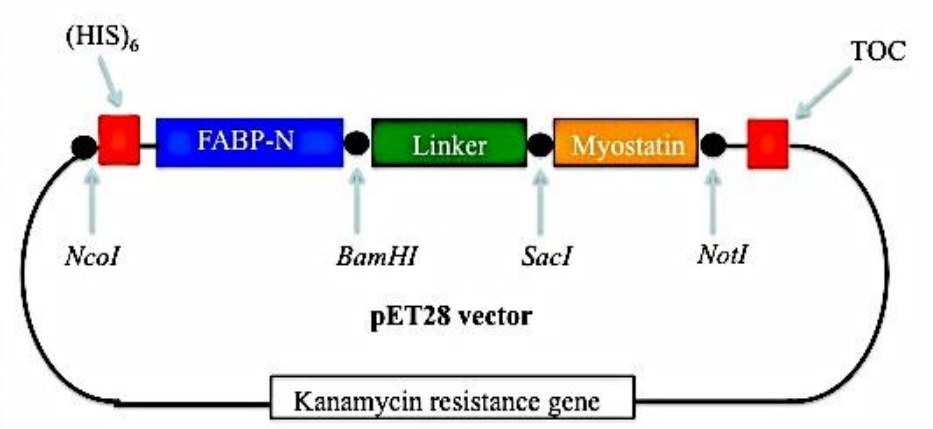

Figure 3.15. Map of pET28b (+)-hFABP vector.

The map locates the N-terminal hFABP gene, the linker sequence, the myostatin stuffer molecule, the HIS-Tag, the kanamycin resistant gene and the restriction sites, SacI, NotI, NcoI, BamHI, on the pET28b (+) vector.

3.5.2 SFRP-2 gene amplification from the pUC57 vector

The SFRP-2 gene was cloned into a pUC57 vector by Genscript USA Inc. Primers were designed to amplify the SFRP-2 gene from the pUC57 vector. The sense primer contains a sequence tail that corresponds to the *Sac* I restriction site and the antisense primer contains a sequence tail that corresponds to the *Not* I restriction site for ligation into pET-28b (+)-hFABP vector. Large-scale amplification (10X) of the SFRP-2 gene was performed using MyTaq^{TM} Red Mix DNA polymerase High Fidelity. The amplified gene was resolved by agarose gel electrophoresis and purified through gel extraction. Successful amplification and purification at approximately 374 bps was observed.

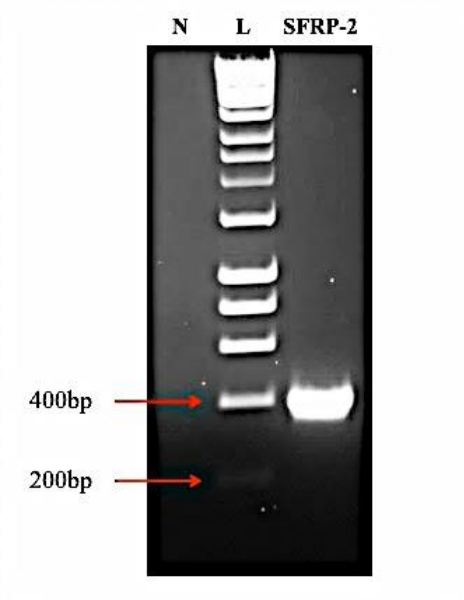

Figure 3.16. Amplification of the SFRP-2 gene from the pUC57 vector.

Large-scale amplification of the SFRP-2 gene was carried out. The PCR product from this experiment was resolved on a 1.5% (w/v) agarose gel. A band at ~400bp was obtained which was the predicted size of the SFRP-2 gene. A negative control (N) consisting of all the necessary PCR components in the absence of DNA was included in this PCR in order to ensure no contamination was present in the sample. The DNA ladder (L) used in this PCR was the Hyperladder 1.

3.5.3 Cloning of the SFRP-2 gene into the pET-28b (+)-hFABP vector

The amplified SFRP-2 gene containing the *Sac* I and *Not* I restriction sites compatible with the pET-28b (+)-hFABP vector was digested with the fast digest *Sac* I and *Not* I restriction enzymes, creating cohesive ends. The pET-28b (+)-hFABP vector was also digested with the fast digest *Sac* I and *Not* I restriction enzymes, creating cohesive ends. Digesting the SFRP-2 gene with two different enzymes guarantees unidirectional cloning of the gene into the vector and prevents the vector re-ligating. The pET-28b (+)-hFABP vector and the SFRP-2 gene were mixed in a 1:3 (vector: insert) ratio and the cohesive ends were ligated by T4 DNA ligase enzyme.

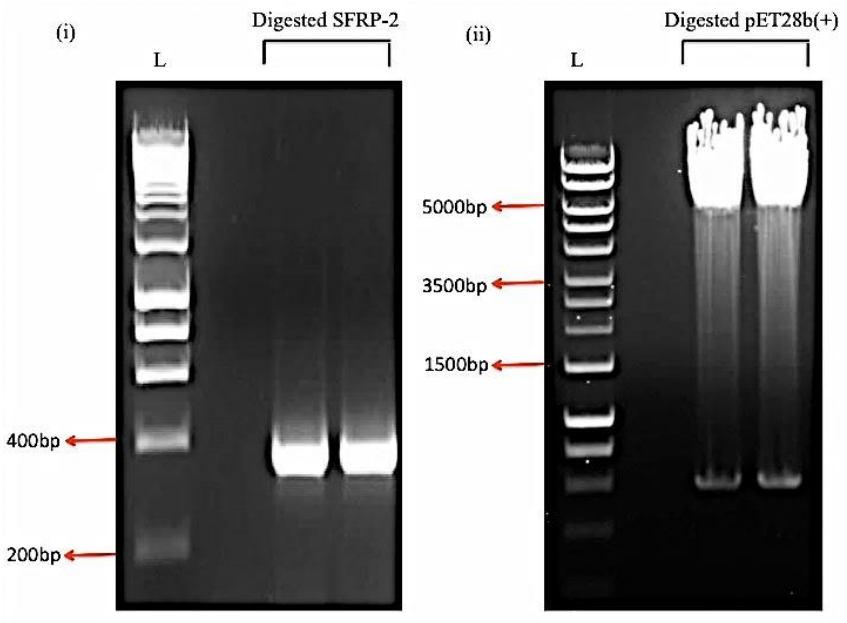

Figure 3.17. pET28b (+)-hFABP vector and SFRP-2 digestion with *NotI* and *SacI* FastDigest enzymes.

(i) *Visualisation on a 1.5% (w/v) agarose gel of the digested SFRP-2 gene using Not I and Sac I FastDigest enzymes.*

(ii) *Visualisation on a 1% (w/v) agarose gel of the digested pET-28b (+)-hFABP vector using FastDigest Not I and Sac I enzymes. The Bioline Hyperladder 1 used in this figure is represented by the letter L.*

3.5.4 Transformation of ligated pET-28b (+)-hFABP vector into Tuner chemically competent cells and colony pick PCR

The ligated vector containing the SFRP-2 gene was next transformed into the chemically competent Tuner (DE3) strain of *E. coli* cells following a heat shock protocol. Transformed colonies were randomly picked from kanamycin-supplemented agar plates and incorporated into a colony pick PCR in order to determine which colonies were harboring the SFRP-2 gene. A total of 10 colonies were picked, two of which contained the SFRP-2 gene.

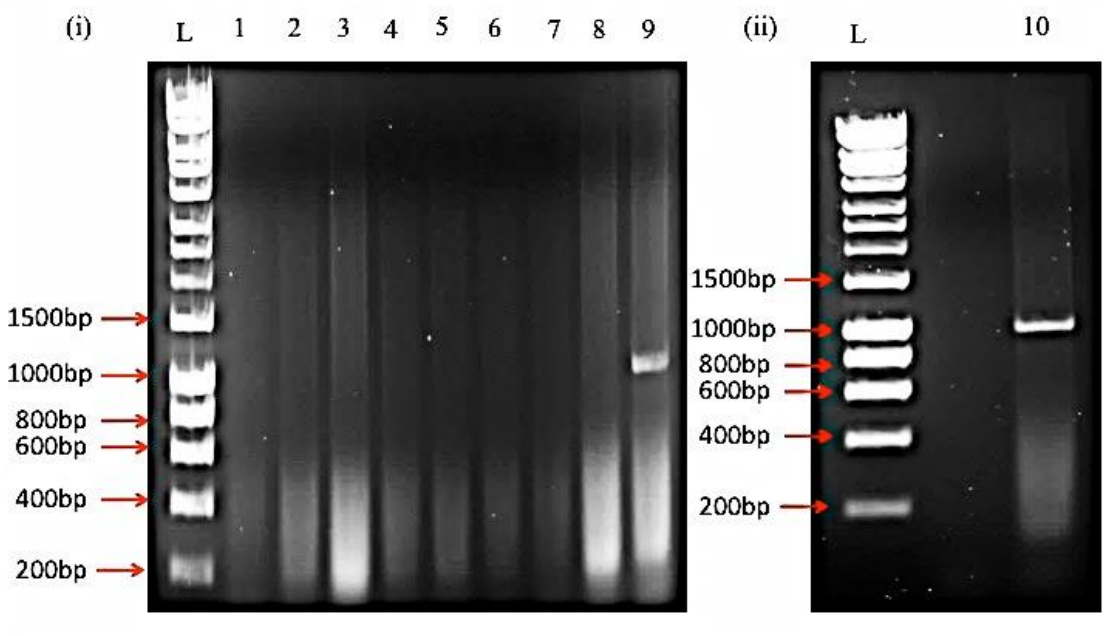

Figure 3.18. Colony-pick PCR for pET28b (+)-hFABP clones.

(i) and (ii) Visualisation of a colony pick PCR performed on 10 (designated 1-9, gel (i) and 10 (gel ii)) clones picked from kanamycin-supplemented agar plates. The PCR products from this experiment were resolved on 1.5% (w/v) agarose gels. The ladder (L) used was the Hyperladder 1 Bioline.

3.5.5 Positive expression of SFRP-2 colony picked clones

In order to ensure positive expression of the SFRP-2 transformed clones, the positive clones, 9 and 10, obtained from the colony pick PCR were inoculated into 10mL of SB (containing 25µg/mL kanamycin) and incubated overnight at 37°C. The following day an aliquot of the overnight cultures was subcultured into 10mL of fresh SB media (containing 25µg/mL kanamycin). The samples were then incubated at 37°C until an OD_{600nm} of ~0.7 was obtained. When an OD_{600nm} of 0.7 was obtained 5mL of each culture was removed and added to a fresh 50mL tube. IPTG (0.1mM) was added to one tube only and the temperature was reduced to 25°C. This provided an uninduced and induced set of samples for each clone and the control. After 4 hours of induction a 1mL sample was taken from each culture and centrifuged at 11,000 x g at 4 °C. The pellets were resuspended in 1X sterile PBS and 4X SDS-PAGE loading dye. The samples were boiled for 2 minutes at 98°C and then analysed through SDS-PAGE and Western blotting.

The predicted size of the SFRP-2 recombinant protein was ~29 kDa. Results from the SDS show that a strong band was obtained at approximately 29 kDa for both clone number 9 and 10. The control showed no expression band at 29 kDa. The anti-SFRP-2 Western blot showed strong bands at approximately 29 kDa for both the uninduced and induced set of samples for both clone number 9 and 10. However, the bands obtained for the induced samples for both clones appeared stronger than those of the uniduced showing the effect of IPTG on expression. Both clones were sent for sequencing to ensure the intact plasmid containing the SFRP-2 sequence was present.

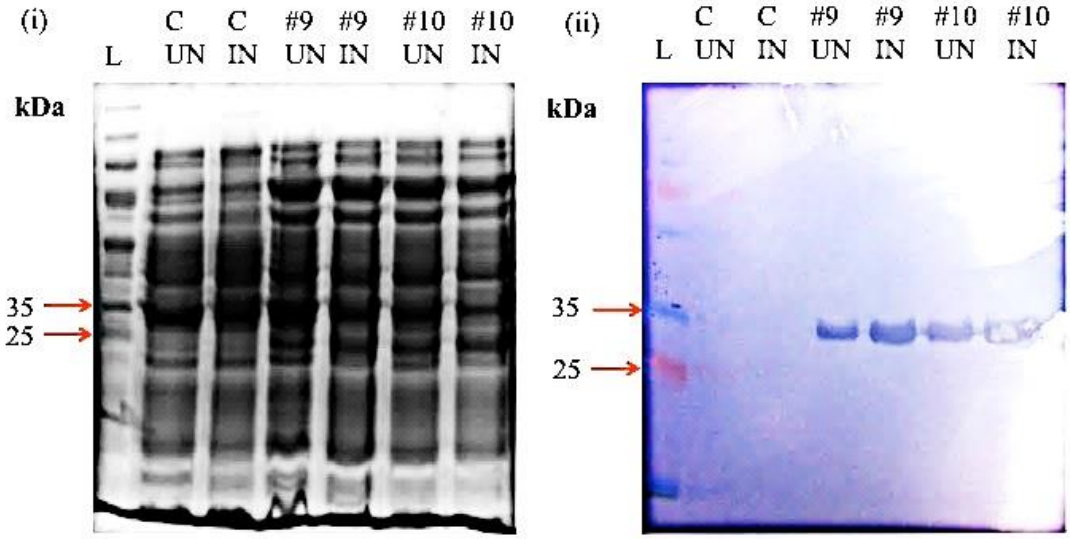

Figure 3.19. SFRP-2-hFABP protein expression in Tuner *E. coli* cells.

(i) *SDS PAGE*

(ii) *Anti-SFRP-2 Western blot. The pellets from the uninduced (UN) and induced (IN) SFRP-2-hFABP transformed clones including the control samples were re-suspended in 1X PBS and SDS-PAGE loading dye. Following a 2 minute incubation at 98 °C, the samples were analysed on a 12.5% SDS-PAGE Gel and by Western blotting. The Western blot was probed initially with a anti-SFRP-2 antibody raised in goat, followed by a HRP-labelled anti-goat (IgG) secondary antibody. The ladder, represented by the letter L in this figure, was a Page Ruler Plus pre-stained protein ladder.*

3.5.6 Sequencing of SFRP-2-hFABP recombinant fusion protein transformant 9

To ensure that the intact plasmid containing the SFRP-2 sequence was present in transformant 9 and 10, a bacterial stock of both clones, containing the transformed plasmids, was sent for sequencing to Source Biosciences. The DNA sequences were received and subsequently translated into the amino acid sequence using ExPASy translation tool. The sequencing data for clone number 10 was very poor. Sequencing

was repeated numerous times and no improvement was observed (data not shown). As can be seen in Figure 3.20, cloning of the SFRP-2 gene into the pET28b (+) vector in clone number 9 was successful. The myostatin stuffer molecule was successfully excised from the vector using the *Sac*I and *Not*I restriction enzymes and the SFRP-2 gene was successfully ligated into the vector in its place.

MVDAFLGTWKLVDSKNFDDYMKSLGVGFATRQVASMTKPTTIIEKNGDILTL
KTHSTFKNTEISFKLGVEFDETTADDRKVKSIVTLDGGKLVHLQKWDGQETT
LVRELIDGKLILTLTHGTAVCTRTYE***KE***GSGGSSRSSSSGGGGSGGGG***EL***ATE
EAPKVCEACKNKNDDDNDIMETLCKNDFALKIKVKEITYINRDTKIILETKSK
TIYKLNGVSERDLKKSVLWLKDSLQCTCEEMNDINAPYLVMGQKQGGELVIT
SVKRWQKGQREAAALEHHHHHH

Figure 3.20. Plasmid gene sequence of transformant 9.

The hFABP sequence is highlighted in red, the linker is highlighted in brown, the SFRP-2 sequence is highlighted in yellow and the histidine tag is highlighted in grey. The amino acid sequence in bold and italics corresponds to the restriction enzyme cut sites SacI and NotI respectively.

3.5.7 Soluble expression of SFRP-2-hFABP clone

The next step was to determine if SFRP-2 was present in the soluble or insoluble fraction. The result from this experiment was critical in determining the success of the N-FABP fusion strategy. Previous attempts carried out by Dr. Gillian O'Hurley to obtain active, soluble SFRP-2 protein were unsuccessful, as the fusion protein was found to be insoluble in the form of bacterial fusion proteins trapped within the bacterial cell periplasm. This experiment was carried out to determine two things: (i) if the production of soluble SFRP-2 protein was possible using this fusion strategy, and (ii) how much insoluble protein was produced. If the results show the production of soluble protein in addition to insoluble protein, an optimisation of expression will be carried out in order to attempt to increase the production of soluble SFRP-2 protein and reduce the amount of insoluble protein produced. Post optimisation of expression, this experiment will be repeated in the hope that the result will show a reduction in the amount of insoluble protein and an increase in the production of soluble SFRP-2 protein.

SFRP-2 clone 9 was inoculated in 10mL of SB (containing 25µg/mL kanamycin) and incubated overnight at 37°C. The following day, the overnight culture was subcultured into two 250mL flasks containing 50mL fresh SB and kanamycin. These samples were incubated at 37°C until an OD_{600nm} of ~0.7 was obtained. The temperature was then dropped to 25°C and 0.1mm IPTG was added to one of the flasks and the samples were incubated for 4 hours. This provided an uninduced and induced set of samples. After 4 hours a 1mL sample was taken from both flasks (uninduced and induced) and centrifuged at 11,000 x g at 4 °C. The cells were lysed with 1mg/mL lysozyme and three freeze thaw cycles were carried out. The samples were then centrifuged at 11,000 x g at 4 °C. Both the supernatant and the pellet were analysed through SDS-PAGE and Western blotting.

The results from the anti-SFRP-2 Western blot, presented here (Figure 3.21), showed that the SFRP protein was present in both the soluble and the insoluble fraction. The Western blot showed a stronger band at approximately 29 kDa for the insoluble fraction, which was expected based on results obtained previously when this protein was expressed. However, a clear sufficient band was also obtained for the soluble fraction, indicating the success of the FABP fusion strategy to produce soluble SFRP-2 recombinant protein. Optimisation of expression for the SFRP-2 protein was next completed in order to determine the optimum expression conditions. Optimising expression may also allow for an improvement in the production of soluble SFRP-2 protein.

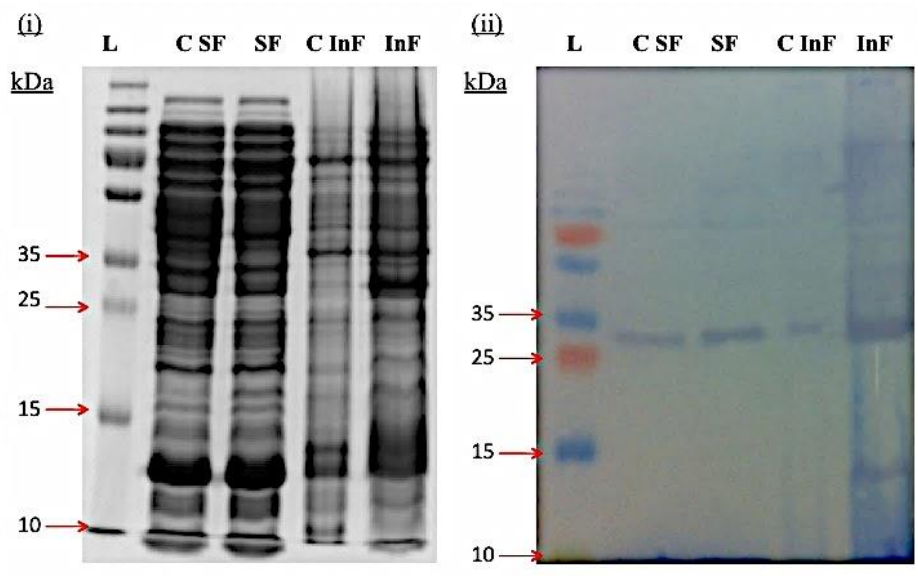

Figure 3.21. Soluble expression of SFRP-2-hFABP.

(i) *SDS-PAGE.*

(ii) *Anti-SFRP-2 Western blot. Following 4 hours of induction with 0.1mM IPTG, SDS-PAGE and Western blot analysis were performed to analyse the soluble (SF) and insoluble (InF) sample fractions of SFRP-2-hFABP recombinant fusion protein clone number 9. A control sample was run alongside both test samples (control soluble fraction (CSF) and control insoluble fraction (CInF). The control sample contained lysate from an SFRP-2 culture expressed in the absence of IPTG. The SDS and anti-SFRP-2 Western blot show clear expression of SFRP-2 (~29 kDa) in both the soluble and insoluble fractions. The ladder, represented by the letter L in this figure, was a Page Ruler Plus pre-stained protein ladder.*

3.5.8 Optimisation of expression of SFRP-2 varying IPTG concentration, induction time and temperature

To determine the optimal induction conditions for the expression of the SFRP-2 recombinant fusion protein in Tuner (DE3) cells, a number of different parameters were varied. The IPTG concentration was varied from 0.05mM – 0.2mM at different time courses, at two different temperatures (20 and 25 °C). The IPTG concentration for this optimisation experiment was kept low in addition to the use of cooler induction temperatures to promote soluble protein expression. Clone number 9 was inoculated into 10mL of SB (containing 25µg of kanamycin) and incubated overnight at 37 °C. The following day the overnight sample was subcultured into 6 x 250mL

flasks (50mL SB supplemented with 25µg of kanamycin). The samples were then incubated at 37 °C until an $OD_{(600nm)}$ of ~0.7 was obtained.

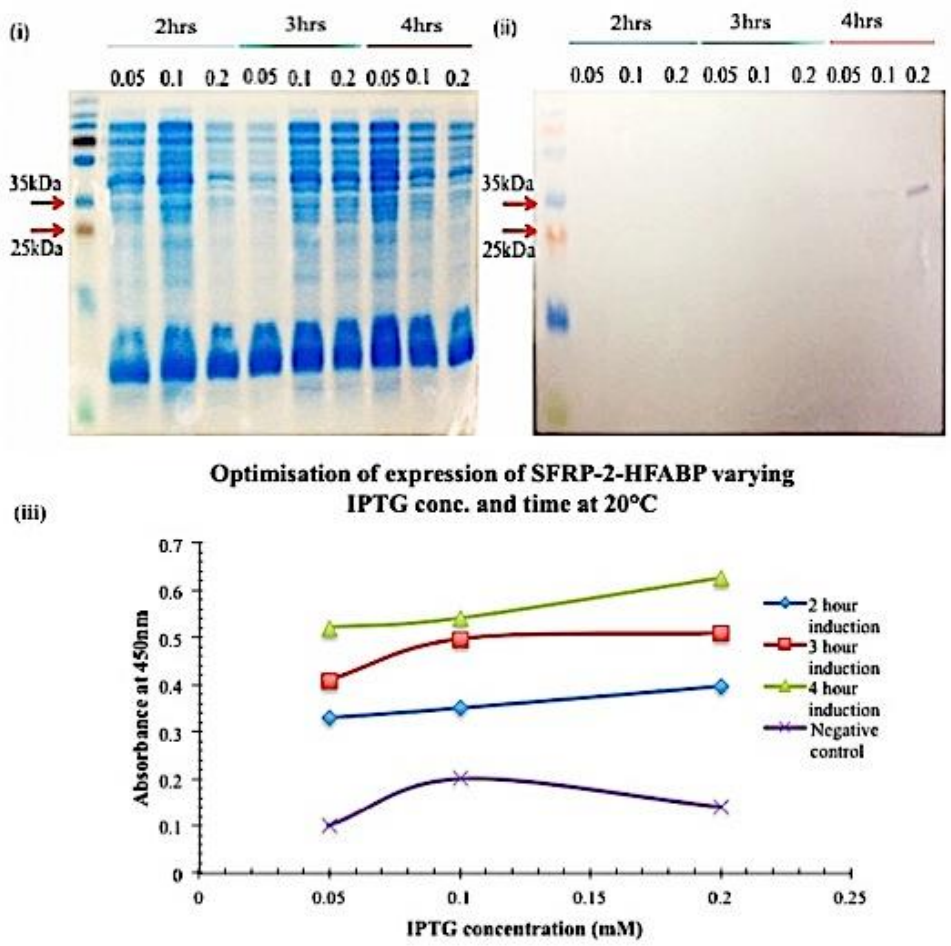

Figure 3.22. Optimisation of expression of clone number 9 at 20 °C.

(i) *SDS-PAGE.*

(ii) *Anti-SFRP-2 Western blot. Optimisation of IPTG concentration, time and temperature was completed in order to identify the optimum conditions for the SFRP-2 protein. The IPTG concentration was varied from 0.05 – 0.2mM. Samples were taken after 2, 3, and 4 hours of induction at the various IPTG concentrations at 20 °C. The results from the anti-SFRP-2 Western blot show that optimum expression was achieved using 0.2mM IPTG after 4 hours.*

(iii) *An ELISA plate was coated with lysate obtained at each time point at 37 °C for 1 hour. Following blocking with 5% (w/v) MM in 1X PBS for 1 hour at 37 °C, the protein was probed with a commercial anti-SFRP-2 polyclonal antibody raised in goat (Abcam) for 1 hour at 37 °C. The plate was washed 3 times with 1X PBS and 1X PBS(T) (0.05% (v/v)). Bound SFRP-2 antibody was detected using an HRP-labelled anti-goat (IgG) secondary antibody. Absorbance was read at 450nm.*

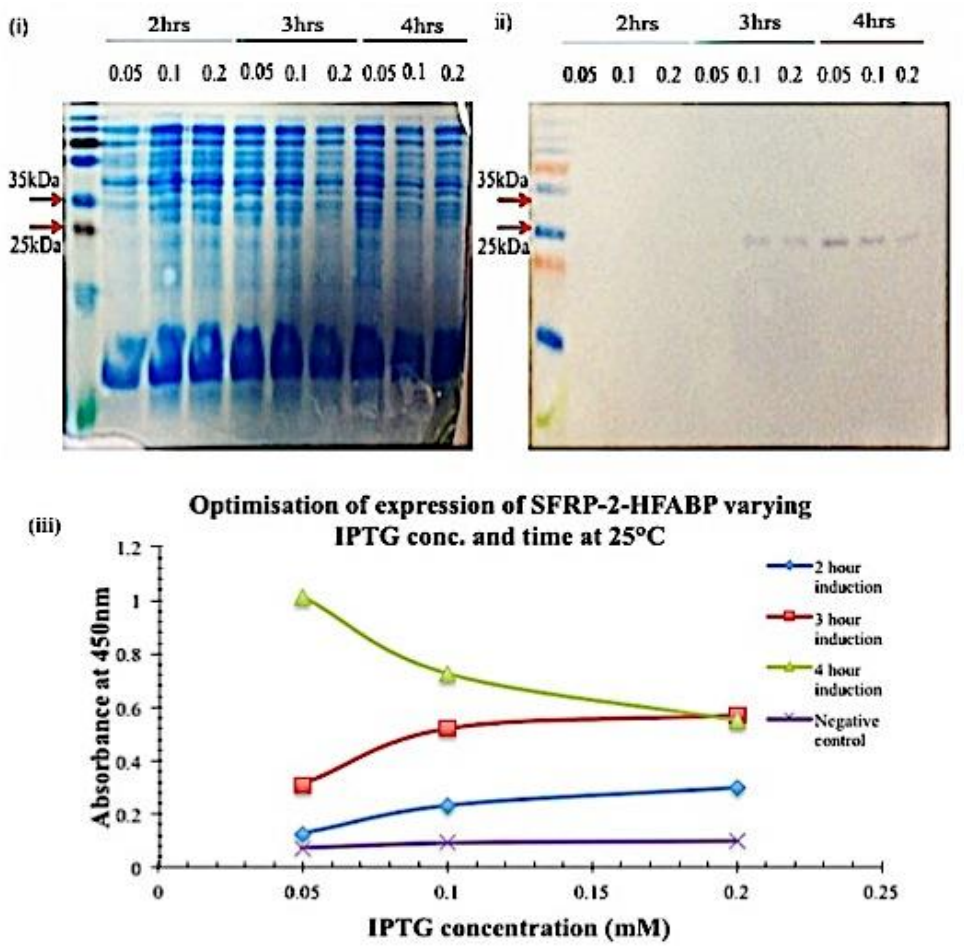

Figure 3.23. Optimisation of expression of clone number 9 at 25 °C.

(i) SDS-PAGE.

(ii) Anti-SFRP-2 Western blot. Optimisation of IPTG concentration, time and temperature was completed in order to identify the optimum conditions for the SFRP-2 protein. The IPTG concentration was varied from 0.05 – 0.2mM. Samples were taken after 2, 3, and 4 hours of induction at the various IPTG concentrations at 25 °C. The results from the anti-SFRP-2 Western blot show that optimum expression was achieved using 0.05mM IPTG after 4 hours.

(iii) *An ELISA plate was coated with lysate obtained at each time point at 37 °C for 1 hour. Following blocking with 5% (w/v) MM in 1X PBS for 1 hour at 37 °C, the protein was probed with a commercial goat anti-SFRP-2 polyclonal antibody (Abcam) for 1 hour at 37 °C. The plate was washed 3 times with 1X PBS and 1X PBS(T) (0.05% (v/v)). Bound SFRP-2 antibody was detected using an HRP-labelled anti-goat (IgG) secondary antibody. Absorbance was read at 450nm.*

When an $OD_{(600nm)}$ of ~0.7 was reached the temperature was reduced to 25 °C for three of the flasks and 20 °C for the remaining three followed by the addition of 0.05mM, 0.1mM, and 0.2mm IPTG. After 2, 3 and 4 hours a 1mL sample was taken

from each sample and centrifuged in a bench-top centrifuge at 11,000 x g at 4 °C. The cells were lysed with 1mg/mL lysozyme and three freeze thaw cycles were carried out. The samples were then centrifuged as before and 30µL of the supernatant was mixed with SDS-PAGE loading dye for SDS-PAGE and anti-SFRP-2 Western blot analysis. Additionally the supernatant taken at each time point was analysed by ELISA to ensure the results correlated with the Western blot and SDS-PAGE. Optimum expression was achieved at 25 °C after 4 hours using an IPTG concentration of 0.05mM. Once expression conditions were optimised, the soluble and insoluble fractions from the optimum induction conditions were analysed by SDS-PAGE and Western blotting. The results from the SDS-PAGE and Western blots show a significant reduction in the production of insoluble protein, indicated by the presence of a very faint SFRP-2-specific band in the insoluble fraction lane. In comparison, the soluble fraction contained a clear SFRP-2-specific band. This experiment proves, not only the success of the FABP fusion strategy but also the importance of optimizing expression and how varying specific parameters can have a major effect on the production of soluble protein.

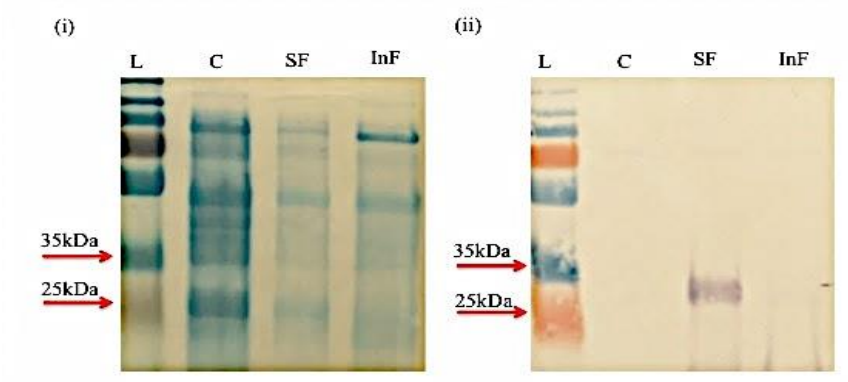

Figure 3.24. SDS-PAGE and WB analysis of the soluble and insoluble fractions from the optimum induction conditions.

(i) *SDS-PAGE.*

(ii) *Anti-SFRP-2 Western blot. Following 4 hours of induction with 0.05mM IPTG at 25 °C SDS-PAGE and Western blot analysis was performed to analyse the soluble (SF) and insoluble (InF) sample fractions of the SFRP-2-hFABP recombinant fusion protein. Results from the SDS and WB indicate a clear reduction in the production of insoluble SFRP-2 protein using the optimum expression conditions. The ladder, represented by the letter L in this figure, was a Page Ruler Plus pre-stained protein ladder. The control, represented by C, was lysate from an SFRP-2 protein culture expressed in the absence of IPTG.*

3.5.9 Small-scale expression and purification of the SFRP-2 recombinant protein

The SFRP-2-hFABP-expressing clone number 9 was used for small-scale production of the SFRP-2 fusion protein. A 10mL culture of the clone was grown up overnight followed by subsequent subculture and 0.05mM IPTG induction for 4 hours at 25 °C. The small-scale sample was then centrifuged (Eppendorf^{TM} Centrifuge with swing-bucket rotor (A-4-62) and fixed-angle rotor (F-45-30-11) at 11,000 x g at 4 °C and the supernatant poured to waste. The pellet was re-suspended in lysis buffer and three freeze thaw cycles were performed. The sample was centrifuged at 11,000 x g at 4 °C again and the pellet obtained was resuspended in equilibration buffer. The filtered protein lysate was purified using immobilized metal affinity chromatography (IMAC). PBS-based buffers were used throughout this experiment. Each buffer was brought to a pH of 8.0 prior to purification except for the elution buffer (100mM sodium acetate), which was pH 4.2. The imidazole concentrations used for wash A, B and C were 10, 15 and 20mM, respectively. Increasing the imidazole concentration over each wash ensured the removal of non-specific proteins that may have been loosely bound to the column. This experiment was carried out at 4 °C.

The purification was analysed by performing SDS-PAGE and anti-SFRP-2 Western blotting on the lysate, unfiltered lysate, 'flow-through', wash and eluted protein. The results show the small-scale expression and purification of the SFRP-2-hFABP recombinant fusion protein was successful. The anti-SFRP-2 antibody used to probe the Western blot generated strong bands at approximately 29 kDa for the unfiltered lysate, "flow-through" 1, "flow-through" 2 and the concentrated protein. No SFRP-2-specific bands were obtained in the either wash sample. The protein concentration was obtained using the NanoDrop Protein A_{280} settings. The yield obtained was 0.15 mg/mL.

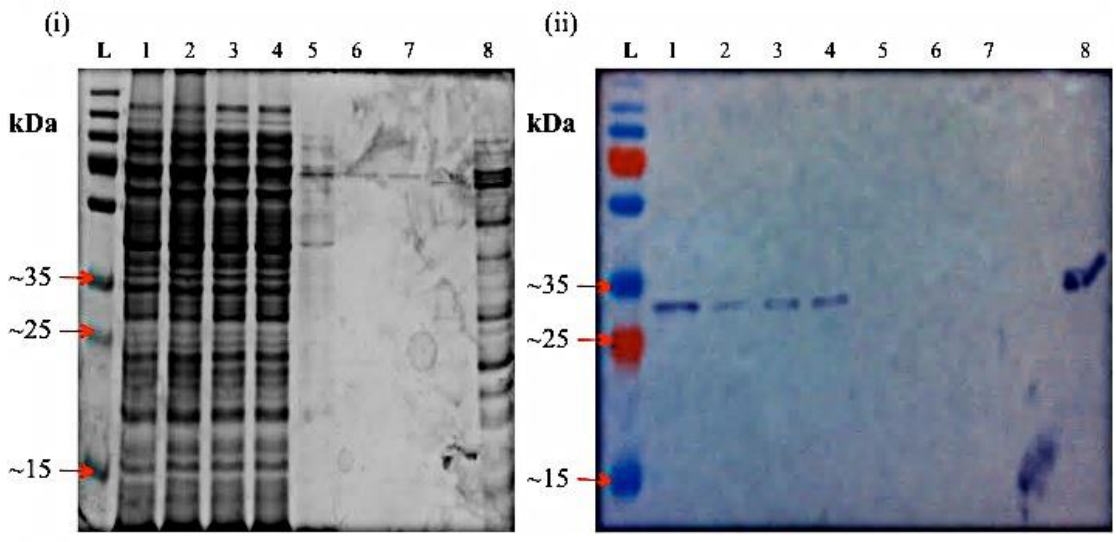

Figure 3.25. Small-scale SFRP-2-hFABP recombinant fusion protein expression in Tuner cells and IMAC purification of the expressed protein.

(i) *SDS-PAGE.*

(ii) *Anti-SFRP-2 Western blot. In (i) and (ii) lane 1 contains the unfiltered lysate from clone number 9 (following 0.05mM IPTG induction for four hours at 25 °C). Lane 2 contained the filtered lysate from clone number 9 (filtered through 0.45 and 0.22 µM filters). Lanes 3 and 4 contain the "flow-through" with all unbound proteins that passed through the resin. Lanes 5, 6 and 7 contain any impure non-specific proteins, which may have weakly bound to the resin and were removed using an increased concentration of imidazole (10mM (Wash A), 15mM (Wash B) and 20mM (Wash C)) and Tween20.* Lane 8 contains the purified eluted SFRP-2 recombinant fusion protein. This purification was carried out at 4 °C. *The ladder, represented by the letter L in this figure, was a Page Ruler Plus pre-stained protein ladder.*

3.5.10 Large-scale expression of the SFRP-2 protein and subsequent purification using PBS-based buffers

Following successful small-scale purification of the SFRP-2 recombinant fusion protein, large-scale purification was carried out in order to obtain a sufficient amount of soluble protein for immunisation purposes. Ten mL of SB containing clone number 9 supplemented with 25µg kanamycin was grown overnight at 37 °C. On the following day, the overnight culture was subcultured into 5 X 1L flasks containing fresh SB supplemented with 25µg kanamycin. IPTG induction was completed, using 0.05mM IPTG, once the appropriate OD was obtained, for 4 hours at 25 °C. The purification of this protein was completed using PBS-based buffers and immobilized

metal affinity chromatography (IMAC). Protease inhibitors were added to the lysate prior to purification to avoid potential degradation of the recombinant protein by endogenous proteases. The success of the purification was assessed by performing SDS-PAGE and anti-SFRP-2 Western blot on the filtered lysate, "flow-through', wash and eluted protein fractions. From the results obtained it is clear that WA removed a significant amount of contaminating proteins in comparison to WB. The concentrated protein fraction, despite containing some additional non-specific protein bands, was of sufficient purity for immunisation purposes. The protein yield, determined using the NanoDrop, was 1mg/mL for this sample. This soluble recombinant protein was utilized in an immunisation campaign (results shown in chapter 4) and allowed the production of recombinant anti-SFRP-2 scFv and scAb antibodies

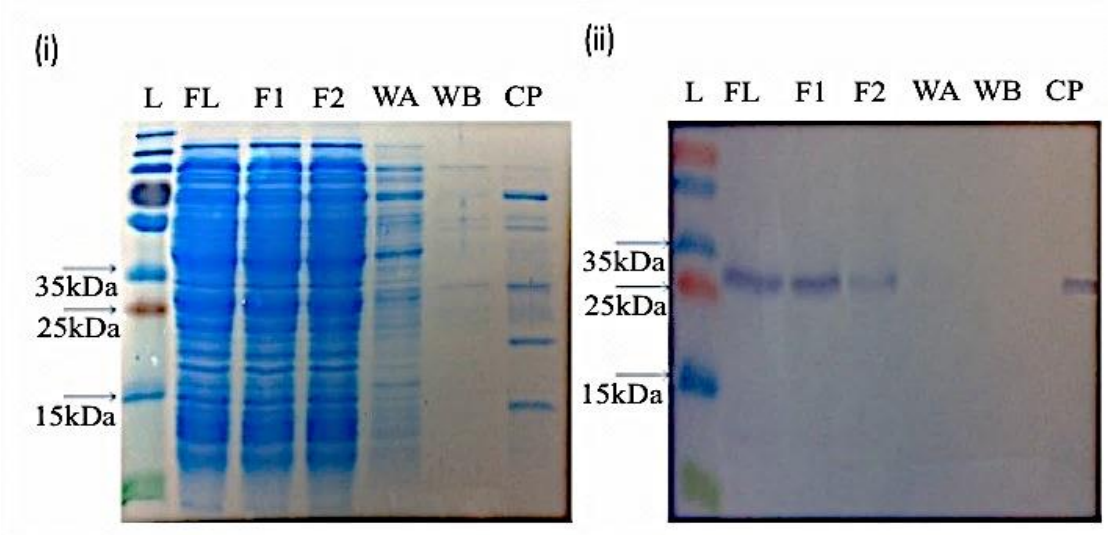

Figure 3.26. SDS-PAGE and WB analysis of the fractions obtained during the purification of SFRP-2 protein.

(i) *SDS-PAGE.*

(ii) *Anti-SFRP-2 Western blot. In (i) and (ii) FL: Filtered lysate from clone number 9 (filtered through 0.45 and 0.22 μM filters). Lanes F1 and F2 contain the "flow-through" with all unbound proteins that passed through the resin. WA: Wash A (15mM Imidazole), WB: Wash B (20mM Imidazole). CP contains the purified concentrated SFRP-2 recombinant fusion protein. This purification was carried out at 4 °C. The ladder, represented by the letter L in this figure, was a Page Ruler Plus pre-stained protein ladder.*

3.5.11 Application of the C-terminal Fusion Cassette to promote soluble protein expression in *E. coli*

3.5.11.1 Optimisation of expression of SFRP-2 using a novel fusion strategy with C-Terminal FABP

The amplified SFRP-2 gene was cloned into a pET28b (+) vector modified to contain a C-terminal h-FABP (Figure 3.29). This experiment was completed in order to analyse the effect that changing the position of the h-FABP would have on the expression of the recombinant SFRP-2 protein. As detailed in section 3.1 – 3.3, the majority of commercially available solubility enhancing fusion proteins function optimally when positioned at the N-terminal of their partner protein.

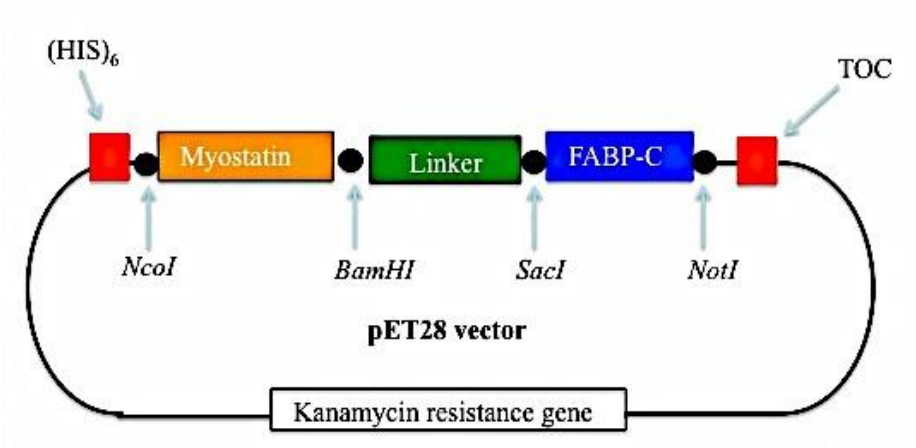

Figure 3.27. Map of pET28b (+)-hFABP vector.

The map indicates the locations of the C-terminal hFABP gene, the linker sequence, the myostatin stuffer molecule, the His-Tag, the kanamycin resistant gene and the restriction sites, SacI, NotI, NcoI, BamHI on the pET28b (+) vector. The 'tag-of-choice' (TOC) site is an optional small amino acid stretch (e.g. HA or FLAG tag) that can be targeted for secondary purification steps, or as a generic handle for detection in immunoassay or oriented capture.

A colony pick PCR was carried out and one of the positive clones, containing the SFRP-2 insert, was brought forward into optimisation of expression studies. All ten clones analysed by the colony pick PCR contained the SFRP-2 insert. Optimisation of expression of the C-terminal FABP-SFRP-2 protein was carried out varying IPTG concentrations, times and temperatures. After 2, 3 and 4 hours a 1mL sample was taken from each sample and centrifuged at 11,000 x g at 4 °C. The cells were lysed with 1mg/mL lysozyme and three freeze thaw cycles were carried out. The samples were then centrifuged as before and 30µL of the supernatant was mixed with SDS-

PAGE loading dye for SDS-PAGE and anti-SFRP-2 Western blot analysis. Additionally the supernatant taken at each time point was analysed by ELISA to ensure the results correlated with the Western blot and SDS-PAGE. Results from the SDS and Western blot show no SFRP-2-specific bands were obtained, indicating that soluble SFRP-2 protein was not produced using this fusion strategy ((Figure 3.30). The ELISA data confirmed the latter (Figure 3.31 and 3.32). These results suggest that the FABP fusion protein promotes soluble SFRP-2 expression only when positioned at the N-terminal of the target protein.

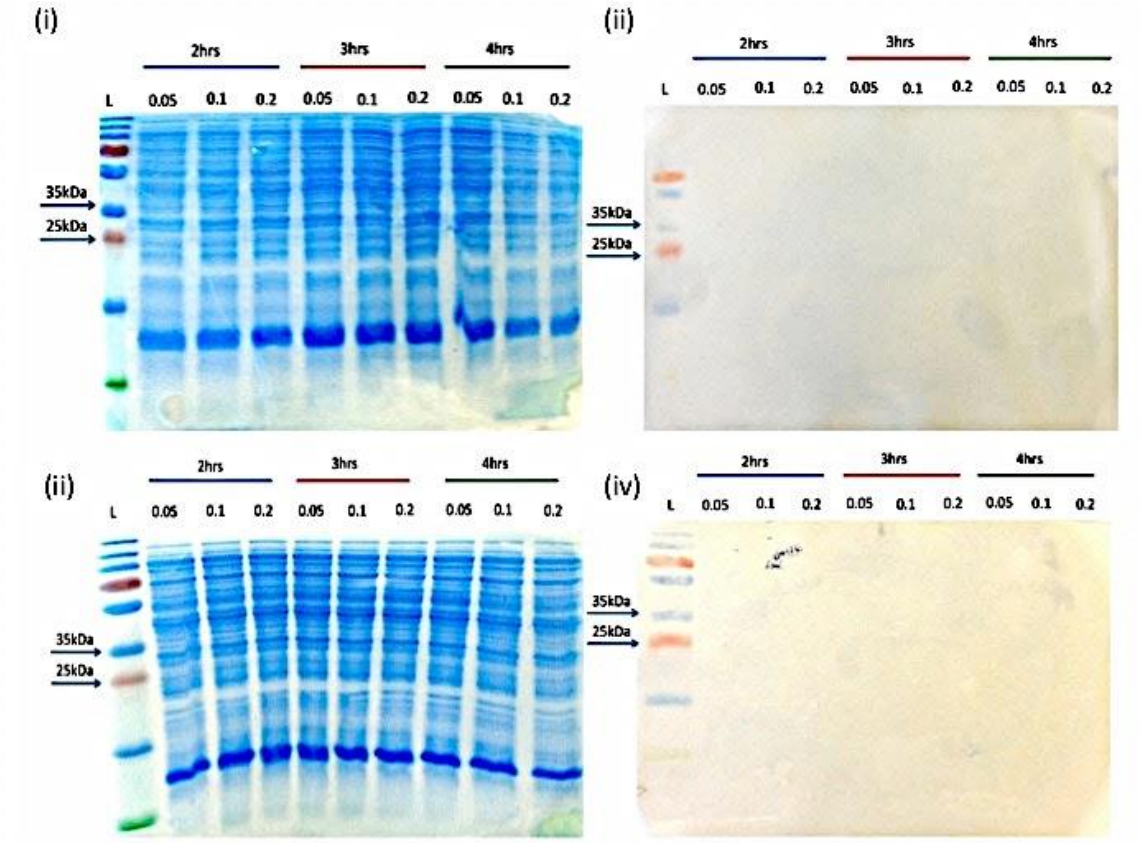

Figure 3.28. Optimisation of expression of SFRP-2 using the C-terminal FABP expression strategy.

Optimisation of expression of SFRP-2 at 20 °C (i) and (ii) and 25 °C (iii) and (iv). (i) and (ii) SDS-PAGE (ii) and (iv) anti-SFRP-2 Western blot. Optimisation of IPTG concentration, time and temperature was completed in order to identify the optimum conditions for production of soluble SFRP-2 protein. The IPTG concentration was varied from 0.05 – 0.2mM. Samples were taken after 2, 3, and 4 hours of induction at the various IPTG concentrations at 20 °C and 25 °C. The ladder, represented by the letter L in this figure, was a Page Ruler Plus pre-stained protein ladder.

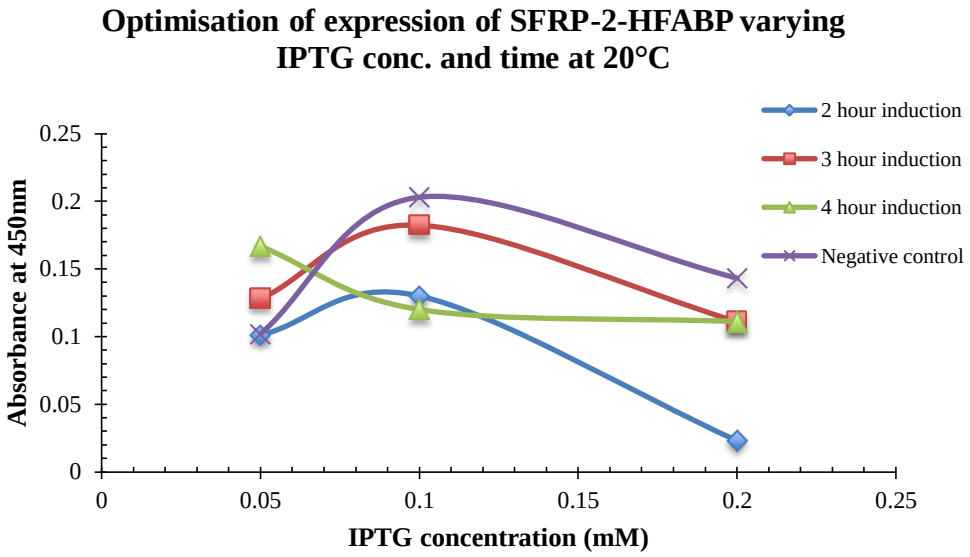

Figure 3.29. ELISA analysis of the optimisation of expression of SFRP-2 at 20 °C.

An ELISA plate was coated with lysate obtained at each time point at 37 °C for 1 hour. Following blocking with 5% (w/v) MM in 1X PBS for 1 hour at 37 °C, the protein was probed with a commercial (suggested to work in WB and ELISA) anti-SFRP-2 polyclonal antibody raised in goat (Abcam) for 1 hour at 37 °C. The plate was washed 3 times with 1X PBS and 1X PBS(T) (0.05% (v/v)). Bound SFRP-2 antibody was detected using an HRP-labelled anti-goat (IgG) secondary antibody. Absorbances were read at 450nm.

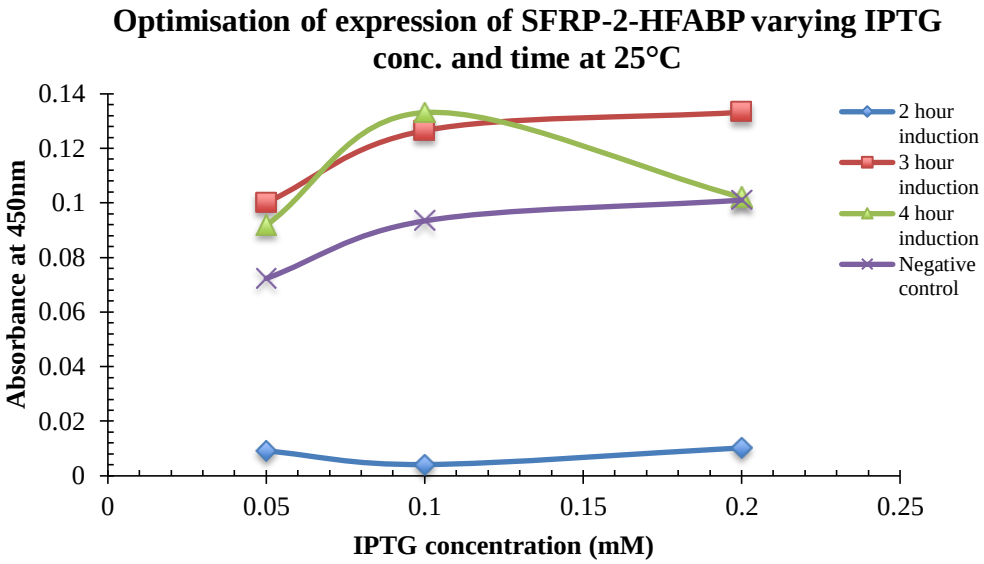

Figure 3.30. ELISA analysis of the optimisation of expression of SFRP-2 at 25 °C.

An ELISA plate was coated with lysate obtained at each time point at 37 °C for 1 hour. Following blocking with 5% (w/v) MM in 1X PBS for 1 hour at 37 °C, the protein was probed with a commercial anti-SFRP-2 polyclonal antibody raised in goat (Abcam) for 1 hour at 37 °C. The plate was washed 3 times with 1X PBS and 1X PBS(T) (0.05% (v/v)). Bound SFRP-2 antibody was detected using an HRP-labelled goat anti-SFRP-2 secondary antibody. Absorbances were read at 450nm.

3.5.12 Soluble expression of a 'difficult-to-express' antibody using a novel expression strategy containing a N-terminally positioned fusion protein

3.5.12.1 Expression of a 'difficult-to-express' antibody using a novel fusion strategy

In addition to SFRP-2, this strategy was applied for the expression of a recombinant anti-cTnI antibody, developed in house, which proved to be 'difficult-to-express'. This study was carried out to complete the 'proof-of-concept' studies behind this novel expression system. The anti-cTnI antibody clone MG4 was amplified using specific primers. The sense primer contains a sequence tail that corresponds to the *Sac*I restriction site and the antisense primer contains a sequence tail that corresponds to the *Not*I restriction site for ligation into pET-28b (+)-hFABP vector. Large-scale amplification (10X) of the anti-cTnI antibody was performed using MyTaq^{TM} Red

Mix DNA polymerase High Fidelity. The amplified gene was resolved by agarose gel electrophoresis (Figure 3.33) and purified through gel extraction. Successful amplification and purification at approximately 800bp was observed.

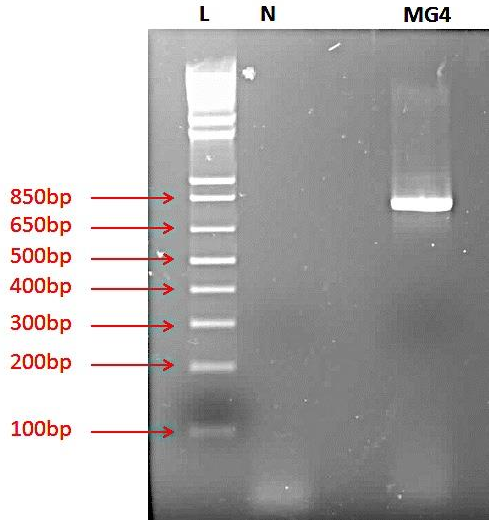

Figure 3.31. Amplification of the anti-cTnI antibody large-scale.

Large-scale amplification of the anti-cTnI antibody (MG4 in this figure) was carried out. The PCR product from this experiment was resolved on a 1.5% (w/v) agarose gel. A band at ~800bp was obtained which was the predicted size of the anti-cTnI antibody. A negative control (N) consisting of all the necessary PCR components in the absence of DNA was included in this PCR in order to ensure no contamination was present in the sample. L represents the ladder in this figure.

3.5.13 Cloning of the anti-cTnI antibody into the pET28b (+)-hFABP vector and subsequent colony pick PCR

The amplified anti-cTnI antibody containing the *Sac*I and *Not*I restriction sites compatible with the pET-28b (+)-hFABP vector was digested with the fast digest *Sac*I and *Not*I restriction enzymes, creating cohesive ends. The pET-28b (+)-hFABP vector was also digested with the fast digest *Sac*I and *Not*I restriction enzymes, creating cohesive ends. The pET-28b (+)-hFABP vector and the anti-cTnI antibody were mixed in a 1:3 (vector: insert) ratio and the cohesive ends were ligated by T4 DNA ligase enzyme. The ligated vector containing the anti-cTnI antibody was next transformed into the chemically competent Tuner (DE3) strain of *E. coli* cells following a heat shock protocol. Transformed colonies were randomly picked from kanamycin-supplemented agar plates and incorporated into a colony pick PCR in order to determine which colonies were harboring the anti-cTnI antibody. A total of 10 colonies were picked, two of which contained the insert (Figure 3.34). Clone 8 was

brought forward for expression studies in order to determine if this novel expression strategy would promote improved soluble expression of the anti-cTnI antibody.

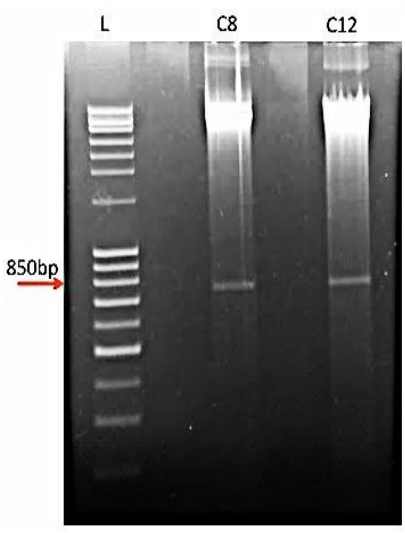

Figure 3.32. Colony-pick PCR for pET28b (+)-hFABP clones.

Visualisation of the positive clones (Clone 8 (C8) and Clone 12 (C12)) identified from a colony pick PCR. The PCR products from this experiment were resolved on 1.5% agarose gels. L represents the ladder in this figure.

3.5.14 Optimisation of expression of the anti-cTnI antibody varying IPTG concentration, induction time and temperature using a novel expression strategy

To determine the optimal induction conditions for the expression of the anti-cTnI antibody in Tuner (DE3) cells a number of different parameters were varied. The IPTG concentration was varied from 0.05mM – 0.2mM at different time courses, varying the temperature from 20 to 25 °C. Clone number 8 was inoculated in 10mL of SB (containing 25µg of kanamycin) and incubated overnight at 37 °C. The following day the overnight sample was subcultured into 6 x 250mL flasks (50mL SB supplemented with 25µg of kanamycin). The samples were then incubated at 37 °C until an $OD_{(600nm)}$ of ~0.7 was obtained. When an $OD_{(600nm)}$ of ~0.7 was obtained, the temperature was reduced to 25 °C for three of the flasks and 20 °C for the remaining three followed by the addition of 0.05mM, 0.1mM, and 0.2mm IPTG. After 2, 3 and 4 hours a 1mL sample was taken from each sample and centrifuged in a bench-top centrifuge at 11,000 x g at 4 °C. The cells were lysed with 1mg/mL lysozyme and three freeze thaw cycles were carried out. The samples were then centrifuged as before and 30µL of the supernatant was mixed with SDS-PAGE loading dye for SDS-

PAGE and anti-His Western blot analysis. Successful soluble expression of this 'difficult-to-express' antibody was achieved using the N-terminal expression cassette at both temperatures included in the optimisation studies. Optimum expression of this antibody was achieved at 20 °C after 2 hours of induction with 0.1mM IPTG.

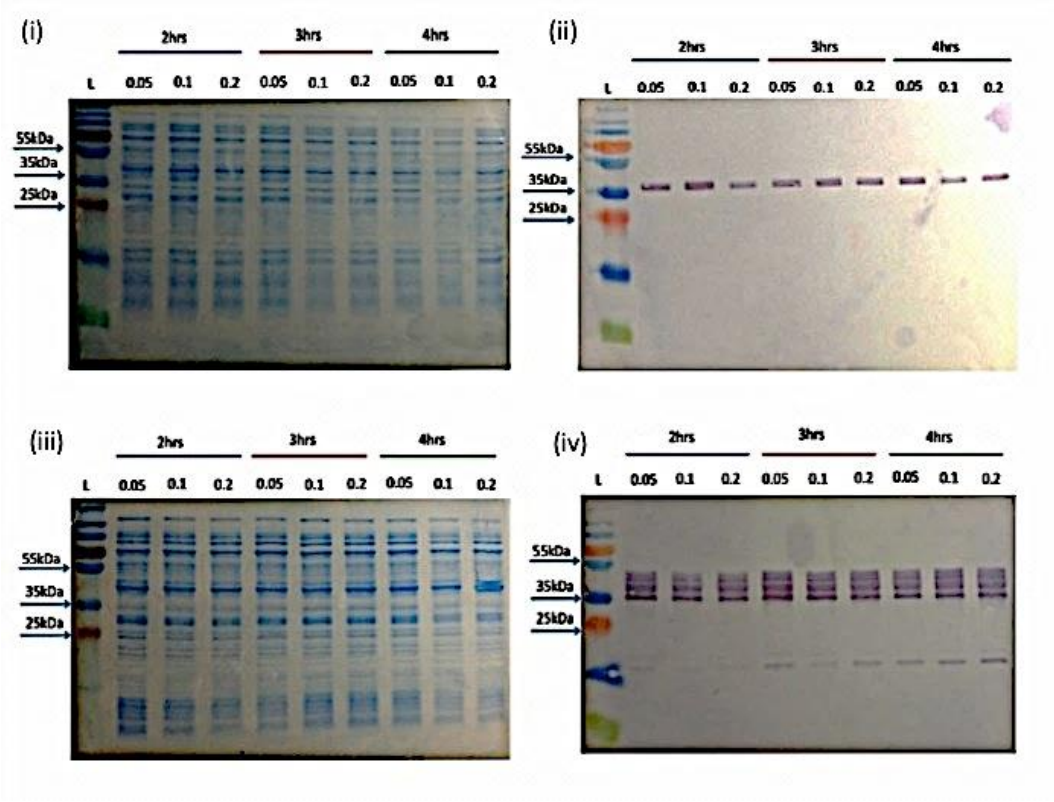

Figure 3.33. Optimisation of expression of anti-cTnI antibody using the N-terminal FABP expression strategy.

Optimisation of expression at 20 °C (i) and (ii) and 25 °C (iii) and (iv). The corresponding SDS-PAGE (i) and (iii) anti-His Western blotting (ii) and (iv) outputs are shown. Optimisation of IPTG concentration, time and temperature was completed in order to identify the optimum conditions for the anti-cTnI antibody. The IPTG concentration was varied from 0.05 – 0.2mM. Samples were taken after 2, 3, and 4 hours (hrs) of induction at the various IPTG concentrations at 20 °C and 25 °C. The ladder, represented by the letter L in this figure, was a Page Ruler Plus pre-stained protein ladder.

3.5.15 Soluble expression of a difficult to express antibody using a novel expression strategy containing a C-terminally positioned fusion protein

3.5.15.1 Optimisation of expression of anti-cTnI clone MG4 using a novel fusion strategy with C-Terminal FABP

The amplified anti-cTnI antibody was cloned into a pET28b (+) vector modified to contain a C-terminal h-FABP to determine the effect that changing the position of the

h-FABP protein would have on the expression of the recombinant antibody. A colony pick PCR was carried out and the positive clone, containing the anti-cTnI insert, was brought forward for expression. Optimisation of expression of the C-terminal FABP-anti-cTnI antibody was carried out varying IPTG concentration, time and temperature. After 2, 3 and 4 hours a 1mL sample was taken from each sample and centrifuged in a bench-top centrifuge at 11,000 x g at 4 °C. The cells were lysed with 1mg/mL lysozyme and three freeze thaw cycles were carried out. The samples were then centrifuged as before and 30µL of the supernatant was mixed with SDS-PAGE loading dye for SDS-PAGE and anti-His Western blotting analysis. Results from the SDS and Western blot show no anti-cTnI antibody-specific bands were obtained, indicating that soluble antibody was not produced using this fusion strategy (Figure 3.36). These results confirm, as with the SFRP-2 protein, that the FABP fusion protein promotes soluble expression when positioned at the N-terminal of the target protein.

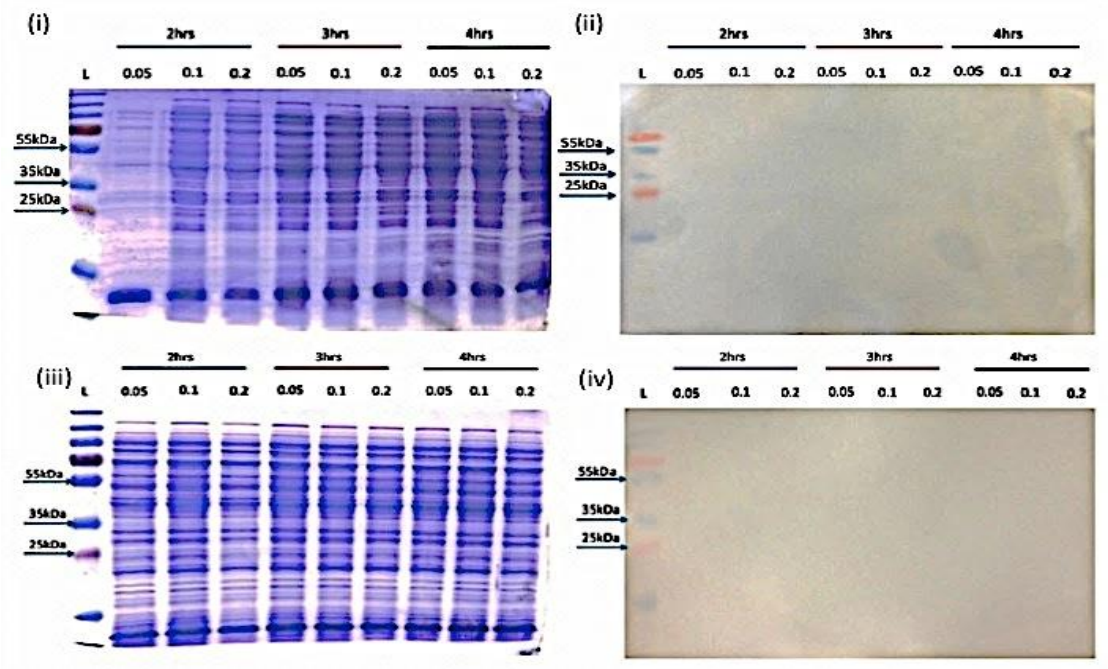

Figure 3.34. Optimisation of expression of the anti-cTnI antibody using the C-terminal FABP expression strategy.

Optimisation of expression at 20 °C (i) and (ii) and 25 °C (iii) and (iv). The corresponding SDS-PAGE (i) and (iii) anti-HIS Western blotting (ii) and (iv) outputs are shown. Optimisation of IPTG concentration, time and temperature was completed in order to identify the optimum conditions for production of soluble anti-cTnI antibody. The IPTG concentration was varied from 0.05 – 0.2mM. Samples were taken after 2, 3, and 4 hours of induction at the various IPTG concentrations at 20 °C

and 25 °C. The ladder, represented by the letter L in this figure, was a Page Ruler Plus pre-stained protein ladder.

3.6 Discussion and Conclusion

Proteins are now widely produced in diverse microbial cell factories. The benefits of cost, ease-of-use and scale make *E. coli* one of the most widely used host systems for recombinant protein production, but one must be aware that success is not always guaranteed in this prokaryotic host system, especially when working with recombinant proteins of human origin, such as SFRP-2 (Costa *et al.,* 2014). With the aid of genetic and protein engineering, novel tailor-made strategies can be designed to suit users or process requirements. Gene fusion technology has been widely implemented for the improvement of soluble protein production and/or purification in *E. coli*. New fusion partners are constantly emerging and complementing the traditional solutions, such as the Fh8 fusion tag that has been recently studied and ranked among the best solubility enhancer proteins. This chapter described the rationale behind the application of a novel fusion strategy for the enhanced expression and solubility of a 'difficult-to-express' protein and antibody that offers advantageous characteristics not provided by current fusion tags such as MBP, NusA or GST.

3.6.1 A novel fusion strategy to enhance the soluble expression of a 'difficult-to-express' protein, SFRP-2

The codon optimised SFRP-2 gene sequence was cloned into two separate pET28b (+) expression vectors modified to contain novel fusion cassettes. The expression cassettes outlined in Figure 3.15 and Figure 3.29 comprise a N- (Figure 3.15) or C-terminally (Figure 3.29) positioned fusion protein, namely heart fatty acid binding protein, to facilitate the expression of 'difficult-to-express' proteins.

Post Tuner *E. coli* transformation of the intact pET28b (+)-hFABP plasmids containing the SFRP-2 gene inserts, optimisation of expression studies commenced. Optimisation of IPTG concentration, time and temperature was carried out to identify the optimum conditions for soluble SFRP-2 expression. The level of recombinant protein expression is greatly affected by inducer concentration. High concentration of IPTG can lead to the production of insoluble, aggregated protein. Hence, for this study, low IPTG concentrations (0.05mM, 0.1mM and 0.2mM) were applied.

Generally the optimum temperature for recombinant protein production in *E. coli* is 37 °C (Sadeghi *et al.*, 2011). However, studies have demonstrated that rate of expression and culture temperature can affect the proper folding of recombinant proteins and inclusion body formation (Li *et al.*, 2009). Reducing culture temperature potentially leads to slower growth of bacteria, slower rate of protein production and lower aggregation of target protein (Vera *et al.*, 2007). Therefore, for the purpose of this study, it was concluded that low induction temperatures were essential to promote soluble protein production. From the optimisation of expression studies, applying the N-terminally positioned hFABP fusion protein cassette, soluble SFRP-2 protein was obtained using 0.05mM IPTG at 25 °C after 4 hours of induction. Results from the expression studies applying the C-terminal hFABP cassette indicated a lack of soluble protein production, suggesting that this fusion partner is more effective at the N-terminal of the target protein. The His-tag incorporated into the fusion cassette allowed for one-step purification of the soluble SFRP-2 recombinant protein, using IMAC post large-scale expression. Sufficient protein yield (1mg/mL) was achieved, and an avian immunisation campaign commenced applying this protein for the subsequent production of anti-SFRP-2 recombinant antibodies (Chapter 4).

3.6.2 A novel fusion strategy to enhance the soluble expression of a 'difficult-to-express' anti-cTnI antibody

In addition to SFRP-2, this novel fusion strategy for enhanced soluble protein expression was applied for the expression of a 'difficult-to-express' anti-cTnI scFv antibody. Currently, the soluble expression of scFv antibodies remains an awkward problem. Thus, the majority of work in this field focuses on developing a strategy based on molecular manipulation to improve the stability and solubility of these antibodies. A number of methods have been applied to express scFv antibodies, including expression of affinity tag fusion (Esposito & Chatterjee, 2006), co-expression of molecular chaperones, and folding modulators (De Marco & De Marco, 2004; Sonoda *et al*., 2011), extracellular accumulation in a defined medium (Fu, 2010), refolding scFv using detergent and additive (Kudou *et al*., 2011) and expression in different host systems (Goulding & Perry, 2003). The anti-cTnI scFv antibody was amplified and cloned into the two fusion cassettes presented in this study and optimisation of expression studies as completed by varying the same

parameters as with the SFRP-2 protein. Based on the data obtained from the SDS-PAGE and WB results, it is clear that the N-terminally positioned hFABP protein greatly enhanced the soluble expression of this antibody. Clear anti-cTnI-specific soluble expression bands were obtained after 2 hours of induction, and remained consistent at each IPTG concentration and time point for both the 20 °C and 25 °C samples. Cleaner expression of the scFv was achieved at 20 °C, with an optimum IPTG concentration of 0.1mM after 2 hours. The results from the expression studies of this scFv using the N-terminal FABP cassette, correlated with the SFRP-2 data, confirming that the hFABP protein is more effective as a fusion partner when positioned at the N-terminal of its target protein.

The expression strategy presented here provides unique characteristics that none of the current systems can provide. The fusion of a FABP protein for improved heterologous expression of proteins/peptides is completely novel. FABP is a stable cytoplasmic human protein that yields soluble fusion protein when positioned at the N-terminal of the target protein. As a stable, soluble, obligately monomeric human protein, it is predicted to function equally well in yeast and mammalian cells in addition to the prokaryote system. Due to the novelty of this work an invention disclosure form (IDF) was generated and is now being examined for patentability with initial responses indicating significant potential and possible commercial value. A Nature Methods paper is in preparation but will not progress until the intellectual property (IP) is fully protected.

Chapter 4

Generation and characterisation of an anti-SFRP-2 recombinant antibody

Chapter outline

Secreted frizzled related protein-2 (SFRP-2) is a novel immunohistochemical marker in PCa (O'Hurley *et al.*, 2011) and is proposed as a key marker of histochemically benign glands and a subgroup of Gleason grade 5 tumours that may predict prognosis. Additionally, the epigenetic biomarker discovery group has shown that SFRP-2 hypermethylation is a common event in prostate cancer and SFRP-2 methylation in combination with other epigenetic markers may be a useful biomarker of PCa.

This chapter describes the production and isolation of avian anti-SFRP-2 polyclonal and recombinant antibodies. The focus of this chapter is the use of phage display technology for the production of recombinant avian anti-SFRP-2 scFv. A chicken was subjected to a standard immunisation routine with a purified SFRP-2 protein expressed using a novel fusion strategy (Chapter 3). After each injection, a bleed was taken, and the serum titre analysed. Following 4 boosts, the spleen and bone marrow cells were harvested from the chicken and the RNA was subsequently extracted. This RNA was converted to cDNA and a scFv library was constructed. The library was panned against a mammalian SFRP-2 protein, to enrich and select for SFRP-2 binders. Monoclonal ELISA and Biacore analysis was performed on 384 scFv antibodies to identify single clones exhibiting SFRP-2 binding. The lead anti-SFRP-2 scFv antibody was subsequently characterised by ELISA and Western blotting. Reformatting this scFv to a scAb led to a significant improvement in expression. IHC analysis applying this scAb is currently underway in Beaumont Hospital.

4.1 Epigenetic abnormalities in Prostate cancer

Secreted Frizzled Related Protein-2 (SFRP-2), a novel immunohistochemical marker in PCa, functions as a negative modulator of the Wingless (WNT) signalling transduction pathway. The WNT signalling transduction pathway is essential for numerous biological processes and abnormal activation or deactivation of this pathway is suggested to play a role in the development of many cancers, including PCa.

Results obtained from a recent study carried out by the epigenetic biomarker discovery group suggest SFRP-2 hypermethylation as a common event in PCa. Epigenetic aberration of the SFRP-2 gene could potentially alter or inhibit the function of this gene in the WNT signalling pathway, possibly leading to the development or progression of PCa. The following section provides a detailed background into the most common epigenetic aberrations in PCa and the effect that epigenetic aberrations have on genes that regulate the WNT signalling pathway, such as SFRP-2.

PCa is the most commonly diagnosed non-skin malignancy and the second most common cause of cancer-associated death among men worldwide. It is well established that cancer is a disease driven by progressive genetic and epigenetic abnormalities (Perry *et al.*, 2010; Hanahan & Weinberg, 2011). Epigenetics is the study of genetic changes in gene expression that are not caused by changes in the underlying DNA sequences (Albany *et al.*, 2011). Unlike mutations, which result in permanent changes in the sequence of DNA, epigenetic aberration does not alter the coding sequence of genes (Albany *et al.*, 2011). Instead, it induces conformational changes in the double helix of DNA and modifies access of transcription factors to promoter regions upstream of coding sequences (Perry *et al.*, 2010; Albany *et al.*, 2011; Hanahan & Weinberg, 2011). The field of epigenetics has rapidly evolved and influenced research in different biological phenotypes such as aging, memory formation, and embryological development. DNA methylation, histone modifications, nucleosome remodeling and RNA-associated silencing are the most common epigenetic mechanisms that have demonstrated critical roles in cancer growth and metastasis (Albany *et al.*, 2011).

The most prominent epigenetic aberrations in PCa are DNA methylation and histone modifications. DNA methylation is an essential regulator of gene transcription, and the role it plays in cancer has been a topic of considerable interest for a number of years (Goering *et al.*, 2012; Yang *et al.*, 2012). It is a covalent chemical modification catalyzed by DNA methyltransferases (DNMTs), resulting in the addition of a methyl ($-CH_3$) group to the 5'-carbon of cytosine in CpG sequences (Li *et al.*, 2005). To date only three active DNA methyltransferase, have been identified in mammals: (DNA (cytosine-5)-methyltransferase 1 (*DNMT1*), DNA (cytosine-5)-methyltransferase 3A (*DNMT3A*), and DNA (cytosine-5)-methyltransferase 3B (*DNMT3B*)) (Albany *et al.*, 2011). *DNMT1*, the most abundant DNA methyltransferase in mammalian cells, is a large, highly dynamic enzyme that is principally responsible for the maintenance of the cell methylation profile, in addition to *de novo* methylation of tumour suppressor genes (Albany *et al.*, 2011). *DNMT3A* and *DNMT3B* are responsible for maintenance and *de novo* methylation activities and play a functional role in the wave of methylation that occurs during embryogenesis (Albany *et al.*, 2011). Aberrations in DNA methylation can occur as either hypo- (a decrease in the epigenetic methylation of cytosine and adenosine residues in DNA) or hypermethylation (increase in the epigenetic methylation of cytosine and adenosine residues in DNA), which can result in chromosomal instability and transcriptional gene silencing (Li *et al.*, 2005). Both forms have been implicated in a plethora of human malignancies, including PCa.

The second type of epigenetic aberration in PCa is histone modifications. Histones are alkaline proteins found in eukaryotic cell nuclei that package and order DNA into nucleosomes. They are subject to a wide variety of post-translational modifications including acetylation, methylation, phosphorylation, and ubiquitination by specific chromatin-modifying enzymes (Li *et al.*, 2005). These modifications occur primarily within the histone amino-terminal (N-terminal) tails, positioned peripheral to the nucleosome core, as well as on the globular core region (Cosgrove *et al.*, 2004; Li *et al.*, 2005). There are three key enzymes involved in the regulation of histone modification, namely, histone deacetylases (HDACs), histone acetyltransferases (HAT), and histone methyltransferases. The rate of acetylation and methylation of specific lysine residues contained within the tails of nucleosomal core histones is known to have a critical role in regulating chromatin structure and gene expression (Albany *et al.*, 2011). Histone modifications, together with DNA methylation, play a

pivotal role in organizing nuclear architecture, which, in turn, is involved in regulating transcription and other nuclear processes (Albany *et al.*, 2011). Variations or aberrant alterations of histone modification patterns have the potential to affect the structure and integrity of the genome and to disrupt normal patterns of gene expression, which could be key factors in many cancers including PCa (Albany *et al.*, 2011). Histone acetylation mediated by HATs is correlated with transcriptional activation and leads to an increase in gene expression. "Histone deacetylation mediated by HDACs is linked to gene silencing. The removal of acetyl groups from histone proteins creates non-permissive chromatin conformation that prevents the transcription of genes that encode proteins involved in tumourigenesis. Histone methylation on arginine and lysine can be associated with either gene activation or suppression depending on the amino acid position and the number of methylated residues (Albany *et al.*, 2011)."

These two epigenetic regulatory mechanisms, DNA methylation and histone modifications, are closely related. Successful epigenetic control of gene expression often requires the cooperation and interaction of both mechanisms, and disruption of either processes leads to aberrant gene expression seen in almost all human cancers (Li *et al.*, 2005).

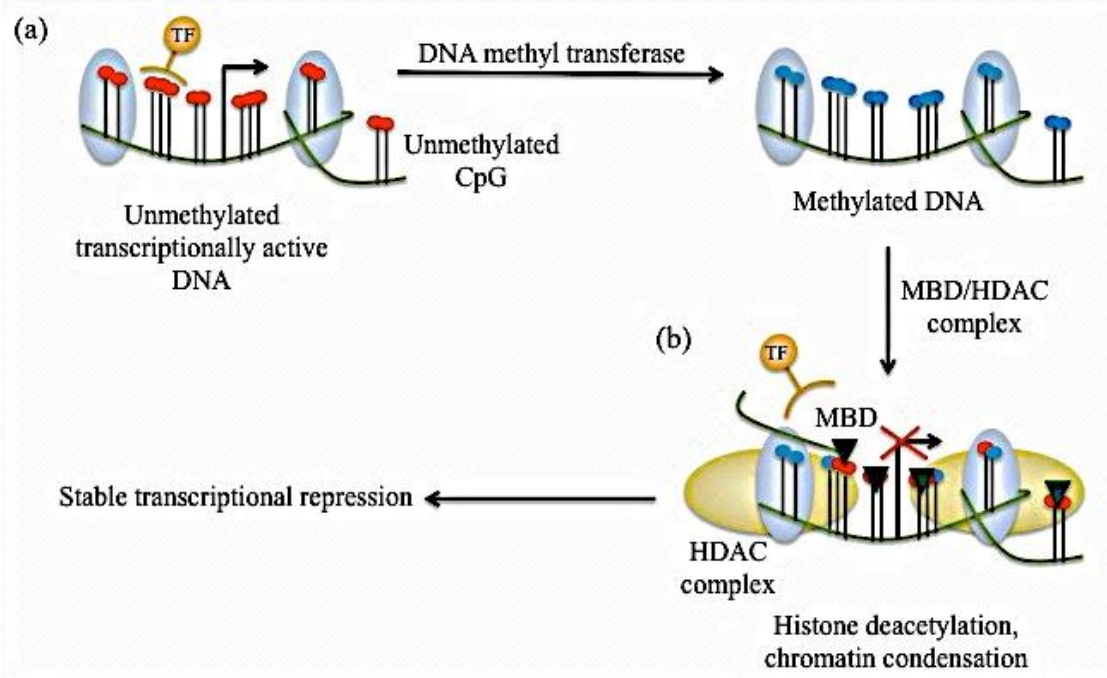

Figure 4.35. Epigenetic mechanisms of gene expression silencing.

(a) *In unmethylated DNA (depicted by red filled-in circles on the left) transcription factors (TF) are free to bind gene promotor regions. In hypermethylated DNA (depicted in blue filled-in circles on the right) TF are blocked from binding to gene promotor regions, leading to functional silencing of gene expression.*
(b) *Histone deacetylation by methyl-CpG-binding domain protein (MBD)/histone deacetylase (HDAC) complexes promotes a condensed structure which inhibits normal gene transcription. (Adapted from Albany et al., 2011).*

Targeting epigenetic regulation of gene expression has become a very appealing topic of investigation in diseases such as cancer from a therapeutic viewpoint. The ability to reverse epigenetic aberrations, for example, with modulators that can demethylate DNA, inhibit histone deacetylases and reactivate silenced genes, has made them very attractive targets for cancer treatment (Cameron *et al.*, 1999; Ou *et al.*, 2007; Li *et al.*, 2005). Moreover, the detection and quantification of specific methylation patterns of genes in biopsies or bodily fluids such as urine and serum could be hugely beneficial diagnostically. Several reviews have recently highlighted the importance of epigenetics in PCa initiation and progression (Gonzalgo & Isaacs, 2003; Diaw *et al.*, 2007; Knudsen & Vasioukhin, 2010). Among all recognised epigenetic alterations, promotor hypermethylation is the most important and best characterised change in PCa (Majumdar *et al.*, 2010). Aberrant DNA methylation, particularly hypermethylation, in PCa is especially documented, leading to the silencing of many

classic tumour suppressor genes such as p16, APC, RASSF1A, as well as hormone response genes like AR, ER, RARβ2, cell adhesion genes such as CD44, ECAD, TIG1, TSLC1, cell cycle control genes including CCND2 and CDKN4, and anti-apoptotic genes such as DCR1, DCR2, DAPK, RTVP1.

Epigenetic mechanisms play a crucial role in cellular proliferation, migration and differentiation in both normal and neoplastic development. One of the key signaling pathways whose components are altered through the epigenetic mechanisms is the Wingless (WNT) signaling pathway.

4.1.1 Wingless (WNT) signalling

The WNT signaling pathway plays an important role in embryonic development, tissue homeostasis, carcinogenesis and neurodegenerative diseases (Surana *et al.*, 2014). The embryonic processes this pathway controls include cell proliferation, migration and differentiation (Surana *et al.*, 2014). These processes are essential for accurate formation of tissues including bone, heart and muscle. Cancer is the most commonly studied disease related to dysregulation of the WNT signalling pathway. Aberrant activation of the WNT pathway has been shown to be associated with tumour development, tumour progression and metastatic spread in various human cancers including colorectal cancer (Giles *et al.*, 2003; Lustig & Behrens, 2005), melanoma (Larue *et al.*, 2006), non-small cell lung cancer (NSCLC) (Stewart *et al.*, 2014), leukemia (Thanendrarajan *et al.*, 2011), mesothelioma (Uematsu *et al.*, 2003), and prostate cancer (O'Hurley *et al.*, 2011; Surana *et al.*, 2014). WNT signalling pathways are characterised as β-catenin dependent (canonical) and β-catenin independent (non-canonical). All three WNT pathways (described below) are activated by the binding of a WNT-protein ligand to a Frizzled family receptor, which passes the biological signal to the protein, Dishevelled, inside the cell (Shi *et al.*, 2007). WNT-proteins are a diverse family of secreted lipid-modified signalling glycoproteins that are 300-400 amino acids in length. In WNT signalling, these WNT-proteins act as ligands to activate different WNT pathways.

4.1.2 The Canonical WNT signalling pathway

β-catenin is a key mediator in the canonical WNT signalling pathway. During the inactive ('WNT-off') state no WNT ligand binds to the frizzled/low density lipoprotein receptor-related protein (LRP) receptor complex (Shi *et al.*, 2007; Komiya

& Habas, 2008; Surana *et al.*, 2014). Thus, β-catenin is bound by a multi-protein destruction complex that consists of adenomatous polyposis coli (APC), Axin, and glycogen synthase kinase-3β (GSK-3β). At this point, β-catenin is phosphorylated by GSK-3β and targeted to undergo ubiquitin-mediated proteasomal degradation.

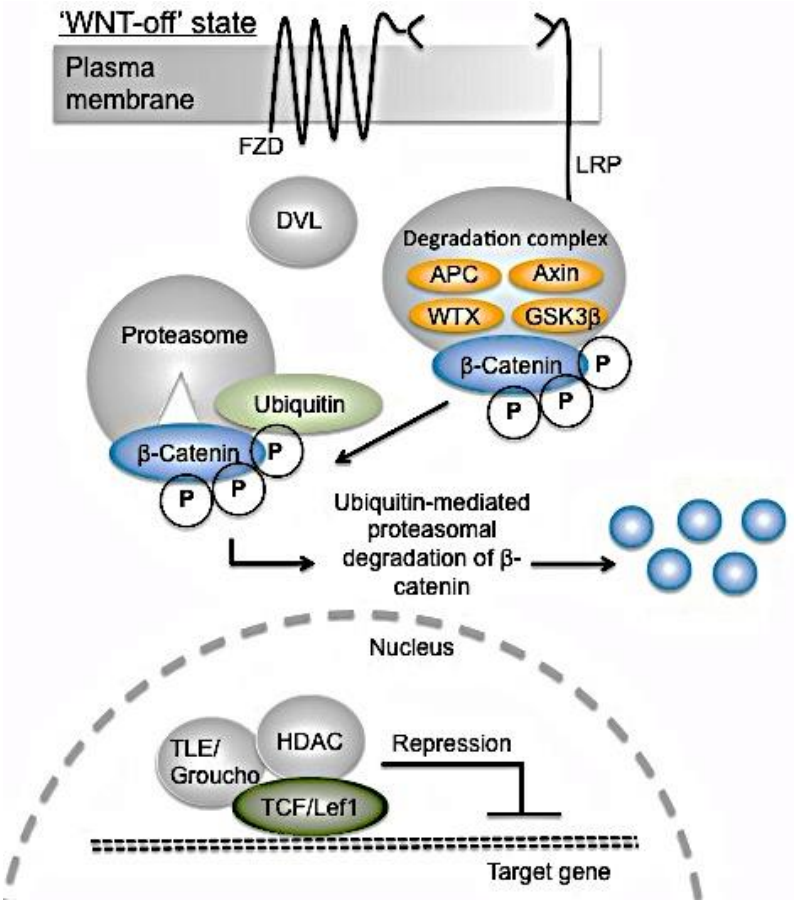

Figure 4.36. 'WNT-off' state.

In the absence of WNT ligands a β-catenin degradation complex (containing axin, APC (adenomatous polyposis coli), WTX, and GSK3β) promotes N-terminal phosphorylation of β -catenin. This leads to ubiquitin-mediated proteasomal degradation of β-catenin and keeps its intracellular levels low. Meanwhile, TCF/Lef1 type transcription factors recruit TLE/Groucho and histone deacetylases (HDAC) to repress WNT target genes. The abbreviations used in this figure are: APC, adenomatous polyposis coli; GSK, glycogen synthase kinase, WTX, Wilms tumour gene on the X-chromosome. (Adapted from Schmidt-Ott & Barasch, 2008).

In the activated ('WNT-on') state, WNT ligand binds to the FZD membrane receptor protein and low-density lipoprotein receptor-related proteins (LRP-5/6) (Surana *et al.*, 2014). This binding interaction causes axin and the phosphoprotein disheveled (DVL)

to bind to phosphorylated LRP5/6, which inhibits the function of the destruction complex and leads to an increased level of β-catenin in the cytoplasm (Komiya & Habas, 2008; Surana *et al.*, 2014). The accumulated β-catenin translocates to the nucleus to interact with members of the T-cell factor/lymphocyte enhancer factor (TCF/LEF) family of transcription factors (Surana *et al.*, 2014). This interaction promotes the expression of WNT-response genes.

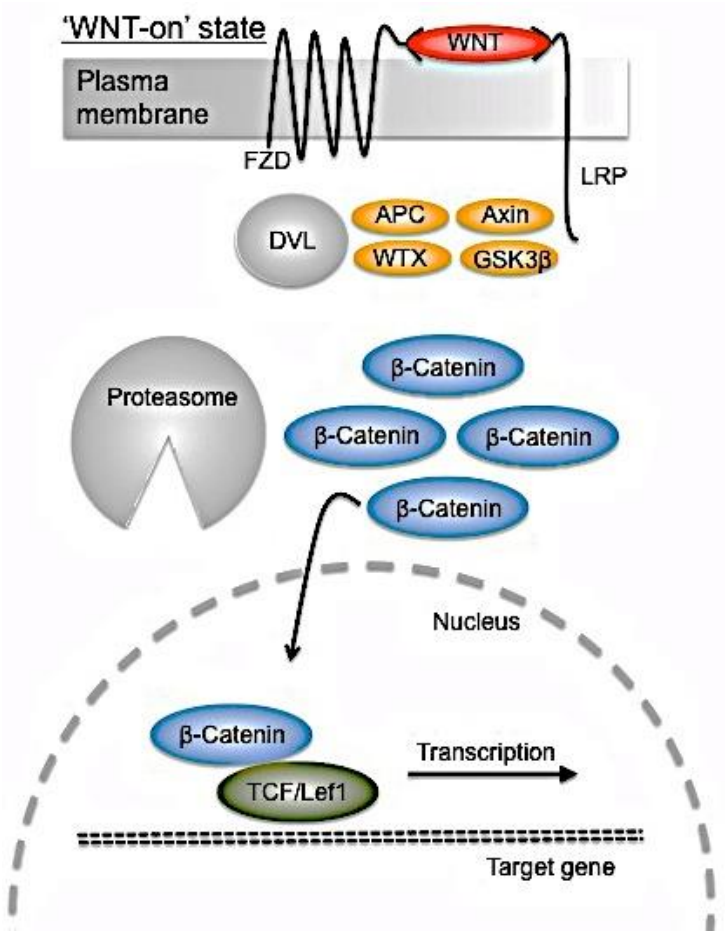

Figure 4.37. 'WNT-on' state.

Once WNT ligands bind to FZD (Frizzled)/LRP (lipoprotein receptor-related protein) co-receptors, the β-catenin degradation complex is inhibited through recruitment of its components to the FZD/LRP/DVL (Dishevelled) complex. Consequently, β -catenin accumulates intracellularly, translocates to the nucleus, and displaces transducin-like enhancer protein (TLE)/Groucho from T cell-specific transcription factor/lymphoid enhancer-binding factor 1(TCF/Lef1). This interaction promotes the transcription of WNT target genes. The abbreviations used in this figure are: APC, adenomatous polyposis coli; GSK, glycogen synthase kinase, WTX, Wilms tumour gene on the X-chromosome. (Adapted from Schmidt-Ott & Barasch, 2008).

4.1.3 The Non-Canonical WNT signalling pathway

The non-Canonical WNT signalling pathways, similar to the Canonical pathway, are activated when a WNT ligand binds to a frizzled family receptor, but differ in their dependency on the type of G-protein they require for activation (Surana *et al.*, 2014). These pathways do not stimulate accumulation of β-catenin and do not require phosphorylation of all three domains of the dishevelled protein (Dsh) for signal transduction. The two non-canonical pathways are able to antagonise the function of the canonical pathway, activate a variety of signalling cascades and trigger the transcription of different gene-sets (Komiya & Habas, 2008; Surana *et al.*, 2014).

4.1.4 The Non-Canonical WNT/Ca^{2+} pathway

The Non-Canonical WNT/Ca^{2+} pathway functions to control protein kinase C (PKC) and calcium/calmodulin-dependent kinase II (CamKII) and regulates cell adhesion and motility. In the Non-Canonical WNT/Ca^{2+} pathway, when a WNT ligand binds to a Fzd receptor, the intracellular concentration of calcium is increased which results in the activation of a number of enzymes (Komiya & Habas, 2008; Surana *et al.*, 2014). These enzymes include CamKII, PKC and calcineurin. The activation of these enzymes leads to activation of nuclear factors of activated T-cells (NF-AT). NF-AT is a family of transcription factors (NFATc1, NFATc2, NFATc3, NFATc4, and NFAT5) that are regulated by calcium signaling (Komiya & Habas, 2008). The NF-AT family can regulate activation-induced transcription of several immunologically important genes and are known to play a role in the development of cardiac and skeletal muscle, and of the nervous system.

4.1.5 The Non-Canonical WNT/JNK pathway

In the Non-Canonical WNT/JNK pathway or the planar cell polarity pathway, frizzled activates JUN-N-terminal kinase (JNK) and directs asymmetric cytoskeletal organization and coordinated polarization of cells within the plane of epithelial sheets. This pathway involves the cadherin-related transmembrane molecule flamingo (Fmi), the proteoglycan knypek (Kny), and the PDZ molecule strabismus (Stbm) and branches at the level of Dsh from the canonical pathway (Komiya & Habas, 2008). Dishevelled (Dsh) is connected via dishevelled associated activator of morphogenesis 1 (Daam1) to downstream effectors such as the small GTPase Rho and Rho-associated kinase (ROCK). The product of the WNT target gene *naked* (Nkd) was

recently identified as an antagonist for WNT signaling that binds to Dsh and blocks β-catenin but stimulates the JNK pathway (Rousset *et al.*, 2001).

4.1.6 Regulation of the WNT signalling pathway

Several classes of negative modulators partially regulate the WNT signalling pathways. These antagonists can be divided into two classes based on their mechanism of action. The first class of antagonists includes the secreted frizzled related protein (SFRP) family, WNT inhibitory factor (WIF)-1 and Cerberus (Surana *et al.*, 2014). These types of antagonists bind to WNT proteins in addition to FZD and are capable of blocking all WNT signalling pathways. The second class of antagonists, which consists of members of the Dickkopfs (DKKs) family, are able to bind to WNT co-receptors LRP5/6 and can inhibit only the canonical β–catenin pathway (Surana *et al.*, 2014).

4.1.6.1 Secreted Frizzled Related Protein (SFRP) Family and SFRP-2

Secreted frizzled related proteins (SFRPs), the first WNT antagonists to be identified, are secreted glycoproteins that regulate the WNT signal transduction pathway. SFRPs are modular proteins, which fold into two separate domains (Bovolenta *et al.*, 2008). Their N-terminus contains a secretion signal peptide followed by a 'cysteine-rich' domain (CRD), which is composed of ten cysteine residues at conserved positions (Bovolenta *et al.*, 2008). These cysteine residues form a pattern of disulphide bridges. The CRD of SFRPs shares 30-50% sequence similarity with the CRD of Fzd proteins (Shi *et al.*, 2007). Due to this sequence similarity, SFRPs may interact with WNT ligands and antagonise WNT signalling. Alternatively, the CRD of SFRPs could interact with Fzd to form non-functional complexes, thereby interfering with the WNT signalling pathway. The C-terminal of SFRPs contains segments of positively charged residues, which confer heparin-binding capacity, and a netrin (NTR) domain which is defined by six cysteine residues, that form three disulphide bridges (Shi *et al.*, 2007; Bovolenta *et al.*, 2008). The function of the NTR domain in SFRPs is not well defined (Shi *et al.*, 2007) and the role it plays in the WNT signalling pathway is yet to be discovered. The SFRP family is made up of five members; SFRP-1, SFRP-2, SFRP-3, SFRP-4 and SFRP-5. The chromosomal locations of SFRP-1, SFRP-2 and SFRP-5 are 8p12-p11.2, 4q31.3 and 10q24.1, respectively, and SFRP-3 and 4 are

encoded by six exons on chromosomes 2q31-q33 and 7p14-p13, respectively (Shi *et al.*, 2007).

Secreted frizzled related protein-2 (SFRP-2) is a novel immunohistochemical marker in PCa (O'Hurley *et al.*, 2011). Under non-malignant conditions, SFRP-2 acts as a negative modulator of the wingless (WNT) signalling pathway by interacting with the WNT proteins, through their 'cysteine-rich' domain (CRD), and preventing frizzled (FZD) receptors from binding to WNT ligands (Surana *et al.*, 2014). Epigenetic inactivation of SFRP-2 by promoter hypermethylation has been reported for human gastric cancer (Cheng *et al.*, 2007), colorectal cancer (Huang *et al.*, 2007; Oberwalder *et al.*, 2008; Wang *& Tang*, 2008), breast cancer (Suzuki *et al.*, 2008; Veeck *et al.*, 2008) and prostate cancer (PCa) (O'Hurley *et al.*, 2011), suggesting that SFRP-2 plays a role in tumour suppression. In a study by O'Hurley *et al*. (2011), immunohistochemical analysis on prostate cancer tissue microarrays with samples from 216 patients was conducted. A strong to moderate cytoplasmic SFRP-2 expression was observed in benign prostatic hyperplasia (BPH) epithelium and negative to weak expression was observed in tumour epithelium particularly in Gleason grade 3 and 4. However, in Gleason grade 5 carcinoma there was a 40:60 split in the immunoexpression of SFRP-2, where 40% displayed strong cytoplasmic SFRP-2 expression and 60% displayed negative SFRP-2 expression in epithelial cells. A morphological difference was noted in the Gleason grade 5 tumours that had strong expression of SFRP-2 (Type A) and the Gleason grade 5 tumours that had no SFRP-2 expression (Type B). It was also noted that biochemical recurrence occurred after 5 years in all patients that had strong SFRP-2 expression in Gleason grade 5 tumours with "Type A" morphology and no evidence of biochemical recurrence occurred in patients with negative SFRP-2 expression in Gleason grade 5 tumours with "Type B" morphology. These results propose SFRP-2 as a key marker of histochemically benign glands and a subgroup of Gleason grade 5 tumours that may predict prognosis and biochemical recurrence.

4.1.6.2 Identification of secreted frizzled related protein-2 (SFRP-2) hypermethylation in Prostate cancer

This section describes the results obtained from a study completed in 2011. Results obtained from a methylation analysis of WNT molecules and their antagonists by the

epigenetic biomarker discovery group (Prostate Molecular Oncology, Institute of Molecular Medicine, Trinity College Dublin) within the Prostate Cancer Research Consortium (PCRC) using Quantitative Methylation-Specific PCR (QMSP) revealed hypermethylation of WNT antagonist SFRP-2 in 65% (48/74) of pooled tumours, 30% (6/20) of high-grade PIN, 11% of BPH glands from prostate cancer patients and 9% (7/69) of histologically benign tissue from patients with no evidence of prostate cancer (Perry *et al.*, 2012). Individual Gleason grades (G3, G4, and G5 areas) were also microdissected from 33 patients to assess SFRP-2 methylation by QMSP within the individual Gleason grades of prostate cancer. Overall, 73% (24/33) of patients displayed SFRP-2 methylation in at least one tumour focus (Perry *et al.*, 2012). Within individual grades, there was a slight trend in methylation frequency, with hypermethylation more frequent in low-grade rather than high-grade disease (Perry *et al.*, 2012). Taking these results into consideration, it is possible that the loss of SFRP-2 expression noted in prostate cancer tissue by O' Hurley *et al.* (2011) (section 4.1.6.1) may be related to methylation of the SFRP-2 gene and that the 40% of Gleason grade 5 carcinomas that either retain or regain SFRP-2 expression may be due to de-methylation of the gene. The results from this study show that SFRP-2 hypermethylation is a common event in prostate cancer and SFRP-2 methylation in combination with other epigenetic markers may be a useful biomarker of prostate cancer.

Owing to a paucity of high quality antigen or antigen surrogates, at present there are no clinically validated, reliable anti-SFRP-2 antibodies available. In general, the available reagents are polyclonal in nature and are not targeted to specific histochemically relevant epitopes. Using a novel expression system (described in chapter 3 of this thesis) biologically relevant recombinant SFRP-2 protein was successfully expressed and purified and utilized in an immunisation campaign in an avian host. The following section describes the results obtained for the generation of an anti-SFRP-2 recombinant scAb with potential applications in IHC.

4.2 Results

4.2.1 Avian immune response to an injected SFRP-2 recombinant protein produced in *E. coli*

A female leghorn chicken was initially immunised sub-cutaneously with a mixture of equal parts of purified SFRP-2 recombinant fusion protein in sterile 1X PBS and Freund's complete adjuvant. The final concentration of the initial immunisation was 100 μg/mL. The first boost (day 14) was then administered using 75 μg/mL of purified protein in 1X PBS, mixed in a 1:1 ratio with Freund's incomplete adjuvant, in a final volume of 1mL. The 3 boosts that followed (days 36, 52 and 66) all contained a reduced concentration of SFRP-2 in 1X PBS (50, 25 and 10μg/mL) and were administered in the same manner as the first boost. A bleed was taken from the chicken 7 days after each boost and an antibody serum titre was performed by ELISA. The antibody serum titre was completed to ensure SFRP-2-specific antibodies were being generated and the titre was sufficiently high for recombinant antibody library production. A series of dilutions ranging from 1 in 100 to 1 in 1,000,000 of chicken serum obtained after the final boost, diluted in 1% (w/v) Milk Marvel prepared in PBST (0.05% (v/v)) (pH, 7.2), was tested against the full-length SFRP-2 protein (produced in mammalian cells in a collaboration with Monash University) in a direct ELISA format. A titre in excess of 1/50,000 was observed from the ELISA, indicating a high level of specific mRNA that could be used for the generation of a recombinant antibody library against the SFRP-2 antigen (Figure 4.40).

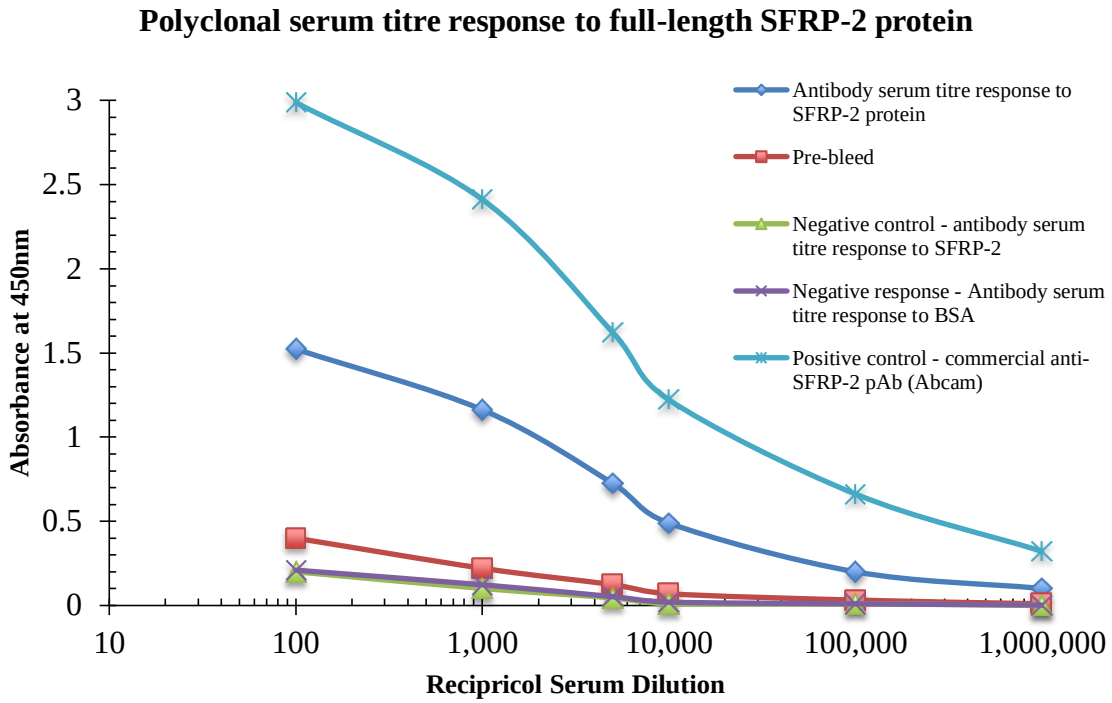

Figure 4.38. Avian anti-serum titration for a chicken sensitised with SFRP-2.

An ELISA plate was coated with 1µg/mL of a recombinant full-length SFRP-2 protein. Serum was collected from an adult Leghorn chicken (female) 7 days prior to sacrifice, diluted in 1% (w/v) PBSTM and bound IgY (chicken antibody) was detected using anti-chicken-Fc-specific HRP-labelled antibody. The graph indicates a significant antibody response for the full-length SFRP-2 protein.

4.2.2 Isolation of anti-SFRP-2 polyclonal antibodies using a Pierce Thiophilic Adsorption kit

Avian IgY is the major globular protein produced by chickens. It is continually synthesized by B cells, secreted into the blood stream and accumulated in the egg yolk (Warr, Magor & Higgens, 1995). The IgY of hens provides their progeny with immunity against avian pathogens until they have a fully matured immune system. Only three avian immunoglobulin subclasses have been identified, IgM, IgA and IgY (Dias da Silva & Tambpurgi, 2010). Like IgG, IgY consists of two heavy (65 kDa) and two light (18 kDa) chains. The IgY differs in that the heavy chain consists of one variable and four constant domains while the light chain comprises of one variable and one constant region. A large amount of IgY is prevalent in the blood (~5 mg/mL); therefore, the serum obtained from the avian model after each immunisation is an

ideal source for the isolation of antigen-specific polyclonal antibodies (Dong *et al*., 2008). The IgY was purified from serum obtained from a chicken immunised with a SFRP-2 protein using a Pierce Thiophilic adsorption kit. The quality of the polyclonal antibodies isolated was determined by SDS-PAGE and Western blotting analysis (Figure 4.41 (a) and (b)). The eluted fractions containing the highest concentration of polyclonal antibodies, determined using a NanoDrop ND^{TM} 1000, were pooled and concentrated in a 30,000 molecular weight 'cut-off' (MWCO) concentrator. In total, 40mg/mL of polyclonal antibody was isolated using this kit for subsequent downstream application. The polyclonal antibodies were diluted to a working stock of 1mg/mL and stored in PBS prepared with 0.02% (w/v) NaN_3.

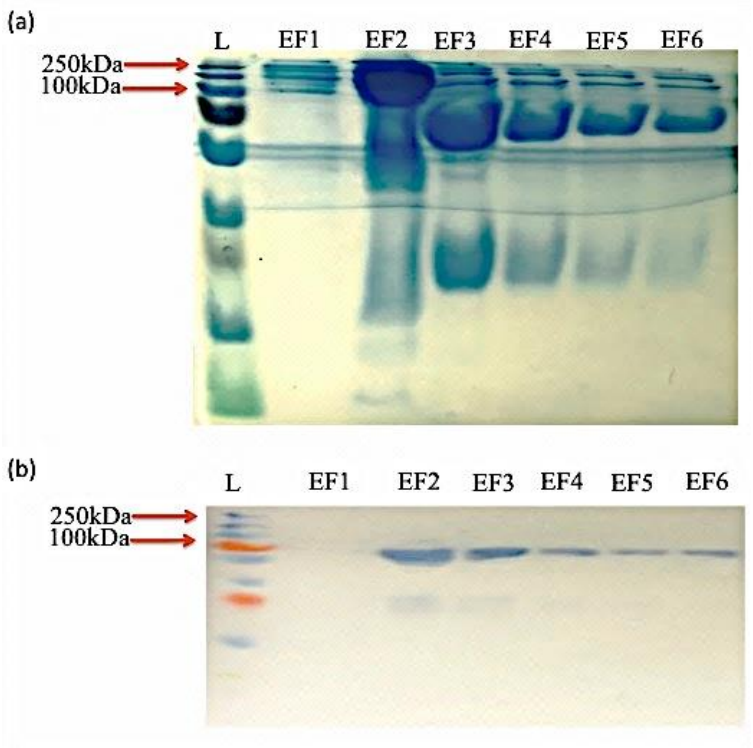

Figure 4.39. SDS-PAGE and WB analysis of the fractions obtained during isolation of anti-SFRP-2 polyclonal antibodies using a Thiophilic adsorption kit.

(a) *SDS-PAGE gel showing the six fractions eluted off the Thiophilic column. A sample from each eluted fraction was run on a 12.5% SDS-PAGE gel at 120V for 50 minutes. Instant blue was then applied to the gel in order to visualise the protein bands. The lanes are labelled as follows; EF1: eluted fraction 1, EF2: eluted fraction 2, EF3: eluted fraction 3, EF4: eluted fraction 4, EF5: eluted fraction 5, and EF6: eluted fraction 6. The ladder, represented by the letter L in this figure, was a Page Ruler Plus pre-stained protein ladder.*

(b) *Western blot showing the eluted polyclonal antibodies. The gel was transferred to a membrane and blocked using 5% milk marvel prepared in 1XPBS. A rabbit anti-chicken (IgG) antibody, conjugated with horseradish-peroxidase (HRP) (1:2,000 dilution) was used to detect the polyclonal antibodies present in each eluted fraction. The lanes are labelled as in (a).*

4.2.3 Characterisation of the isolated anti-SFRP-2 polyclonal antibodies by Western blotting and ELISA

Once purified, the anti-SFRP-2 polyclonal antibodies were used to probe a western blot, which had been transferred from resolved SFRP-2 protein on an SDS-PAGE gel. To compare the efficacy of the polyclonal antibodies isolated 'in-house' blotting was performed using the commercial anti-SFRP-2 polyclonal antibody and the 'in-house' antibody simultaneously. The optimum working concentration of the commercial polyclonal antibody was a 1 in 1,000 dilution. To determine if similar results could be

obtained using the 'in-house' polyclonal antibody, a 1 in 1,000 dilution was also applied. From the results shown in Figure 4.42 it is evident that the 'in-house' isolated antibody worked to the same high standard as the commercial antibody, showing a clear SFRP-2-specific band at approximately 33kDa. This result not only indicated that the purified antibodies were SFRP-2-specific but confirmed the success of the SFRP-2 immunisation campaign allowing the production of SFRP-2-specific antibodies.

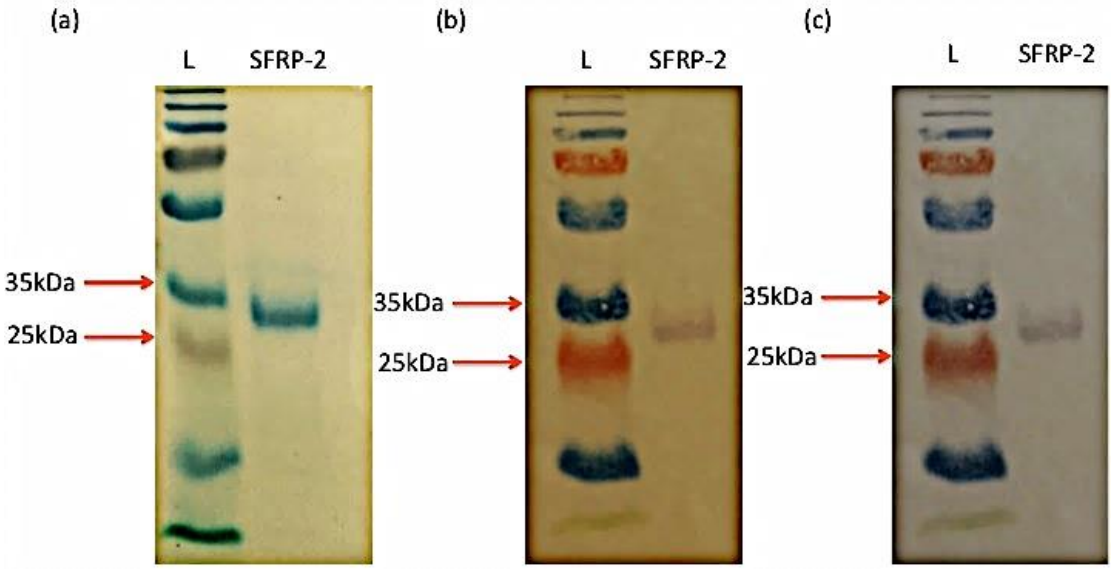

Figure 4.40. SDS-PAGE and WB analysis of a commercial anti-SFRP-2 polyclonal antibody versus anti-SFRP-2 polyclonal antibodies isolated 'in-house'.

(a) *SDS-PAGE gel showing the SFRP-2 pure protein. Five µg of the full-length SFRP-2 protein was run on a 12.5% SDS-PAGE gel in order to ensure protein purity and that the correct size protein was present (~33kDa). The ladder, represented by the letter L in this figure, was a Page Ruler Plus pre-stained protein ladder.*

(b) *Western blot of a SFRP-2 protein probed with a commercial anti-SFRP-2 antibody at a 1:1,000 dilution. The anti-SFRP-2 commercial polyclonal antibody was used to probe a western blot, which had been transferred from resolved SFRP-2 protein on an SDS-PAGE gel. Prior to addition of the polyclonal antibody the blot was blocked with 5% (w/v) MM in 1XPBS. Post incubation with the polyclonal antibody the blot was probed with a rabbit anti-chicken antibody, conjugated with horseradish-peroxidase (HRP) at a 1:2,000 dilution. L is the pre-stained protein ladder.*

(c) *Western blot of a SFRP-2 protein probed with the 'in-house' isolated polyclonal anti-SFRP-2 antibody at a 1:1,000 dilution. This blot was treated in the same manner as (b). Both Western blots were developed using TMB. The ladder, represented by the letter L in this figure, was a Page Ruler Plus pre-stained protein ladder.*

ELISA analysis was carried out to compare the binding activity of the anti-SFRP-2 polyclonal antibodies isolated from serum with the commercial anti-SFRP-2 polyclonal antibody (positive control). Two negative controls were included in this assay to ensure the results obtained were valid. All samples were run in duplicate. The results indicate that the commercial polyclonal antibody produced a stronger signal for the target protein in ELISA when compared to the 'in-house' polyclonal antibody. However, the 'in-house' polyclonal antibody still produced a sufficient target-specific signal in ELISA at a dilution of 1 in 5,000. This polyclonal antibody will be brought forward for future IHC analysis along side the generated anti-SFRP-2 recombinant antibodies.

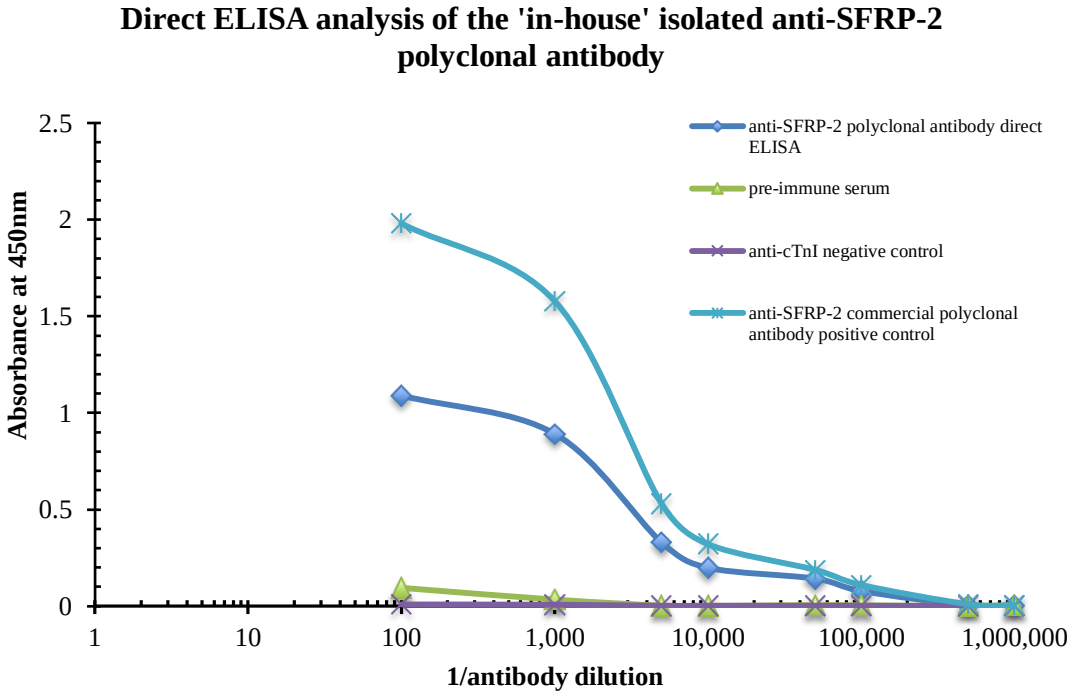

Figure 4.41. Direct ELISA analysis of the 'in-house' isolated anti-SFRP-2 antibodies.

A microtitre plate was coated with 1µg/mL of the SFRP-2 protein. The plate was blocked with 5% (w/v) Milk Marvel in 1X PBS (pH 7) and probed with varying dilutions of the anti-SFRP-2 polyclonal antibody, prepared in 1% (w/v) PBSTM, diluted from 1:100 to 1:1,000,000. A rabbit anti-chicken antibody, conjugated with horseradish-peroxidase (HRP) (1:2,000) was used to detect any antibodies binding to SFRP-2. A commercial anti-SFRP-2 polyclonal antibody (Abcam) was used as the positive control in this ELISA and an anti-cTnI antibody along with the pre-immune serum was used as the negative control.

4.2.4 Construction of an anti-SFRP-2 scFv library

The preliminary testing of immune serum from the immunised chicken demonstrated a clear response to SFRP-2. The spleen and bone marrow were removed from the immunised chicken. The total RNA was extracted from the tissue samples, quantified using a NanoDrop^{TM} 1000 and first-strand cDNA synthesised by reverse transcription. The cDNA template was used in the amplification of the avian variable heavy (V_H) and light (V_L) chain genes.

4.2.4.1 Avian Library construction by PCR – Amplification of variable heavy and light chain genes

Post sacrifice, RNA extraction and cDNA synthesis, the variable domains from the avian bone marrow (BM) and spleen (SP) were amplified using high fidelity Platinum® PCR SuperMix. Platinum® SuperMix is a proprietary formulation which enables robust DNA amplification with minimal optimisation of reaction conditions. It is a ready-to-use mixture of DNA polymerase, salts, magnesium, and dNTPs for highly efficient PCR amplification. The long linker primer CSCVHo-FL is paired with the CSCG-B reverse primer to amplify V_H fragments using the cDNA as a template. The sense primers have a sequence tail that is compatible with the linker sequence that is used in the overlap extension PCR. The reverse primer has a sequence tail containing a S*fi*I site; this site is recognized by the reverse extension primer used in the second-round PCR. The CSCVK sense primer is combined with the CKJo-B reverse primer to amplify the V_L gene segments and a 5'- sequence tail that contains an S*fi*I site that is recognized by the sense extension primer in the second-round PCR. The reverse primer has a linker sequence tail that is used in the overlap extension.

The PCR products for each variable domain for both the BM and SP were resolved on 1.5% (w/v) agarose gels. These indicated similar yield, shown by discrete-specific band formation at approximately 400bp for V_H and 350bp for V_L. Post large-scale amplification, the correct size amplicons were isolated by gel extraction and clean up (as per the manufacturers' guidelines). Both the V_H and V_L were brought together by the inclusion of a flexible serine-glycine linker [$(G_4S)_4$] in a spice-by-overlap extension (SOE) PCR.

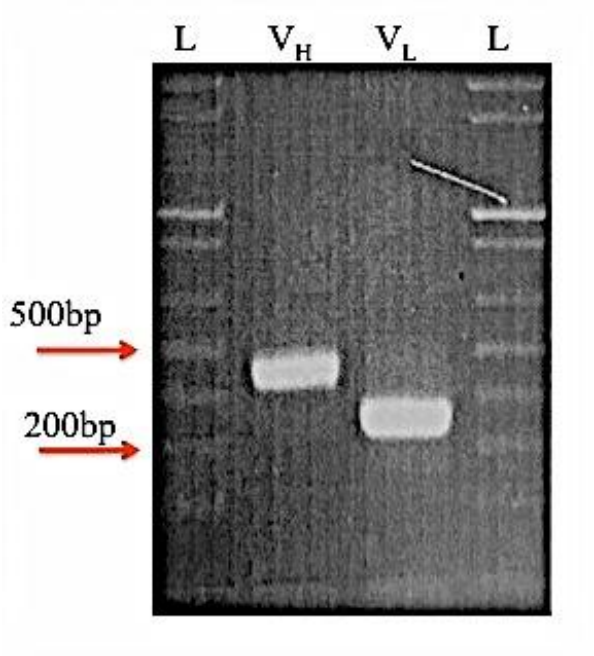

Figure 4.42. Bone marrow (BM) variable heavy (V_H) and variable light (V_L) chain PCR amplification.

Visualisation of the variable heavy and light chain products amplified using the cDNA synthesised from the bone marrow RNA. The lanes are labelled as follows; L: Ladder, V_H: variable heavy, V_L: variable light.

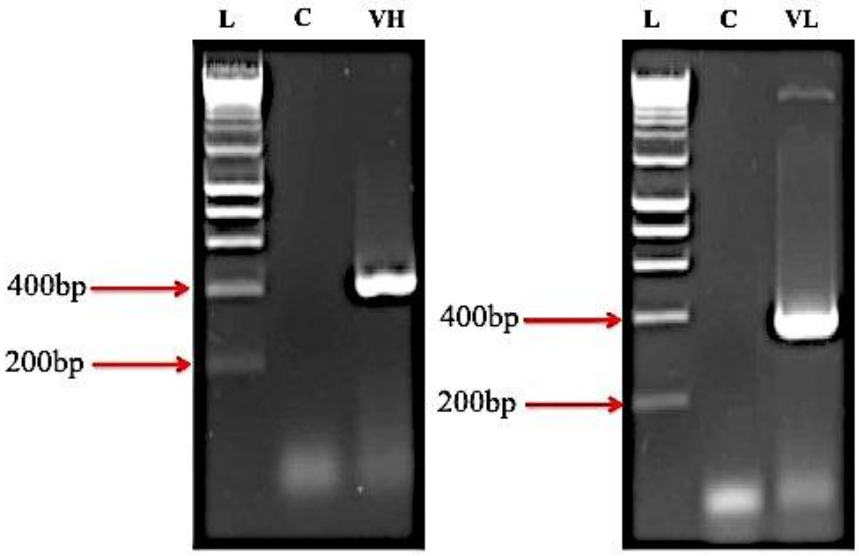

Figure 4.43. Spleen (SP) variable heavy (VH) and variable light (VL) chain PCR amplification.

Visualisation of the variable heavy and light chain products amplified using the cDNA synthesised from spleen RNA. The lanes are labelled as follows; L: Ladder, C: negative control, V_H: variable heavy, V_L: variable light.

4.2.4.2 Splice-by-overlap extension (SOE) PCR of the variable light and heavy region to generate a spleen and bone marrow anti-SFRP-2 scFv libraries

The purified variable domains were incorporated in equimolar ratios into a SOE-PCR. The sense and the reverse primers used (CSC-F and CSC-B) recognize the sequence tails from the first round of amplifications. This PCR produced the desired 750bp fusion product of the two chains alone, joined via a serine-glycine linker, to form the full-length scFv gene fragment. Platinum® *Taq* DNA polymerase High Fidelity was used for this overlap in order to ensure correct formation of the scFv. The large-scale reactions were visualised on 0.8% (w/v) agarose gels and showed a diffuse band that was discrete enough to be isolated and purified.

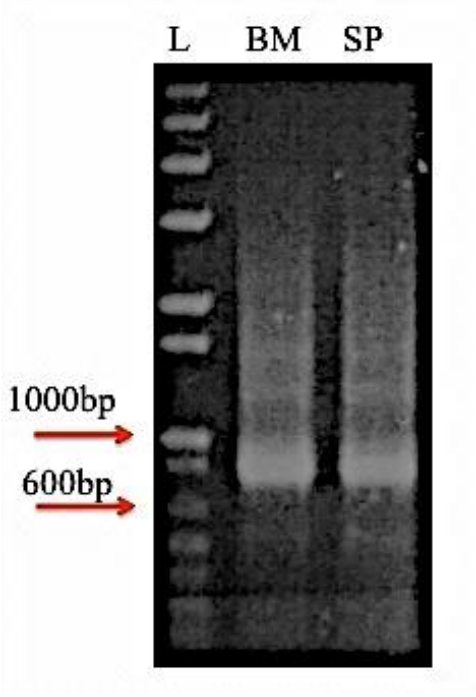

Figure 4.44. Splice-by-Overlap Extension PCR of the amplified V_H and V_L chain genes from the synthesised cDNA of an avian model immunised with purified SFRP-2 protein.

Visualisation of the SOE product for both the spleen (SPSOE) and bone marrow (BMSOE) on a 0.8% (w/v) agarose gel. Both the spleen and bone marrow samples show formation of a specific band at ~750bp corresponding to the scFv SOE product. The lanes are labelled as follows: L: Ladder, BM: bone marrow, SP: spleen.

4.3 Construction of scFv library in the pComb3xSS vector

The pComb3xSS vector was made available by Professor Carlos Barbas III of the Scripps Institute, La Jolla, California, USA. The vector was previously transformed into dcm^-/dam^- *E. coli* for vector purification (Dr. Paul Conroy, Monash University, Melbourne, Australia) and stored in glycerol aliquots. An overnight culture of the pComb3xSS vector was prepared, followed by plasmid preparation of the vector prior to digestion. Large-scale digestion of the vector to incorporate the anti-SFRP-2 scFv library was carried out in a stepwise, triple digestion protocol. Digestion of the vector with S*fi*I may result in a large amount of intact stuffer fragment or undigested vector, leading to library contamination despite de-phosphorylation of the cut vector. To overcome this, subsequent digestion of the vector with X*ho*I and X*ba*I further degraded the stuffer fragment into three products (S*fi*I – X*ba*I, X*ba*I – X*ho*I, X*ho*I – S*fi*I, see Figure 4.47). In addition, Antarctic phosphatase treatment of the entire vector digestion results in a de-phosphorylated vector, thus further preventing re-ligation.

Successful S*fi*I digestion of the SOE products was confirmed on a 1.5% (w/v) agarose gel with cleavage of the restriction site plus the $(GAG)_6$ sequence readying the insert for ligation into the triple digested pComb3x vector. Post ligation, the antibody libraries (BM and SP) were transformed into XL1Blue electrocompetent *E. coli* cells generating a combined library size of 6.1×10^7 members, which was subsequently rescued with helper-phage for screening via phage display. The background re-ligation/contamination of this library was found to be zero. This highlights the success of the triple digest approach in combination with de-phosphorylation of the pComb3xSS vector during the library building process in generating a specific and uncompromised library.

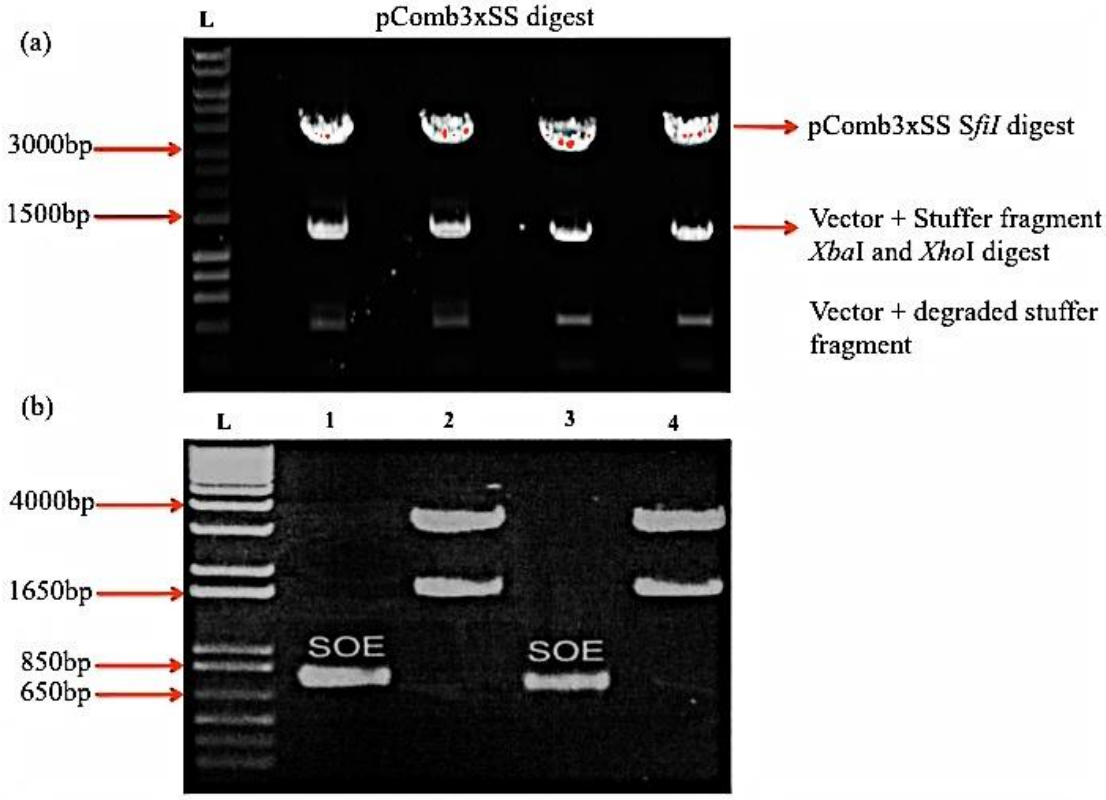

Figure 4.45. pComb3xSS vector triple digest and SfiI digest of BM and SP.

(a) *Triple digestion involved further degradation of the stuffer fragment (already SfiI digested) with XhoI and XbaI (Table 24 in Section 2.4.10 outlines the triple digest approach). The triple digestion reduces the potential for contamination of the downstream library building process. The digestions were resolved on a 0.5% (w/v) agarose gel and were compared to a 1Kb+ DNA ladder. The letter L represents the ladder in this figure. The four additional lanes contain triple digested pComb vector product.*

(b) *Visualisation of successful SfiI digestion of spleen and bone marrow anti-SFRP-2 scFv SOE-PCR inserts (Lane 1 and 3 respectively) on a 1.5% (w/v) agarose gel run along-side the SfiI digested pComb3xSS vector for comparison (Lane 2 and 4).*

4.4 Phage display of anti-SFRP-2 scFv antibodies

The library was evaluated in a highly stringent antigen presentation manner to maximize the probability of selecting anti-SFRP-2-specific scFv antibodies. The scFv fragments were rescued by helper-phage and displayed on filamentous phage surface. The panning strategy outlined in chapter 2 was exploited incorporating panning conditions and stringencies that are delineated in Table 46. Due to the fact that the antigen used for immunisation was a fusion protein, it was essential to screen this library against the SFRP-2 protein in the absence of FABP in order to avoid the potential of obtaining anti-FABP antibodies. Hence, a project-specific collaboration

was set-up with Prof. James Whisstock's Lab in Monash University, Melbourne. The full length SFRP-2 protein was expressed in mammalian cells by Prof. Whisstock's Lab and applied as the antigen in this screening strategy. A high density (100μg/mL and 50 μg/mL) of SFRP-2 protein was used for the first two rounds of panning to ensure enrichment of the library. To complement the stringency element introduced by this presentation strategy, a further level of selective pressure was introduced by gradual limitation of the concentration of antigen available for binding, in addition to an increased number of wash steps throughout (Table 46). After four rounds of panning the phage preparations for each round were analysed by polyclonal-phage ELISA (section 4.5).

Table 45. Panning conditions applied for screening the anti-SFRP-2 scFv library.

The stringency of each consecutive round of panning was altered by increasing the number of washes and decreasing the antigen coating concentration.

Panning round	SFRP-2 antigen coating conc. (μg/mL)	Washing frequency
1	100	3 X PBS, 3 X PBST
2	50	5 X PBS, 5 X PBST
3	25	7 X PBS, 7 X PBST
4	10	10 X PBS,10 X PBST

Table 46. Panning input anf output titres over 4 rounds of panning of the avian anti-SFRP-2 scFv library.

Anti-SFRP-2 scFv panning input and output titres from 4 rounds of panning		
Round 1	**Input titre**	**Output titre**
	1.4×10^{12}	2.6×10^{6}
Round 2	**Input titre**	**Output titre**
	3.2×10^{11}	1.6×10^{6}
Round 3	**Input titre**	**Output titre**
	2.1×10^{11}	1.2×10^{5}
Round 4	**Input titre**	**Output titre**
	1.3×10^{10}	1×10^{6}

4.5 Polyclonal phage ELISA analysis of precipitated phage obtained after each round of panning to identify the round in which significant enrichment of the anti-SFRP-2 scFv library was achieved

Post-panning, the selected antibody-displaying phage from each round of selection were evaluated in a polyclonal-phage ELISA for enrichment against SFRP-2. To increase confidence in the result, a helper phage negative control and BSA-coated wells were included in the assay. The presence of specific-antibody-displaying phage was detected by an HRP-labelled mouse anti-M13 secondary antibody. Figure 4.48 illustrates the dramatic increase in specific-antibody-displaying phage at round three, suggesting enrichment of scFv-harbouring phage within the panned library. There was minimal or no background binding with any of the included controls. Phage from round 3 were subsequently infected into mid-exponential *E. coli* Top 10F' for expression of soluble scFv fragments and taken forward into the screening campaign.

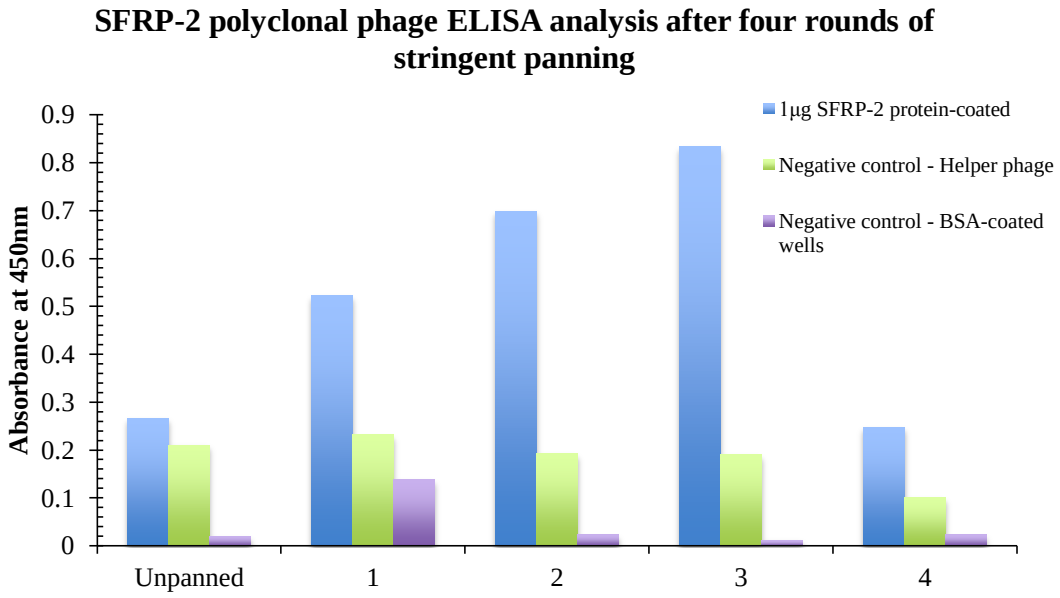

Figure 4.46. Polyclonal-phage ELISA analysis to identify the panning round in which significant enrichment for SFRP-2 occured.

The phage preparations were assayed for specific binding against SFRP-2. Phage from each of the rounds (1-4) were diluted 1 in 5 in 1% (w/v) PBSTM and 100µl applied to each well. Bound phage were detected using HRP-labelled anti-M13 secondary antibody. The ELISA plate was developed using TMB and the absorbance read after quenching with 10% (v/v) HCl at 450nm. The graph shows the dramatic increase in phage-displaying SFRP-2-specific scFv up to round 3.

4.6 Screening analysis of specific-antibody-displaying phage

Three hundred and eighty four single colonies were isolated and grown up for screening. The screening approach was carried out at a protein level to assess binding in two ways: i) ELISA and ii) Biacore^{TM} 4000 high throughput (HT)-ranking by stability early and late analysis. The acquired data, most notably on the refined HT-system, offered a wealth of information to judiciously aid the screening process.

4.6.1 Monoclonal phage ELISA analysis of 384 clones picked following polyclonal phage ELISA analysis of precipitated phage from panning of the anti-SFRP-2 scFv library

Initial protein-specificity screening was performed as a preliminary evaluation of the success of the panning strategy post polyclonal phage ELISA analysis and prior to HT-screening on the Biacore^{TM} 4000. Three hundred and eight four scFv clones were included in this analysis to identify potential SFRP-2-specific binders. A positive clone was defined as having a SFRP-2-specific binding response greater than an absorbance of 0.3A.U. The screen highlighted the success of the panning strategy, but was merely a pre-screen for more rigorous HT analysis.

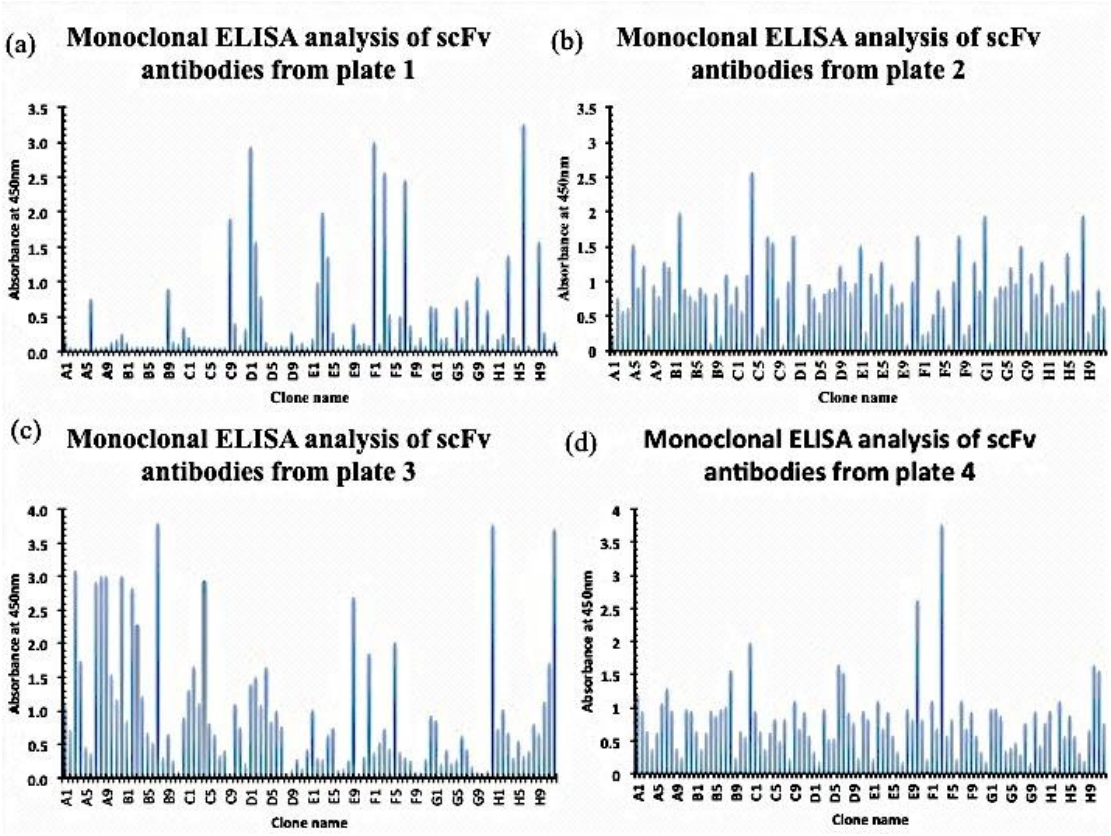

Figure 4.47. Initial screening of four scFv panned library output plates.

This direct binding ELISA permitted approximate determination of the percentage of positive binders for SFRP-2. A large percentage of clones bound to the SFRP-2 protein. One µg/mL of SFRP-2 was coated on four ELISA plates blocked with 5% (w/v) PBSTM, to which diluted crude supernatants from overnight expressed single colonies were applied. Specific scFv were detected using an HRP-labelled mouse anti-HA- secondary antibody.

4.6.2 Stability early vs. stability late analysis of 384 anti-SFRP-2 scFv clones post Biacore 4000 screening

Three hundred and eight-four scFv clones were ranked by percentage left analysis and stability early versus late in a direct binding format, where the full-length SFRP-2 protein was immobilised on the chip surface using standard amine coupling chemistry. Amine coupling chemistry covalently attaches the amine groups of the SFRP-2 protein to the carboxyl groups of the dextran CM5 biosensor chip. Figure 4.50 diagrammatically illustrates the flow cell setup. There are four flow cells, each with five independently addressable and monitored spots, within the system. A SFRP-2 protein surface was created by immobilisation of approximately 4,500 response units (RU) of covalently attached protein onto spots 1, 2, 4 and 5 via primary amine groups. Crude lysates from overnight expressed clones were diluted in running buffer (HBS-EP+) and run over all 5 flow cells, where flow cell three was the reference (control) flow cell. The clones were ranked by the response unit (RU) level at two time points (stability early (SE) and stability late (SL)). Stability late was set 16 minutes after stability early to allow for dissociation to occur. Twenty mM NaOH was used for the regeneration of the chip surface after each run. Figure 4.51 is a plot of stability early versus stability late for the 384-clone screen where 100% left (or no dissociation) is signified by a diagonal, dotted black line. All clones resided within three sub-populations, namely, those with percentage left values $\geq$ 60%, < 60% and non-binders.

Antibody screening data were acquired in a relatively short timeframe, where the analysis of 384 clones took <18 hours. Combined with the monoclonal ELISA analysis screening, appropriate information was available to rationally select a panel of clones to carry forward.

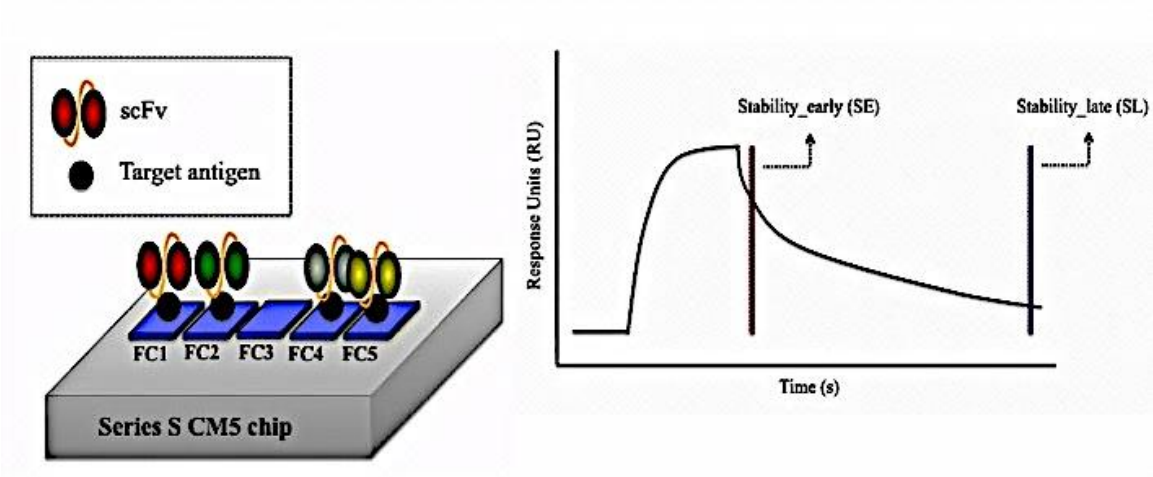

Figure 4.48. Overview of the experimental flow cell setup.

The surface was composed of full-length SFRP-2 protein on spots 1, 2, 4 and 5 of each flow cell (FC). Spot 3 was used as the reference flow cell (control flow cell).

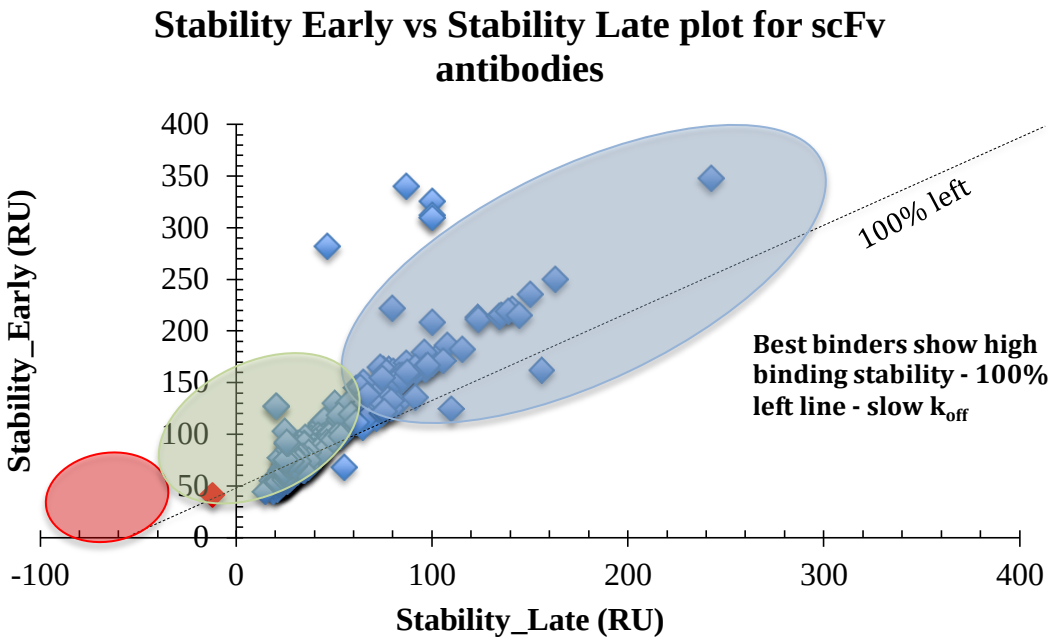

Figure 4.49. High-throughput stability early (SE) versus stability late (SL) ranking of anti-SFRP-2 scFv antibodies.

A plot of stability early versus stability late values for each of the 384 clones illustrated the overall stability of the binding events. From the graph, three distinct populations were identified - red circle: non-binders, green circle: higher expressing clones with % left vales ≥ 60 (blue circle) and those clones with % left values < 60 (green circle). The black diagonal, dotted line signifies a percentage left value of 100% where no dissociation has occurred. The best binders show high binding stability and are situated along the 100% left line.

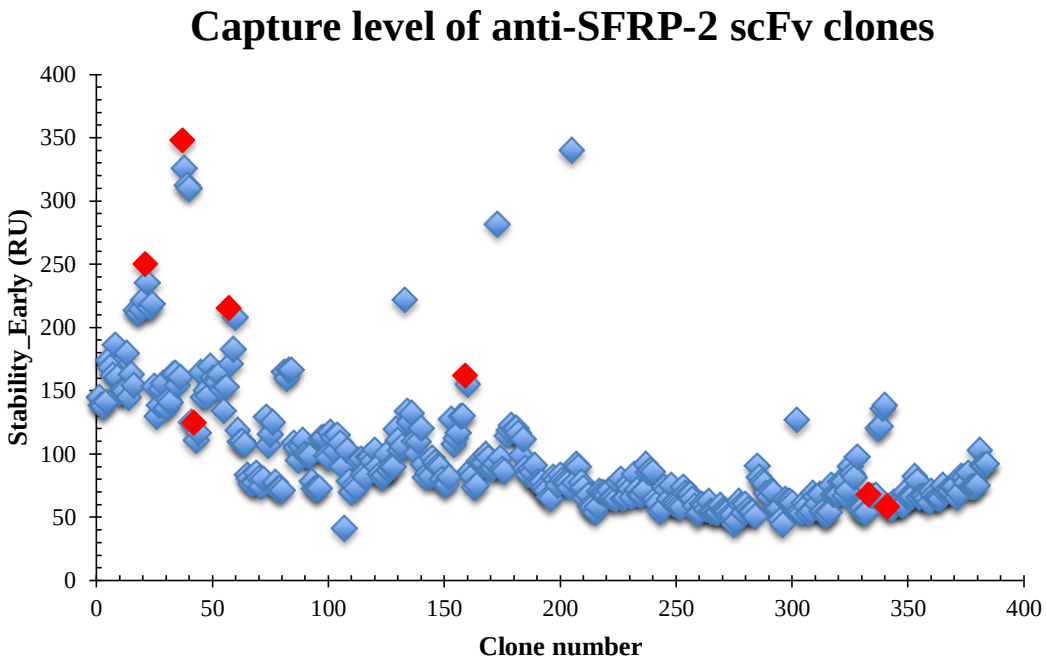

Figure 4.50. High-throughput scFv capture level plot for anti-SFRP-2 scFv clones.

Plot of the scFv capture level by clone number shown for 384 clones in the analysis. Capture level can be related to expression, as all clones were cultured in equal volumes and diluted in the same fashion. Taking the data obtained from the (i) monoclonal phage ELISA, (ii) stability early versus stability late results, and (iii) percentage left plot in to consideration, seven lead candidates were identified for further analysis. If a clone was positive in the monoclonal ELISA and had a percentage left value greater than 65% it was brought forward for sequencing analysis. These antibodies are highlighted in red in this figure.

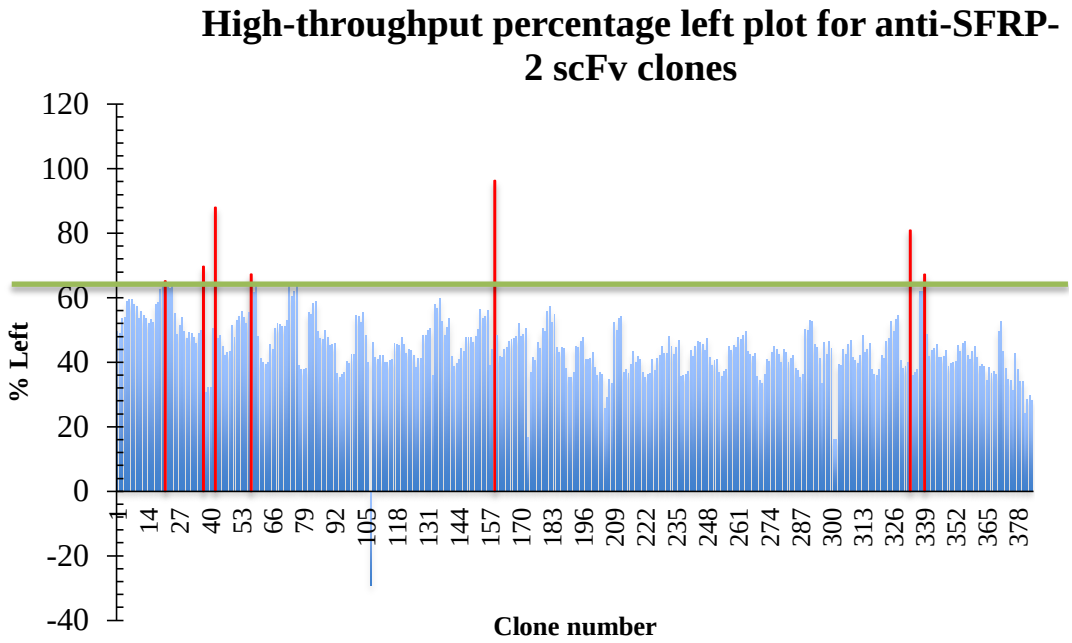

Figure 4.51. High-throughput percentage left plot for anti-SFRP-2 scFv clones.

Percentage left values were calculated using the equation (SL/SE)(100/1). Percentage left values were plotted versus clone number and broken into two groupings. All clones with a percentage left value of over 65% (above the green line) were brought forward for sequencing analysis. Glycerol stocks of all clones with % left values lower than 65% (below the green line) were prepared and stored at -80^{o}C for long-term storage. Out of the 384 clones screened, seven had a % left value of over 65%. These seven clones were brought forward for sequencing analysis.*

Table 47. Rational selection of anti-SFRP-2 scFv clones based on % left >65% and positive response (PR) in monoclonal phage ELISA.

All clones in this table are colour co-ordinated. Clones of the same colour were identified as being identical clones in the sequencing data.

Clone number	%Left	Clone I.D.	SFRP-2-specific positive response in monoclonal phage ELISA
21	65	**P1B2**	Yes
37	69	**P3B3**	Yes
42	87	**P3C3**	Yes
57	67	**P3C4**	Yes
159	96	**P4F3**	Yes
333	80	**P1H9**	Yes
339	67	**P4E10**	Yes

4.7 Sequencing analysis of three selected anti-SFRP-2 scFv antibodies

The results obtained from sequencing analysis of the seven selected anti-SFRP-2 clones indicated that out of the seven clones, only two different clones were present. X-ray crystallographic analysis of antigen: antibody complexes has demonstrated that the hypervariable loops (complementarity-determining regions) of immunoglobulin V regions determine the specificity of antibodies. With protein antigens, the antibody molecule contacts the antigen over a broad area of its surface that is complementary to the surface recognized on the antigen. Electrostatic interactions, hydrogen bonds, van der Waals forces and hydrophobic interactions can all contribute to binding. However, amino acid side chains in most or all of the hypervariable loops make contact with the antigen and determine both the specificity and the affinity of the interaction. Hence, knowledge of the amino acid sequence of an antibody is essential.

The CDRH3 region is known to contain the greatest sequence diversity when compared to the five remaining CDRs and makes a significant contribution to antigen binding. The CDRH3 region for all sequences was 17 amino acids in length and was dominated by the presence of serine, glycine, aspartic acid, tyrosine, tryptophan and isoleucine residues. Tyrosine, tryptophan and arginine residues are involved in mediating various intermolecular interactions, which are desirable in the composition of the CDRs. The tyrosine residue content of the CDRs is attributed to specific antibodies in synthetic libraries with glycine, serine and tyrosine being dominant in the naïve loops. The frequency of tryptophan and arginine residues increases in antibodies that have undergone affinity maturation, but it is tyrosine side-chains that mediate ~25% of antigen contacts. Furthermore, small residue prevalence in the CDR loops confers conformational flexibility which is crucial for effective antigen recognition.

Taking this into consideration, almost all CDRs presented here are dominated by the small amino acids serine, glycine and aspartic acid. Four of the six CDRs in all sequences contain tyrosine residues with the CDRH regions showing higher frequencies. Interestingly, only two arginine residues occur in the CDRs (L2 and L3). Based on what is known about flexibility and tyrosine content, this would suggest that the CDRH regions for the antibodies presented here may be important for SFRP-2

binding. However, in the absence of any structural data this observation remains a supposition.

Table 48. Sequencing data for anti-SFRP-2 scFv clones 21, 37, 57 and 339.

The CDRL regions are highlighted in blue, the linker is highlighted in orange, the CDRH regions are highlighted in red and the tag highlighted in green. Source Biosciences Ltd., Ireland, performed DNA sequencing of 7 anti-SFRP-2 scFv antibodies in triplicate. Clone number 57, in this table, is the cycle name on Biacore for clone P3C4 or clone C4. See Table 48 for more detail on clone number and clone I.D.

Clone 21	LTLPSSVSANPGETVKITCSGGSNNYGWYQQKSPGSAPVTLIYQNDKRPSGIPS
Clone 37	LTLPSSVSANPGETVKITCSGGSNNYGWYQQKSPGSAPVTLIYQNDKRPSGIPS
Clone 57	LTLPSSVSANPGETVKITCSGGSNNYGWYQQKSPGSAPVTLIYQNDKRPSGIPS
Clone 339	LTLPSSVSANPGETVKITCSGGSNNYGWYQQKSPGSAPVTLIYQNDKRPSGIPS
Clone 21	SFSGSKSGSTNTLTITGVRAEDEAVYFCGSGDINSRVGIFGAGTTLTVLGGSSRSS
Clone 37	SFSGSKSGSTNTLTITGVRAEDEAVYFCGSGDINSRVGIFGAGTTLTVLGGSSRSS
Clone 57	SFSGSKSGSTNTLTITGVRAEDEAVYFCGSGDINSRVGIFGAGTTLTVLGGSSRSS
Clone 339	SFSGSKSGSTNTLTITGVRAEDEAVYFCGSGDINSRVGIFGAGTTLTVLGGSSRSS
Clone 21	GGGGSGGGGSSAVTLDESGGGLXTPGGAVSLICKASGFDFYSYYMQFWARQA
Clone 37	GGGGSGGGGSSAVTLDESGGGLXTPGGAVSLICKASGFDFYSYYMQFWARQA
Clone 57	GGGGSGGGGSSAVTLDESGGGLXTPGGAVSLICKASGFDFYSYYMQFWARQA
Clone 339	GGGGSGGGGSSAVTLDESGGGLXTPGGAVSLICKASGFDFYSYYMQFWARQA
Clone 21	PGKGLEYVAGITSEDGDTTDYYAAVKGRATIYRDNGPSTVRLYLYNLYAYDTG
Clone 37	PGKGLEYVAGITSEDGDTTDYYAAVKGRATIYRDNGPSTVRLYLYNLYAYDTG
Clone 57	PGKGLEYVAGITSEDGDTTDYYAAVKGRATIYRDNGPSTVRLYLYNLYAYDTG
Clone 339	PGKGLEYVAGITSEDGDTTDYYAAVKGRATIYRDNGPSTVRLYLYNLYAYDTG
Clone 21	TYFCAKDVDGCGSGSWIGIYIDAWGYGTIYLVSSTSGQAGQHHHHHHGAYPY
Clone 37	TYFCAKDVDGCGSGSWIGIYIDAWGYGTIYLVSSTSGQAGQHHHHHHGAYPY
Clone 57	TYFCAKDVDGCGSGSWIGIYIDAWGYGTIYLVSSTSGQAGQHHHHHHGAYPY
Clone 339	TYFCAKDVDGCGSGSWIGIYIDAWGYGTIYLVSSTSGQAGQHHHHHHGAYPY
Clone 21	DVPDYTS
Clone 37	DVPDYTS
Clone 57	DVPDYTS
Clone 339	DVPDYTS

Table 49. Sequencing data for anti-SFRP-2 scFv clones 42, 159 and 333.

See Table 49 for details. Clone 159, in this table, is the cycle name on Biacore for clone P4F3 or clone F3.

Clone 42	AAPGGVAANDGETVKIT**C**SNYGSNYG**WYQ**QLSNGYIPVAL**IY**DNDTRSSGIPS
Clone 159	AAPGGVAANDGETVKIT**C**SNYGSNYG**WYQ**QLSNGYIPVAL**IY**DNDTRSSGIPS
Clone 333	AAPGGVAANDGETVKIT**C**SNYGSNYG**WYQ**QLSNGYIPVAL**IY**DNDTRSSGIPS
Clone 42	SFSGSKSGSTNTLTITGVRAEDEAVYF**C**GSGDINSRVGI**FGAG**TTLTVLGGSSRSS
Clone 159	SFSGSKSGSTNTLTITGVRAEDEAVYF**C**GSGDINSRVGI**FGAG**TTLTVLGGSSRSS
Clone 333	SFSGSKSGSTNTLTITGVRAEDEAVYF**C**GSGDINSRVGI**FGAG**TTLTVLGGSSRSS
Clone 42	GGGGSGGGGSSAVTLDESGGGLALSGVSLI**CKAS**GSDYYSYYAGI**MQ**FWARQA
Clone 159	GGGGSGGGGSSAVTLDESGGGLALSGVSLI**CKAS**GSDYYSYYAGI**MQ**FWARQA
Clone 333	GGGGSGGGGSSAVTLDESGGGLALSGVSLI**CKAS**GSDYYSYYAGI**MQ**FWAGGA
Clone 42	AGKKLEWAGIINRNDGDIYDYYSSV**K**SSRTNYLDNGYRTRRLYLYLLYAYDTG
Clone 159	AGKKLEWAGIINRNDGDIYDYYSSV**K**SSRTNYLDNGYRTRRLYLYLLYAYDTG
Clone 333	AGKKLEWAGIINRNDGDIYDYYSSV**K**SSRTNYLDNGYRTRRLYLYLLYAYDTG
Clone 42	AYI**CAK**SVDGDGSGSWYGIYIDY**WGYG**AILLVSSTSGSASSQHHHHHHSAYPY
Clone 159	AYI**CAK**SVDGDGSGSWYGIYIDY**WGYG**AILLVSSTSGSASSQHHHHHHSAYPY
Clone 333	AYI**CAK**SVDGDGSGSWYGIYIDY**WGYG**AILLVSSTSGSASSQHHHHHHSAYPY
Clone 42	DVPDYTA
Clone 159	DVPDYTA
Clone 333	DVPDYTA

4.8 Direct and sandwich ELISA analysis of anti-SFRP-2 scFv lysates by varying antigen concentration

Direct ELISA and sandwich ELISA analysis were carried out on the two anti-SFRP-2 scFv clones, C4 and F3, identified from the screening and sequencing analysis. Direct analysis was completed initially to determine the optimal working dilution of each antibody by probing an ELISA plate coated with 0.5µg/mL SFRP-2 protein with varying dilutions of the scFv antibodies. An HRP-labelled mouse anti-HA secondary was used to detect the anti-SFRP-2 scFv antibodies. All samples were tested in triplicate. One negative and one positive control were included in this assay. Optimal dilutions of lysate were determined for each clone to give an absorbance of ~1.0AU. Anti-SFRP-2 scFv clone F3 showed an almost identical binding pattern to the anti-SFRP-2 commercial polyclonal antibody with an optimum working dilution

determined to be 1 in 1,000, as with the commercial antibody (determined by the manufacturer). Anti-SFRP-2 scFv clone C4 showed no target-specific binding, as the response of this antibody to SFRP-2 was similar to that of the negative control.

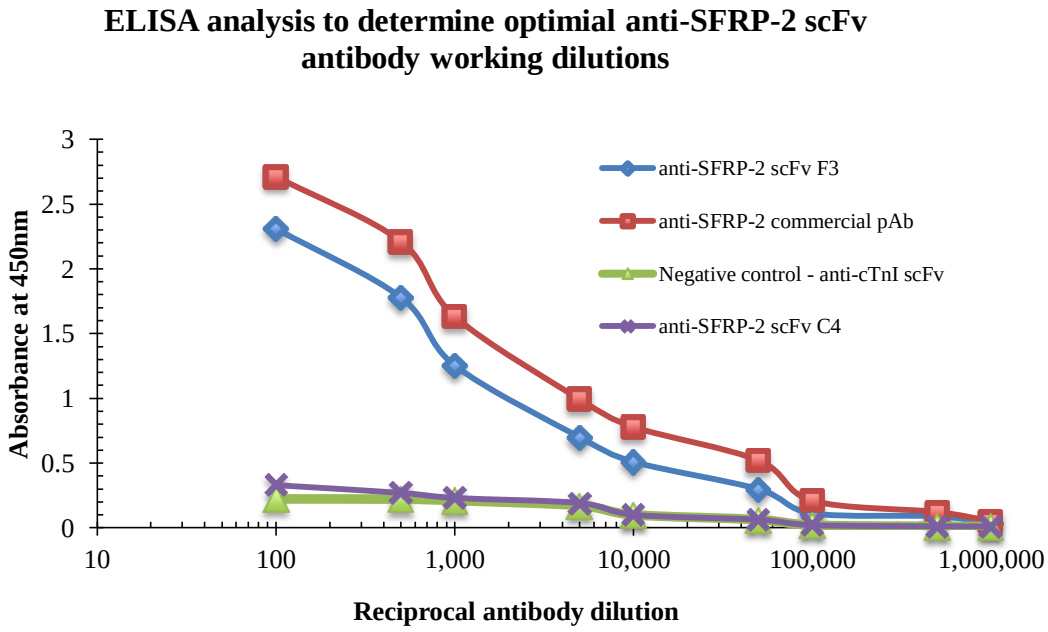

Figure 4.52. Titration of scFv against SFRP-2 by ELISA.

Supernatants were diluted in 1% (w/v) PBSTM and applied to individual wells. Bound scFv were detected using HRP-labelled mouse anti-HA- secondary antibody. Optimal dilutions of lysate were determined for each clone to give an absorbance of 1.0AU.

Figure 4.55, a sandwich assay, illustrates the scFv antibody lysates as the capture reagents for various concentrations of the SFRP-2 protein (0.5-2,000ng/mL). In this assay, bound SFRP-2 was detected using the commercial anti-SFRP-2 pAb or the 'in-house' purified anti-SFRP-2 polyclonal antibody. Clone F3 again out performed clone C4 in this assay and was brought forward for purification and characterisation in WB and dot blot analyses.

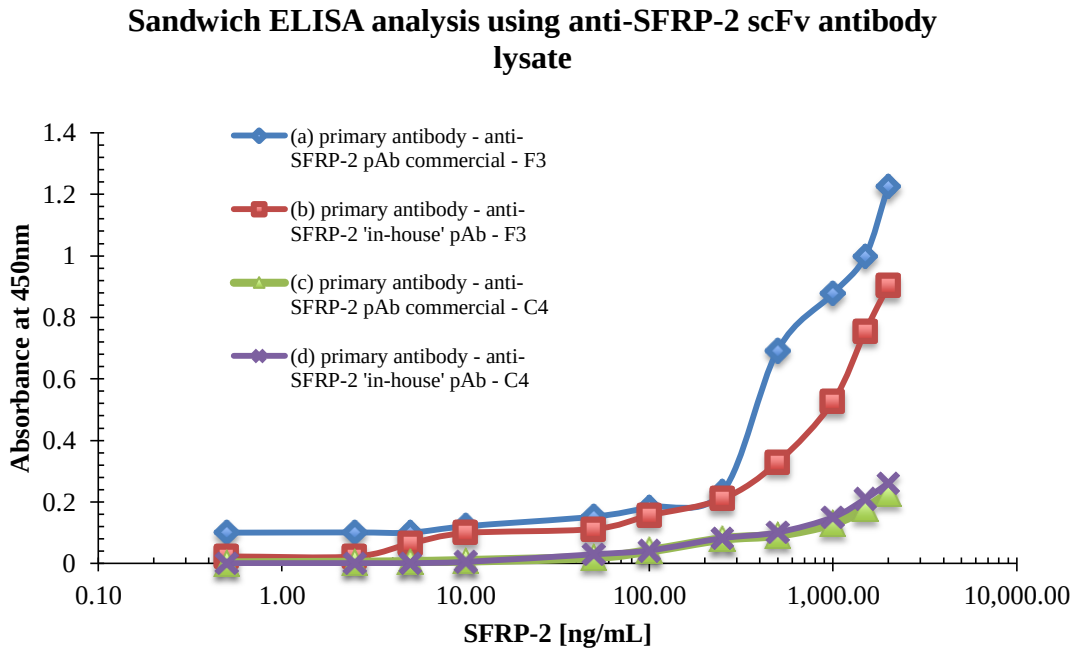

Figure 4.53. Sandwich ELISA analysis of anti-SFRP-2 scFv clones.

Anti-SFRP-2 scFv supernatants were applied to an ELISA plate to form the antibody capture surface. Varying concentrations of SFRP-2 (0.5-2,000ng/mL) were applied to the immobilised scFv antibodies. Captured SFRP-2 was detected using an anti-SFRP-2 commercial pAb or the 'in-house' purified anti-SFRP-2 pAb, which completed the sandwich format. Bound commercial pAb (raised in goat) was detected using a commercial rabbit HRP-labelled anti-goat polyclonal antibody. Bound 'in-house' pAb was detected using a commercial HRP-labelled anti-chicken antibody.

4.9 IMAC purification of anti-SFRP-2 scFv antibody F3 using osmotic shock approach

An optimisation of expression of this scFv was completed post purification by varying a number of parameters, such as IPTG concentration, induction time and temperature. However, in general the expression of this clone was quite poor. The optimum conditions were determined to be 0.8mM IPTG, overnight at 25°C. Optimised large-scale expression (results of optimisation process not shown) of the anti-SFRP-2 scFv clone F3 was completed using 0.8mM IPTG for induction overnight at 25°C. The anti-SFRP-2 scFv clone F3 was purified, using osmotic shock-based buffers. The scFv was purified by virtue of the 6xHis tag encoded on the pComb3x vector by immobilised metal affinity chromatography (IMAC). The purification was carried out from 5 x 200mL cultures induced overnight. The eluted

protein was concentrated and buffer exchanged into PBS. The concentrated sample was analysed by SDS-PAGE and WB, alongside the 'flow-through', wash A (WA) and wash B (WB) fractions. Protein concentration was obtained by A_{280} on a NanoDrop™ 1000 and is shown in Table 51. The results from the SDS and WB show significant loss of the antibody in 'flow-through' 1 and Wash A. Additionally, the protein yield post concentration was quite low (~0.4mg/mL). This experiment was repeated numerous times and an optimisation of purification was performed, but no significant improvement in antibody yield could be achieved. Despite this, the protein membrane binding capability of the scFv was assessed by dot and western blotting in order to determine if, in addition to ELISA, this antibody could recognise its target in a membrane format. The following section shows the application of this purified scFv as a primary antibody in a SFRP-2 western and dot blot analysis.

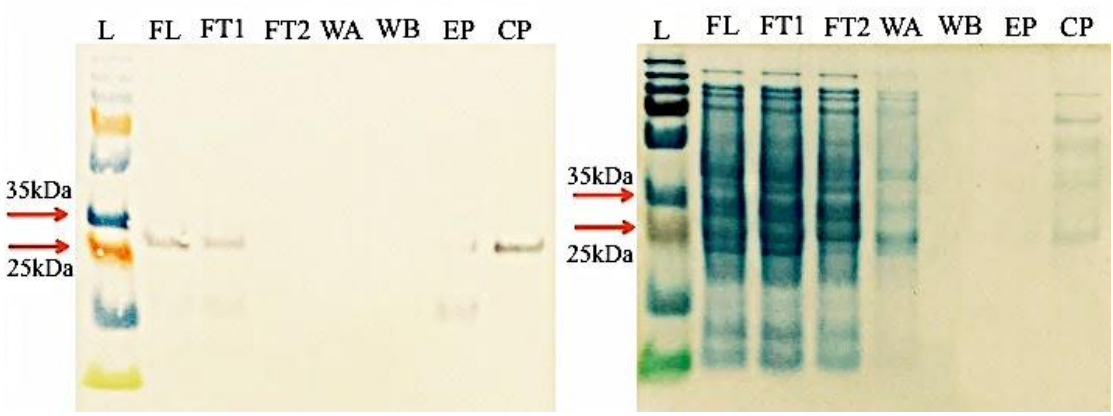

Figure 4.54. WB and SDS-PAGE analysis of anti-SFRP-2 scFv F3 purification steps.

In the large-scale purification, samples of each step of the process were analysed. The lanes are labelled as follows; FL: filtered lysate, FT1: flow-through 1, FT2: flow-through 2, WA: wash A, WB: wash B, EP: eluted protein and CP: concentrated protein. The ladder, represented by the letter L in this figure, was a Page Ruler Plus pre-stained protein ladder.

Table 50. IMAC-purified anti-SFRP-2 scFv F3 protein yield determined using the NanoDrop 1000.

Protein fraction	Volume (mL)	Protein yield as determined by the NanoDrop™ 1000
Eluted protein	4.0	0.1mg/mL
Concentrated protein	0.2	0.4mg/mL

4.10 Analysis of the anti-SFRP-2 scFv F3 protein membrane binding capability in dot and Western blotting

The epitopes of antigens are divided into two categories, conformational and linear, based on their structure and interaction with the paratope (part of an antibody that binds to the epitope). A conformational epitope is composed of discontinuous sections of the antigen's amino acid sequence. By contrast, a linear epitope is formed by a continuous sequence of amino acids from the antigen. The aim of this research was to generate PCa-specific antibodies for application in IHC. Typically, in IHC antigen structure is preserved and thus the protein assumes its natural three-dimensional conformation, exposing its conformational epitope. However, some antigen retrieval approaches can lead to conformational changes in the protein structure and can expose slightly denatured protein (i.e. the linear epitope). Hence, the discovery of an anti-SFRP-2 scFv antibody that can recognise both the linear and conformational epitopes would be highly advantageous.

Western and dot blotting analysis were performed in order to determine the ability of the anti-SFRP-2 scFv antibody to recognise and bind its target antigen in a membrane format. If the antibody was capable of binding to its target in western blot, it recognizes the linear epitope of the antigen (denatured). In contrast, if the antibody recognizes its target in dot blot it recognizes the conformational epitope (target native state). One μg of SFRP-2, which was prepared in 4X SDS-PAGE loading dye and denatured and 95°C for 5 minutes, was loaded per well. The protein was separated by electrophoresis at 120V for 60 minutes. The separated protein bands were then transferred to a nitrocellulose carrier membrane and blocked for 1 hour with 5% (w/v)

PBSM. Varying dilutions of the anti-SFRP-2 scFv F3 were prepared in 1% (w/v) PBSTM and were used to probe SFRP-2 Western blots for 1 hour at RT. A negative control was included in this analysis; whereby, one SFRP-2 protein blot was probed with an anti-cTnI antibody. Bound scFv antibody was detected using an HRP-labeled mouse anti-chicken (IgG) secondary antibody for 1 hour at room temperature, followed by the addition of TMB substrate. Three washes with 1XPBS and 1XPBSTM were completed after each incubation step. A positive anti-SFRP-2 commercial pAb was also included. Results from this analysis show the anti-SFRP-2 scFv F3 antibody performing well in WB even at a dilution of 1 in 1,000. The commercial anti-SFRP-2 pAb showed a stronger band in the WB when compared to the anti-SFRP-2 scFv; however, one must take in to account the difference in antibody concentration before making this comparison. The stock concentration of the commercial antibody was 1mg/mL, whereas the scFv stock concentration was 0.4 mg/mL. Additionally, the difference in molecular weight between the scFv (~30kDa) and the commercial polyclonal antibody (~150kDa) needs to be considered. Hence, in order to truly compare both antibodies and conclude one was out performing the other, the relative molar concentrations would need to be identical.

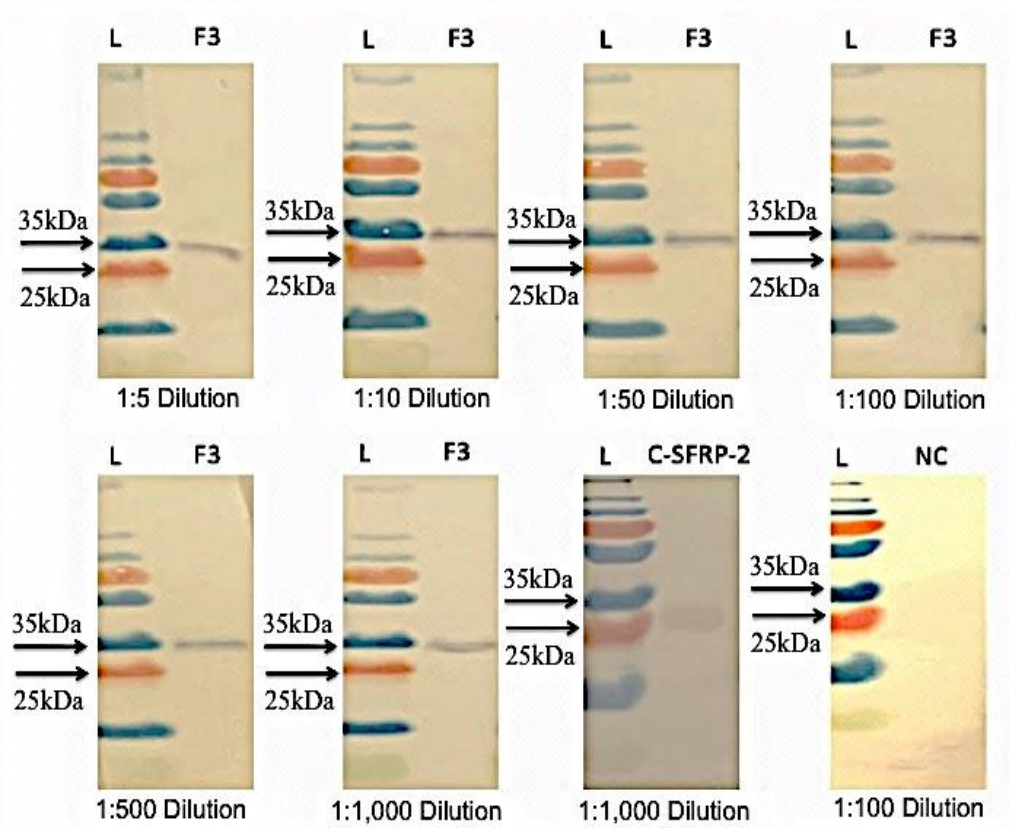

Figure 4.55. Application of anti-SFRP-2 scFv F3 as the primary antibody in a western blot analysis.

Varying dilutions (1 in 5, 1 in 10, 1 in 50, 1 in 100, 1 in 500 and 1 in 1,000) of the anti-SFRP-2 scFv F3 antibody were used to probe a western blot, which had been transferred from resolved SFRP-2 protein on an SDS-PAGE gel, for 1 hour at RT. Bound scFv was detected using an HRP-labelled anti-HA secondary antibody (produced in mouse). C-SFRP-2 represents the positive control (anti-SFRP-2 commercial antibody). NC represents the negative control. The ladder, represented by the letter L in this figure, was a Page Ruler Plus pre-stained protein ladder.

For the dot blot analysis, 2µg/mL of SFRP-2, prepared in molecular grade H_2O, was dotted onto a pre-activated Polyvinylidene fluoride (PVDF) membrane and allowed to dry. The blot was blocked with 5% (w/v) PBSM for 20 minutes at RT. Varying dilutions (1 in 50, 1 in 100, 1 in 500, and 1 in 1,000) of the scFv clone F3, prepared in 1% (w/v) PBSTM, were used to probe the dot blots. Bound scFv was detected using an HRP-labelled anti-chicken (IgG) antibody. Anti-cTnI scFv was included as a control (negative), in addition to the positive commercial control (anti-SFRP-2 commercial pAb raised in goat). Results obtained from the dot blot analysis show the scFv antibody working well even at a dilution of 1 in 1,000.

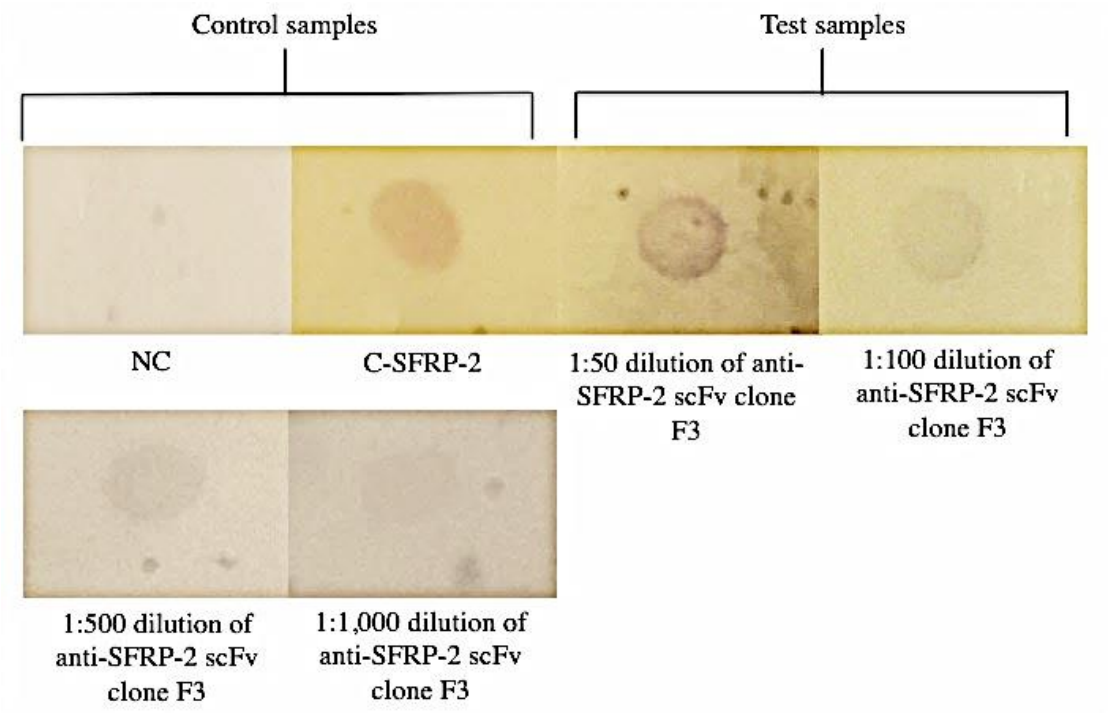

Figure 4.56. Dot blot analysis of anti-SFRP-2 scFv antibody F3.

Two μg/mL of SFRP-2, prepared in molecular grade H_2O, was dotted on to pre-activated PVDF membrane and allowed to dry. The blot was blocked with 5% (w/v) PBSM for 20 minutes at RT. Varying dilutions of the anti-SFRP-2 scFv F3 antibody, prepared in 1% (w/v) PBSTM, were used to probe the dot blots. Bound scFv was detected using a HRP-labelled anti-chicken antibody raised in mouse. C-SFRP-2 represents the positive control (anti-SFRP-2 commercial polyclonal antibody raised in goat). NC represents the negative control (anti-cTnI scFv).

The results obtained from both the western blotting analysis and the dot blot analysis show that this scFv is capable of binding its target antigen in both membrane formats at a dilution as low as 1 in 1,000. These results suggest that this antibody recognises both the conformational and linear epitope of the SFRP-2 protein, suggesting that it could be applicable for use in IHC. However, problems associated with this antibody, such as poor expression and low antibody yield post purification, are a hindrance. In order for an antibody to be appealing commercially for use in IHC, ease of expression and purification, allowing for the production of high quality antibody with high yield, is essential. Three studies completed to date in Prof. O' Kennedy's Lab have shown a significant improvement in antibody expression and yield when the scFv was reformatted to a scAb. Hence, this anti-SFRP-2 scFv was reformatted to a scAb.

4.11 Reformatting the anti-SFRP-2 scFv to a scAb

A plasmid prep of the anti-SFRP-2 scFv F3 clone was prepared and incorporated into a PCR reaction with the primers ChiVL-VHPac-F and ChiVL-VHPac-R to prime the insert for insertion into the pMoPAC vector. The PCR was run under the conditions outlined in Table 29. The PCR product was resolved on a 1.5% (w/v) agarose gel. Figure 59 shows the success of the amplification with the visualisation of the scFv at ~750bp.

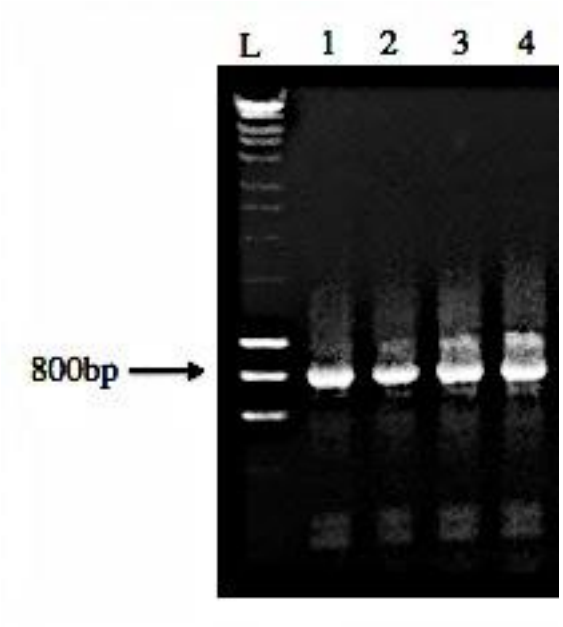

Figure 4.57. Visualisation of the amplification of anti-SFRP-2 scFv F3 using the primers ChiVL-VHPac-F and ChiVL-VHPac-R.

A PCR reaction was set up with the plasmid DNA of clone F3 in order to prime the DNA to allow this insert to be cloned into the pMoPAC vector. MyTaq™ Red Mix was used for this PCR. A large-scale reaction was set up using the components and volumes outlined in Table 28. The PCR was run under the conditions outlined in Table 29. The results were visualised on a 1.5% (w/v) agarose gel. The lanes are labelled as follows; L: Ladder, 1, 2, 3 and 4: PCR amplified anti-SFRP-2 scFv F3, using the primers ChiVL-VHPac-F and ChiVL-VHPac-R.

4.12 Colony-pick PCR to determine whether the pMoPac vector was harbouring the anti-SFRP-2 gene post transformation

Post ligation of the scFv insert into the pMoPAC vector and transformation in Top 10F' chemically competent cells, a colony pick PCR was performed to ensure the pMoPAC vector was harbouring the anti-SFRP-2 gene insert. The results from the

colony pick PCR showed that all clones picked contained the scFv F3 insert. Glycerol stocks were prepared for all clones and one was used as the working stock.

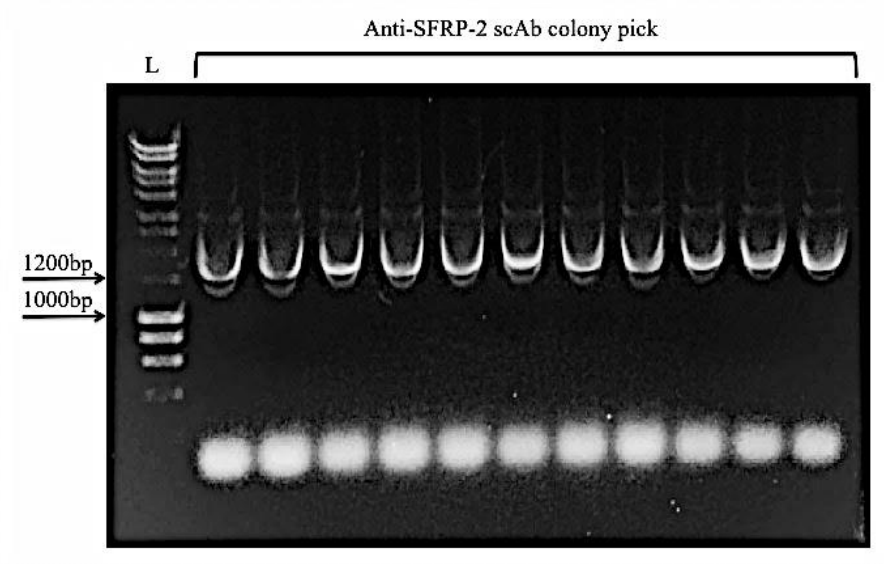

Figure 4.58. Visualisation on a 1.5% (w/v) agarose gel of the colony pick PCR of the transformed pMoPAC vector containing the scFv F3 insert.

Eleven single colonies were picked and incorporated into a colony pick PCR. The gene was amplified using the PCR primers ChiVL-VHPac-F and ChiVL-VHPac-R and MyTaq™ Red PCR mix. L in this figure represents the ladder. Each additional lane contains the PCR product from the colony pick PCR.

4.13 Optimisation of expression of anti-SFRP-2 scAb F3 by varying IPTG concentration and time

Optimisation of expression of the anti-SFRP-2 scAb F3 was carried out to determine the optimum conditions to apply when expressing the scAb on a large-scale. Varying concentrations of IPTG (0.2, 0.5, 0.8, and 1mM) and time were assessed throughout this analysis. The lysates representing each IPTG concentration and time were analysed via WB in order to visualise the optimum conditions. A HRP-labelled anti-chicken (IgG) secondary antibody (raised in mouse) was used to detect the antibody lysate. The results from this optimisation experiment showed that the optimum expression of this clone was achieved with overnight induction using 0.8mM IPTG at 25 °C.

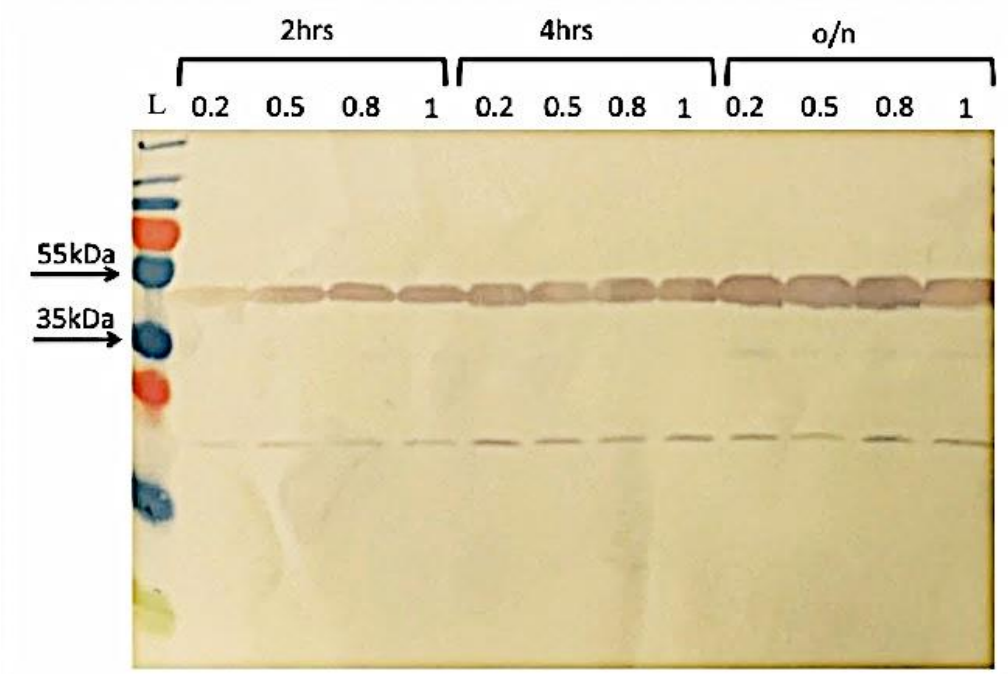

Figure 4.59. Optimisation of expression of the anti-SFRP-2 scAb F3 varying IPTG concentration and times.

An overnight culture of scAb F3 was used to inoculate four 10mL cultures. The cultures were grown at 37 °C, shaking at 220rpm, until an OD_{600} of ~0.7 was obtained. At this point, all cultures were induced with varying concentrations of IPTG (0.2mM, 0.5mM, 0.8mM and 1mM) and the temperature reduced to 25°C. A 1mL sample was taken from each tube after 2hrs, 4hrs and overnight for WB analysis in order to determine the optimum induction conditions for this scAb. ScAb-specific bands were detected using an HRP-labelled anti-chicken (IgG) secondary antibody raised in mouse. L is the pre-stained protein ladder.

4.14 Large-scale expression and subsequent purification of anti-SFRP-2 scAb F3 using an osmotic shock approach

Optimised large-scale expression of the anti-SFRP-2 scAb clone F3 was completed using 0.8mM IPTG for induction overnight at 25°C. The anti-SFRP-2 scAb clone F3 was purified using osmotic shock-based buffers (as described in section 2.2.23) using osmotic shock based buffers delineated in section 2.1.5.2.3). The scAb was purified by virtue of the 6xHis tag encoded on the pMoPAC vector by immobilised metal affinity chromatography (IMAC). The purification was carried out from 5 x 200mL cultures induced overnight.

The concentrated sample was analysed by SDS-PAGE and WB, alongside the filtered lysate, 'flow-through', WA and WB fractions, and showed a very pure protein

preparation. Protein concentration was obtained by A_{280} on a NanoDrop™ 1000 and is outlined in Table 52. The purified antibody was diluted to a working stock concentration of 1mg/mL in sterile PBS containing 0.02% (w/v) NaN_3.

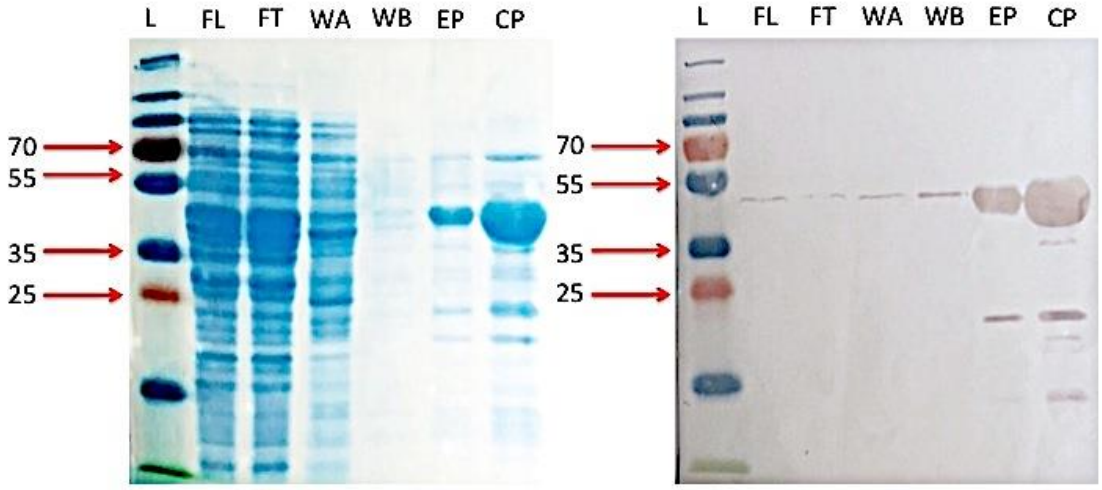

Figure 4.60. SDS-PAGE and WB analysis of anti-SFRP-2 scAb F3 purification steps.

In the large-scale purification, samples of each step of the process were analysed. The lanes are labelled as follows; FL: filtered lysate, FT: 'flow-through', WA: wash A, WB: wash B, EP: eluted protein and CP: concentrated protein. L is the pre-stained protein ladder.

Table 51. IMAC-purified anti-SFRP-2 scAb F3 protein yield determined using the NanoDrop 1000.

Protein fraction	Volume (mL)	Protein yield determined by the NanoDrop™ 1000
Eluted protein	4.0	5.4 mg/mL
Concentrated protein	1.0	22.0 mg/mL

In order to visually compare the difference in protein yield between the scFv and scAb, 10µg of both pure antibodies were run alongside each other on a SDS-PAGE gel. The results shown in Figure 4.63 show a significant difference in antibody-specific yield. The band obtained for the scAb is the strongest band present on the gel whereas the scFv-specific band is weak and not the most prominent protein band present. The anti-SFRP-2 scAb was brought forward for testing in western and dot

blotting and used as the primary antibody in a fluorescent microscopic analysis of prostate tissue.

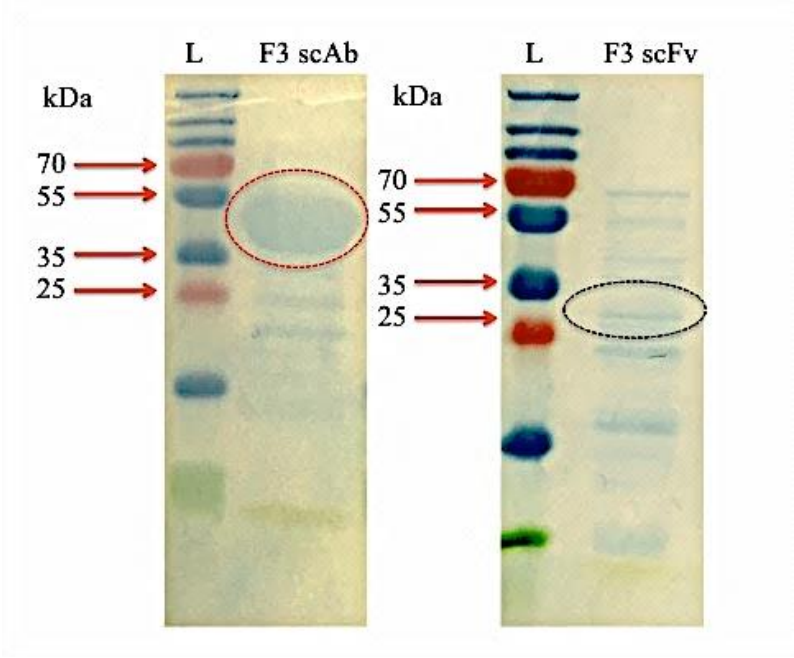

Figure 4.61. Visual comparison of the improvement of antibody yield by reformatting a scFv to a scAb.

Ten µg of both the anti-SFRP-2 scFv and scAb were run alongside each other on a SDS-PAGE gel in order to visually compare the purity and yield. The result shows the advantage of reformatting this scFv to a scAb. L is the pre-stained protein ladder.

4.15 Western and dot blot analysis of purified anti-SFRP-2 F3 scAb

Varying dilutions of the purified scAb were prepared in 1% (w/v) PBSTM and used to probe SFRP-2 western and dot blots. Bound scAb was detected using HRP-labelled anti-chicken- secondary antibody. Results from this experiment show the anti-SFRP-2 scAb working efficiently as a primary antibody in both WB and dot blot analysis at a dilution of 1 in 2,000. This antibody dilution was applied in the fluorescence-based microscopic analysis described in the following section.

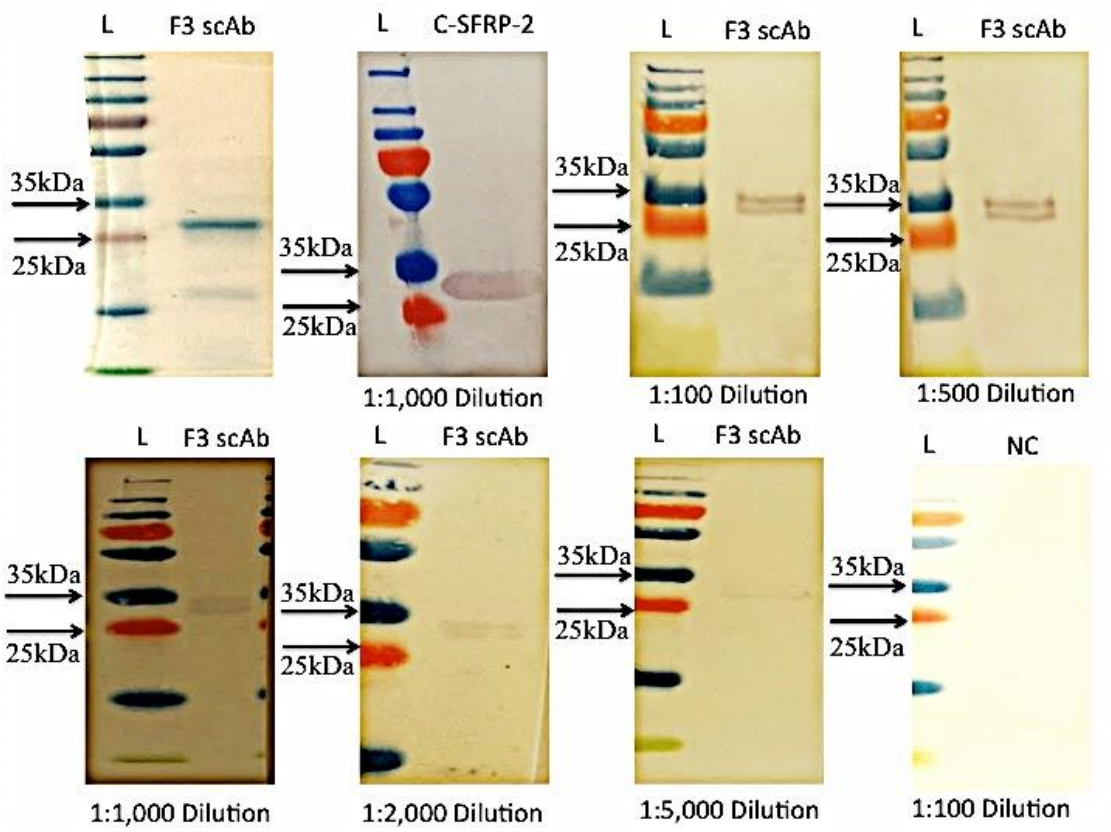

Figure 4.62. Application of an anti-SFRP-2 scAb F3 clone as the primary antibody in a western blot.

Varying dilutions (1 in 100, 1 in 500, 1 in 1,000, 1 in 2,000 and 1 in 5,000) of the anti-SFRP-2 scAb F3 antibody were used to probe western blots, which had been transferred from resolved SFRP-2 protein on an SDS-PAGE gel, for 1 hours at RT. Bound scFv was detected using an HRP-labelled anti-HA secondary antibody raised in mouse. L is the pre-stained protein ladder. A commercial anti-SFRP-2 polyclonal antibody (Abcam) was applied as the control (C-SFRP-2) in this experiment.

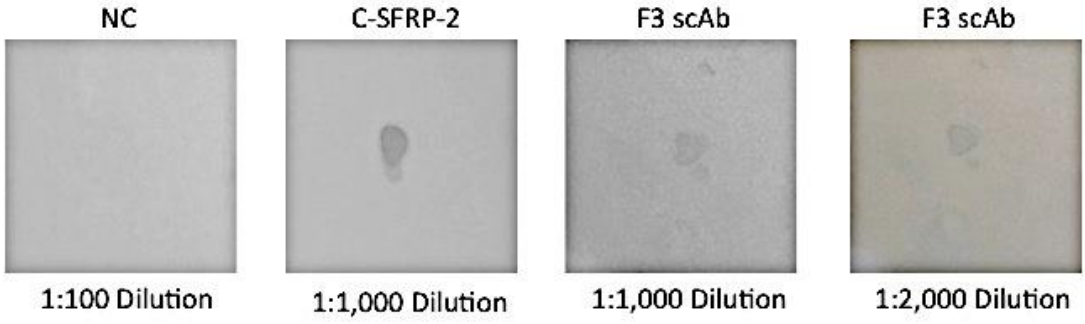

Figure 4.63. Application of an anti-SFRP-2 scAb F3 clone as the primary antibody in a dot blot.

Two µg/mL of SFRP-2, prepared in molecular grade H_2O, was dotted on to pre-activated PVDF membrane and allowed to dry. The blot was blocked with 5% (w/v) PBSM for 20 minutes at RT. Varying dilutions of the anti-SFRP-2 scAb F3, prepared in 1% (w/v) PBSTM, were used to probe the dot blots. Bound scAb was detected using an HRP-labelled anti-chicken (IgG) antibody raised in mouse. The images are labelled are follows; NC: Negative control, C-SFRP-2: Positive control (anti-SFRP-2 commercial polyclonal antibody raised in goat).

4.16 Fluorescence-based microscopic analysis of normal, benign prostatic hyperplasia and malignant prostate tissue probed with anti-SFRP-2 scAb F3 and anti-chicken H/L Dylight488-labelled polyclonal antibody

Epigenetic silencing, as described in detail in section 4.1, of the SFRP-2 gene has been implicated to be associated with a number of different cancers, suggesting the potential role of this marker in tumour suppression (Guo *et al*., 2014; Saito *et al*., 2014; Sui *et al.*, 2014; Xiao *et al*., 2001). However, todate, there is only one study suggesting SFRP-2 as a potential prognostic biomarker for PCa. O' Hurley *et al*. (2011), have proposed this marker as a key marker for histochemically benign prostate glands and a subgroup of Gleason grade 5 tumours that may predict prognosis.

O' Hurley *et al*. (2011) struggled to source an anti-SFRP-2 antibody applicable for use in their research. The majority of antibodies tested either did not work in tissue, or provided very weak SFRP-2-specific staining. The antibody applied in their research was removed from the market prior to this project for unknown reasons. Hence, the generation of histochemically relevant anti-SFRP-2 antibodies is highly warranted in order to allow one to gain an in depth insight into the potential use of this marker for PCa. This study has shown the generation of an anti-SFRP-2 recombinant antibody

applicable as a primary antibody in WB and dot blotting. Additionally this antibody was characterised by ELISA and Biacore analysis. The anti-SFRP-2 antibody presented here shows potential for application in IHC. The TMAs available for this study were of limited supply, hence preliminary testing of prostate tissue was carried out prior to IHC application on clinical samples. Normal, benign prostatic hyperplasia and malignant (adenocarcinoma) prostate tissue slides were obtained commercially from Abcam and incorporated into fluorescence-based microscopic analysis, where the primary antibody was the anti-SFRP-2 scAb.

This analysis was completed to determine the ability of the scAb to bind its target antigen in varying forms of prostate tissue. One negative (anti-cTnI scFv antibody (raised in chicken) probed with an anti-chicken H/L Dylight488-labelled polyclonal antibody) and one positive (anti-SFRP-2 pAb) control were included in this experiment. The anti-cTnI negative control was included to ensure the response/signal obtained for the test antibody was specific. Additionally, the anti-chicken H/L Dylight488-labelled polyclonal antibody was included as a secondary antibody for the control to assess the extent of background staining that could potentially lead to the production of false positive results. The prostate tissues were prepared and probed with a 1 in 2,000 dilution of the scAb, alongside the control slides overnight at 4 °C. Bound scAb was detected using an anti-chicken H/L Dylight488-labelled polyclonal antibody. The results from this study were inconclusive as the auto-fluorescence of the secondary antibody, in the absence of cover slides (prevent drying out of the tissue), prevented clear imaging of the tissue samples from being achieved. Due to time constraints and the high cost of the commercial tissue, this experiment could not be repeated. IHC analysis, of various prostate tissue samples, applying this antibody is currently ongoing in Beaumont Hospital.

4.17 Chapter discussion and conclusion

O' Hurley *et al.* (2011), implicate SFRP-2 as a novel immunohistochemical marker for prostate cancer (results from this study discussed in detail in section 4.1.6.1 of this chapter). However, further evaluation on larger patient numbers with longer follow-up will address whether SFRP-2 expression has true prognostic relevance. If the results from future studies concur with the preliminary results presented by O' Hurley *et al.* (2011), SFRP-2 could become a useful marker for predicting prognosis and biochemical recurrence, particularly in patients with advanced prostate cancer.

This chapter presents the successful generation of a recombinant SFRP-2 antibody. IHC analysis applying this antibody is currently underway in Beaumont hospital to confirm the results described above and add to the current research on SFRP-2 as a potential marker for the improvement of PCa diagnosis.

Due to the lack in availability of biologically relevant SFRP-2 protein, a novel expression system (described in detail in Chapter 3 of this thesis) was utilized for the successful production of a recombinant SFRP-2 fusion protein. This protein was subsequently utilised as a primary antigen to induce an SFRP-2-specific immune response in an avian host. Following a full immunisation schedule, high anti-SFRP2 antibody titre responses were observed in avian serum. The animal was sacrificed and both the spleen and bone marrow were harvested. RNA was extracted from both sources and used as a template for cDNA synthesis. Successful amplification of full-length scFv gene fragments was carried out using consecutive PCR steps. Purified pComb3xSS vector and the anti-SFRP-2 spleen and bone marrow scFv libraries were digested using the S*fi*I restriction enzyme, ligated and transformed into electrocompetent *E. coli* XL-1 Blue cells generating a combined library size of 6.1 x 10^7 members, which was subsequently rescued with helper-phage for screening via phage display.

The immunogen utilized in the immunisation campaign described in this chapter was an SFRP-2-FABP fusion protein. Hence, the potential of isolating anti-FABP antibodies alongside the anti-SFRP-2 scFv antibodies would be quite high if this protein was used as the antigen in the screening approach. In order to enhance the potential of obtaining target-specific antibodies a collaboration was set up between

Prof. O' Kennedy's research group and Prof. Whisstock's research group in Monash University. Prof. Whisstock's group are renowned for large-scale expression of human proteins for subsequent crystallisation. During the development phases of this project it was realised that the crystal structure for both the partial and full-length SFRP-2 proteins are absent and are of high value. Solving the crystal structure of this protein is of considerable importance as, once elucidated, the information will provide insights into the structure and function of this novel disease-associated protein which, in addition to cancer, has roles in CVD, myogenesis and retinal development. Hence, the expression of this protein was beneficial for both parties involved. Dr. Paul Conroy, a postdoctoral fellow in Prof. Whisstock's Lab, expressed and purified the full length SFRP-2 protein in mammalian CHO cells. This protein was utilised in this project as the antigen for screening the anti-SFRP-2 scFv library, allowing the identification of numerous potential anti-SFRP-2 lead antibody candidates. Additionally, research is currently ongoing to solve the crystal structure of this full-length protein in Monash University.

A conventional phage display method was applied for screening the anti-SFRP-2 scFv library, whereby, the antigen (full-length SFRP-2 protein) was absorbed to a solid support (microtitre plate). Following exposure of the scFv phage particles to the target antigen, non-specific binders were removed in the wash steps, and phage bound to the target were recovered in the elution step. The eluted phage were successfully re-amplified in *E. coli* and used in four rounds of panning. Table 47 shows the input and output titres obtained over the four rounds of panning the anti-SFRP-2 scFv library. A polyclonal phage ELISA was performed in order to determine at which round significant enrichment of the anti-SFRP-2 library was achieved. Enrichment of the scFv library to the target protein was achieved after three rounds of panning, as this round showed the strongest target-specific reactivity.

The phage pools from round three of panning were subsequently infected into a non-suppressor (non-SupE) strain of *E. coli* (Top 10 F'). Three hundred and eight four anti-SFRP-2 scFv clones were selected for screening against the SFRP-2 antigen. This screening approach was carried out at a protein level to assess binding in two ways: i) monoclonal phage ELISA and ii) Biacore^{TM} 4000 high throughput (HT)-ranking by stability early and late analysis. The acquired data, most notably on the refined HT-

system, offered a wealth of information to judiciously aid the screening process.

Analysing the data obtained from the screening process allowed the 7 lead anti-SFRP-2 candidates to be identified. Sequencing analysis revealed that out of the 7 antibodies sent for sequencing, only 2 different clones were present (Clone number 57 on Biacore (Plate 3 clone C4 (clone position in ELISA plate) and clone number 159 (Plate 4 C4 (clone position in ELISA plate). The low diversity of the clones sequenced validates the stringent selection and rigorous screening approach applied to identify these anti-SFRP-2 specific scFv antibodies. Both anti-SFRP-2 scFv antibodies were brought forward for further characterisation, allowing the successful identification of anti-SFRP-2 scFv F3 which showed similar efficiency at recognizing its target antigen in ELISA, WB and dot blot to the commercial anti-SFRP-2 polyclonal antibody. Post optimised-large-scale expression of this clone, the antibody was purified by IMAC. The purified antibody was successfully applied as the primary antibody in western blot and dot blot analysis and was capable of binding its target at a dilution as low as 1 in 1,000.

The yield of antibody obtained post purification was quite low (0.4mg/mL from a 1L culture). Optimisation of purification was completed but unfortunately no improvement in yield was achieved. It was concluded that the low yield obtained could have been due to the poor expression of this antibody. Expression and production of scFvs in *E. coli* is greatly influenced by the stability and folding of the antibody fragment in the *E. coli* periplasm which, in turn, depends on several factors, such as, disulphide bonds, salt bridges between oppositely charged amino acids and repulsions between equally charged amino acids, hydrophobic core packing, buried hydrophilic residues and exposed hydrophobic residues. Several studies focused on the effect of various biophysical factors to improve stability (Knappik & Pluckthun, 1995; Forsberg *et al*., 1997; Kipriyanov *et al*., 1997; Nieba *et al*., 1997; Ewert *et al*., 2003). However, previous studies completed in Prof. O' Kennedy's research group showed a significant improved in antibody expression when the scFv was reformatted to a scAb.

Reformatting the anti-SFRP-2 scFv antibody to a scAb significantly improved the expression of this antibody, providing a purified antibody yield ~60 times greater than that obtained by the scFv. The purified antibody was diluted to a working stock

concentration of 1mg/mL and used as the primary antibody in a fluorescence-based microscopic analysis of various forms of prostate tissue (normal, benign and malignant). All tissues were obtained from donors aged between 50 and 60 years old. The tissue slides were fixed in paraformaldehyde, processed to paraffin wax and cut to a thickness of 5μM. Three slides for each type of tissue were provided at a cost of ~900 euro. Hence, it was essential to carefully plan the experimental approach taken and the necessary controls to include ensuring success of the experiment. One negative and one positive control were included in this analysis. An indirect fluorescent microscopic approach was applied for this study, whereby the fluorophore (Alexa488 in this study) was conjugated to the secondary anti-chicken antibody specific for the primary antibody (anti-SFRP-2 scAb F3, raised in chicken). The results from this study were inconclusive as the auto-fluorescence of the secondary antibody, in the absence of cover slides (prevent drying out of the tissue), prevented clear imaging of the tissue samples from being achieved. Due to time constraints and the high cost of the commercial tissue, this experiment could not be repeated.

IHC analysis of prostate tissue applying this antibody is currently underway to gain more of an insight into the expression pattern of this protein in PCa and how it could potentially aid in improving PCa diagnosis and overcome current issues associated with the PSA test. In addition to IHC analysis, Prof. James Whisstock's research group, are working on resolving the crystal structure of this scAb in order to show it in complex with the full length SFRP-2 protein. Knowledge of protein structure and function is vital in order to fully appreciate the interactions that occur between proteins, for example, an antibody and its cognate antigen.

In conclusion, SFRP-2 has been highlighted as a key marker in prostate cancer research. This chapter presents the successful generation of an anti-SFRP-2 recombinant antibody, which could be applied in the future to improve the diagnosis of prostate cancer.

Chapter 5

Generation and characterisation of an anti-prostate-specific membrane (PSMA) recombinant antibody

Chapter outline

Prostate–specific membrane antigen (PSMA) is the most well-established, highly specific prostate epithelial cell membrane marker known. Pathology studies, carried out to date, indicate that virtually all prostate cancers express PSMA. Moreover, PSMA expression increases progressively in higher-grade cancers, metastatic disease and castration-resistant prostate cancer (CRPC). Although first thought to be entirely prostate-specific, subsequent studies demonstrated that cells of the small intestine, proximal renal tubules, and salivary glands also express PSMA. However, the expression levels of PSMA in normal cells is 100–1000-fold less than in prostate tissue, and the site of expression is not typically exposed to circulating intact antibodies (Tagawa *et al.*, 2010)

This chapter describes the approach taken to generate an anti-PSMA scFv and scAb, the screening methods applied to identify key PSMA-specific antibodies, and the characterisation of these antibodies. A female Leghorn chicken was immunised with two prostate cancer-specific cell lines that overexpress PSMA, namely LNCaP and 22RV1. After a 3-month immunisation programme, the animal was sacrificed. Both the spleen and bone marrow were harvested and the ribonucleic acid (RNA) extracted using standard protocols. The amplified antibody variable genes were assembled by splice overlap extension polymerase chain reaction (SOE-PCR) and ligated into the Barbas pComb3xSS vector (Barbas *et al.*, 2001). The recombinant phage display libraries were screened against a commercial full-length PSMA protein. ELISA analysis and high throughput Biacore^{TM} screening were performed in order to select for PSMA-specific antibodies. The lead anti-PSMA scFv antibody was subsequently characterised by ELISA and Western blotting. Reformatting this scFv to a scAb led to an improvement in expression and binding affinity in Western blotting. The scAb was brought forward for preliminary testing in fluorescent microscopic analysis.

5.1 Introduction to Prostate-specific membrane antigen

Efforts to evaluate and discover diagnostic and therapeutic markers for prostate cancer continue. One of these, prostate-specific membrane antigen (PSMA), a transmembrane protein expressed in all types of prostatic tissue, remains a useful diagnostic and possibly therapeutic target. PSMA is a type II membrane protein originally characterised by the murine monoclonal antibody (mAb) 7E11-C5.3 and is expressed in all forms of prostate tissue, including carcinoma. The PSMA protein has a unique 3-part structure: a 19-amino-acid internal portion, a 24-amino-acid transmembrane portion, and a 707-amino-acid external portion (Leek *et al.*, 1995; Denekamp *et al.*, 1998). The PSMA gene is located on the short arm of chromosome 11 in a region that is not commonly deleted in prostate cancer (O'Keefe *et al.*, 1998).

PSMA is up regulated and strongly expressed on prostate cancer cells associated with high grade primary, androgen independent, and metastatic tumours (Ben Jemaa e*t al.*, 2014). The expression in other tissues is significantly lower compared to the expression in prostate cancer (Mhawech-Fauceglia e*t al.*, 2007). PSMA expression differs between benign prostatic tissue, localized prostate cancer, and lymph node metastases and is increased in the more advance stages of prostate cancer (Mhawech-Fauceglia e*t al.*, 2007).

PSMA is found in all adenocarcinomas, but its expression is greatest in high-grade adenocarcinoma. PSMA's expression was found to increase from benign epithelium to high-grade prostatic intraepithelial neoplasias (Bernacki *et al.*, 2014). Its expression is also associated with prostate cancer cells responsive to androgens with an increase in activity as cells transition to become more androgen-independent (Bernacki *et al.*, 2014). PSMA has become an established biomarker for the progression of prostate cancer (Mhawech-Fauceglia e*t al.*, 2007; Bernacki *et al.*, 2014) and has attracted significant attention as a target for the delivery of imaging (Bouchelouche *et al.*, 2010) and therapeutic agents (Bouchelouche *et al.*, 2010).

The ability to selectively detect PSMA overexpression in prostate cancer tissue offers the promise for new avenues of diagnosis and earlier therapeutic intervention for patients at risk of an aggressive metastatic stage of the disease. The aim of this chapter was to generate anti-PSMA recombinant antibodies applicable for use in IHC for the analysis of various forms of prostate tissue.

5.2 Results

5.2.1 Immunisation response to full-length PSMA protein

A serum titration was performed to determine whether a sufficient response had been achieved following immunization with PSMA. A series of dilutions of chicken serum, ranging from 1 in 100 to 1 in 1,000,000 following dilution in 1% (w/v) Milk Marvel prepared in PBST (0.05% (v/v)); (pH, 7.2), were tested against commercially available PSMA in a direct ELISA format. A titre in excess of 1/50,000 was observed from the ELISA, suggesting the presence of a high level of specific mRNA, which could be used for the generation of a recombinant antibody library against PSMA (Figure 5.66).

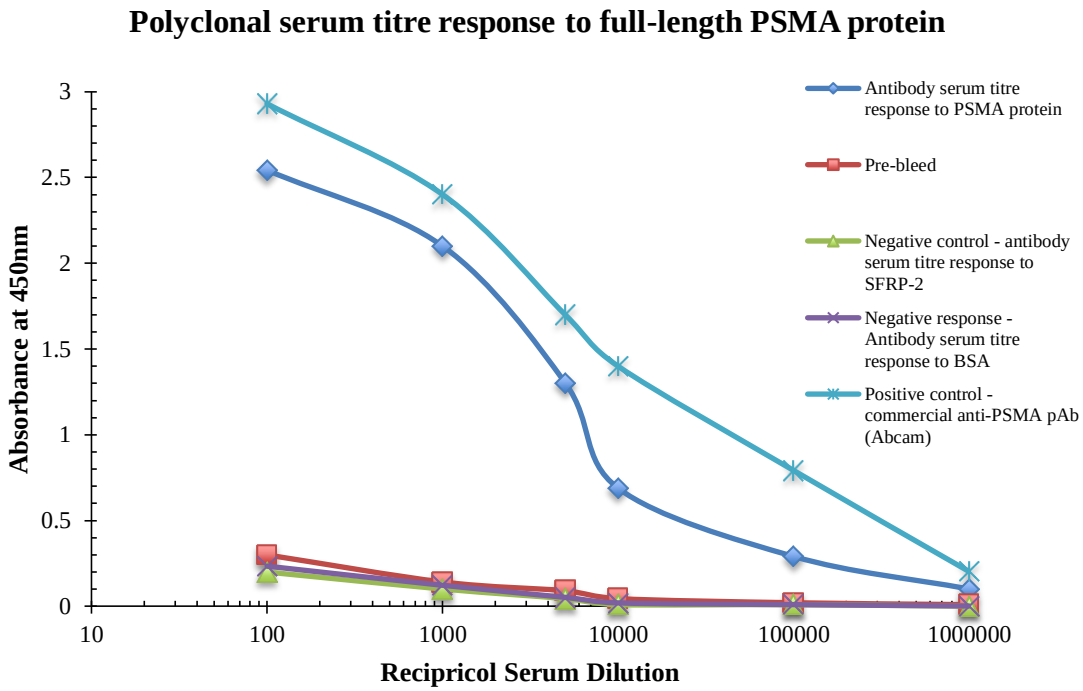

Figure 5.64. Avian anti-serum titration for a chicken sensitised with two prostate cancer cell lines, LNCaP and 22RV1.

Serum was collected from an adult Leghorn chicken (female) 7 days prior to sacrifice, diluted in 1% (w/v) PBSTM and bound IgY (chicken antibody) detected using anti-chicken-Fc-specific HRP-labelled antibody. The graph indicates a significant antibody response for the commercial PSMA full-length protein.

5.2.2 Construction of an anti-PSMA avian scFv library

The preliminary testing of immune serum from the immunised chicken demonstrated a clear response to PSMA. The antibody encoding genes were then isolated. In the first stage of recombinant antibody generation, the variable heavy (V_H) and the variable light (V_L) genes were amplified from avian spleen and bone marrow cDNA.

5.2.2.1 Chicken variable heavy and light chain PCR amplification

Initially, the $MgCl_2$ concentration for the PCR was optimised for the V_L and V_H of both the bone marrow (BM) and spleen (SP). $MgCl_2$ optimisation allows for optimal yield with greatest specificity. The yield is influenced by activity of the Taq polymerase and the magnesium ion-dependent incorporation of dNTPs, which also affects the specificity of primer for the template. The PCR products for each variable domain at each $MgCl_2$ concentration for both the BM and SP were resolved on 1.5% (w/v) agarose gels. These indicated similar yield, shown by discrete-specific band formation at approximately 450bp for V_H and 350bp for V_L (Figure 5.67). Post large-scale amplification the correct size amplicons were isolated by gel extraction and clean up (as per the manufacturers' guidelines). Both the V_L and V_H genes were then brought together by the inclusion of a flexible serine glycine linker [$(G_4S)_4$] in a splice-by-overlap extension (SOE) PCR (section 5.2.2.2).

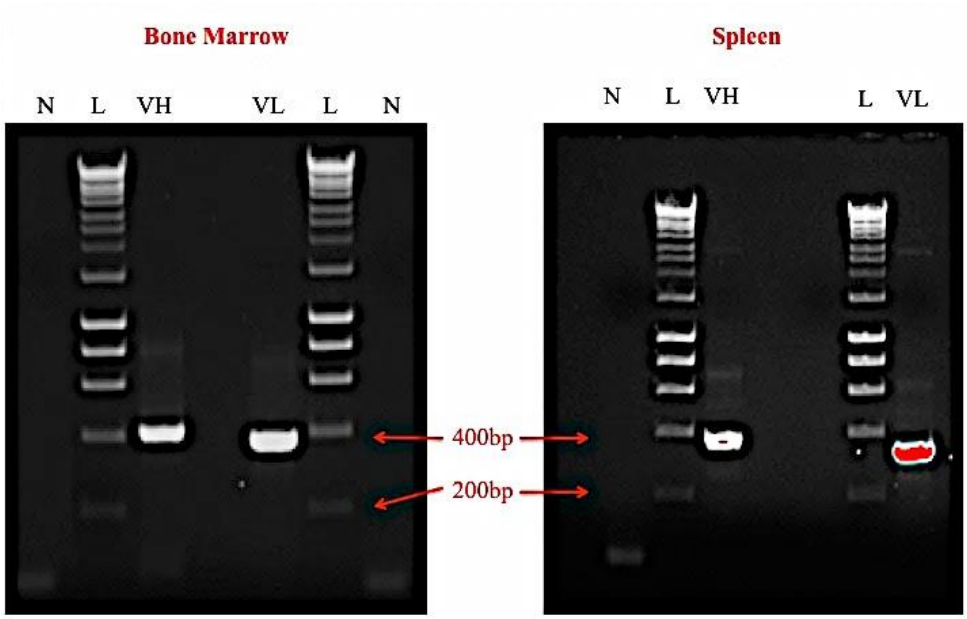

Figure 5.65. Optimised large-scale amplification of spleen and bone marrow V_L and V_H from cDNA.

Visualisation of large-scale amplification of V_L and V_H from SP (right) and BM (left) from cDNA obtained from a chicken immunised with LNCaP and 22RV1 prostate cancer cell lines, post $MgCl_2$ optimisation. In both cases V_L amplicons were observed at ~350bp and V_H amplicons at ~450bp. A negative control (N) PCR showed no contaminating bands. The 1Kb+ DNA ladder (L) allowed approximation of DNA fragment size following resolution on a 1.5% (w/v) agarose gel.

5.2.2.2 SOE PCR of the variable heavy and light region to generate an anti-PSMA scFv library

Following the successful amplification of the avian variable domain genes, the purified variable domains were incorporated in equimolar ratios into the SOE product corresponding to the scFv fragment (approximately 750-800bp) using the CSC-F and CSC- B primers. At this stage of the library construction process a high fidelity enzyme, MyTaq™ Red Mix, was used to ensure correct formation of the scFv fragment. The large-scale reactions were visualised on 2% (w/v) agarose gel and showed a diffuse band that was sufficiently discrete to be isolated and purified.

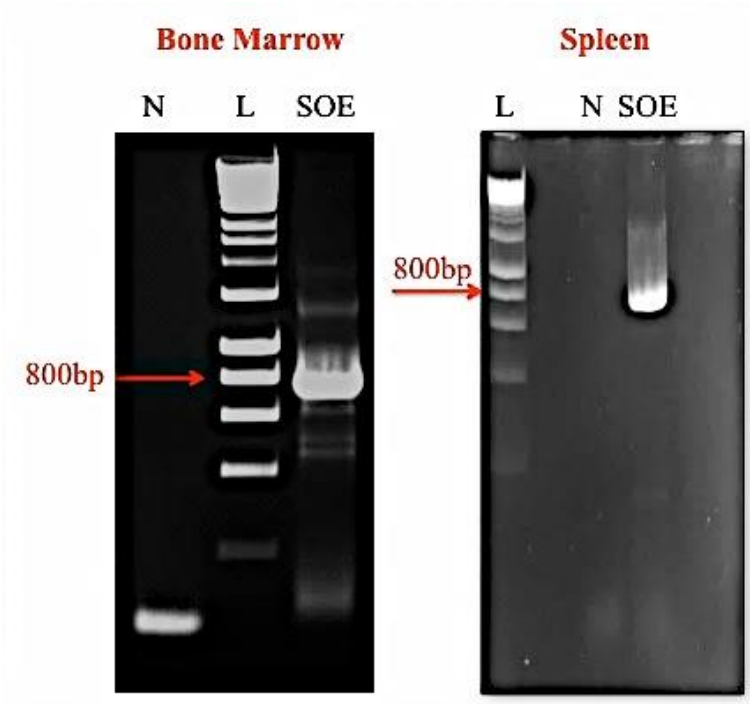

Figure 5.66. Optimised large-scale SOE-PCR for SP (right) and BM (left).

An equimolar mix of V_L and V_H was overlapped by virtue of the overlap extension tails on the V_L reverse and V_H forward primers. Both the SP and BM show the formation of a specific band at ~800bp corresponding to the scFv SOE product. Negative control reactions showed that no non-specific products were amplified.

5.3 S*fi*I restriction digest of the pComb3xSS vector plasmid

The pComb3xSS vector was made available by Professor Carlos Barbas III of the Scripps Institute, La Jolla, California, USA. The vector is a variant of pComb3x (accession number AF268281) containing a stuffer fragment. The vector contains both *E. coli* and phage origins of replication and can act as a shuttle vector for DNA encoding scFv (or Fab) fragments between *E. coli* cells and expression of the scFv on the surface of phage as a fusion to the geneIII protein. The vector was previously transformed into dcm$^-$/dam$^-$ *E. coli* for vector purification (Dr. Paul Conroy, Monash University, Melbourne, Australia) and stored in glycerol aliquots. An overnight culture of the pComb3xSS vector was prepared, followed by plasmid preparation of the vector prior to digestion.

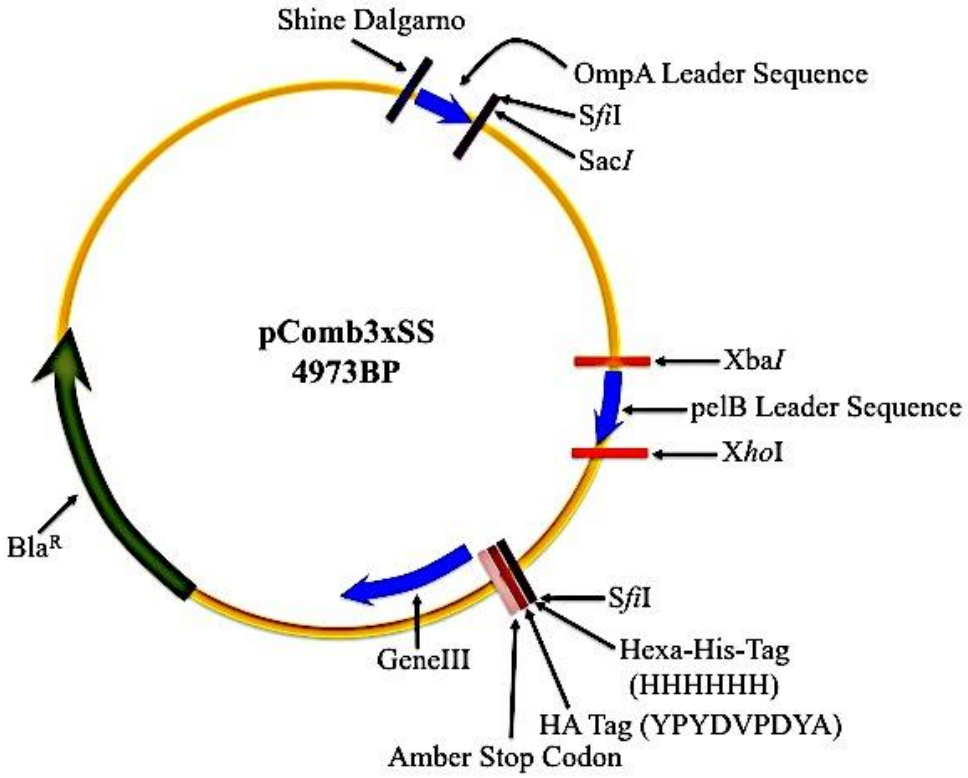

Figure 5.67. pComb3xSS vector map.

The pComb3xSS vector is approximately 4973bp. The "SS" in the vector name refers to the double stuffer fragment, located between the two SfiI sites. This vector contains a His-TAG and HA-tag allowing ease of purification and detection. The amber stop codon incorporated into the vector 'turns-off' expression of the pIII fusion protein by switching to a non-suppressor strain of E. coli allowing production of soluble protein without sub-cloning.

Large-scale digestion of the vector to incorporate the anti-PSMA scFv library was carried out in a stepwise, triple digestion protocol. Digestion of the vector with S*fi*I may result in a significant amount of intact stuffer fragment or undigested vector, leading to library contamination, as observed in previous experiments despite de-phosphorylation of the cut vector (personal communication: Dr. Stephen Hearty and Dr. Paul Conroy, DCU, Ireland/Monash University, Melbourne). To overcome this, subsequent digestion of the vector with X*ho*I and X*ba*I further degraded the stuffer fragment into three products (S*fi*I –X*ba*I, X*ba*I – X*ho*I and X*ho*I – S*fi*I), which were observed on a 0.5% (w/v) agarose gel. In addition, Antarctic phosphatase treatment of the entire vector digestion results in a de-phosphorylated vector, thus further preventing re-ligation. The fully digested, treated and purified pComb3xSS vector was visualised on 0.5% (w/v) gel showing a single band at approximately 3300bp

(results not shown).

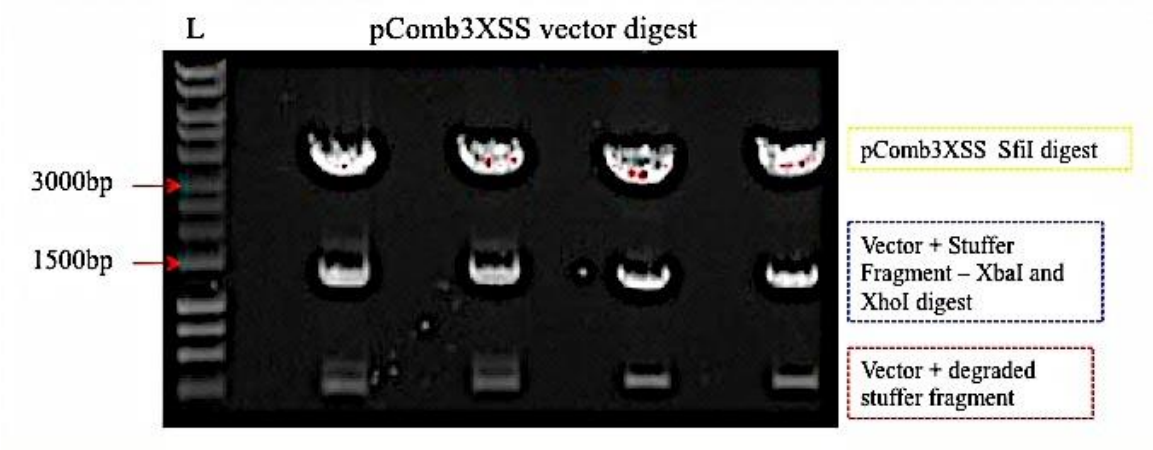

Figure 5.68. Large-scale triple digestion of pComb3xSS vector.

Triple digestion involved further degradation of the stuffer fragment (already SfiI digested) with XhoI and XbaI (Table 24 in Section 2.4.10). The triple digestion reduces the potential for contamination of the downstream library building process. The digestions were resolved on a 0.5% (w/v) agarose gel and were compared to a 1Kb+ DNA ladder.

5.3.1 S*fi*I restriction digest of the anti-PSMA scFv library

Successful S*fi*I digestion of the SOE products was confirmed on a 1.5% (w/v) agarose gel with cleavage of the restriction site plus the $(GAG)_6$ sequence readying the insert for ligation into the triple digested pComb3x vector. Post ligation the antibody libraries (BM and SP) were transformed into XL1Blue electrocompetent *E. coli* cells generating a combined library size of 1.2 x 10^7 members, which was subsequently rescued with helper-phage for screening via phage display. The background re-ligation/contamination of this library was found to be less than 1000, as confirmed by the completion of a control titre, which was composed of a vector re-ligation reaction without the presence of the insert. This highlights the success of the triple digestion methodology in combination with de-phosphorylation of the pComb3xSS vector during the library building process, generating a specific and uncompromised antibody library.

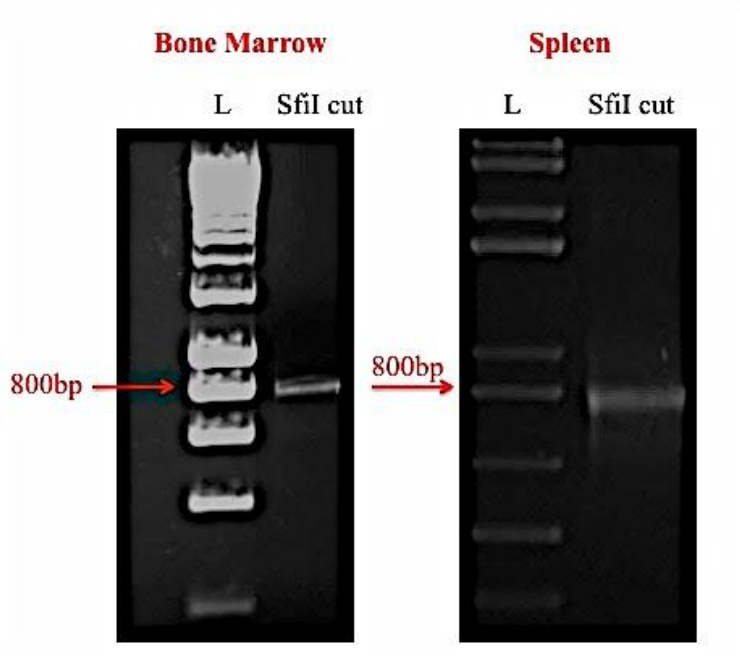

Figure 5.69. Large-scale SfiI digestion of avian anti-PSMA scFv SOE-PCR inserts.

Visualisation of successful SfiI digestion of spleen and bone marrow anti-PSMA scFv SOE-PCR inserts on a 1.5% (w/v) agarose gel.

5.3.2 Phage display of anti-PSMA scFv antibodies

The library was evaluated in a highly stringent antigen presentation manner to maximize the probability of selecting anti-PSMA-specific scFv antibodies. The scFv fragments were rescued by helper-phage and displayed on filamentous phage surface. The panning strategy outlined in section 2.5.13 of this thesis was exploited incorporating panning conditions and stringencies that are delineated in Table 53. A high density (100µg/mL and 50 µg/mL) of PSMA protein was used for the first two rounds of panning to ensure enrichment of the library. To complement the stringency element introduced by this presentation strategy, a further level of selective pressure was introduced by gradual limitation of the concentration of antigen available for binding, in addition to, an increased number of wash steps throughout. After four rounds of panning the phage preparations for each round were analysed by polyclonal-phage ELISA (section 5.4).

Table 52. Panning conditions for the generation of the PSMA-specific chicken scFv library using varying concentration of PSMA coated on the wells of an ELISA plate.

The stringency of each consecutive round of panning was altered by increasing the number of washes and decreasing the antigen coating concentration.

Panning round	PSMA antigen coating conc. (µg/mL)	Washing frequency
1	100	3 X PBS, 3 X PBST
2	50	5 X PBS, 5 X PBST
3	25	7 X PBS, 7 X PBST
4	10	10 X PBS, 10 X PBST
5	5	15 X PBS, 15 X PBST

Table 53. Phage input and output titres.

The phage input and output titres over 4 rounds of panning of the avian anti-PSMA scFv library.

Anti-PSMA scFv panning input and output titres from 4 rounds of panning		
Round 1	**Input titre**	**Output titre**
	1.4×10^{12}	2.6×10^{6}
Round 2	**Input titre**	**Output titre**
	3.2×10^{11}	1.6×10^{6}
Round 3	**Input titre**	**Output titre**
	2.1×10^{11}	1.2×10^{5}
Round 4	**Input titre**	**Output titre**
	1.3×10^{10}	1×10^{6}

5.4 Polyclonal phage ELISA analysis of precipitated phage obtained after each round of panning to identify the round in which significant enrichment of the anti-PSMA scFv library occurred

Post-panning, the selected antibody-displaying phage from each round of selection were evaluated for enrichment against PSMA in a polyclonal-phage ELISA. To increase confidence in the result, a helper phage negative control, and BSA coated wells were included in the assay. The presence of specific-antibody-displaying phage was detected by an anti-M13 HRP-labelled secondary antibody. Figure 5.72 illustrates the dramatic increase in specific-antibody-displaying phage at round four, suggesting enrichment of scFv-harbouring phage within the panned library. There was minimal or no background binding to any of the included controls. Round four phage were subsequently infected into mid-exponential *E. coli* Top 10F' for expression of soluble scFv fragments and taken forward into the screening campaign.

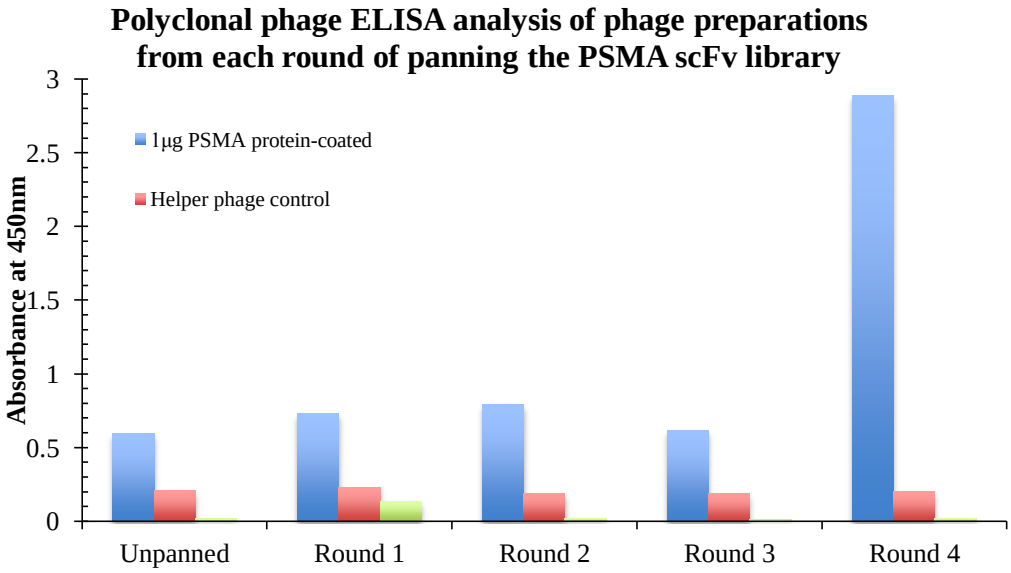

Figure 5.70. Polyclonal-phage ELISA analysis to identify the panning round in which significant enrichment for PSMA occurred.

The phage preparations were assayed for specific binding against PSMA. Phage from each round was diluted 1 in 5 in 1% (w/v) PBSTM and 100µl applied to each well. Bound phage were detected using anti-M13-HRP-labelled secondary antibody. The ELISA plate was developed using TMB and the absorbance read at 450nm. The graph shows the dramatic increase in phage-displaying PSMA-specific scFv after four rounds of panning.

5.5 Screening analysis of specific-antibody-displaying phage

Three hundred and eighty four single colonies were isolated and grown up for

screening. The screening approach was carried out at a protein level to assess binding in two ways: i) ELISA and ii) Biacore^{TM} 4000 high throughput (HT)-ranking by stability early and late analysis. The acquired data, most notably on the refined HT-system, offered a wealth of information to judiciously aid the screening process.

5.5.1 Monoclonal phage ELISA analysis of 384 clones picked following polyclonal phage ELISA analysis of precipitated phage from panning of the anti-PSMA scFv library

Initial protein-specificity screening was performed as a preliminary evaluation of the success of the panning strategy post polyclonal phage ELISA analysis and prior to HT-screening on the Biacore^{TM} 4000 (as described in section 2.5.18 and 2.5.19). Three hundred and eighty four scFv clones were included in this analysis to identify potential PSMA-specific binders. A positive clone was defined as having a PSMA-specific binding response greater than an absorbance of 0.3A.U. The screen highlighted the success of the panning strategy, but was merely a pre-screen for more rigorous HT analysis.

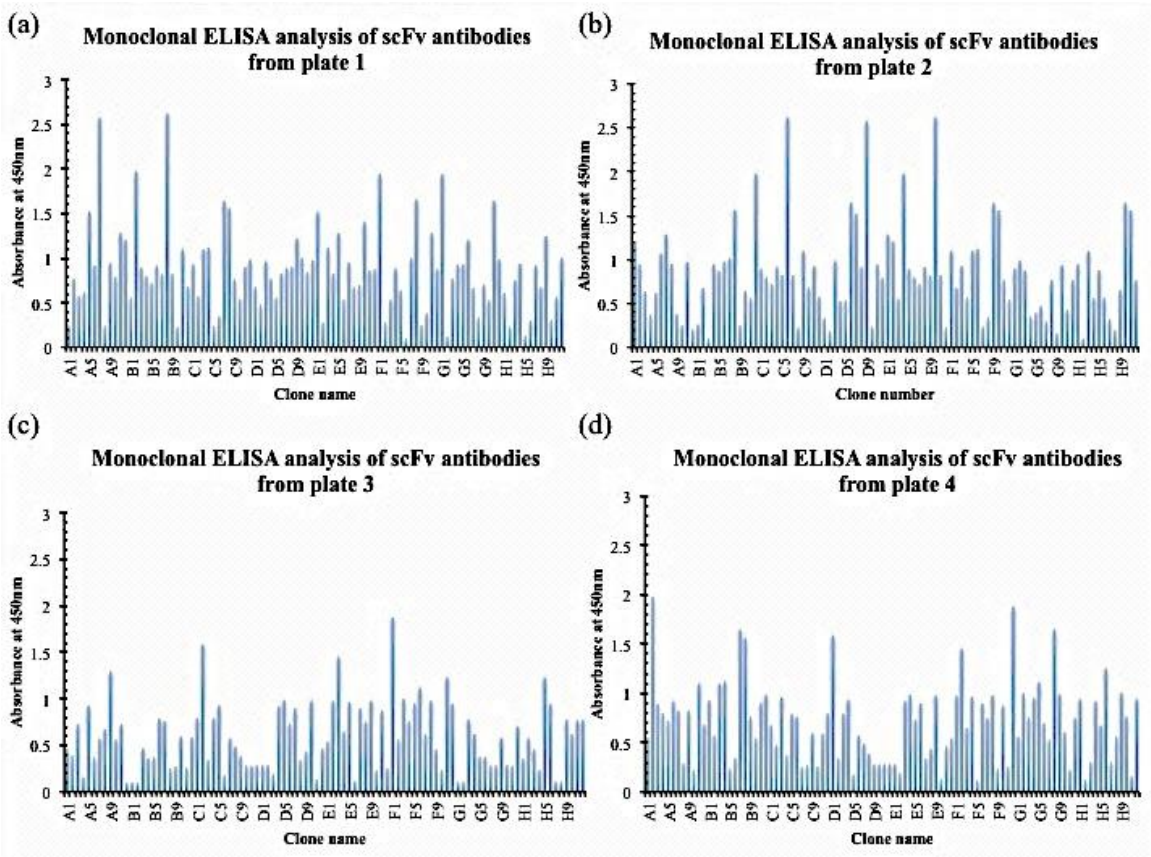

Figure 5.71. Initial screening of four scFv panned library output plates.

This direct binding ELISA permitted approximate determination of the percentage of positive binders for PSMA. A large percentage of clones bound to the PSMA protein. One µg of PSMA was coated on four ELISA plates, blocked with 5% (w/v) PBSTM, to which diluted crude supernatants from overnight expressed single colonies were applied. Specific scFv were detected using an anti-HA HRP-labelled secondary antibody.

5.5.2 Stability early vs. stability late analysis of 384 anti-PSMA scFv clones post Biacore 4000 screening

Three hundred and eight-four scFv clones were ranked by percentage left analysis and stability early versus late in a direct binding format, where the full-length PSMA protein was immobilised on the chip surface using standard amine coupling chemistry. Amine coupling chemistry covalently attaches the amine groups of the PSMA protein to the carboxyl groups of the dextran CM5 biosensor chip. Figure 4.50 in section 4.6.2 diagrammatically illustrates the flow cell setup. There are four flow cells each with five independently addressable and monitored spots within the system. A PSMA protein surface was created by immobilisation of approximately 6000 response units (RU) of covalently attached protein onto spots 1, 2, 4 and 5 via primary amine groups. Crude lysates from overnight expressed clones were diluted in running

buffer (HBS-EP+) and run over all 5 flow cells, where flow cell three was the reference (control) flow cell. The clones were ranked by the response unit (RU) level at two time points (stability early (SE) and stability late (SL)). Stability late was set 16 minutes after stability early to allow for dissociation to occur. Twenty mM NaOH was used for the regeneration of the chip surface after each run. Figure 5.74 is a plot of stability early versus stability late for the 384-clone screen where 100% left (or no dissociation) is signified by a diagonal, dotted black line. All clones resided within three sub-populations. Those with percentage left values ≥ 60%, < 60% and non-binders.

Vast amounts of data wer acquired in a relatively short timeframe where the analysis of 384 clones took <18 hours. Combined with the monoclonal ELISA analysis screening, substantial information was available to rationally select a panel of clones to carry forward. Table 55 is the correlated data for the top 75 performing clones from the HT-screening. This was then related to the monoclonal ELISA screening and a decision was made to bring all seventy-five clones forward for sequencing analysis.

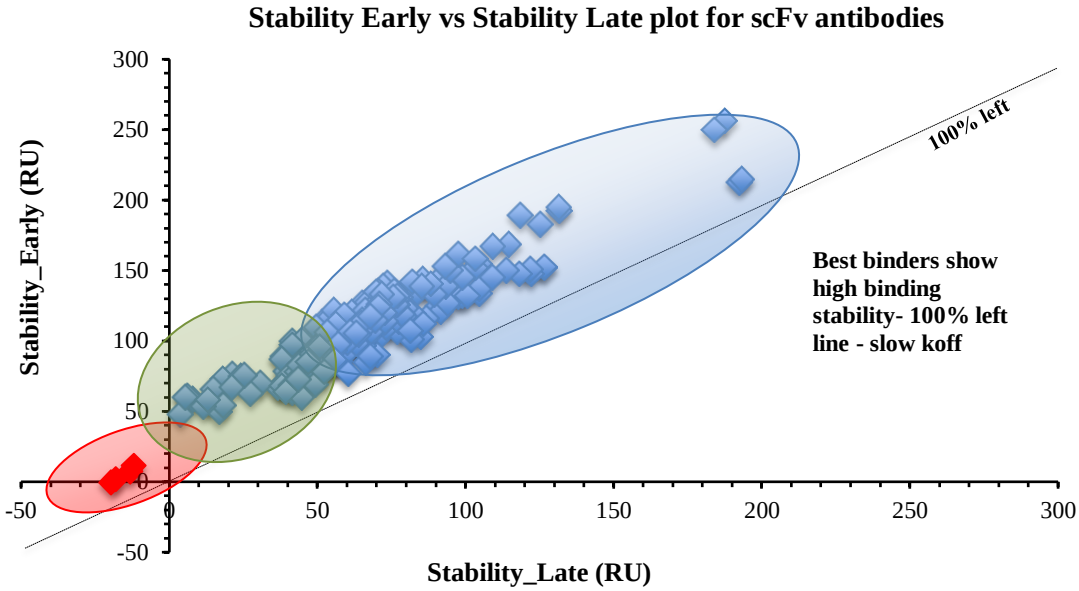

Figure 5.72. High-throughput ranking of anti-PSMA scFv: stability early versus stability late.

A plot of stability early versus stability late values for each of the 384 clones illustrated the overall stability of the binding events. From the graph, three distinct populations were identified - red circle: non-binders, green circle: higher expressing clones with % left vales ≥ 60 (blue circle) and those clones with % left values < 60 (green circle). The black diagonal, dotted line signifies a percentage left value of 100% where no dissociation has occurred. The best binders show high binding stability and lie high along the 100% left line.

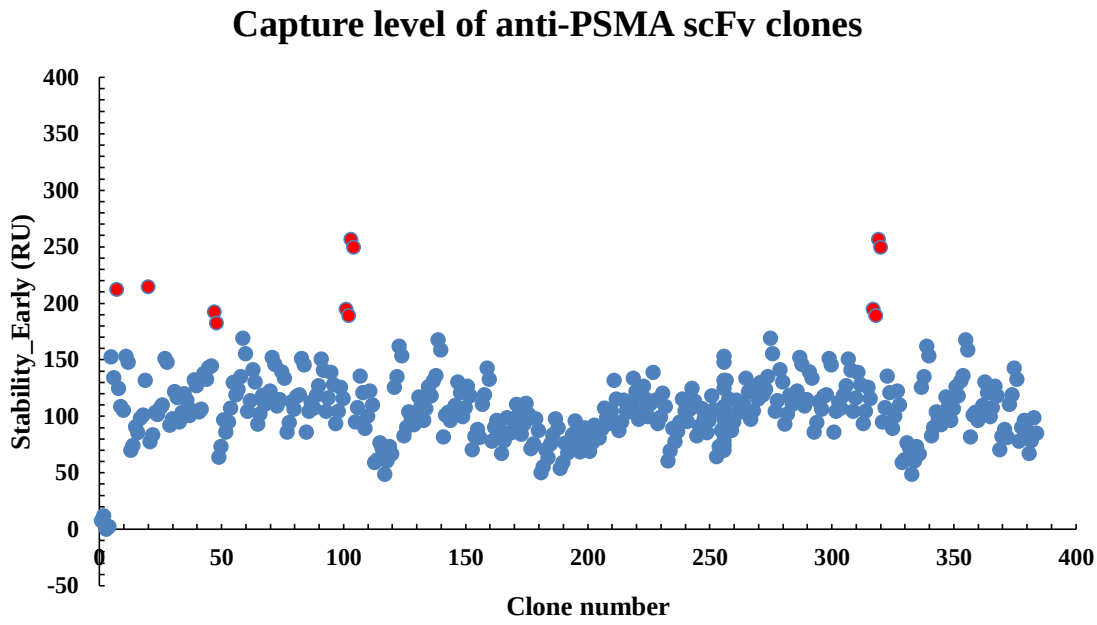

Figure 5.73. High-throughput scFv capture level plot for anti-PSMA scFv clones.

Plot of the scFv capture level by clone number shown for 384 clones in the analysis. High capture level clones are highlighted in red. Capture level can be related to expression, as all clones were cultured in equal volumes and diluted in the same fashion.

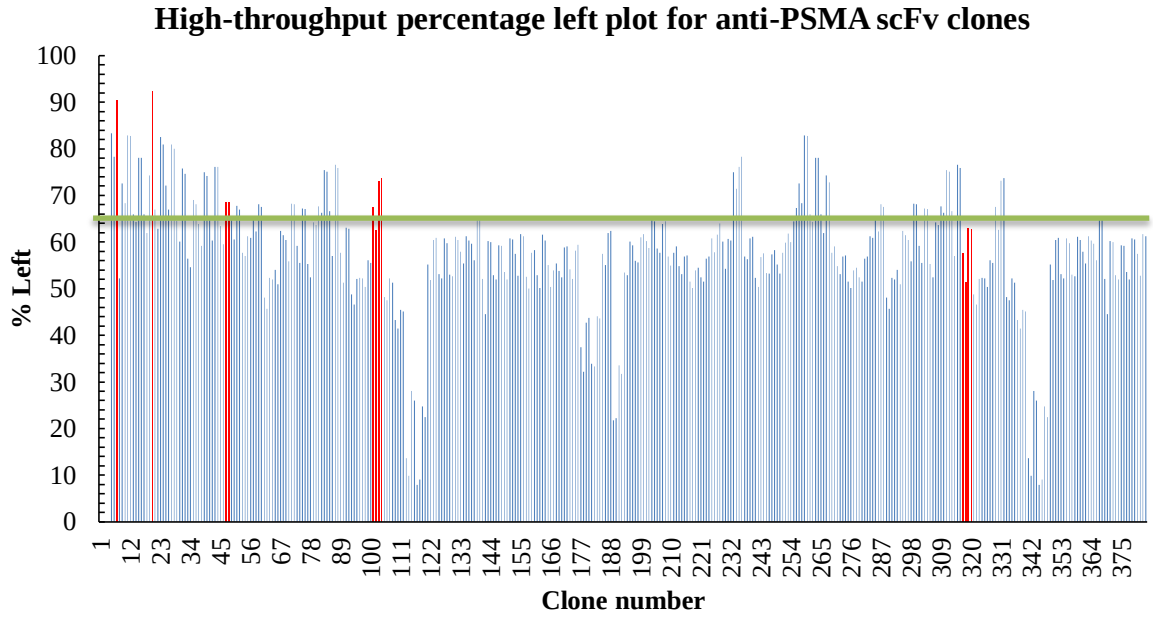

Figure 5.74. High-throughput percentage left plot for anti-PSMA scFv clones.

Percentage left values were calculated using the equation (SL/SE)(100/1). Percentage left values were plotted versus clone number and broken into two groupings. All clones with a percentage left value of over 65% (above the green line) were brought forward for sequencing analysis. Glycerol stocks of all clones with % left values lower than 65% (below the green line) were prepared and stored at -80^{o}C for long-term storage. The high expressing clones identified from the Capture level plot having high expression levels, have been identified in this plot also (highlighted in red). Seven of the twelve clones identified from the capture level plot were brought forward for sequence analysis.*

Table 54. Rational selection of anti-PSMA scFv clones based on % Left >65% and positive response (PR) in monoclonal phage ELISA.

Clones highlighted in red and underlined in the 'clone number' column were clones identified as having a high capture level in Figure 5.75. All clones in this table are colour co-ordinated. Clones of the same colour were identified as being identical clones in the sequencing data.

Clone number	%Left	Clone I.D.	PSMA-specific positive response in monoclonal phage ELISA
5	83	P1A5	Yes
6	78	P1A6	Yes
7	90	P1A7	Yes
9	72	P1A9	Yes
10	68	P1A10	Yes
111	82	P1A11	Yes
12	82	P1A12	Yes
15	78	P1B3	Yes
16	78	P1B4	Yes
19	74	P1B7	Yes
20	92	P1B8	Yes
21	66	P1B9	Yes
23	82	P1B11	Yes
24	80	P1B12	Yes
25	72	P1C1	Yes
26	66	P1C2	Yes
27	80	P1C3	Yes
28	80	P1C4	Yes
31	75	P1C7	Yes
32	74	P1C8	Yes
35	68	P1C11	Yes
36	68	P1C12	Yes
39	74	P1D3	Yes
40	74	P1D4	Yes
43	76	P1D7	Yes
44	76	P1D8	Yes
47	68	P1D11	Yes
48	68	P1D12	Yes
51	67	P1E3	Yes
52	67	P1E4	Yes
59	68	P1E11	Yes
60	67	P1E12	Yes
71	68	P1F11	Yes
72	68	P1F12	Yes
75	67	P1G3	Yes
76	67	P1G4	Yes

81	67	**P1G9**	Yes
82	66	**P1G10**	Yes
83	75	**P1G11**	Yes
84	75	**P1G12**	Yes
85	66	**P1H1**	Yes
87	76	**P1H3**	Yes
88	75	**P1H4**	Yes
101	67	**P2A5**	Yes
103	73	**P2A7**	Yes
104	73	**P2A8**	Yes
233	74	**P3D5**	Yes
234	71	**P3D6**	Yes
235	76	**P3D7**	Yes
236	78	**P4D8**	Yes
256	67	**P3F4**	Yes
257	72	**P3F5**	Yes
258	68	**P3F6**	Yes
259	**82**	**P3F7**	Yes
260	**82**	**P3F8**	Yes
263	78	**P3F11**	Yes
264	78	**P3F12**	Yes
267	74	**P3G3**	Yes
268	72	**P3G4**	Yes
287	68	**P3H11**	Yes
288	67	**P3H12**	Yes
299	68	**P4A11**	Yes
300	68	**P4A12**	Yes
303	67	**P4B3**	Yes
304	67	**P4B4**	Yes
309	67	**P4B9**	Yes
310	66	**P4B10**	Yes
311	75	**P4B11**	Yes
312	75	**P4B12**	Yes
313	66	**P1C1**	Yes
315	76	**P1C3**	Yes
316	75	**P1C4**	Yes
329	67	**P4D5**	Yes
331	73	**P4D7**	Yes
332	73	**P4D8**	Yes

5.6 Sequencing analysis of the selected anti-PSMA scFv antibodies

Examination of the seventy-five sequences indicated a 'jackpot library' with ~95% sequence similarity. Out of the 75 clones sent for sequencing, only five different clones were present. This 'jackpot' is a desirable outcome, because in a library of 1.2 x 10^7 members the probability of the same sequence appearing at random is low (Lerner, 2006). This was a relatively small cohort of clones to sequence, considering the output library size from the final round of panning was 1 x 10^6. However, after four stringent rounds of selection and rigorous, specific screening it was anticipated that the diversity would be narrow given the focused immunisation and stringent panning regimes applied. This 'jackpot' result further validates the procedures followed. The clones highlighted in Table 55 in purple were not brought forward for further characterisation due to the presence of a stop codon in their sequence (See sequence in Table 60).

Table 55. Sequence data for anti-PSMA scFv clone 20 and 7.

The CDRL regions are highlighted in blue, the linker is highlighted in orange, the CDRH regions are highlighted in red and the tag highlighted in green. Bold and underlined letters are the key amino acids to look for when identifying the start or the end of a CDR region. Source Biosciences Ltd., Ireland, performed DNA sequencing of 75 anti-PSMA scFv antibodies in triplicate. Clone number 20 is the Biacore screening name from clone P1B8. See Table 55 for further details on clone number and clone I.D.

Clone_20 LGVSKPGRNRQDX**C**SGDSNNYG**WYQ**QKSPGSAPVTV**IY**QNTNRPSNIPSRFSGALSGSTATLT
Clone_7 LGVSKPGRNRQDX**C**SGDSNNYG**WYQ**QKSPGSAPVTV**IY**QNTNRPSNIPSRFSGALSGSTATLT

Clone_20 ITGVQADDEAVYY**C**GSADRSTDAGDAGI**FGAG**TTLTVLGGSSRSSGGGG**SGGGGSS**AVTLDE
Clone_7 ITGVQADDEAVYY**C**GSADRSTDAGDAGI**FGAG**TTLTVLGGSSRSSGGGG**SGGGGSS**AVTLDE

Clone_20 SGGGLQTPGGALSLV**CKAS**GFTFSSYAMQMQ**WV**RQAPGKG**LEWVG**VINTGSYTYYGAAV
Clone_7 SGGGLQTPGGALSLV**CKAS**GFTFSSYAMQMQ**WV**RQAPGKG**LEWVG**VINTGSYTYYGAAV

Clone_20 **K**GRATITRDNGQSTVRLQLNNLRAEDTATYY**CAK**SAGRSIYPHGTDNIDA**WGYG**TEVIVSST
Clone_7 **K**GRATITRDNGQSTVRLQLNNLRAEDTATYY**CAK**SAGRSIYPHGTDNIDA**WGYG**TEVIVSST

Clone_20 SGQAGQ**HHHHHH**GA**YPYDVPDYA**S
Clone_7 SGQAGQ**HHHHHH**GA**YPYDVPDYA**S

Table 56. Sequence data for anti-PSMA scFv clones 5, 11, 12, 23, 259 and 260.

See Table 56 for details. Clone number 5 is the Biacore screening name for clone P1A5, which was brought forward for further analysis.

Clone_5
LTXPSSVSANPGETVKIT**C**SGGSNNYG**WYQ**QKSPGSAPVTV**IY**QNDKRPSDIPSRFSGSKSGST
Clone_11
LTXPSSVSANPGETVKIT**C**SGGSNNYG**WYQ**QKSPGSAPVTV**IY**QNDKRPSDIPSRFSGSKSGST
Clone_12
LTXPSSVSANPGETVKIT**C**SGGSNNYG**WYQ**QKSPGSAPVTV**IY**QNDKRPSDIPSRFSGSKSGST
Clone_23
LTXPSSVSANPGETVKIT**C**SGGSNNYG**WYQ**QKSPGSAPVTV**IY**QNDKRPSDIPSRFSGSKSGST
Clone_259
LTXPSSVSANPGETVKIT**C**SGGSNNYG**WYQ**QKSPGSAPVTV**IY**QNDKRPSDIPSRFSGSKSGST
Clone_260
LTXPSSVSANPGETVKIT**C**SGGSNNYG**WYQ**QKSPGSAPVTV**IY**QNDKRPSDIPSRFSGSKSGST

Clone_5 NTLTITGVQADDEAVYF**C**GSADSSPGHDDDI**F**GAGTTLTVLGGSSRSSGGGG**SGGGGS**AVT
Clone_11 NTLTITGVQADDEAVYF**C**GSADSSPGHDDDI**F**GAGTTLTVLGGSSRSSGGGG**SGGGGS**AVT
Clone_12 NTLTITGVQADDEAVYF**C**GSADSSPGHDDDI**F**GAGTTLTVLGGSSRSSGGGG**SGGGGS**AVT
Clone_23 NTLTITGVQADDEAVYF**C**GSADSSPGHDDDI**F**GAGTTLTVLGGSSRSSGGGG**SGGGGS**AVT
Clone_259 NTLTITGVQADDEAVYF**C**GSADSSPGHDDDI**F**GAGTTLTVLGGSSRSSGGGG**SGGGGS**AVT
Clone_260 NTLTITGVQADDEAVYF**C**GSADSSPGHDDDI**F**GAGTTLTVLGGSSRSSGGGG**SGGGGS**AVT

Clone_5 LDESGGGLQTPGGALSLV**C**KAS**GFTFSSYAMQF**W**V**RQAPGKG**LEFVAG**ISDSGSSTYYAPA**
Clone_11 LDESGGGLQTPGGALSLV**C**KAS**GFTFSSYAMQF**W**V**RQAPGKG**LEFVAG**ISDSGSSTYYAPA**
Clone_12 LDESGGGLQTPGGALSLV**C**KAS**GFTFSSYAMQF**W**V**RQAPGKG**LEFVAG**ISDSGSSTYYAPA**
Clone_23 LDESGGGLQTPGGALSLV**C**KAS**GFTFSSYAMQF**W**V**RQAPGKG**LEFVAG**ISDSGSSTYYAPA**
Clone_259 LDESGGGLQTPGGALSLV**C**KAS**GFTFSSYAMQF**W**V**RQAPGKG**LEFVAG**ISDSGSSTYYAPA**
Clone_260 LDESGGGLQTPGGALSLV**C**KAS**GFTFSSYAMQF**W**V**RQAPGKG**LEFVAG**ISDSGSSTYYAPA**

Clone_5 **V**K**G**RATISRDNGQNTVRLQLNNLRAXDTAIYY**C**GK**TTCGACWYAGDAIDT**W**GHG**TEVIVS
Clone_11 **V**K**G**RATISRDNGQNTVRLQLNNLRAXDTAIYY**C**GK**TTCGACWYAGDAIDT**W**GHG**TEVIVS
Clone_12 **V**K**G**RATISRDNGQNTVRLQLNNLRAXDTAIYY**C**GK**TTCGACWYAGDAIDT**W**GHG**TEVIVS
Clone_23 **V**K**G**RATISRDNGQNTVRLQLNNLRAXDTAIYY**C**GK**TTCGACWYAGDAIDT**W**GHG**TEVIVS
Clone_259 **V**K**G**RATISRDNGQNTVRLQLNNLRAXDTAIYY**C**GK**TTCGACWYAGDAIDT**W**GHG**TEVIVS
Clone_260 **V**K**G**RATISRDNGQNTVRLQLNNLRAXDTAIYY**C**GK**TTCGACWYAGDAIDT**W**GHG**TEVIVS

Clone_5 STSGQAGQ**HHHHHH**GA**YPYDVPDYA**S
Clone_11 STSGQAGQ**HHHHHH**GA**YPYDVPDYA**S
Clone_12 STSGQAGQ**HHHHHH**GA**YPYDVPDYA**S
Clone_23 STSGQAGQ**HHHHHH**GA**YPYDVPDYA**S
Clone_259 STSGQAGQ**HHHHHH**GA**YPYDVPDYA**S
Clone_260 STSGQAGQ**HHHHHH**GA**YPYDVPDYA**S\

Table 57. Sequence data for anti-PSMA scFv clones 24, 27, 28, 6, 15, 16, 236, 263 and 264.

See Table 56 for details. Clone 6 is the Biacore screening name for clone P1A6, which was brought forward for further analysis.

Clone_24
LSANPGETVXIT**C**SGVSSSGHGYG**WYQ**QKSPGSAPVTL**IY**SNDKRPSGIPSRFSGSKSGSTATLT
Clone_27
LSANPGETVXIT**C**SGVSSSGHGYG**WYQ**QKSPGSAPVTL**IY**SNDKRPSGIPSRFSGSKSGSTATLT
Clone_28
LSANPGETVXIT**C**SGVSSSGHGYG**WYQ**QKSPGSAPVTL**IY**SNDKRPSGIPSRFSGSKSGSTATLT
Clone_6
LSANPGETVXIT**C**SGVSSSGHGYG**WYQ**QKSPGSAPVTL**IY**SNDKRPSGIPSRFSGSKSGSTATLT
Clone_15
LSANPGETVXIT**C**SGVSSSGHGYG**WYQ**QKSPGSAPVTL**IY**SNDKRPSGIPSRFSGSKSGSTATLT
Clone_16
LSANPGETVXIT**C**SGVSSSGHGYG**WYQ**QKSPGSAPVTL**IY**SNDKRPSGIPSRFSGSKSGSTATLT
Clone_236
LSANPGETVXIT**C**SGVSSSGHGYG**WYQ**QKSPGSAPVTL**IY**SNDKRPSGIPSRFSGSKSGSTATLT
Clone_263
LSANPGETVXIT**C**SGVSSSGHGYG**WYQ**QKSPGSAPVTL**IY**SNDKRPSGIPSRFSGSKSGSTATLT
Clone_264
LSANPGETVXIT**C**SGVSSSGHGYG**WYQ**QKSPGSAPVTL**IY**SNDKRPSGIPSRFSGSKSGSTATLT

Clone_24
ITGVQADDEAVYF**C**GTYDSSYVGI**FGAG**TTLTVLGGSSRSSGGGG**SGGGGSS**AVTLDESGGGL
Clone_27
ITGVQADDEAVYF**C**GTYDSSYVGI**FGAG**TTLTVLGGSSRSSGGGG**SGGGGSS**AVTLDESGGGL
Clone_28
ITGVQADDEAVYF**C**GTYDSSYVGI**FGAG**TTLTVLGGSSRSSGGGG**SGGGGSS**AVTLDESGGGL
Clone_6
ITGVQADDEAVYF**C**GTYDSSYVGI**FGAG**TTLTVLGGSSRSSGGGG**SGGGGSS**AVTLDESGGGL
Clone_15
ITGVQADDEAVYF**C**GTYDSSYVGI**FGAG**TTLTVLGGSSRSSGGGG**SGGGGSS**AVTLDESGGGL
Clone_16
ITGVQADDEAVYF**C**GTYDSSYVGI**FGAG**TTLTVLGGSSRSSGGGG**SGGGGSS**AVTLDESGGGL
Clone_236
ITGVQADDEAVYF**C**GTYDSSYVGI**FGAG**TTLTVLGGSSRSSGGGG**SGGGGSS**AVTLDESGGGL
Clone_263
ITGVQADDEAVYF**C**GTYDSSYVGI**FGAG**TTLTVLGGSSRSSGGGG**SGGGGSS**AVTLDESGGGL
Clone_264
ITGVQADDEAVYF**C**GTYDSSYVGI**FGAG**TTLTVLGGSSRSSGGGG**SGGGGSS**AVTLDESGGGL

Clone_24
LQTPGGAXSLV**CKAS**GFTFSSYGMQG**WV**RQAPGKG**LEWVAG**IGSTDSETNYGSAV**K**GRAT
Clone_27
LQTPGGAXSLV**CKAS**GFTFSSYGMQG**WV**RQAPGKG**LEWVAG**IGSTDSETNYGSAV**K**GRAT
Clone_28
LQTPGGAXSLV**CKAS**GFTFSSYGMQG**WV**RQAPGKG**LEWVAG**IGSTDSETNYGSAV**K**GRAT
Clone_6
LQTPGGAXSLV**CKAS**GFTFSSYGMQG**WV**RQAPGKG**LEWVAG**IGSTDSETNYGSAV**K**GRAT
Clone_15
LQTPGGAXSLV**CKAS**GFTFSSYGMQG**WV**RQAPGKG**LEWVAG**IGSTDSETNYGSAV**K**GRAT
Clone_16
LQTPGGAXSLV**CKAS**GFTFSSYGMQG**WV**RQAPGKG**LEWVAG**IGSTDSETNYGSAV**K**GRAT
Clone_236
LQTPGGAXSLV**CKAS**GFTFSSYGMQG**WV**RQAPGKG**LEWVAG**IGSTDSETNYGSAV**K**GRAT
Clone_263
LQTPGGAXSLV**CKAS**GFTFSSYGMQG**WV**RQAPGKG**LEWVAG**IGSTDSETNYGSAV**K**GRAT
Clone_264
LQTPGGAXSLV**CKAS**GFTFSSYGMQG**WV**RQAPGKG**LEWVAG**IGSTDSETNYGSAV**K**GRAT

Clone_24
ISRDNGQSTVRLQLNNLRAEDTGTYFCAKRTDAGGGYCWSCADNIDAWGHGTEVIVSSTSG
Clone_27
ISRDNGQSTVRLQLNNLRAEDTGTYFCAKRTDAGGGYCWSCADNIDAWGHGTEVIVSSTSG
Clone_28
ISRDNGQSTVRLQLNNLRAEDTGTYFCAKRTDAGGGYCWSCADNIDAWGHGTEVIVSSTSG
Clone_6
ISRDNGQSTVRLQLNNLRAEDTGTYFCAKRTDAGGGYCWSCADNIDAWGHGTEVIVSSTSG
Clone_15
ISRDNGQSTVRLQLNNLRAEDTGTYFCAKRTDAGGGYCWSCADNIDAWGHGTEVIVSSTSG
Clone_16
ISRDNGQSTVRLQLNNLRAEDTGTYFCAKRTDAGGGYCWSCADNIDAWGHGTEVIVSSTSG
Clone_236
ISRDNGQSTVRLQLNNLRAEDTGTYFCAKRTDAGGGYCWSCADNIDAWGHGTEVIVSSTSG
Clone_263
ISRDNGQSTVRLQLNNLRAEDTGTYFCAKRTDAGGGYCWSCADNIDAWGHGTEVIVSSTSG
Clone_264
ISRDNGQSTVRLQLNNLRAEDTGTYFCAKRTDAGGGYCWSCADNIDAWGHGTEVIVSSTSG

Clone_24 QAGQHHHHHHGAYPYDVPDYAS
Clone_27 QAGQHHHHHHGAYPYDVPDYAS
Clone_28 QAGQHHHHHHGAYPYDVPDYAS
Clone_6 QAGQHHHHHHGAYPYDVPDYAS
Clone_15 QAGQHHHHHHGAYPYDVPDYAS
Clone_16 QAGQHHHHHHGAYPYDVPDYAS
Clone_236 QAGQHHHHHHGAYPYDVPDYAS
Clone_263 QAGQHHHHHHGAYPYDVPDYAS
Clone_264 QAGQHHHHHHGAYPYDVPDYAS

Table 58. Sequence data for anti-PSMA scFv clones 9,19,25, 31, 32, 39, 40, 43, 44, 48, 83, 84, 87, 88, 103, 104, 233, 234, 235, 257, 267, 268, 311, 312, 315, 316, 331 and 332.

See Table 56 for details.Clone 9 is the Biacore screening name for clone P1A9, which was brought forward for further analysis.

Clone_9 LTQPSSVSANPGETVKITCSGVSSSGHGYGWYQQKSPGSAPVTLIYSNDKRPSNIPSRFSGSKS
Clone_19 LTQPSSVSANPGETVKITCSGVSSSGHGYGWYQQKSPGSAPVTLIYSNDKRPSNIPSRFSGSKS
Clone_25 LTQPSSVSANPGETVKITCSGVSSSGHGYGWYQQKSPGSAPVTLIYSNDKRPSNIPSRFSGSKS
Clone_31 LTQPSSVSANPGETVKITCSGVSSSGHGYGWYQQKSPGSAPVTLIYSNDKRPSNIPSRFSGSKS
Clone_32 LTQPSSVSANPGETVKITCSGVSSSGHGYGWYQQKSPGSAPVTLIYSNDKRPSNIPSRFSGSKS
Clone_39 LTQPSSVSANPGETVKITCSGVSSSGHGYGWYQQKSPGSAPVTLIYSNDKRPSNIPSRFSGSKS
Clone_40 LTQPSSVSANPGETVKITCSGVSSSGHGYGWYQQKSPGSAPVTLIYSNDKRPSNIPSRFSGSKS
Clone_43 LTQPSSVSANPGETVKITCSGVSSSGHGYGWYQQKSPGSAPVTLIYSNDKRPSNIPSRFSGSKS
Clone_44 LTQPSSVSANPGETVKITCSGVSSSGHGYGWYQQKSPGSAPVTLIYSNDKRPSNIPSRFSGSKS
Clone_83 LTQPSSVSANPGETVKITCSGVSSSGHGYGWYQQKSPGSAPVTLIYSNDKRPSNIPSRFSGSKS
Clone_84 LTQPSSVSANPGETVKITCSGVSSSGHGYGWYQQKSPGSAPVTLIYSNDKRPSNIPSRFSGSKS
Clone_87 LTQPSSVSANPGETVKITCSGVSSSGHGYGWYQQKSPGSAPVTLIYSNDKRPSNIPSRFSGSKS
Clone_88 LTQPSSVSANPGETVKITCSGVSSSGHGYGWYQQKSPGSAPVTLIYSNDKRPSNIPSRFSGSKS
Clone_103 LTQPSSVSANPGETVKITCSGVSSSGHGYGWYQQKSPGSAPVTLIYSNDKRPSNIPSRFSGSKS
Clone_104 LTQPSSVSANPGETVKITCSGVSSSGHGYGWYQQKSPGSAPVTLIYSNDKRPSNIPSRFSGSKS
Clone_233 LTQPSSVSANPGETVKITCSGVSSSGHGYGWYQQKSPGSAPVTLIYSNDKRPSNIPSRFSGSKS
Clone_234 LTQPSSVSANPGETVKITCSGVSSSGHGYGWYQQKSPGSAPVTLIYSNDKRPSNIPSRFSGSKS
Clone_235 LTQPSSVSANPGETVKITCSGVSSSGHGYGWYQQKSPGSAPVTLIYSNDKRPSNIPSRFSGSKS
Clone_257 LTQPSSVSANPGETVKITCSGVSSSGHGYGWYQQKSPGSAPVTLIYSNDKRPSNIPSRFSGSKS
Clone_267 LTQPSSVSANPGETVKITCSGVSSSGHGYGWYQQKSPGSAPVTLIYSNDKRPSNIPSRFSGSKS
Clone_268 LTQPSSVSANPGETVKITCSGVSSSGHGYGWYQQKSPGSAPVTLIYSNDKRPSNIPSRFSGSKS
Clone_311 LTQPSSVSANPGETVKITCSGVSSSGHGYGWYQQKSPGSAPVTLIYSNDKRPSNIPSRFSGSKS
Clone_312 LTQPSSVSANPGETVKITCSGVSSSGHGYGWYQQKSPGSAPVTLIYSNDKRPSNIPSRFSGSKS

Clone_315 LTQPSSVSANPGETVKITCSGVSSSGHGYGWYQQKSPGSAPVTLIYSNDKRPSNIPSRFSGSKS
Clone_316 LTQPSSVSANPGETVKITCSGVSSSGHGYGWYQQKSPGSAPVTLIYSNDKRPSNIPSRFSGSKS
Clone_331 LTQPSSVSANPGETVKITCSGVSSSGHGYGWYQQKSPGSAPVTLIYSNDKRPSNIPSRFSGSKS
Clone_332 LTQPSSVSANPGETVKITCSGVSSSGHGYGWYQQKSPGSAPVTLIYSNDKRPSNIPSRFSGSKS

Clone_9 GSTATLTITGVRAEDEAVYFCATADSSDIFGAGTTLTVLGGSSRSSGGGGSGGGGSSAVTLDE
Clone_19 GSTATLTITGVRAEDEAVYFCATADSSDIFGAGTTLTVLGGSSRSSGGGGSGGGGSSAVTLDE
Clone_25 GSTATLTITGVRAEDEAVYFCATADSSDIFGAGTTLTVLGGSSRSSGGGGSGGGGSSAVTLDE
Clone_31 GSTATLTITGVRAEDEAVYFCATADSSDIFGAGTTLTVLGGSSRSSGGGGSGGGGSSAVTLDE
Clone_32 GSTATLTITGVRAEDEAVYFCATADSSDIFGAGTTLTVLGGSSRSSGGGGSGGGGSSAVTLDE
Clone_39 GSTATLTITGVRAEDEAVYFCATADSSDIFGAGTTLTVLGGSSRSSGGGGSGGGGSSAVTLDE
Clone_40 GSTATLTITGVRAEDEAVYFCATADSSDIFGAGTTLTVLGGSSRSSGGGGSGGGGSSAVTLDE
Clone_43 GSTATLTITGVRAEDEAVYFCATADSSDIFGAGTTLTVLGGSSRSSGGGGSGGGGSSAVTLDE
Clone_44 GSTATLTITGVRAEDEAVYFCATADSSDIFGAGTTLTVLGGSSRSSGGGGSGGGGSSAVTLDE
Clone_83 GSTATLTITGVRAEDEAVYFCATADSSDIFGAGTTLTVLGGSSRSSGGGGSGGGGSSAVTLDE
Clone_84 GSTATLTITGVRAEDEAVYFCATADSSDIFGAGTTLTVLGGSSRSSGGGGSGGGGSSAVTLDE
Clone_87 GSTATLTITGVRAEDEAVYFCATADSSDIFGAGTTLTVLGGSSRSSGGGGSGGGGSSAVTLDE
Clone_88 GSTATLTITGVRAEDEAVYFCATADSSDIFGAGTTLTVLGGSSRSSGGGGSGGGGSSAVTLDE
Clone_103 GSTATLTITGVRAEDEAVYFCATADSSDIFGAGTTLTVLGGSSRSSGGGGSGGGGSSAVTLDE
Clone_104 GSTATLTITGVRAEDEAVYFCATADSSDIFGAGTTLTVLGGSSRSSGGGGSGGGGSSAVTLDE
Clone_233 GSTATLTITGVRAEDEAVYFCATADSSDIFGAGTTLTVLGGSSRSSGGGGSGGGGSSAVTLDE
Clone_234 GSTATLTITGVRAEDEAVYFCATADSSDIFGAGTTLTVLGGSSRSSGGGGSGGGGSSAVTLDE
Clone_235 GSTATLTITGVRAEDEAVYFCATADSSDIFGAGTTLTVLGGSSRSSGGGGSGGGGSSAVTLDE
Clone_257 GSTATLTITGVRAEDEAVYFCATADSSDIFGAGTTLTVLGGSSRSSGGGGSGGGGSSAVTLDE
Clone_267 GSTATLTITGVRAEDEAVYFCATADSSDIFGAGTTLTVLGGSSRSSGGGGSGGGGSSAVTLDE
Clone_268 GSTATLTITGVRAEDEAVYFCATADSSDIFGAGTTLTVLGGSSRSSGGGGSGGGGSSAVTLDE
Clone_311 GSTATLTITGVRAEDEAVYFCATADSSDIFGAGTTLTVLGGSSRSSGGGGSGGGGSSAVTLDE
Clone_312 GSTATLTITGVRAEDEAVYFCATADSSDIFGAGTTLTVLGGSSRSSGGGGSGGGGSSAVTLDE
Clone_315 GSTATLTITGVRAEDEAVYFCATADSSDIFGAGTTLTVLGGSSRSSGGGGSGGGGSSAVTLDE
Clone_316 GSTATLTITGVRAEDEAVYFCATADSSDIFGAGTTLTVLGGSSRSSGGGGSGGGGSSAVTLDE
Clone_331 GSTATLTITGVRAEDEAVYFCATADSSDIFGAGTTLTVLGGSSRSSGGGGSGGGGSSAVTLDE
Clone_332 GSTATLTITGVRAEDEAVYFCATADSSDIFGAGTTLTVLGGSSRSSGGGGSGGGGSSAVTLDE

Clone_9 SGGGLQTPGGALSLVCKASGFTFSSYAMQWVRQAPGKGLEWVGVINTGSYTYGAAVKGR
Clone_19 SGGGLQTPGGALSLVCKASGFTFSSYAMQWVRQAPGKGLEWVGVINTGSYTYGAAVKGR
Clone_25 SGGGLQTPGGALSLVCKASGFTFSSYAMQWVRQAPGKGLEWVGVINTGSYTYGAAVKGR
Clone_31 SGGGLQTPGGALSLVCKASGFTFSSYAMQWVRQAPGKGLEWVGVINTGSYTYGAAVKGR
Clone_32 SGGGLQTPGGALSLVCKASGFTFSSYAMQWVRQAPGKGLEWVGVINTGSYTYGAAVKGR
Clone_39 SGGGLQTPGGALSLVCKASGFTFSSYAMQWVRQAPGKGLEWVGVINTGSYTYGAAVKGR
Clone_40 SGGGLQTPGGALSLVCKASGFTFSSYAMQWVRQAPGKGLEWVGVINTGSYTYGAAVKGR
Clone_43 SGGGLQTPGGALSLVCKASGFTFSSYAMQWVRQAPGKGLEWVGVINTGSYTYGAAVKGR
Clone_44 SGGGLQTPGGALSLVCKASGFTFSSYAMQWVRQAPGKGLEWVGVINTGSYTYGAAVKGR
Clone_83 SGGGLQTPGGALSLVCKASGFTFSSYAMQWVRQAPGKGLEWVGVINTGSYTYGAAVKGR
Clone_84 SGGGLQTPGGALSLVCKASGFTFSSYAMQWVRQAPGKGLEWVGVINTGSYTYGAAVKGR
Clone_87 SGGGLQTPGGALSLVCKASGFTFSSYAMQWVRQAPGKGLEWVGVINTGSYTYGAAVKGR
Clone_88 SGGGLQTPGGALSLVCKASGFTFSSYAMQWVRQAPGKGLEWVGVINTGSYTYGAAVKGR
Clone_103 SGGGLQTPGGALSLVCKASGFTFSSYAMQWVRQAPGKGLEWVGVINTGSYTYGAAVKGR
Clone_104 SGGGLQTPGGALSLVCKASGFTFSSYAMQWVRQAPGKGLEWVGVINTGSYTYGAAVKGR
Clone_233 SGGGLQTPGGALSLVCKASGFTFSSYAMQWVRQAPGKGLEWVGVINTGSYTYGAAVKGR
Clone_234 SGGGLQTPGGALSLVCKASGFTFSSYAMQWVRQAPGKGLEWVGVINTGSYTYGAAVKGR
Clone_235 SGGGLQTPGGALSLVCKASGFTFSSYAMQWVRQAPGKGLEWVGVINTGSYTYGAAVKGR
Clone_257 SGGGLQTPGGALSLVCKASGFTFSSYAMQWVRQAPGKGLEWVGVINTGSYTYGAAVKGR
Clone_267 SGGGLQTPGGALSLVCKASGFTFSSYAMQWVRQAPGKGLEWVGVINTGSYTYGAAVKGR
Clone_268 SGGGLQTPGGALSLVCKASGFTFSSYAMQWVRQAPGKGLEWVGVINTGSYTYGAAVKGR
Clone_311 SGGGLQTPGGALSLVCKASGFTFSSYAMQWVRQAPGKGLEWVGVINTGSYTYGAAVKGR
Clone_312 SGGGLQTPGGALSLVCKASGFTFSSYAMQWVRQAPGKGLEWVGVINTGSYTYGAAVKGR
Clone_315 SGGGLQTPGGALSLVCKASGFTFSSYAMQWVRQAPGKGLEWVGVINTGSYTYGAAVKGR
Clone_316 SGGGLQTPGGALSLVCKASGFTFSSYAMQWVRQAPGKGLEWVGVINTGSYTYGAAVKGR
Clone_331 SGGGLQTPGGALSLVCKASGFTFSSYAMQWVRQAPGKGLEWVGVINTGSYTYGAAVKGR
Clone_332 SGGGLQTPGGALSLVCKASGFTFSSYAMQWVRQAPGKGLEWVGVINTGSYTYGAAVKGR

Clone_9 ATITRDNGQSTVRLQLNNLRAEDTATYYCAKPSGDAGGWLADDIDAWGHGTEVIVSSTSGQ
Clone_19 ATITRDNGQSTVRLQLNNLRAEDTATYYCAKPSGDAGGWLADDIDAWGHGTEVIVSSTSGQ
Clone_25 ATITRDNGQSTVRLQLNNLRAEDTATYYCAKPSGDAGGWLADDIDAWGHGTEVIVSSTSGQ
Clone_31 ATITRDNGQSTVRLQLNNLRAEDTATYYCAKPSGDAGGWLADDIDAWGHGTEVIVSSTSGQ
Clone_32 ATITRDNGQSTVRLQLNNLRAEDTATYYCAKPSGDAGGWLADDIDAWGHGTEVIVSSTSGQ
Clone_39 ATITRDNGQSTVRLQLNNLRAEDTATYYCAKPSGDAGGWLADDIDAWGHGTEVIVSSTSGQ

Clone_40 ATITRDNGQSTVRLQLNNLRAEDTATYY**CAK**PSGDAGGWLADDIDA**WGHG**TEVIVSSTSGQ
Clone_43 ATITRDNGQSTVRLQLNNLRAEDTATYY**CAK**PSGDAGGWLADDIDA**WGHG**TEVIVSSTSGQ
Clone_44 ATITRDNGQSTVRLQLNNLRAEDTATYY**CAK**PSGDAGGWLADDIDA**WGHG**TEVIVSSTSGQ
Clone_83 ATITRDNGQSTVRLQLNNLRAEDTATYY**CAK**PSGDAGGWLADDIDA**WGHG**TEVIVSSTSGQ
Clone_84 ATITRDNGQSTVRLQLNNLRAEDTATYY**CAK**PSGDAGGWLADDIDA**WGHG**TEVIVSSTSGQ
Clone_87 ATITRDNGQSTVRLQLNNLRAEDTATYY**CAK**PSGDAGGWLADDIDA**WGHG**TEVIVSSTSGQ
Clone_88 ATITRDNGQSTVRLQLNNLRAEDTATYY**CAK**PSGDAGGWLADDIDA**WGHG**TEVIVSSTSGQ
Clone_103 ATITRDNGQSTVRLQLNNLRAEDTATYY**CAK**PSGDAGGWLADDIDA**WGHG**TEVIVSSTSGQ
Clone_104 ATITRDNGQSTVRLQLNNLRAEDTATYY**CAK**PSGDAGGWLADDIDA**WGHG**TEVIVSSTSGQ
Clone_233 ATITRDNGQSTVRLQLNNLRAEDTATYY**CAK**PSGDAGGWLADDIDA**WGHG**TEVIVSSTSGQ
Clone_234 ATITRDNGQSTVRLQLNNLRAEDTATYY**CAK**PSGDAGGWLADDIDA**WGHG**TEVIVSSTSGQ
Clone_235 ATITRDNGQSTVRLQLNNLRAEDTATYY**CAK**PSGDAGGWLADDIDA**WGHG**TEVIVSSTSGQ
Clone_257 ATITRDNGQSTVRLQLNNLRAEDTATYY**CAK**PSGDAGGWLADDIDA**WGHG**TEVIVSSTSGQ
Clone_267 ATITRDNGQSTVRLQLNNLRAEDTATYY**CAK**PSGDAGGWLADDIDA**WGHG**TEVIVSSTSGQ
Clone_268 ATITRDNGQSTVRLQLNNLRAEDTATYY**CAK**PSGDAGGWLADDIDA**WGHG**TEVIVSSTSGQ
Clone_311 ATITRDNGQSTVRLQLNNLRAEDTATYY**CAK**PSGDAGGWLADDIDA**WGHG**TEVIVSSTSGQ
Clone_312 ATITRDNGQSTVRLQLNNLRAEDTATYY**CAK**PSGDAGGWLADDIDA**WGHG**TEVIVSSTSGQ
Clone_315 ATITRDNGQSTVRLQLNNLRAEDTATYY**CAK**PSGDAGGWLADDIDA**WGHG**TEVIVSSTSGQ
Clone_316 ATITRDNGQSTVRLQLNNLRAEDTATYY**CAK**PSGDAGGWLADDIDA**WGHG**TEVIVSSTSGQ
Clone_331 ATITRDNGQSTVRLQLNNLRAEDTATYY**CAK**PSGDAGGWLADDIDA**WGHG**TEVIVSSTSGQ
Clone_332 ATITRDNGQSTVRLQLNNLRAEDTATYY**CAK**PSGDAGGWLADDIDA**WGHG**TEVIVSSTSGQ

Clone_9 QAGQ**HHHHHH**GA**YPYDVPDYA**
Clone_19 QAGQ**HHHHHH**GA**YPYDVPDYA**
Clone_25 QAGQ**HHHHHH**GA**YPYDVPDYA**
Clone_31 QAGQ**HHHHHH**GA**YPYDVPDYA**
Clone_32 QAGQ**HHHHHH**GA**YPYDVPDYA**
Clone_39 QAGQ**HHHHHH**GA**YPYDVPDYA**
Clone_40 QAGQ**HHHHHH**GA**YPYDVPDYA**
Clone_43 QAGQ**HHHHHH**GA**YPYDVPDYA**
Clone_44 QAGQ**HHHHHH**GA**YPYDVPDYA**
Clone_83 QAGQ**HHHHHH**GA**YPYDVPDYA**
Clone_84 QAGQ**HHHHHH**GA**YPYDVPDYA**
Clone_87 QAGQ**HHHHHH**GA**YPYDVPDYA**
Clone_88 QAGQ**HHHHHH**GA**YPYDVPDYA**
Clone_103 QAGQ**HHHHHH**GA**YPYDVPDYA**
Clone_104 QAGQ**HHHHHH**GA**YPYDVPDYA**
Clone_233 QAGQ**HHHHHH**GA**YPYDVPDYA**
Clone_234 QAGQ**HHHHHH**GA**YPYDVPDYA**
Clone_235 QAGQ**HHHHHH**GA**YPYDVPDYA**
Clone_257 QAGQ**HHHHHH**GA**YPYDVPDYA**
Clone_267 QAGQ**HHHHHH**GA**YPYDVPDYA**
Clone_268 QAGQ**HHHHHH**GA**YPYDVPDYA**
Clone_311 QAGQ**HHHHHH**GA**YPYDVPDYA**
Clone_312 QAGQ**HHHHHH**GA**YPYDVPDYA**
Clone_315 QAGQ**HHHHHH**GA**YPYDVPDYA**
Clone_316 QAGQ**HHHHHH**GA**YPYDVPDYA**
Clone_331 QAGQ**HHHHHH**GA**YPYDVPDYA**
Clone_332 QAGQ**HHHHHH**GA**YPYDVPDYA**

Table 59. Sequence data for anti-PSMA scFv clone 10.

See Table 56 for details.

Clone_10
LTXPSSVSANPGEGVKIG**C**XGGSNNYG**WYQ**QKSPGSAPVTV**IY**QNDKRGSGI**STOP**GSGSKSG

Clone_10 STNTLTITGXRAEDEAVYF**C**GSGDINSRVGI**FGAG**TTLTVLGQSXRGGSSRSSGGGG**SGGGGS**

Clone_10
SAVTLDESGGGLQTPGGAVSLI**CKAS**GFDFSSYAMQF**WA**RQAPGKG**LEYVAG**ITSEDGDTTD

Clone_10 YGAAV**K**GRATISRDNGPSTVRLQLSNLRAEDTGTYF**CAK**DVDGCGSGSWCGINIDA**WGYG**T

Clone_10 EVIVSSTSGQAGQ**HHHHHH**GA**YPYDVPDYA**S

5.7 Direct and sandwich ELISA analysis of anti-PSMA scFv lysate

Direct ELISA and sandwich ELISA analysis were carried out on the four anti-PSMA scFv clones identified from the screening and sequencing analysis. Direct analysis was completed initially to determine the optimal working dilution of each antibody by probing an ELISA plate coated with 0.5µg/mL PSMA protein with varying dilutions of the scFv antibodies. An anti-HA-HRP-labelled secondary antibody was used to detect the anti-PSMA scFv antibodies. All samples were tested in triplicate. One negative and one positive control were included in this assay. Optimal dilutions of lysate were determined for each clone to give an absorbance of ~1.0AU. Anti-PSMA scFv clone B8 showed an almost identical binding pattern to the anti-PSMA commercial polyclonal antibody with an optimum working dilution determined to be 1 in 1,000, as with the commercial antibody (determined by the manufacturer).

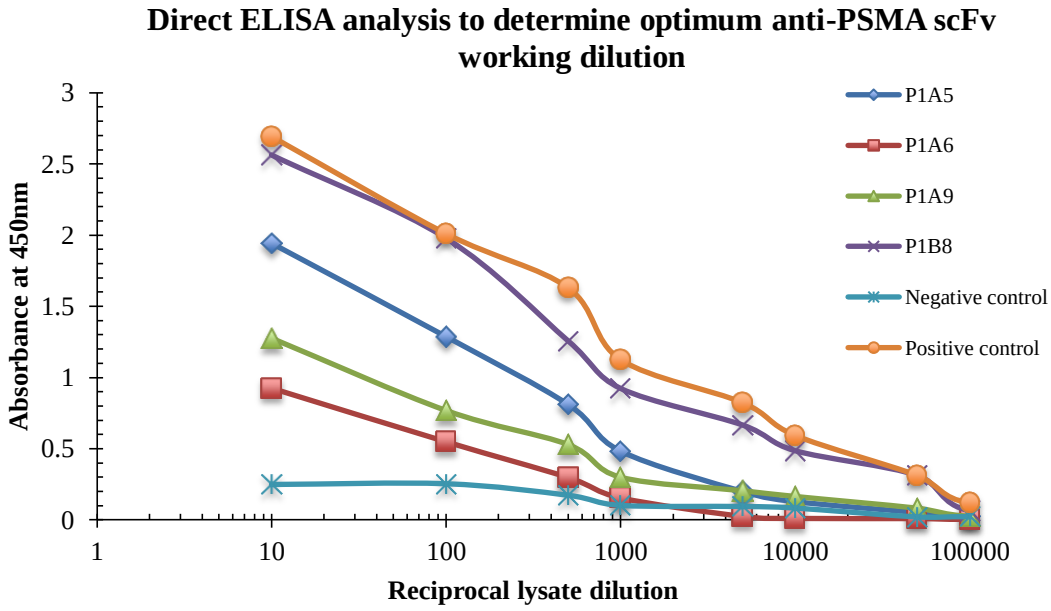

Figure 5.75. Titration of scFv against PSMA by ELISA.

Supernatants were diluted in 1% (w/v) PBSTM and applied to individual wells. Bound scFv was detected using anti-HA HRP-labelled secondary antibody. Optimal dilutions of lysate were determined for each clone to give an absorbance of 1.0AU.

Figure 5.78, a sandwich assay, illustrates the scFv antibody lysates as the capture reagents for various concentrations of PSMA (0.5-2000ng/mL). In this assay, bound PSMA was detected using the commercial anti-PSMA pAb.

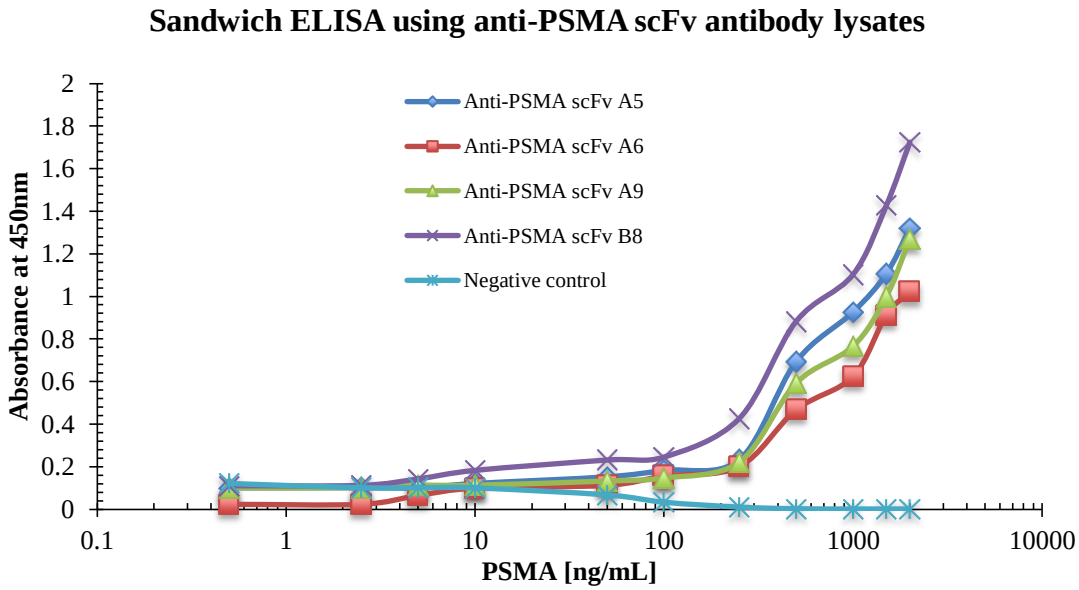

Figure 5.76. Sandwich ELISA analysis of anti-PSMA scFv clones.

Anti-PSMA scFv supernatants were applied to an ELISA plate to form the antibody capture surface. Varying concentrations of PSMA (0.5-2,000ng/mL) were applied to the immobilised scFv antibodies. One negative control was included (0.5-2,000ng/mL SFRP-2) to ensure there were no non-specific interactions with the scFv antibodies. Captured PSMA was probed using an anti-PSMA commercial pAb (raised in rabbit), which completed the sandwich format. Bound pAb was detected using a commercial mouse anti-rabbit-HRP-labelled secondary antibody.

5.8 Analysis of the protein-membrane binding capability of anti-PSMA scFv antibodies in western and dot blots

Western and dot blotting analysis were performed in order to determine the ability of the anti-PSMA scFv antibodies to recognise and bind their target antigen in a membrane format. If the antibody was capable of binding to its target in western blot, it recognizes the linear epitope of the antigen. In contrast, if the antibody recognizes its target in dot blot it recognizes the conformational epitope. The aim of this experiment was to identify an antibody that would work in both formats.

One µg of PSMA, which was prepared in 4X SDS-PAGE loading dye and denatured and 95°C for 5 minutes, was loaded per well. The protein was separated by electrophoresis at 120V for 60 minutes. The separated protein bands were then transferred to a nitrocellulose carrier membrane and blocked for 1 hour with 5% (w/v) PBSTM. A 1 in 100 dilution of scFv crude lysate was prepared in 1% (w/v) PBSTM and used to probe the PSMA membrane for 1 hour at RT. Bound scFv was detected

using an anti-HA-HRP-labelled secondary antibody. TMB substrate for membranes was applied to each blot to visualise the result. The results indicated that out of the four scFv antibodies tested, only one, namely anti-PSMA scFv B8, was capable of binding to the PSMA protein in a western blot format in addition to a dot blot. Anti-PSMA scFv clone B8 was taken forward for large-scale expression and purification.

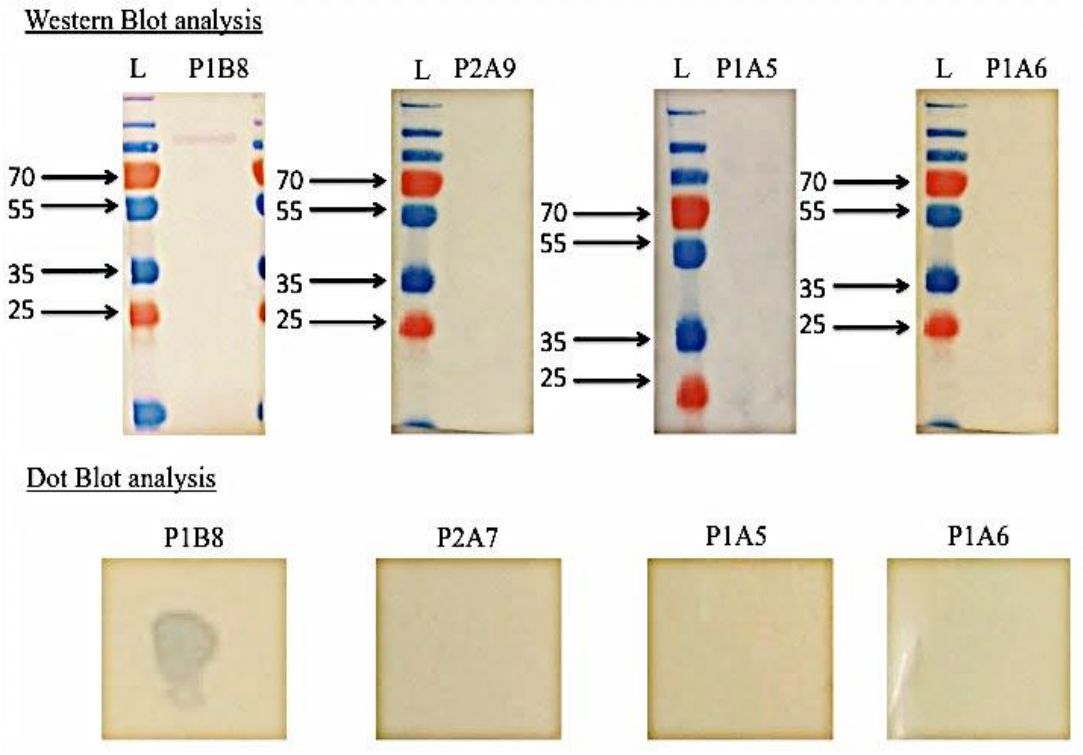

Figure 5.77. Application of anti-PSMA scFv antibodies as primary antibodies in a WB and dot blot format.

Western blot: a 1 in 100 dilution of each scFv clone was used to probe a PSMA membrane for 1 hour at RT. Bound scFv was detected using an anti-HA-HRP-labelled secondary antibody. Dot blot: 2µg/mL of PSMA, prepared in molecular grade H_2O, was dotted on to pre-activated PVDF membrane and allowed to dry. The blot was blocked with 5% (w/v) PBSM for 20 minutes at RT. A 1 in 100 dilution of each scFv clone, prepared in 1% (w/v) PBSTM, was used to probe the dot blots. Bound scFv was detected using an anti-HA-HRP-labelled antibody.

5.9 Purification of anti-PSMA scFv clone B8 using osmotic shock approach (visualization on SDS and WB)

Optimised large-scale expression (results not shown) of the anti-PSMA scFv clone B8 was completed and 1mM IPTG was selected for induction overnight at 25°C. The anti-PSMA scFv clone B8 was purified, as described in section 2.5.22, using osmotic shock-based buffers delineated in section 2.1.5.2.3. The scFv was purified by virtue of

the 6xHis tag encoded on the pComb3x vector by immobilised metal affinity chromatography (IMAC). The purification was carried out from 5 x 200mL cultures induced overnight. It was noted that a significant amount of non-specific protein was eluted in wash 1 (W1) and wash 2 (W2), whereas the wash 3 (W3) fraction appeared to be very clean. The eluted protein was concentrated and buffer exchanged into PBS. The concentrated sample was analysed by SDS-PAGE and WB, along-side the 'flow-through', W1, W2 and W3 fractions, and showed a very pure protein preparation. Protein concentration was obtained by A^{280} on a ND-1000™ and is outlined in Table 61.

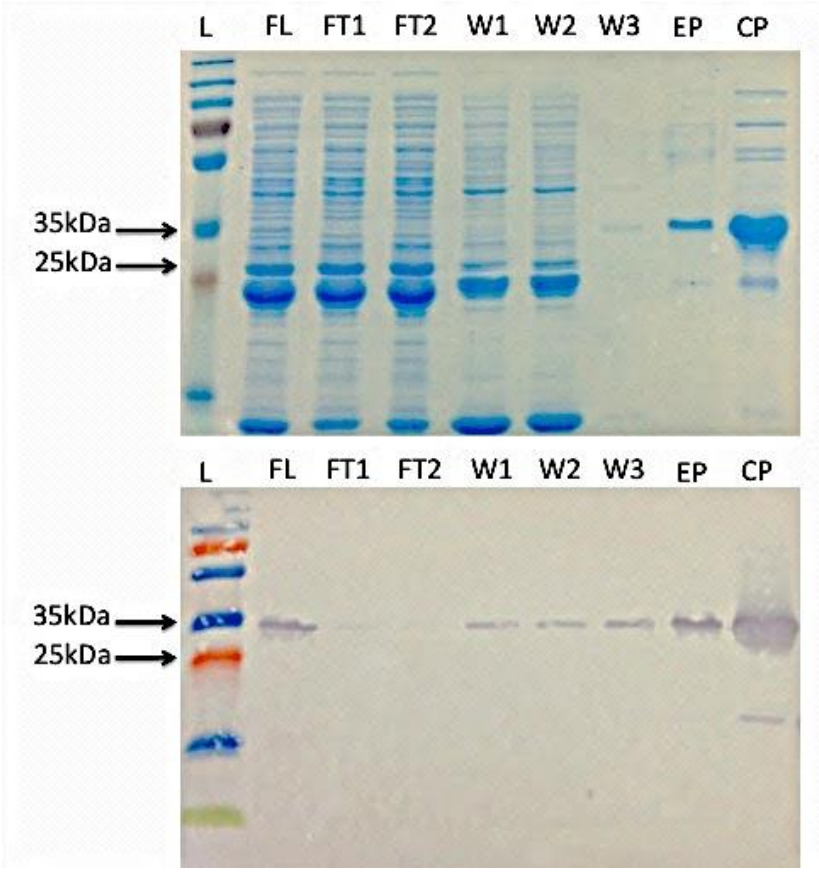

Figure 5.78. SDS-PAGE and WB analysis of anti-PSMA scFv B8 purification steps.

In the large-scale purification, samples of each step of the process were analysed. The lanes are labelled as follows: FL: filtered lysate F1: flow-through 1, F2: flow-through 2, W1: wash 1, W2: wash 2, W3: wash 3, EP: Eluted protein and CP: concentrated protein. L is the pre-stained protein ladder.

Table 60. IMAC-purified anti-PSMA scFv B8 protein yield determined using the NanoDrop™ 1000.

Protein fraction	Volume (mL)	Protein yield determined by the NanoDrop™ 1000
Eluted protein	4.0	0.8mg/mL
Concentrated protein	0.5	4.2mg/mL

To ensure that the purification conditions did not compromise the activity of the purified scFv, a series of ELISAs was carried out. The purified scFv antibody was diluted to a working stock concentration of 1mg/mL. This concentration matched that of the commercial positive control. Initially, the scFv was titrated against PSMA in a direct binding ELISA in parallel to the commercial anti-PSMA pAb antibody to determine the optimal working dilution of the scFv antibody. An anti-SFRP-2 scFv clone F3 was used as the negative control in this ELISA. The scFv titred out at approximately 1 in 30,000 compared to the commercial polyclonal antibody titring at approximately 1 in 50,000.

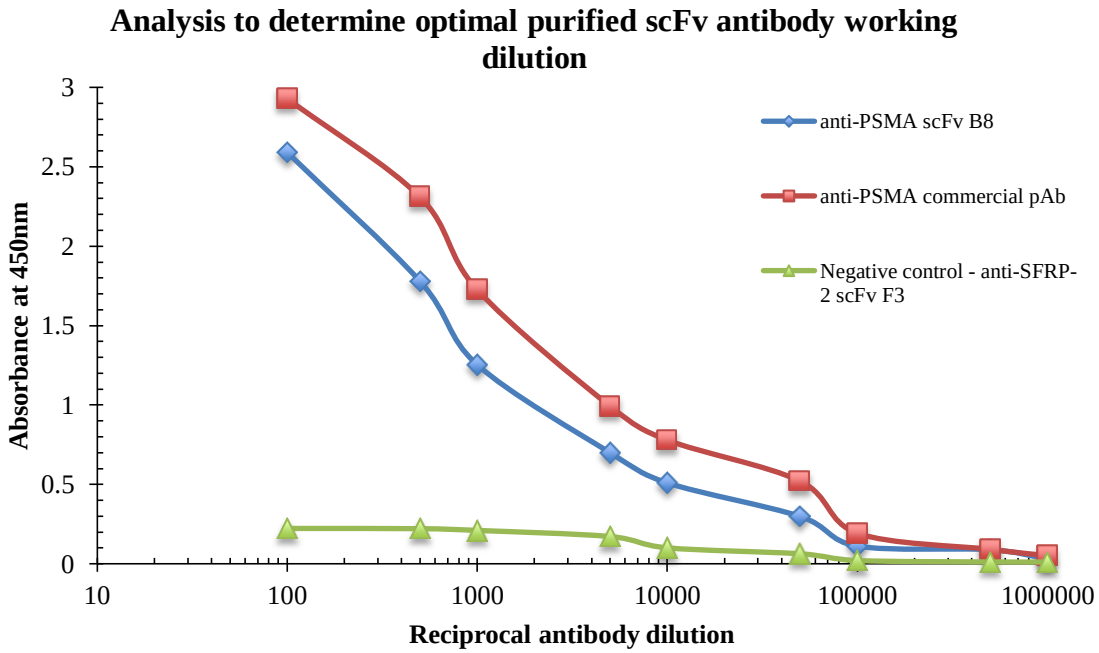

Figure 5.79. Titration of scFv, positive and negative controls against PSMA by ELISA.

Varying dilutions (1 in 100 to 1 in 1,000,000) of the purified anti-PSMA scFv B8, anti-PSMA commercial pAb and the anti-SFRP-2 scFv F3 were diluted in 1% (w/v) PBSTM and applied to PSMA-coated (0.5µg/mL) wells. Bound scFv was detected using anti-HA-HRP-labelled secondary antibody. Bound pAb was detected using anti-rabbit-HRP-labelled secondary antibody and an anti-goat-HRP-labelled secondary was used to probe the negative control. Optimal dilution of scFv was selected to give an absorbance of 1.0AU.

Figure 5.82, a sandwich assay, illustrates purified anti-PSMA scFv B8 as the capture reagent (1µg/mL) (assay type 1) for various concentrations of PSMA (0.5-2,000ng/mL), plotted against a sandwich assay (assay type 2) with the commercial pAb (1 µg/mL) as the capture reagent. In the first assay, bound PSMA was detected using the commercial anti-PSMA pAb and in the second, bound PSMA was detected using the optimal working dilution of the anti-PSMA scFv B8 antibody (1 in 1,000 dilution). The purified scFv antibody compares well in both assay formats with the equivalent commercial antibody. In this non-optimised assay format the anti-PSMA scFv antibody can detect PSMA concentrations between 100-150ng/mL.

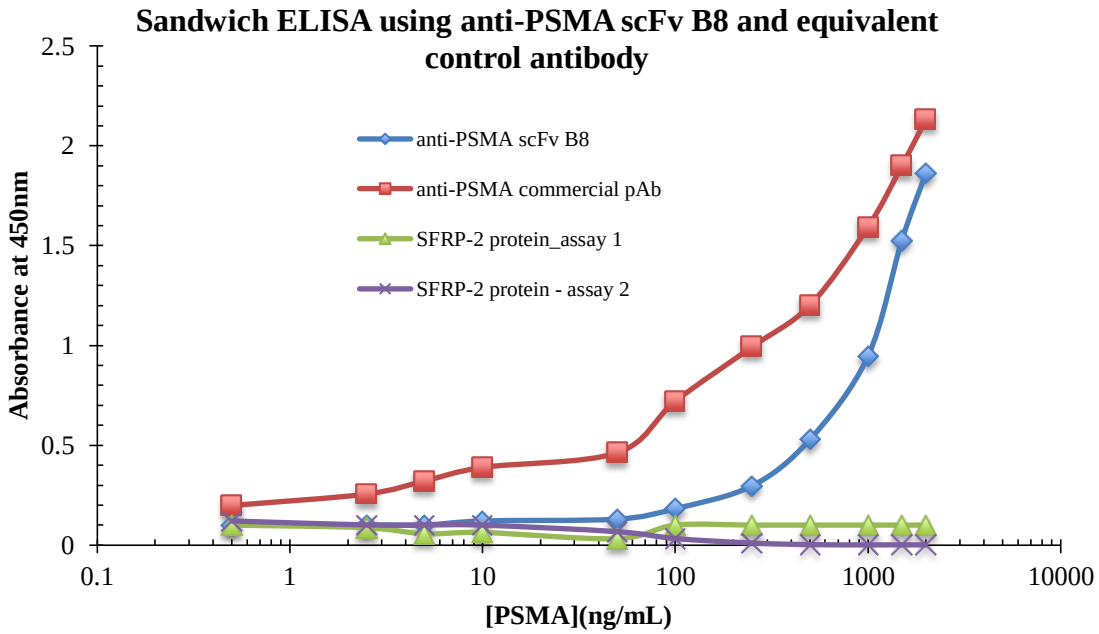

Figure 5.80. Sandwich ELISA using the purified anti-PSMA scFv B8 antibody and equivalent control antibody for PSMA capture.

Anti-PSMA scFv B8 and anti-PSMA commercial pAb were coated onto the surface of an ELISA plate capturing cTnI over a relatively wide concentration range (0.5 to 2,000ng/mL). Captured PSMA was detected using anti-PSMA pAb followed by an anti-rabbit HRP-labelled secondary in assay 1. In assay 2, detection was obtained using the anti-PSMA scFv B8 antibody followed by anti-HA-HRP-labelled secondary. Both the commercial and 'in-house' scFv antibody (P1B8) behaved similarly.

5.10 Analysis of the protein-membrane binding capability of anti-PSMA scFv clone B8 – Western blotting and dot blot

The IMAC-purified anti-PSMA scFv B8 antibody was used to probe PSMA western and dot blots in order to ensure the purification of the antibody did not affect its ability to bind its target antigen in membrane, prior to downstream applications in fluorescent microscopic analysis and IHC. Initially, the determined optimum working dilution of the scFv was applied to probe the blots. The results from this analysis showed that the purified antibody was capable of probing the target protein in dot blot but not in WB. The experiment was repeated applying additional dilutions of the scFv. Varying dilutions (1 in 100, 1 in 500 and 1 in 1,000) of the purified antibody, prepared in 1% (w/v) PBSTM, were used to probe the blocked (5% (w/v) PBSM, 1 hour, at RT) blots for 1 hour at RT. Bound scFv was detected using an anti-HA-HRP-labelled secondary antibody. The purified anti-PSMA scFv B8 antibody, again, worked well in dot blots, binding to the target antigen, at a dilution as low as 1 in

1,000. However, from the result of the western blotting analysis it was clear that, despite the presence of faint PSMA-specific bands at ~110kDa, the purified anti-PSMA scFv B8 antibody did not work efficiently when compared to the result obtained applying the lysate of this clone, even at a 1 in 100 dilution, in WB. This could indicate that the antibody folded in such a way, during the purification process, that the binding site for the linear epitope was not available for interaction, thereby reducing the efficiency of the result. The purification method was altered, in addition to changing the buffers used to purify the antibody, but the results were not improved (data not shown). In fact, altering the purification approach resulted in a reduction in protein yield from purification in addition decreased purity of the fraction.

In chapter 4 of this thesis, reformatting the anti-SFRP-2 scFv F3 to a scAb not only improved the expression of the antibody, but, additionally improved the ability of the antibody to bind in WB and dot blots. Hence, the same approach was applied for the anti-PSMA scFv prior to fluorescence-based microscopic analysis of prostate tissue.

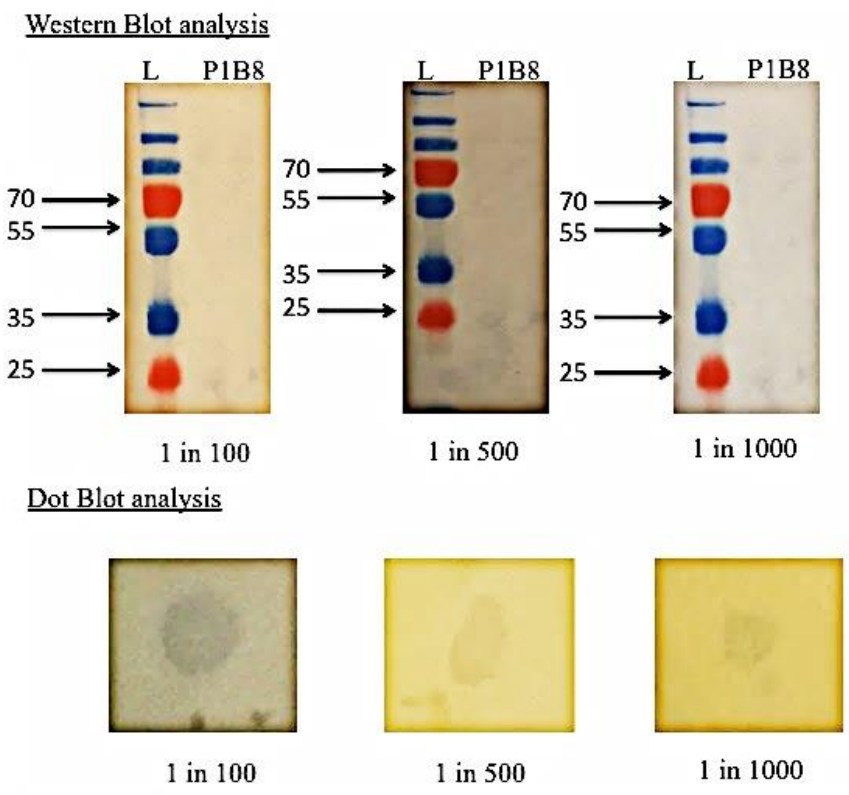

Figure 5.81. The application of an anti-PSMA scFv B8 clone as the primary antibody in a WB and dot blot analysis.

Western blot: varying dilutions (1 in 100, 1 in 500 and 1 in 1,000) of the anti-PSMA scFv B8 antibody were used to probe western blots, which had been transferred from resolved PSMA protein on an SDS-PAGE gel, for 1 hour at RT. Bound scFv was detected using an anti-HA-HRP-labelled secondary antibody. Dot blot: 2µg/mL of PSMA, prepared in molecular grade H_2O, was dotted on to pre-activated PVDF membrane and allowed to dry. The blot was blocked with 5% (w/v) PBSM for 20 minutes at RT. Varying dilutions of the anti-PSMA scFv B8 antibody, prepared in 1% (w/v) PBSTM, were used to probe the dot blots. Bound scFv was detected using an anti-HA-HRP-labelled antibody.

5.11 Reformatting anti-PSMA scFv to scAb

The expression of scFv clones targeted to the periplasm of *E. coli* often results in very low yields of soluble protein, frequently accompanied by host cell growth arrest, and sometimes cell lysis. Reformatting a scFv to a single-chain antibody fragment (scAb) can, in some circumstances, improve expression, protein yield and antibody stability. A scAb is a scFv with a human kappa light chain constant (HuCkappa) domain attached C-terminally. In chapter 4, reformatting the anti-SFRP-2 scFv antibody F3 to a scAb resulted in a 60-fold improvement in expression, with no noted negative effect on antigen binding recognition in ELISA and improved affinity for its target in WB.

Despite the fact that expression of clone B8 was not an issue, once purification of the antibody was carried out, a reduction in the antibody's ability to function in WB was observed. Hence, the same approach was taken, as with the anti-SFRP-2 scFv clone F3, for the anti-PSMA scFv clone B8 in order to determine if an improvement in WB performance could be obtained.

5.12 PCR amplification of anti-PSMA scFv B8 plasmid using primers for scAb

A plasmid prep of the anti-PSMA scFv B8 clone was prepared and incorporated into a PCR reaction with the primers ChiVL-VHPac-F and ChiVL-VHPac-R to prime the insert for insertion into the pMoPAC vector. The PCR was run under the conditions outlined in section 2.4.28.1 in Table 29. The PCR product was resolved on a 1.5% (w/v) agarose gel. Figure 5.84 shows the success of the amplification with the visualisation of the scFv at ~750bp.

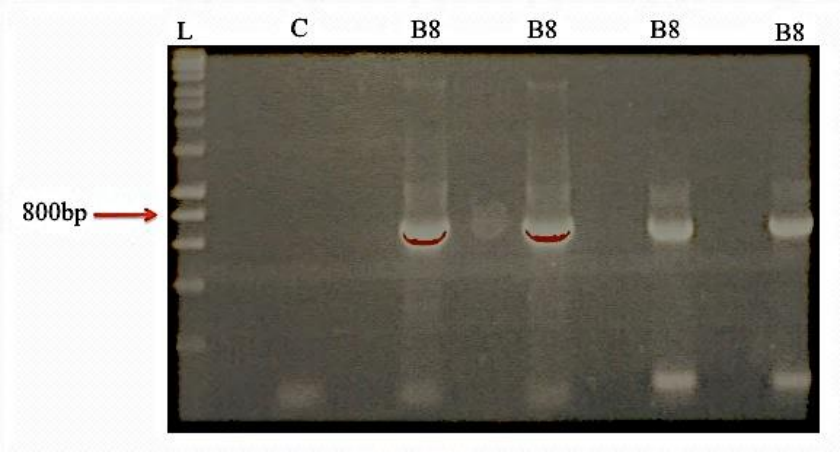

Figure 5.82. Visualisation of the amplification of anti-PSMA scFv B8 using the primers ChiVL-VHPac-F and ChiVL-VHPac-R.

A PCR reaction was set up with the plasmid DNA of clone B8 in order to prime the DNA to allow this insert to be cloned into the pMoPAC vector. MyTaq™ Red Mix was used for this PCR. A large-scale reaction was set up using the components and volumes outlined in Table 28. The PCR was run under the conditions outlined in Table 29 in section 2.4.28.1. The results were visualised on a 1.5% (w/v) agarose gel.

5.13 Colony-pick PCR to determine whether the pMoPac vector was harbouring the anti-PSMA B8 gene post transformation

Post ligation of the scFv insert into the pMoPAC vector and transformation in Top 10F' chemically competent cells, a colony pick PCR was performed to ensure the pMoPAC vector was harboring the anti-PSMA insert. The results from the colony

pick PCR showed that all clones picked contained the scFv B8 insert. Glycerol stocks were prepared for all clones and one was used as the working stock.

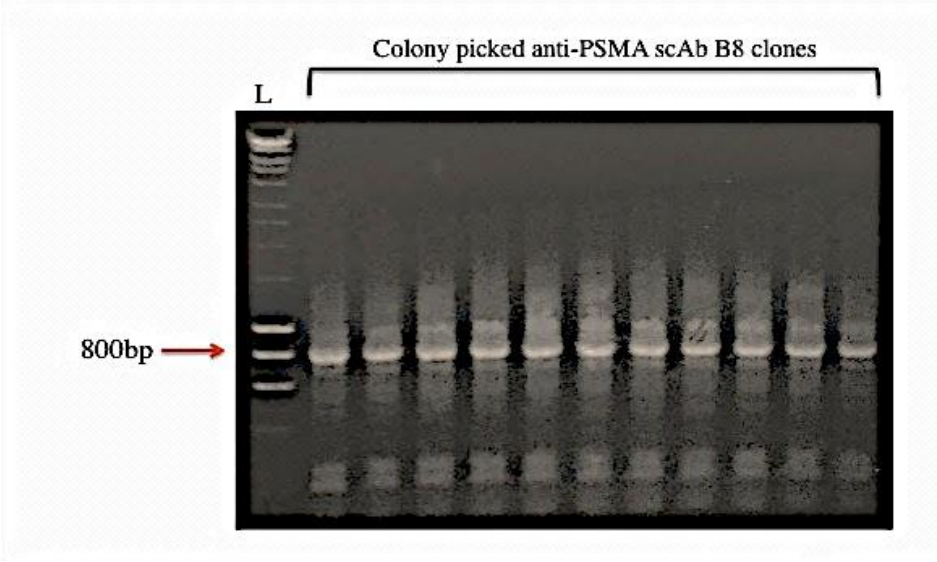

Figure 5.83. Visualisation on a 1.5% (w/v) agarose gel of the colony pick PCR of the transformed pMoPAC vector containing the scFv B8 insert.

Eleven single colonies were picked and incorporated into a colony pick PCR. The gene was amplified using the PCR primers ChiVL-VHPac-F and ChiVL-VHPac-R and MyTaq™ Red PCR mix.

5.14 Optimisation of expression of anti-PSMA scAb B8 varying IPTG concentration and temperature

Optimisation of expression of the anti-PSMA scAb B8 was carried out to determine the optimum conditions to apply when expressing the scAb large-scale. Varying concentrations of IPTG (0.2, 0.5, 0.8, and 1mM) and temperature were assessed throughout this analysis. The lysates representing each IPTG concentration at either 25 °C or 30 °C were analysed via WB in order to visualise the optimum conditions. An anti-chicken-HRP-labelled secondary antibody was used to detect the expressed antibody. The results from this optimisation experiment showed that the expression level of the scAb B8 was consistent at all IPTG concentration at both 25 °C and 30 °C. Therefore, the conditions used for large-scale expression were 1mM IPTG, at 25 °C, overnight.

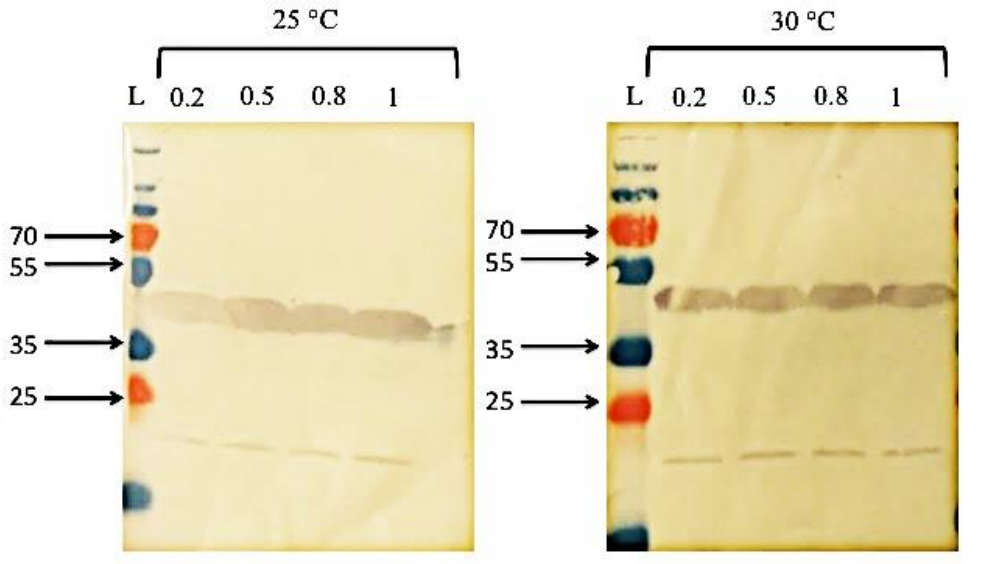

Figure 5.84. Optimisation of expression of the anti-PSMA scAb B8.

An overnight culture of scAb B8 was used to inoculate eight 10mL cultures. The cultures were grown at 37 ^{o} C, shaking at 220rpm, until an OD_{600} of ~0.7 was obtained. At this point four of the cultures were induced with varying concentrations of IPTG and the temperature reduced to 30^{o} C. The remaining four were induced with varying concentrations of IPTG at 25 ^{o} C overnight.

5.15 Large-scale expression and subsequent purification using an osmotic shock approach of anti-PSMA scAb B8

Optimised large-scale expression of the anti-PSMA scAb clone B8 was completed using 1mM IPTG for induction overnight at 25°C. The anti-PSMA scAb clone B8 was purified, as described in section 2.5.22, using osmotic shock-based buffers delineated in section 2.1.5.2.3. From the results, it was noted that a significant amount of non-specific protein was eluted in wash A (WA) whereas wash B (WB) appeared to be very clean. The eluted protein was concentrated and buffer exchanged into PBS. The concentrated sample was analysed by SDS-PAGE and WB, along-side the filtered lysate, 'flow-through', WA and WB fractions, and showed a very pure protein preparation. Protein concentration was obtained by A^{280} on a ND-1000™ and outlined in Table 62. The purified antibody was diluted to a working stock concentration of 1mg/mL in sterile PBS containing 0.02% (w/v) NaN_3.

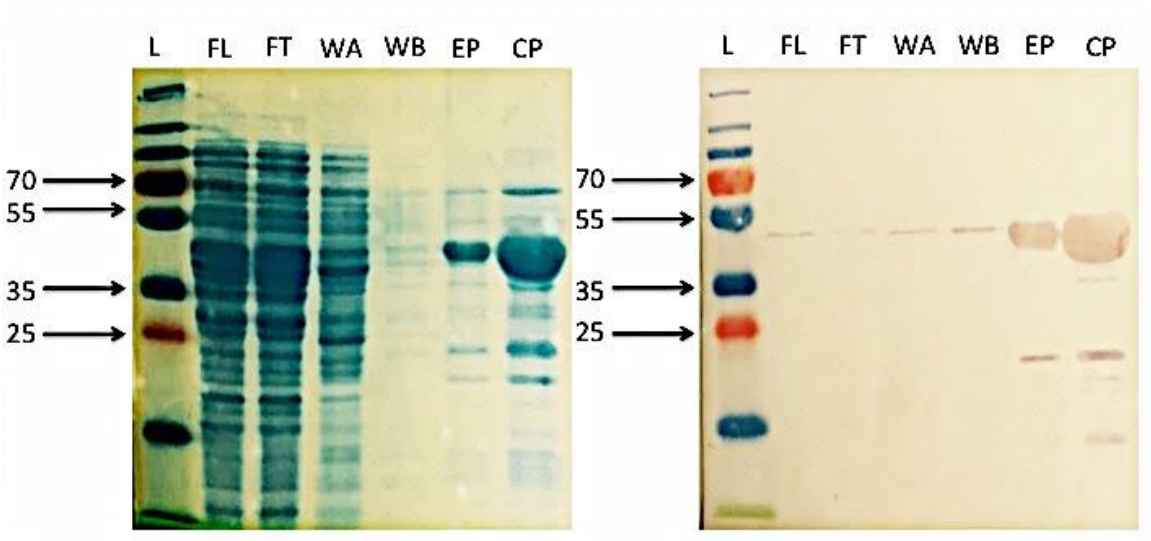

Figure 5.85. SDS-PAGE and WB blot analysis of anti-psma scAb B8 purification steps.

In the large-scale purification, samples of each step of the process were analysed. The lanes are labelled as follows; FL: filtered lysate, FT: 'flow-through' 1, WA: wash A, WB: wash B, EP: Eluted protein and CP: concentrated protein. L is the pre-stained protein ladder.

Table 61. IMAC-purified anti-PSMA scAb B8 protein yield determined using the NanoDrop™ 1000.

Protein fraction	Volume (mL)	Protein yield determined by the NanoDrop™ 1000
Eluted protein	4.0	4.1mg/mL
Concentrated protein	1.0	12.8mg/mL

5.16 Western and dot blot analysis of purified anti-PSMA B8 scAb

Varying dilutions of the purified scAb were prepared in 1% (w/v) PBSTM and used to probe PSMA western and dot blots. Bound scAb was detected using anti-chicken-HRP-labelled secondary antibody. The results from both the western and dot blots show a clear improvement in the binding ability of clone B8 to its target in western blotting, working at a dilution as low as 1 in 2,000. Reformatting the scFv to a scAb not only improved the expression of this clone but also improved its ability to

recognise the linear and conformational epitopes of the PSMA protein. The scAb was then brought forward and used to probe prostate tissue in a fluorescent microscopic analysis at the optimum working dilution, determined by ELISA, WB and dot blot, at 1 in 2,000.

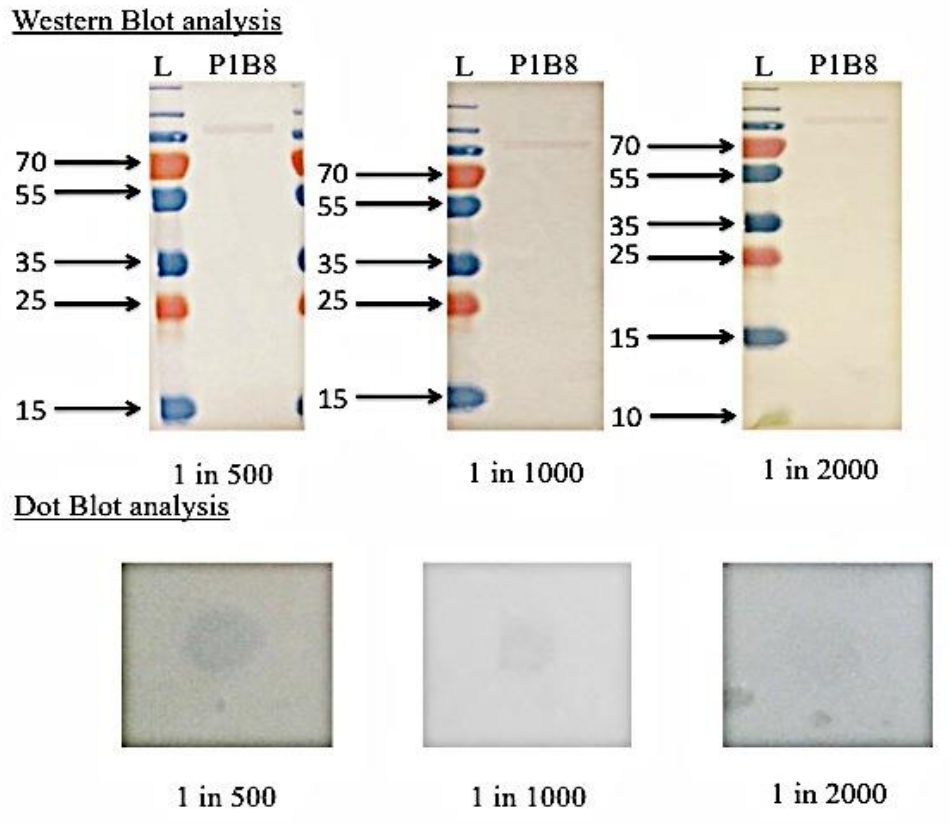

Figure 5.86. The application of an anti-PSMA scAb B8 clone as the primary antibody in a western blot and dot blot format.

Western blot: varying dilutions (1 in 500, 1 in 1,000 and 1 in 2,000) of the anti-PSMA scAb B8 antibody were used to probe a PSMA membrane for 1 hour at RT. Bound scFv was detected using an anti-HA-HRP-labelled secondary antibody. Dot blot: 2µg/mL of PSMA, prepared in molecular grade H_2O, was dotted on to pre-activated PVDF membrane and allowed to dry. The blot was blocked with 5% (w/v) PBSM for 20 minutes at RT. Varying dilutions of the anti-PSMA scAb B8 antibody, prepared in 1% (w/v) PBSTM, were used to probe the dot blots. Bound scAb was detected using an anti-chicken-HRP-labelled antibody.

5.17 Fluorescent microscopic analysis of normal, benign prostatic hyperplasia and malignant prostate tissue probed with anti-PSMA scAb B8 and anti-chicken H/L Dylight488 polyclonal antibody

Prior to IHC analysis of prostate tissue, additional preliminary testing was completed. Normal, benign prostatic hyperplasia and malignant (adenocarcinoma) prostate tissue slides were obtained commercially from Abcam and incorporated into a fluorescent microscopic analysis. Studies have consistently demonstrated PSMA expression in all types of prostate tissue and increased PSMA expression in cancer tissue. This analysis was completed to determine the ability of the scAb to bind its target antigen in varying forms of prostate tissue. See section 4.16 for details on secondary antibodies applied and negative controls included for analysis. The results from this study were inconclusive as the auto-fluorescence of the secondary antibody, in the absence of cover slides (prevent drying out of the tissue), prevented clear imaging of the tissue samples from being achieved. Due to time constraints and the high cost of the commercial tissue, this experiment could not be repeated. IHC analysis applying this antibody is currently ongoing in Beaumont Hospital.

5.18 Chapter discussion and conclusion

Accurate pathologic diagnosis of prostate cancer is vital for optimal patient treatment. Diagnosis of the disease can usually be made on morphological features such as growth pattern, nuclear atypia and the absence of basal cells. However, due to the heterogeneous nature of the disease (discussed in chapter 1), often in morphologically equivocal cases, the use of IHC is applied by the histopathologist to resolve differential diagnosis (Varma & Jasani, 2005). IHC is used essentially in two different clinical settings in prostate cancer: (i) to distinguish low-grade prostatic cancer from benign mimics, in particular on needle biopsies and (ii) in transurethral resection specimens or metastatic tumour samples, to establish the prostatic origin of a poorly differentiated carcinoma (Varma & Jasani, 2005). PSMA is coming to the forefront as a key marker in prostate cancer where increased expression of this marker is linked to aggressive disease. The aim of this chapter was to generate anti-PSMA recombinant antibodies applicable for use in IHC for the analysis of various forms of prostate tissue.

A successful immunisation campaign was completed in an avian host with two PCa cell lines that are known to express high levels of the target protein. The animal was

sacrificed and both the spleen and bone marrow were harvested. RNA was extracted from both sources and used as a template for cDNA synthesis. Successful amplification of full-length scFv gene fragments was carried out using consecutive PCR steps. Purified pComb3xSS vector and the anti-PSMA spleen and bone marrow scFv libraries were digested using the S*fi*I restriction enzyme. Barbas *et al.* (2001) designed the pComb3 phagemid display system so that directional cloning of the scFv gene sequences could be accomplished with a single restriction endonuclease. S*fi*I recognizes an 8-bp sequence (GGCCNNNN^NGGCC) and cuts (between the 4^{th} and 5^{th} N) within the degenerate region of its interrupted palindromic recognition site, leaving an indeterminate 'sticky' end. The freedom in the N nucleotide selection enables the design of different restriction sites that are recognised and cut by the same S*fi*I enzyme. The use of unique 5' (GGCCCAGG^CGGCC) and 3' (GGCCAGGC^CGGCC) S*fi*I sites within the sense and reverse avian primers for the amplification of the variable regions in this work, allowed the scFv fragments to be ligated into the pComb3xSS vector in the correct orientation (Gao *et al.*, 2002). Ligated pComb3xSS-anti-PSMA scFv gene sequences were transformed into electrocompetent *E. coli* XL-1 Blue cells. Dilutions of the electroporated bacteria were plated and the number of scFv-containing clones within the library was estimated. The complexity of an antibody library is defined as the number of clones bearing a suitable selectable marker (antibiotic resistance) and containing the full size antibody gene (Barbas, *et al.*, 2001). In contrast to naïve libraries, the use of animals as the source of immunoglobulin cDNA reduces the need for very large (> billion) antibody libraries. Typically, an immune antibody library has already been enriched with antigen-specific antibodies. Furthermore, some of these antibodies may have undergone natural affinity maturation (Smith *et al.*, 2005b). Even so, the overall immune library size is still an important determinant for successful selection against an antigen. Typically libraries derived from immune animals range in size from 10^7 to 10^8 transformants. Smaller immune libraries are not recommended for screening using the panning strategy, as diversity may be limited due to the absence of certain antibody sequences (Barbas, *et al.*, 2001). A combined anti-PSMA scFv library size of 1×10^7 was incorporated into a stringent panning regime in order to achieve enrichment of the library for the PSMA antigen.

A conventional phage display method was applied for screening the anti-PSMA scFv

library, whereby the antigen was absorbed to a solid support (microtitre plate). Following exposure of the scFv phage particles to the target antigen, non-specific binders were removed in the wash steps, and phage bound to the target were recovered in the elution step. The eluted phage were successfully re-amplified in *E. coli* and used in four rounds of panning. Table 54 shows the input and output titres obtained over the four rounds of panning the anti-PSMA scFv library. Some researchers use their input and output titres as an indication as to whether or not their panning approach has been successful. However, this is not always a reliable approach. Only a small fraction of the titred phage actually display correctly folded antibody fragments on their surface. In addition, phage that have a low propensity to interact with the target antigen but are able to replicate quickly will rapidly dominate the output titre. Furthermore, antibodies that bind to a contaminant with high affinity, rather than to the target antigen, can also dominate the selection process. Therefore, total phage titres do not reveal the amount of functional target-specific phage present (Maynard & Georgiou, 2000; Barbas, *et al.,* 2001; O' Brien & Aitken, 2002; Clackson & Lowman, 2007). Taking this into consideration, in order to clearly determine at which round of panning significant enrichment of anti-PSMA occurred, an ELISA analysis on the phage obtained after each round of selection was completed. As the viral input to the assay is mixed in composition, the assay is termed polyclonal phage ELISA (O' Brien & Aitken, 2002). An increase in ELISA signal as a function of panning round is indicative of enrichment for PSMA binders (O' Brien & Aitken, 2002). Enrichment of the anti-PSMA scFv library was achieved after four rounds of panning, as this round showed the strongest anti-PSMA reactivity.

The phage pools from round four of panning were subsequently infected into a non-suppressor (non-SupE) strain of *E. coli* (Top 10 F'). The pComb3xSS vector contains an amber stop codon positioned between the scFv fragment and pIII genes. This allows for the expression of scFv fragments as either phage-bound pIII fusion proteins (in SupE bacterial strains) or soluble recombinant protein (in non SupE bacterial strains) that are not fused to pIII (Barbas, 2001; O' Brien & Aitken, 2002). Three hundred and eight four anti-PSMA scFv clones were selected for screening against the PSMA antigen. This screening approach was carried out at a protein level to assess binding in two ways: i) monoclonal phage ELISA and ii) Biacore^{TM} 4000 high throughput (HT)-ranking by stability early and late analysis. The acquired data, most

notably on the refined HT-system, offered a wealth of information to judiciously aid the screening process.

Analysing the data obtained from the screening process allowed the 75 lead anti-PSMA candidates to be identified. Sequencing analysis revealed that out of the 75 antibodies sent for sequencing, 5 different clones were present. Out of the 5, only 4 anti-PSMA scFv antibodies were eligible to be brought forward for further characterisation. The low diversity of the clones sequenced validates the stringent selection and rigorous screening approach applied to identify these anti-PSMA-specific scFv antibodies. It is widely accepted that the CDRH3 has by far the greatest sequence diversity compared to the five remaining CDRs and makes a significant contribution to antigen contact (Birtalan *et al*., 2008). The CDRH3 region for all sequences identified varied in length but was dominated by the presence of serine and glycine residues. Tyrosine, aspartic acid and isoleucine residues were also quite prominent. Tyrosine, tryptophan and arginine residues are capable of mediating a wide-array of intermolecular interactions, which are desirable in the composition of the CDRs. The frequency of small residues in the CDR loops confers conformational flexibility, which is crucial for effective antigen recognition. With this in mind, almost all the CDRs are dominated by the small amino acids serine and glycine.

All four anti-PSMA scFv antibodies were brought forward for further characterisation allowing the successful identification of anti-PSMA scFv B8 which showed similar efficiency at recognizing its target antigen in ELISA, WB and dot blot to the commercial anti-PSMA polyclonal antibody. Post purification by IMAC the ability to apply this antibody in WB was reduced. Antibodies, like all proteins, are sensitive to their environment. The purification process applied here may have been too harsh (i.e. inappropriate elution buffer, buffer pH, experimental temperature etc.), and thus had an effect downstream on the antibody binding in WB. As discussed previously, WB is a technique whereby the proteins to be analysed are partially or fully denatured prior to use. Hence, in a WB the target analyte is not presented to the antibody in its native state. The purification process applied here appears to have altered the antibody in such a way that it has affected how the antibody interacts with the non-native form of the antigen (i.e. the linear epitope). Optimisation of the purification process was completed and the antibody was tested in WB numerous times; however, no improvement was observed.

Reformatting the anti-PSMA scFv antibody to a scAb improved both its ability to bind its target in all assays tested and also the expression. ScAbs have proven to be superior to scFv antibodies in a number of studies completed in Prof. O' Kennedy's lab, including the two presented in this thesis.

Due to the limited supply of prostate TMAs for IHC analysis employing this antibody, fluorescent microscopic analysis of various forms of prostate tissue was completed as a preliminary test to determine if staining could be achieved in prostate tissue using the anti-PSMA scAb B8 and a commercial pAb equivalent known to function in IHC. The prostate tissue slides (normal, benign and malignant) were commercially sourced from Abcam. Following a thorough literature search and through personal communication with Dr. Tony O' Grady (Chief Medical Scientist, Pathology Department, Royal College of Surgeons in Ireland Beaumont Hospital) a decision was made on the approach taken to prepare the slides, the most efficient mode of antigen retrieval to utilize, in addition to, the primary and secondary antibody dilutions and incubation times. One negative and one positive control were included in this analysis. Fluorescence microscopy takes advantage of light emission with different spectral peaks against a dark background. The basic principle behind fluorescent microscopy relies on the ability of individual fluorophores to be excited by one wavelength and emit at a longer specific wavelength (a phenomenon known as Stokes shift). An indirect fluorescent microscopic approach was applied for this study, whereby the fluorophore (Alexa488 in this study) was conjugated to the secondary anti-chicken antibody specific for the primary antibody (anti-PSMA scAb B8, raised in chicken). The results from this study were inconclusive as the auto-fluorescence of the secondary antibody, in the absence of cover slides (prevent drying out of the tissue), prevented clear imaging of the tissue samples from being achieved. Due to time constraints and the high cost of the commercial tissue, this experiment could not be repeated.

IHC studies completed to-date, have shown that PSMA is highly expressed in most intraepithelial neoplasia, primary and metastatic prostate tumour specimens. PSMA expression has often been described as heterogeneous with variable staining patterns in tissue, ranging from low-level diffuse cytoplasmic staining in normal prostate epithelium to very intense cytoplasmic and focal membrane staining in high-grade primary carcinomas and metastatic tissue (Wright *et al.*, 1995). The majority of

studies completed have concluded that high PSMA expression is significantly associated with tumour stage and high Gleason grade. Additionally, tumours with strong PSMA expression have a higher risk of biochemical recurrence than those with weak.

In conclusion, an anti-PSMA recombinant antibody was successfully generated showing potential for application in IHC. IHC plays as important role in diagnostic surgical pathology of the prostate. Given the advantageous characteristics associated with PSMA as a biomarker for PCa, employing anti-PSMA antibodies into routine IHC analysis for the diagnosis of this disease, singly, or in combination with other PCa-specific antibodies, such as AMACR, may significantly improve PCa diagnosis and the ability to decipher between benign and malignant disease.

Over the past two decades, PSMA is a molecular target the use of which has resulted in some of the most productive work toward imaging and treating prostate cancer, in addition to diagnosing the disease. A wide variety of imaging agents extending from intact antibodies to low-molecular-weight compounds permeate the literature. In parallel there is a rapidly expanding pool of antibody-drug conjugates, radiopharmaceutical therapeutics, small-molecule drug conjugates, theranostics and nanomedicines targeting PSMA (Kiess *et al.,* 2015). Such productivity is motivated by the abundant expression of PSMA on the surface of prostate cancer cells and within the neovasculature of other solid tumours, with limited expression in most normal tissues. The future for PSMA as a key marker for prostate cancer is bright and targeting this protein may provide a viable alternative or first-line approach to managing this disease in addition to other cancers.

Chapter 6

Development of a unique theoretical approach for the generation of a novel bispecific antibody

Chapter overview

The development of monospecific antibodies for diagnostic or therapeutic application is well documented and has shown some tremendous successes to-date in the clinic. An area of antibody generation that has shown resurgence over the past 10 years, due to the introduction of recombinant DNA technology, is the development of bispecific antibodies. Diagnostically, the main advantage of using bsAbs over monospecific antibodies is that maximum specific activity and functional efficiency can be achieved since every antibody molecule is associated with a signal-generating molecule (Byrne *et al.,* 2013). In addition to making the diagnostic assay rapid, bsAbs enhance sensitivity and specificity of detection. They significantly reduce or even eliminate false positive reactions especially in assays such as ELISA (Kontermann, 2011). In the case of immunohistochemistry, the use of bsAbs leads to decreased background, clear and distinct identification of immune reactivity, and good resolution of ultra-structural details (Milstein & Cuello, 1983; Suresh *et al.*, 1986; Kontermann, 2011). Additional advantages of using bsAbs in immunodiagnostic assays include improvement in signal-to-noise ratios and simplification of the assay procedures, often with the elimination of steps (Byrne *et al.*, 2013). Bispecific antibodies also exhibit a number of characteristics that make them therapeutically appealing, including design flexibility, modularity, optimal selectivity for activating or downregulating ligands, and the delivery of therapeutic molecules (Byrne *et al.*, 2013).

Bispecific antibodies are quickly becoming an integral part of antibody research. Hence, research groups in academia and industry are consistently striving to improve bispecific antibody technology and introduce novel approaches to generate these antibodies. A bispecific/bifunctional antibody generation strategy was devised in Professor O' Kennedy's lab that utilizes PCR technology and primer design for the overlap of two scAb constructs with specificity for two different targets. Throughout this project, PCR technology was applied for cloning, antibody construction and reformatting and gene amplification. Taking this into consideration, it was decided that the skills gained throughout this work would be utilized to complete the first part in the 'proof-of-concept' studies for this bispecific antibody generation strategy, which was to build the bispecific antibody using PCR technology and specifically designed primers. Two highly specific antibodies targeting two different cardiac

markers, namely cardiac thrombin-I (cTnI) and myeloperoxidase (MPO), were readily available and were therefore applied in the 'proof-of-concept' study for this work. Successful amplification of the anti-cTnI x anti-MPO bsAb was achieved, leading to the amplification of a 2400bp product (anti-cTnI scAb (1200bp) and anti-MPO scAb (1200bp)), completing the overall aim of this chapter. The second part in the 'proof-of-concept' studies in currently underway in a separate project for the generation of a anti-prostate cancer specific bispecific antibody.

6.1 Introduction to bispecific antibodies

Bispecific antibodies (bsAb) are antibody-derived proteins with the ability to bind to two different epitopes on the same or different antigens. Recombinant DNA technology has yielded the greatest range of bsAbs, through artificial manipulation of genes (45 formats in the past two decades) (Kontermann, 2012). Several bsAb formats can redirect cytotoxic effector cells against target cells that play key roles in disease processes. They can induce cytotoxicity, phagocytosis, and present antigens or directly suppress deregulated immune responses, depending on the nature of interaction between the bsAb and its target. Furthermore, they can deliver payloads to, for example, tumour cells, including toxins, drugs, pro-drugs and contrast agents (Kontermann, 2012). BsAbs have proven to be of major therapeutic interest over the past 30 years. They possess several advantageous characteristics including design flexibility, modularity, optimal selectivity for activatory or downregulating molecules, oligoreactivity, and the delivery of therapeutic molecules.

The ability of bsAbs to bind simultaneously to a specific antigen and a given detection moiety enables them to additionally function as excellent bifunctional immunoprobes in diagnostic assays. Associated advantages of bsAbs over traditional mAbs include design flexibility and one-step addition of reagents compared to traditional multi-step procedures. Obviating the requirement to label a reagent directly, such as a secondary antibody, reduces the deleterious effects of chemical modification of either the enzyme or the antibody (Byrne *et al.*, 2013). Antibodies are extremely versatile and are incorporated into a variety of different immunodiagnostic assay platforms, such as microtiter plate assays, swabs, strips, filter disks, and 'spinning-disc-type' assays (Byrne *et al.*, 2013). BsAbs are attractive in such assays because they simplify the detection steps and are currently used for the development of simple, rapid, and highly sensitive immunoassays for the analysis of bacterial and viral infectious diseases and in cancer diagnostics. The following section discusses the most popular recombinant bispecific antibody formats and how they are engineered. Table 63 outlines the applications of these bispecific antibodies in cancer therapy and Table 64 displays those that have moved into clinical trials and/or have been approved for clinical use.

6.2 Recombinant bispecific antibody formats

A plethora of different recombinant bsAb formats exist, ranging from whole 'IgG-like' molecules to small recombinant formats such as tandem single chain variable fragment molecules (taFvs), diabodies (Dbs), single chain diabodies (scDbs), and various other derivatives of these. Bispecific tetravalent molecules are produced using Fc-mediated dimerization and possess two binding sites for each antigen, which impart increased avidity. A frequently used approach to produce a tetravalent bispecific molecule is through the fusion of a single-chain Fv fragment to the C terminus of an antibody heavy chain or by substituting the Fab arm with a bispecific single-chain antibody fragment such as a tandem scFv or a scDb (Muller & Kontermann, 2010). It is also possible to fuse a second variable heavy (V_H) and variable light (V_L) domain to the heavy and light chains of an antibody, therefore leading to the production of a dual-variable-domain (DVD) antibody (Wu *et al.*, 2007).

Recombinant strategies can also be used to produce small bsAb fragments. The most common approach for this is the fusion of two different scFv molecules. This strategy forms the basis of the bispecific T cell engager (BiTE) developed for cancer immunotherapy. A further expansion of this strategy is the fusion of an additional scFv fragment molecule, leading to the formation of a trivalent or trispecific antibody (Kellner *et al.*, 2008; Muller & Kontermann, 2010). In an alternative approach, two bispecific Dbs and two bispecific trivalent proteins were expressed within the same cell, produced and tested as potential agents for pre-targeted delivery of radio-labelled bivalent haptens to tumours expressing carcinoembryonic antigen (CEA). These chains assembled in an antiparallel manner to form heterodimeric molecules (Rossi *et al.*, 2003; Muller & Kontermann, 2010). ScFv fragments expressed in bacteria are known to exist in both monomeric and dimeric forms (Griffiths *et al.*, 1993) and this can be exploited to form Dbs, which are generated by linking the V_H domain of one antibody to the V_L domain of another. The linker is deliberately short (3–12 amino acids in length), which induces the two domains to pair with the complementary domain of another chain, thus creating two different antigen-binding sites. ScDbs are a derivative of the Db approach and are produced by introducing an additional peptide linker to join the two antibody fragments, hence, the domains are expressed as a single polypeptide chain (Muller & Kontermann, 2010).

ScFv antibody constructs have been applied as the basic building blocks for a plethora of bispecific antibodies, however, certain forms of scFv have variable and unpredictable expression yields and the linker used can cause spontaneous aggregation. Introducing shortened linkers to produce a Db does not always guarantee success, as the linker can induce deleterious conformational changes resulting in a reduction of antibody functionality (Auf der Maur *et al.*, 2001).

To overcome solubility-related issues, several unique approaches have been undertaken to stabilize recombinant bispecific antibodies (rbsAbs). Single domain antibodies (sdAbs) occur in the natural repertoire of both camelid and cartilaginous fish. These single V domain constructs, known as VHH in camelids and V-NAR in sharks, are of minimal size (15 kDa). In addition, they demonstrate high expression levels, and exhibit high stability and solubility in vitro, which has made them attractive entities for bsAb generation (Els Conrath *et al.*, 2001). SdAbs can be produced in bacteria (or yeast) and their properties support facile conversion to bispecific formats through linkage of two sdAbs directed against two different antigens. The resultant low molecular mass (~30 kDa), although advantageous for bio-distribution, can hamper therapeutic success due to rapid clearance *in vivo* by renal filtration and degradation. The positive attributes associated with sdAbs have made them a key point of therapeutic interest (Els Conrath *et al.*, 2001; Holliger & Hudson, 2005; Chames & Baty, 2009).

The bsAb stable is large with big pharmaceutical companies investing over US$7.5 billion in bsAbs since 2009 (Holmes, 2011; Byrne *et al.*, 2013). Table 63 outlines the recombinant bispecific antibody formats in current research circulation for application in therapy, in addition to, the bispecific antibodies in clinical trials and those approved for clinical use (Table 64).

Table 62. Recombinant bispecific antibodies for therapeutic application.

(Adapted from Byrne *et al.*, 2013)

Format	Target 1	Target 2	Reference
Recombinant bispecific antibodies for application in the treatment of Cancer			
TaFv	CD19	CD3 (CTL)	(Wolf *et al.*, 2005; Brischwein *et al.*, 2006; Buhmann *et al.*, 2009 Seimetz *et al.*, 2010)
	EpCAM	CD3	(Dettmar *et al.*, 2012; Eissler *et al.*, 2012)
	MHC complex	CD16 (NK cells)	(Sharkey *et al.*, 2007)
	ErbB2	CD16	(McBride *et al.*, 2006)
	EGFR	Adenovirus (Ad)	(Khaw *et al.*, 2006; Tekabe *et al.*, 2010; Gada *et al.*, 2011; Patil *et al.*, 2012)
	EpCAM	Ad	(Cattamanchi *et al.*, 2011)
	CD40	Ad	(Davis *et al.*, 2011)
	CEA	Ad	(Sarkar *et al.*, 2012)
	(3E10) Cell penetration	P53 (Apoptosis)	Chen *et al.*, 2007
Db	CD19	CD3	(Manafi *et al.*, 2001; Guittikonda *et al.*, 2007)
	EGFR	IGFR	(Yam *et al.*, 2003)
	VEGFR2	VEGFR3	(Chan *et al.*, 2004)
	PSMA	CD3	(Keyaerts *et al.*, 2005)
scDb	CD19	CD3	(Yamashita *et al.*, 2005)
	Engodlin	CD3	Kammila *et al.*, 2008
	Endoglin	Ad	(Sunwoo *et al.*, 2013)
TaDb	CD19	CD3	(Hemmerle *et al.*, 2012)
scFv-CH3	ErbB2	CD16	(Dreier *et al.*, 2002)
IgG-scFv	TRAIL-R2	LTβR	(Loffler *et al.*, 2003)
scFv-IgG	EGFR	IGFR	(Gruen *et al.*, 2004)
$scFv_2$-	EGFR	IGFR	(Ren-Heindenreich *et al.*, 2004)
	IGFR	------	(Maletz *et al.*, 2001)
IgG-scFv	CEA	DOTA	(Wuest *et al.*, 2001)
$F(ab')_2$	CD20	CD22	(Grosse-Hovest *et al.*, 2004)
TriMab	ErbB	IGF1R	(McCall *et al.*, 2001)
bsFab (sdAb)	CEA	FcγRIIa	(Haisma *et al.*, 2000)
Format	**Target 1**	**Target 2**	**Reference**
***Recombinant bispecific antibodies for application in the treatment of* allergic disease**			
IgG-like	FcεRI	FcγRIIb (CD32B)	(Beusechem *et al.*, 2002)
$F(ab')_2$	IgE	FcγRIIb (CD32B)	(Heideman *et al.*, 2002)
IgG-like	CCR3	CD300a	(Brandao *et al.*, 2003)

Format	Target 1	Target 2	Reference
***Recombinant bispecific antibodies for application in the treatment of* infectious disease**			
IgG-scFv	HIV CCR5 epitope	HIV CCR5 epitope	(Korn *et al.*, 2004)
V_{HH}-C_H	LukS-PV	LukF-PV	(Weisbart *et al.*, 2004)
scFv	Malaria parasite (MSP)	CD3	(Cochlovius *et al.*, 2000)
TaDb	MP65	SAP-2	(Kipriyanov *et al.*, 2002)
***Recombinant bispecific antibodies for application in the treatment of i*nflammatory disease**			
IgG-scFv scFv-Fc TascFv-Fc	IL17A	IL23	(Xiong *et al.*, 2002)
Db	FcγRIIb (CD32B)	CD79b	(Hayashi *et al.*, 2004)
DVD-Ig	IL-1α	IL-1β	(Takemura *et al.*, 2002)

Table 63. Recombinant bispecific antibodies in clinical trials.

(Adapted from Byrne *et al.*, 2013)

Name (format)	Target 1	Target 2	Phase	Reference
MDX-447 ($F(ab')_2$)	EGFR	FcγRI	I	(Lu *et al.*, 2004)
MM-111 (Trimeric scFv)	ErbB2	ErbB3	I-II	(Leonard *et al.*, 2008)
DT2219ARL (Dimeric scFv)	CD19	CD22/DT390	I	(Chames & Baty, 2009)
TF2 (Tri-Fab)	CEA	HSG	I-II	(Buhler et al., 2008)
rM28 (scAb)	Melanoma-associated proteoglycan	CD28	I-II	(Kipriyanov *et al.*, 2003)
MT103 (BiTE)	CD19	CD3	I-II	(Korn *et al.*, 2004)
MT110 (BiTE)	EpCAM	CD3	I	(Nettelbeck *et al.*, 2001)
SAR156597 (Tetravalent bispecific tandem Ig)	IL4	IL13	I	(Nettelbeck *et al.*, 2004)
Ozoralizumab (Trivalent bispecific nanobody)	TNF	HAS	II	(Reusch *et al.*, 2004)

6.3 The application of SOE-PCR technology to construct a bispecific/ bifunctional antibody

The following section introduces a bispecific/bifunctional antibody construction approach that was successfully developed and could be applied in future projects to generate disease-specific bsAbs that may improve the diagnosis and therapy of a number of diseases including PCa. The concept behind this bispecific antibody generation strategy is to use specifically designed primers incorporating the necessary restriction and overlap sites to construct two single-chain antibodies (scAb) (see

Figure 89 and 90), with specificity for two different targets. The two scAbs are then incorporated into a SOE-style PCR, applying the appropriate primers, to link both fragment antibodies leading to the production of a 2400bp product, corresponding to the size of two scAbs overlapped (Figure 6.91). The concept behind this novel bsAb generation strategy, including the primer design, was conceived by Dr. Paul Conroy, a previous postdoctoral researcher in Prof. O' Kennedy's research group.

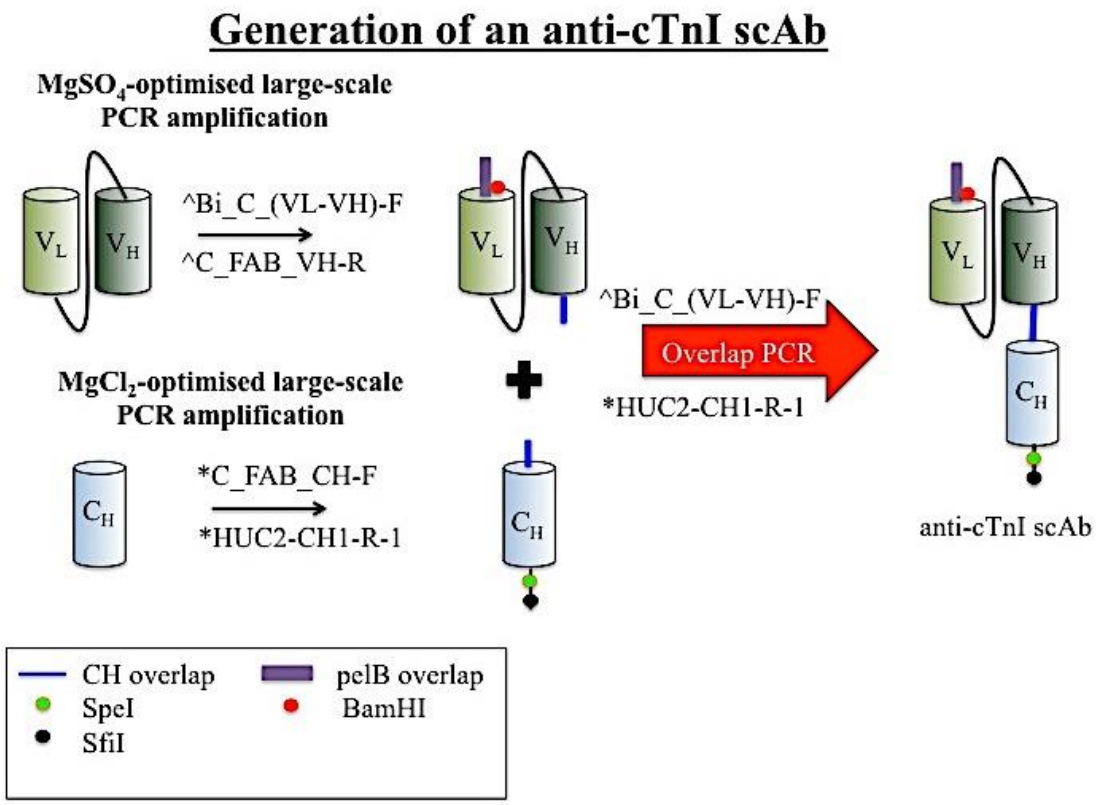

Figure 6.87. Overview of anti-cTnI scAb generation.

The constant heavy (C_H) and anti-cTnI scFv (V_L-V_H) regions were amplified on a large-scale and then incorporated into an overlap PCR to allow the generation of the anti-cTnI scAb construct. The star (*) represents the constant heavy forward and reverse primers, which incorporate a SfiI restriction site and a constant heavy overlap tail (represented by a blue line in Figure 6.89). The anti-cTnI scFv forward and reverse primers incorporating the constant heavy (blue line) and the pelB (dotted purple line) overlap tails are represented by ^. The constant heavy overlap tail (blue line), incorporated into the constant heavy and variable heavy region, allow the overlap extension of the anti-cTnI scFv with the constant heavy region leading to the generation of the anti-cTnI scAb.

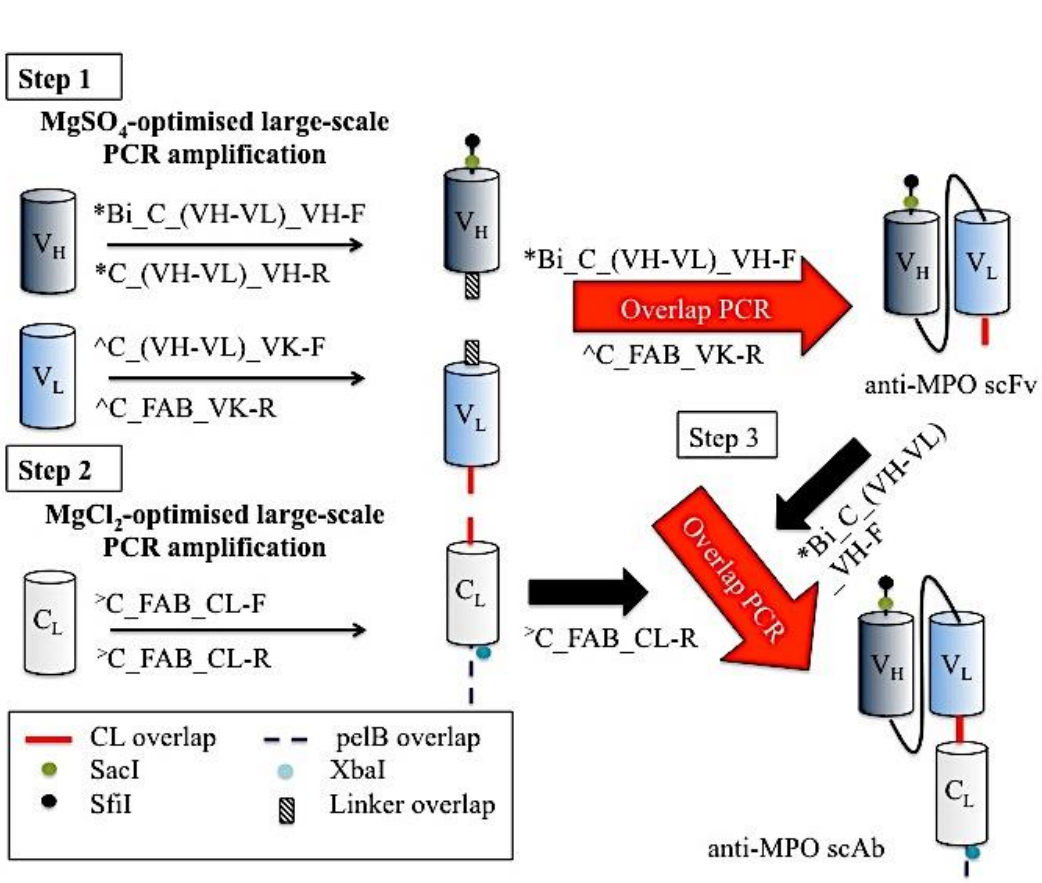

Figure 6.88. Overview of anti-MPO scAb generation.

The constant light (C_L) and anti-MPO scFv (V_H-V_L) regions were amplified on a large-scale basis and then incorporated into an overlap PCR to allow the generation of the anti-cTnI scAb construct. Reformation of the anti-MPO scFv from the V_L-V_H format to the V_H-V_L format was carried out. The star (*) represents the variable heavy forward and reverse primers incorporating the SfiI restriction site and the linker overlap tail (represented by a hatched box in Figure 6.90). The variable light forward and reverse primers incorporating the constant light (red line in this Figure) and linker overlap (lined box) tails are represented by ^. The constant light forward and reverse primers incorporating the constant light (red line) and pelB (purple dotted line) overlap tails are represented by >. The constant light overlap tail (red line), incorporated into the constant light and variable light region, allow the overlap extension of the anti-MPO scFv with the constant light region leading to the generation of the anti-MPO scAb.

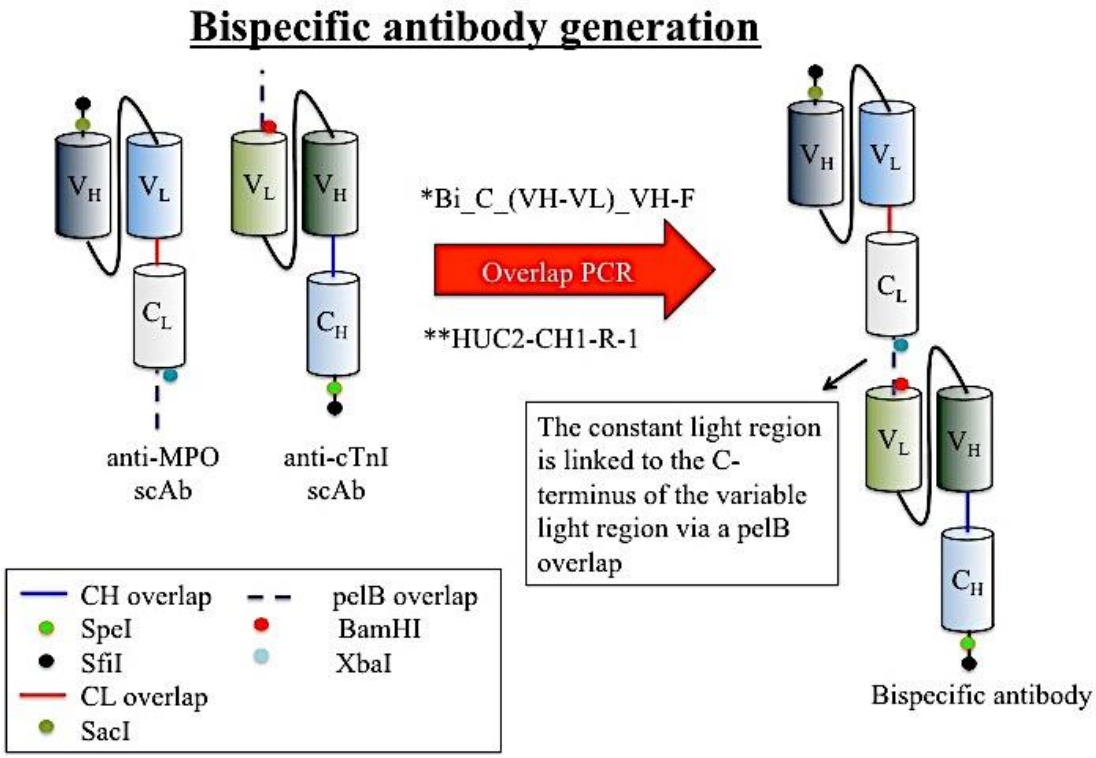

Figure 6.89. Bispecific antibody generation through overlap PCRs.

The purified anti-MPO and anti-cTnI scAb constructs were incorporated in equimolar ratios into an overlap PCR using the variable heavy forward primer and the constant heavy reverse primer. The pelB tail (represented by a dotted purple line) on the constant light and variable heavy constructs allow the overlap extension of both scAbs. The constant light region is linked to the C-terminus on the variable light region so that the binding capability of the anti-MPO scAb would not be affected. The star (*) represents the variable heavy forward primer. The double star (**) represents the constant heavy reverse primer.

6.4 Results

6.4.1 Anti-cTnI scAb construction

GoTaq® Flexi DNA polymerase and Platinum® High Fidelity DNA polymerase were used throughout the construction of this anti-cTnI scAb. Initially, the $MgCl_2$ concentration for each PCR was optimised. $MgCl_2$ optimisation allows for optimal yield with greatest specificity. The yield is influenced by activity of the *Taq* polymerase and the magnesium ion-dependent incorporation of dNTPs, which also affects the specificity of primer for the template. The PCR products for each region were resolved on 1.5% (w/v) agarose gels.

6.4.2 Optimisation of $MgCl_2$ concentration and large-scale amplification of the constant heavy region using chicken cDNA.

GoTaq® Flexi DNA polymerase was used for the amplification of the constant heavy region (C_H). GoTaq® Flexi DNA Polymerase offers robust amplification, and facilitates direct-to-gel analysis of PCR products. Two reaction buffers, Green and colourless GoTaq® Flexi Buffers, are supplied with the kit. Both buffers contain a compound that increases sample density, allowing samples to sink easily into the wells of agarose gels and making it possible to load reactions directly onto a gel after amplification. The 5X Green GoTaq® Flexi Buffer contains two dyes (blue and yellow) that separate during electrophoresis to monitor migration progress. The colourless buffer is used when direct fluorescence or absorbance readings are required without prior purification of the amplified DNA. The forward and reverse primers used for this PCR were designed to incorporate a constant heavy overlap tail (represented by a blue line in Figure 6.89) and S*pe*I (represented by a green circle, outlined in orange) and S*fi*I (represented by a black circle in Figure 6.89) restriction sites. In order to obtain a sufficient quantity of genetic material, a $MgCl_2$ concentration gradient was employed in this PCR. Three mM $MgCl_2$ provided the strongest amplification of the C_H region, at ~400bp. The result from this amplification also indicates the presence of primer dimers (bands below the 200bp marker in the ladder). Primer dimers are common by-products identified in most PCR reactions. They consist of primer molecules that have attached to each other because of strings of complementary bases in the primers. As a result, the DNA polymerase can amplify the primer dimer, leading to competition for PCR reagents, thus potentially reducing

or inhibiting amplification of the target DNA sequence. Physical-chemical optimization of the PCR system can reduce the production of primer dimers i.e., changing the concentrations of primers, magnesium chloride, nucleotides, ionic strength and temperature of the reaction. The amplification of target DNA in this PCR was sufficient despite the presence of primer dimers, hence, no further optimisation was required. Subsequently, large-scale amplification was completed, followed by gel extraction and purification.

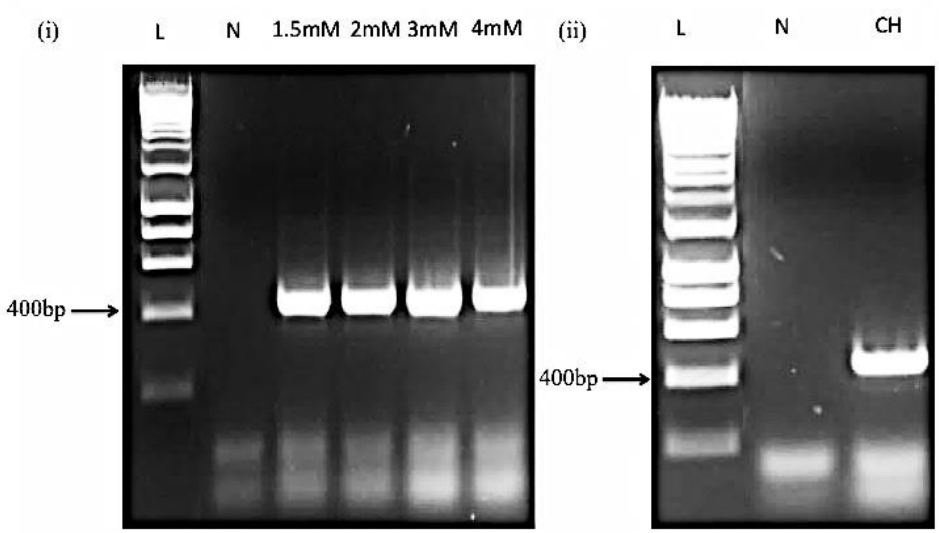

Figure 6.90. Optimisation of the amplification of the constant heavy region from cDNA.

(i) *Visualisation of the effect of $MgCl_2$ concentration for the amplification of the constant heavy (C_H) region on a 1.5% (w/v) agarose gel. The amplification of the constant heavy region from chicken cDNA was initially optimised by magnesium chloride titration. The 1Kb DNA Hyperladder 1, as represented by L in both (i) and (ii), allowed approximation of DNA fragment size.*

(ii) *$MgCl_2$-optimised large-scale amplification of the constant heavy region. Negative control reactions represented by N in both (i) and (ii) for each PCR were made up of all the necessary PCR components without template DNA. Both negative controls showed no non-specific bands, therefore, no contamination occurred throughout this amplification. Bands present in the negative sample below the 200bp mark are primer dimers.*

6.4.3 Optimisation and amplification of the anti-cTnI scFv using a cTnI Ab clone.

In the next stage, a number of optimisations were carried out in order to obtain specific amplification of the anti-cTnI scFv while reducing the amount of non-specific

bands. GoTaq® Flexi DNA polymerase was used initially for this amplification. Optimisation of the $MgCl_2$ concentration was carried out varying the magnesium concentration from 1.5mM – 4mM using an annealing temperature of 56 °C. The PCR products from this experiment were resolved on a 1.5% (w/v) agarose gel. While the results show that the appropriate band at approximately 800bp (450bp for V_H and 350bp for V_L) was obtained a number of other non-specific bands were present. Hence, Platinum® *Taq* DNA Polymerase High Fidelity was applied in order to attempt to reduce the volume of contaminating bands. Platinum® *Taq* DNA polymerase requires the inclusion of $MgSO_4$ in the PCR. Platinum® *Taq* DNA polymerase is a high fidelity enzyme mixture composed of recombinant *Taq* DNA polymerase, *Pyrococcus species* GB-D polymerase, and Platinum® *Taq* Antibody (Innis, 1988; Barnes, 1994). *Pyrococcus species* GB-D polymerase possesses a proofreading ability by virtue of its 3' → 5' exonuclease activity. Mixing the proofreading enzyme with *Taq* DNA polymerase increases fidelity approximately six times more than that of *Taq* DNA polymerase alone, and it allows amplification of simple and complex DNA templates over a large range of target sizes. The enzyme mixture is provided with an optimised buffer that improves enzyme fidelity and amplification of difficult templates. The forward and reverse primers used for the amplification of the scFv were designed to incorporate a pelB (represented by a dotted purple line in Figure 6.91) and constant heavy overlap tail, in addition to a BamHI restriction site into the construct.

Optimisation of the $MgSO_4$ concentration was carried out for the amplification of the anti-cTnI scFv using the Bi_C_(V_L-V_H)_F and C_FAB_V_H-R primers with an annealing temperature of 58 °C (suggested by the manufacturer's guidelines). The $MgSO_4$ concentration was varied from 1.5 - 4mM. The results from this experiment were visualised on a 1.5% (w/v) agarose gel. From the results obtained 2mM $MgSO_4$ was identified as the optimum concentration. However, further optimisation was required in order to achieve cleaner amplification of the scFv.

An annealing temperature gradient was completed using 2mM $MgSO_4$ from 51– 56 °C. These min and max temperatures were chosen according to the manufacturers' guidelines. The results, resolved on a 1.5% (w/v) agarose gel, show that optimum amplification of the scFv was achieved using an annealing temperature of 56 °C. A

$MgSO_4$ optimisation experiment was repeated using the optimised annealing temperature in order to ensure that 2mM remained as the optimum magnesium concentration. The results from this experiment were resolved on a 1.5% (w/v) agarose gel. Two mM was again identified as the optimum magnesium concentration. Optimised large-scale amplification was then carried out, followed by gel extraction and purification.

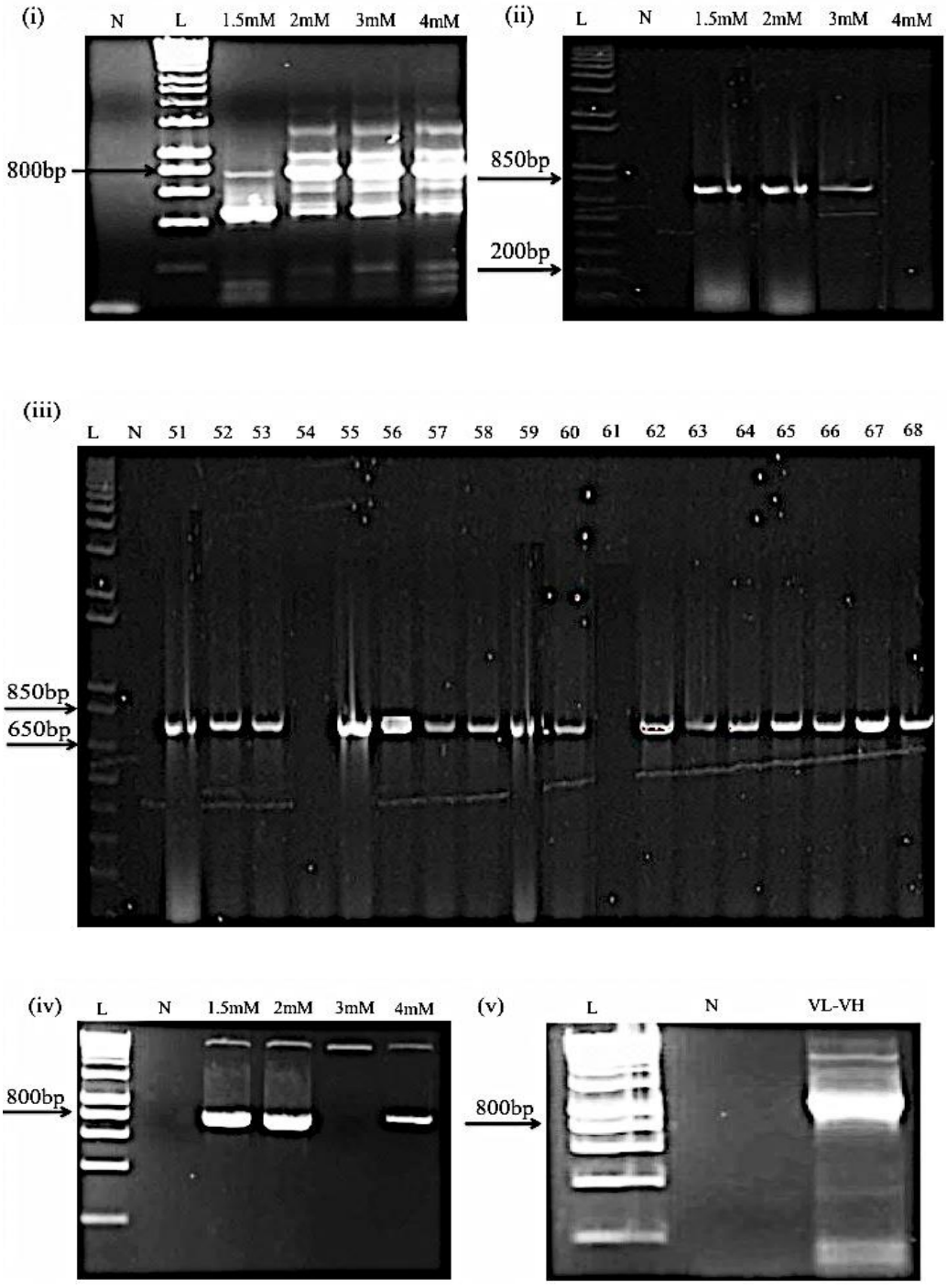

Figure 6.91. Optimisation and large-scale amplification of the anti-cTnI scFv antibody.

(i) *Optimisation of $MgCl_2$ concentration for the amplification of the anti-cTnI scFv from 1.5 – 4mM on a 1.5% agarose gel (w/v).*

(ii) *Optimisation of the $MgSO_4$ concentration from 1.5 – 4mM using an annealing temperature of 58 °C.*

(iii) *Annealing temperature gradient for the amplification of the anti-cTnI scFv from 51–68 °C.*

(iv) *Optimisation of the $MgSO_4$ concentration from 1.5 – 4mM using an annealing temperature of 56 °C.*

(v) *$MgSO_4$-optimised large-scale amplification of V_L-V_H scFv. The V_L-V_H amplicon was observed at ~800bp. Negative control (N) reactions run for all samples, containing the necessary PCR components in the absence of DNA, showed no contaminating bands. The DNA ladder in each image is represented by the letter L.*

6.4.4 Optimisation and amplification of the anti-cTnI scAb

Platinum® High Fidelity DNA polymerase was used for the overlap of the anti-cTnI scFv with the constant heavy region. Optimisation of the $MgSO_4$ concentration was carried out as before by varying the $MgSO_4$ concentration from 1.5 – 4mM. It is clear from the results obtained on a 1.5% (w/v) agarose gel that 3mM $MgSO_4$ provided the strongest scAb amplification at ~1200bp (V_L-V_H scFv = ~ 800bp, C_H = ~ 400bp). $MgSO_4$-optimised large-scale amplification of the anti-cTnI scAb was then carried out. The correct size amplicon (~ 1200bp) was isolated by gel extraction and purified as per the manufacturers' guidelines.

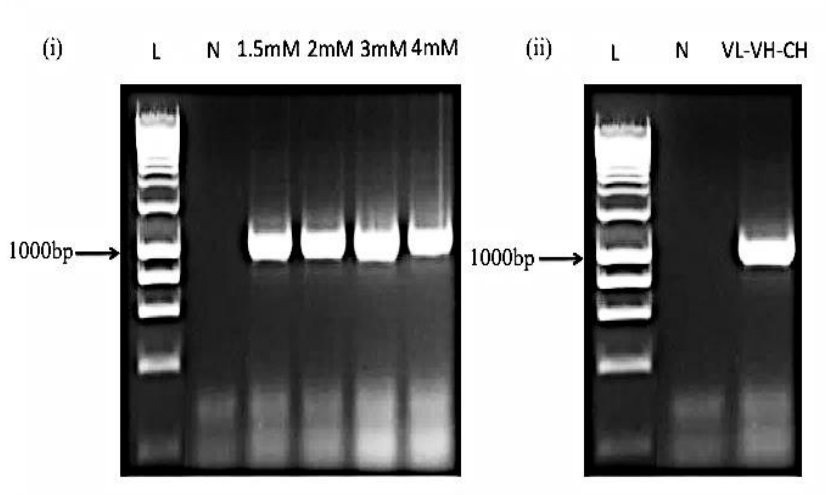

Figure 6.92. Optimisation and amplification of the anti-cTnI scAb construct.

(i) *Visualisation of the effect of $MgSO_4$ concentration for the amplification of the V_H-V_L-C_L region on a 1.5% (w/v) agarose gel. The amplification of the anti-cTnI scAb was initially optimised by varying the $MgSO_4$ concentration, followed by large-scale amplification.*

(ii) *Large-scale amplification using 3mM $MgSO_4$. The 1Kb DNA Hyperladder allowed approximation of DNA fragment size (~1200bp). The negative control consisting of the necessary PCR components in the absence of DNA run for both (i) and (ii) showed no contaminating bands.*

6.4.5 Anti-MPO scAb construction

There were a number of additional PCR steps involved in the construction of the anti-MPO scAb in order to re-orientate the anti-MPO scFv from the traditional V_L-V_H format to a V_H-V_L format in order to allow the overlap extension of the variable light region with the constant light region. Firstly, the V_H and V_L regions were amplified individually using an anti-MPO Ab clone (supplied by Dr. Stephen Hearty). The purified variable domains were then incorporated in equimolar ratios into the SOE product corresponding to the scFv fragment (approximately 800bp) using the Bi_C_(V_H-V_L)_V_H_F and C_FAB_VK-R primers. An additional PCR was then carried out in order to overlap the re-orientated anti-MPO scFv with the constant light region (C_L) using the Bi_C_(V_H-V_L)_V_H_F and C_FAB_C_L-R2-short primers. GoTaq® Flexi DNA polymerase, Platinum® *Taq* DNA polymerase High Fidelity and Phusion® *Taq* High-Fidelity DNA polymerase were used throughout the construction of this scAb.

6.4.6 Optimisation of $MgCl_2$ concentration and large-scale amplification of the constant light region using chicken cDNA.

GoTaq® Flexi DNA polymerase was used for the amplification of the C_L region. The primers used to amplify the constant light domain were designed to incorporate a constant light (represented by a red line in Figure 6.90) and pelB overlap tail, in addition to an X*ba*I restriction site. $MgCl_2$ concentration was varied from 1.5 – 4mM. From the results obtained on a 1.5% (w/v) agarose gel a $MgCl_2$ concentration of 3mM was found to produce the strongest amplification at approximately 350bp. Large-scale amplification was carried out.

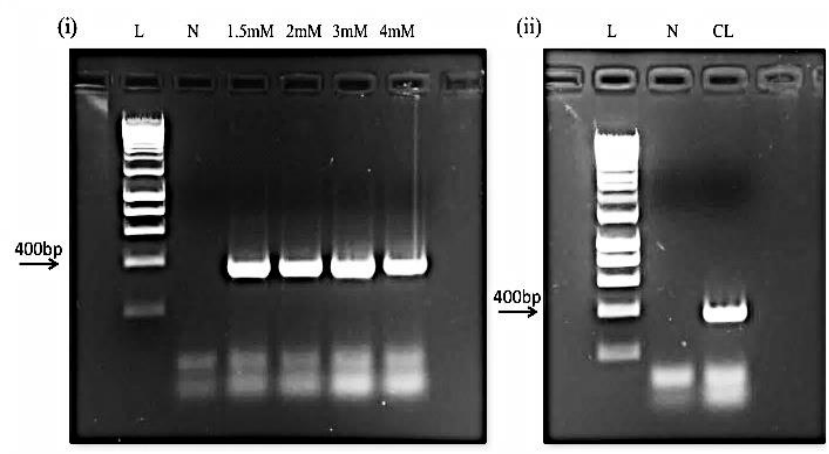

Figure 6.93. Optimisation of the amplification of the constant light region from cDNA.

(i) *Visualisation of the effect of $MgCl_2$ concentration for the amplification of the constant light region on a 1.5% (w/v) agarose gel. The amplification of the constant light region from chicken cDNA was initially optimised by varying the $MgCl_2$ concentration form 1.5 - 4mM. The 1Kb DNA Hyperladder 1 allowed approximation of DNA fragment size (~350bp).*

(ii) *$MgCl_2$-optimised large-scale amplification of the constant light region. The negative control (N) for each PCR in the absence of template DNA showed no non-specific bands. The position of the 400bp band in the ladder varies in each image due to the voltage and time applied to resolve each gel.*

6.4.7 Optimisation and amplification of the variable domains.

The next step in the construction of this scAb was to amplify the variable domains using an anti-MPO Ab clone (supplied by Dr. Stephen Hearty) and Platinum® *Taq* DNA polymerase (High Fidelity). Optimisation of the $MgSO_4$ concentration was carried out for both the V_H and V_L region, using Bi_C_(V_H-V_L)_V_H_F and C_(V_H-

V_L)_V_H_R primers for V_H and C_(V_H-V_L)_VK_F and C_FAB_VK-R primers for V_L. The primers applied for the amplification of the V_H domain were designed to incorporate a linker overlap tail (represented by a lined box in Figure 6.90) to allow the overlap extension of this domain with the V_L. S*ac*I and S*fi*I (represented by a black circle in Figure 6.90) restriction sites were also included. The primers used to amplify the V_L domain were designed to include the linker overlap tail, in addition to, a C_L overlap tail. The PCR products for each variable domain were resolved on 1.5% (w/v) agarose gels. These indicated similar yield, shown by discrete-specific band formation at approximately 450bp for V_H and 350bp for V_L. Large-scale reactions were carried out for both the V_H and V_L, followed by gel extraction and purification. The large-scale reactions were visualised on 1.5% (w/v) agarose gels.

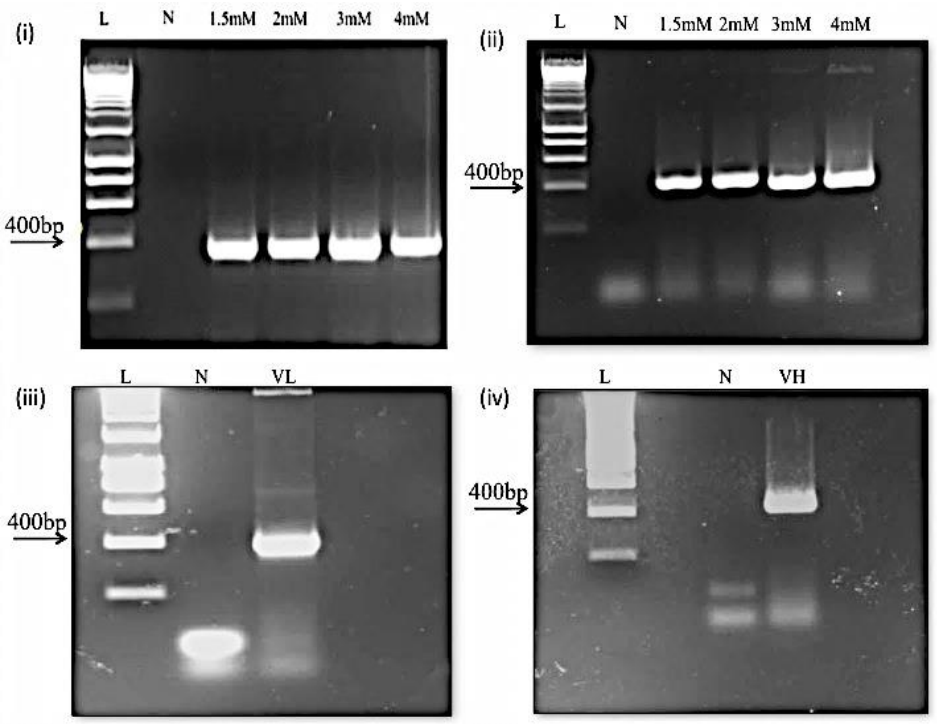

Figure 6.94. Optimisation and amplification of the V_H and V_L regions using an anti-MPO Ab clone.

(i) *Optimisation of the $MgSO_4$ concentration for the V_L region on a 1.5% (w/v) agarose gel. 4mM MgSO4 was determined to be the optimum concentration.*

(ii) *Optimisation of the $MgSO_4$ concentration for the V_H region on a 1.5% (w/v) agarose gel. 3mM was found to be the optimum magnesium concentration for the amplification of V_L.*

(iii) *A large-scale reaction was carried out for the variable light domain and visualised on 1.5% agarose (w/v) gels.*

(iv) *A large-scale reaction was carried out for the variable heavy domain and visualised on 1.5% agarose (w/v) gels. The position of the 400bp band in the ladder varies in each image due to the voltage and time applied to resolve* each gel.

6.4.8 Optimisation and amplification of the V_H-V_L format anti-MPO scFv.

The variable domains, purified through gel extraction, were incorporated in equimolar ratios into a SOE-PCR. Platinum Taq DNA polymerase High Fidelity was initially used for this overlap as it allowed specific amplification of both the V_H and V_L regions. $MgSO_4$ optimisation was carried out varying the concentration from 1.5mM – 4mM. The PCR products from this experiment were resolved on a 1.5% (w/v) agarose gel. Although, specific amplification was obtained at approximately 800bp, a

number of non-specific bands were present in each sample. To overcome this an alternative high fidelity buffer was used. Phusion® DNA polymerase offers both high fidelity and robust performance, and thus can be used for all PCR applications. Its unique structure, a novel *Pyrococcus*-like enzyme fused with a processivity-enhancing domain, increases fidelity and speed. Phusion® DNA Polymerase is an ideal choice for cloning and can be used for long or difficult amplicons. With an error rate >50-fold lower than that of *Taq* DNA Polymerase and 6-fold lower than that of *Pyrococcus furiosus* DNA Polymerase, Phusion® is one of the most accurate thermostable polymerases available. Phusion® DNA Polymerase possesses 5′→ 3′-polymerase activity, 3′→ 5′-exonuclease activity and will generate blunt-ended products. There are two possible reaction buffers for PCR reactions using Phusion® *Taq* polymerase, 5X Phusion GC buffer and 5X Phusion HF buffer, although, the error rate of the HF buffer (4.4×10^{-7}) is lower than that in the GC buffer (9.5×10^{-7}).

Optimisation of the $MgCl_2$ concentration was carried out by varying the concentration as before from 1.5mM – 4mM. Three percent (v/v) DMSO was also included in this PCR in order to reduce the presence of non-specific bands (3% (v/v) DMSO is the optimum DMSO concentration to use in a PCR according to manufacturers' guidelines). Four mM $MgCl_2$ provided the strongest amplification of the anti-MPO scFv at approximately 800bp (V_H = ~ 450bp and V_L = ~350bp). The PCR products for this experiment and subsequent large-scale amplification were resolved on 1.5% (w/v) agarose gels.

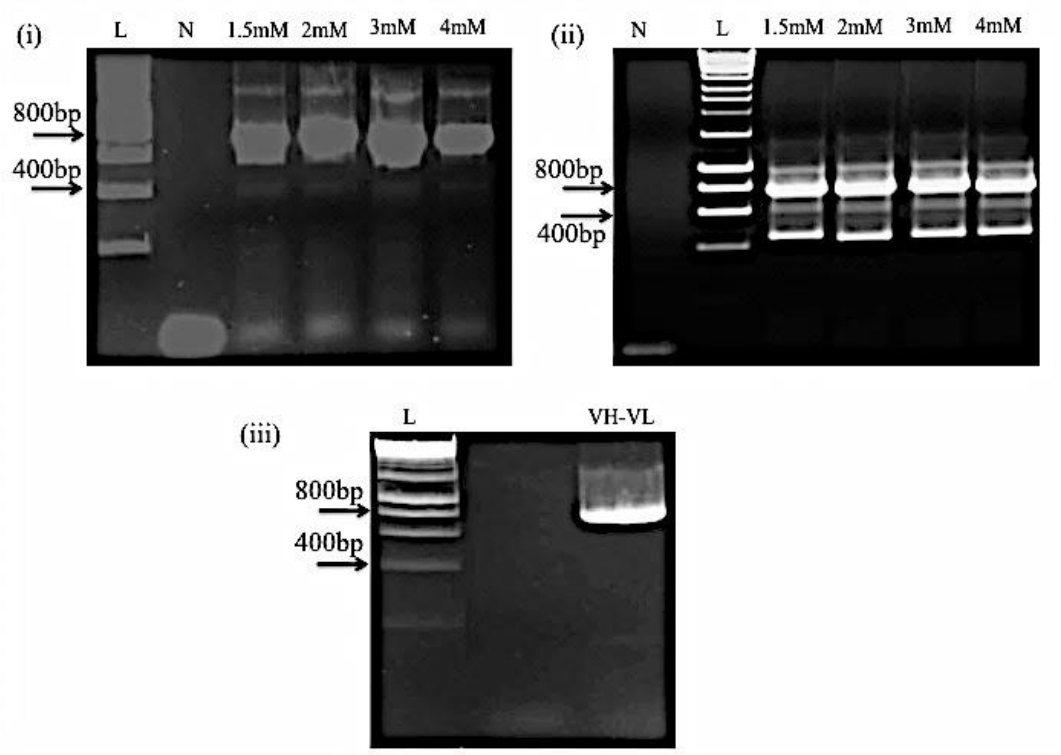

Figure 6.95. Optimisation and large-scale amplification of the anti-MPO scFv.

(i) *Optimisation of $MgSO_4$ concentration for the amplification of the anti-MPO scFv from 1.5 – 4mM on a 1.5% (w/v) agarose gel using Platinum® Taq DNA polymerase High Fidelity.*

(ii) *Optimisation of the $MgCl_2$ concentration for the amplification of the anti-MPO scFv from 1.5 – 4mM using Phusion® High Fidelity DNA polymerase.*

(iii) *$MgCl_2$-optimised large-scale amplification of V_H-V_L. The V_H-V_L amplicon was observed at ~800bp when using Phusion® DNA polymerase. Negative control (N) reactions consisting of all the necessary PCR components in the absence of DNA run for all three amplifications showed no contaminating bands. The ladder used was a Hyperladder 1 (Bioline), which is represented by L in each image.*

6.4.9 Optimisation of the $MgCl_2$ concentration and large-scale amplification of the anti-MPO scAb construct.

Phusion DNA polymerase High Fidelity was used for the overlap of the V_H-V_L anti-MPO scFv and the constant light region using the Bi_C_(V_H-V_L)_V_H_F and C_FAB_C_L-R2 primers and 3% (v/v) DMSO. The $MgCl_2$ concentration for this reaction was varied from 1.5 - 4mM. Three mM $MgCl_2$ provided the strongest amplification at approximately 1200bp (V_H-V_L = ~ 800bp and C_L = ~ 400bp) with the

least amount of non-specific amplification. $MgCl_2$-large-scale amplification was carried out. Resolution of the PCR products for both $MgCl_2$ optimisation and subsequent large-scale amplification was carried out on 1.5% (w/v) agarose gels. Negative control reactions run in the absence of template DNA showed that no non-specific products were amplified.

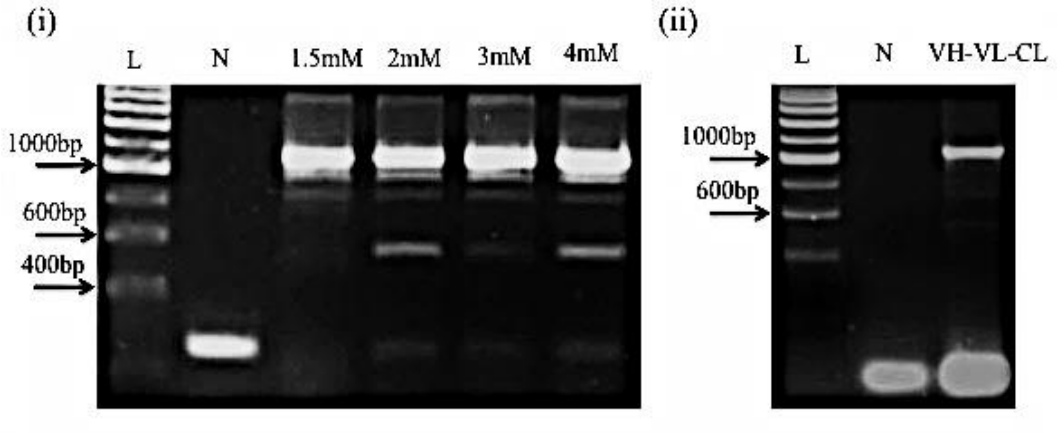

Figure 6.96. Optimisation of the V_H-V_L-C_L amplification.

(i) *Optimisation of the $MgCl_2$ concentration for the overlap of the V_H-V_L scFv with the constant light region.*

(ii) *$MgCl_2$-optimised large-scale amplification of the anti-MPO scAb. PCR products were resolved on 1.5% (w/v) agarose gels. Negative reactions (N) run for both PCRs consisting of all the necessary PCR components in the absence of template DNA contained no contaminating bands. The Bioline DNA Hyperladder 1 is represented by L in this Figure. In both Figures the 1000bp band is located on the gel. The amplification of the scAb was successful showing a clear band at ~1200bp in the gel.*

6.4.10 Optimisation and amplification of the anti-cTnI x anti-MPO bsAb

The final step in the construction of this bispecific antibody was to overlap the two constructs. In order to obtain a sufficient band at approximately 2400bp (V_L-V_H-C_H = ~ 1200bp and V_H-V_L-C_L = ~ 1200bp) several optimisation experiments were carried out. Platinum® *Taq* DNA polymerase High Fidelity and DreamTaq were both used in order to overlap the two scAb constructs but these experiments were unsuccessful. Thus, Phusion® DNA polymerase was applied for this overlap PCR. Optimisation of the DMSO and $MgCl_2$ concentration was carried out using Phusion® *Taq* DNA polymerase. The DMSO concentration ranges varied from 2 - 5% (v/v) while the

$MgCl_2$ concentration was varied from 1.5 – 4mM. A DMSO concentration of 4% (v/v) with a $MgCl_2$ concentration of 3mM was found to give optimum amplification at 2400bp on a 1% (w/v) agarose gel. DMSO-$MgCl_2$-optimised large-scale amplification was carried out.

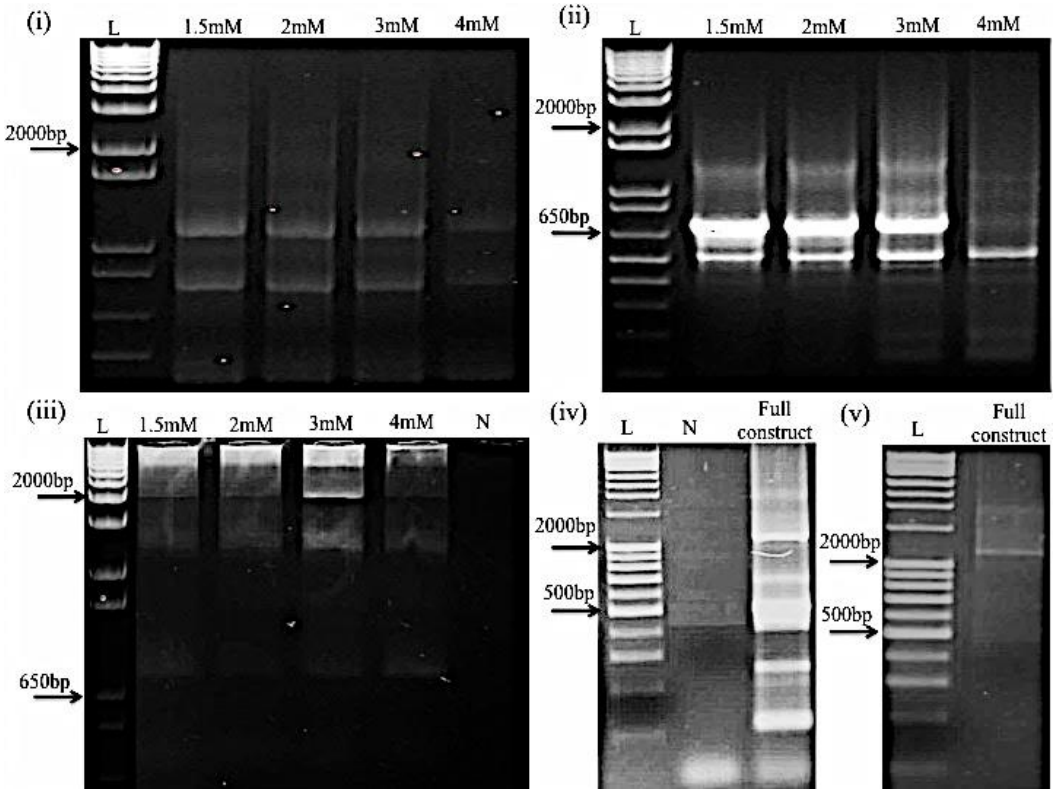

Figure 6.97. Amplification of the anti-cTnI x anti-MPO bispecific antibody.

(i) *Optimisation of $MgSO_4$ concentration for the amplification of anti-cTnI x anti-MPO bsAb using Platinum® Taq DNA polymerase High Fidelity.*

(ii) *Optimisation of the $MgCl_2$ concentration for the amplification of anti-cTnI x anti-MPO bsAb using DreamTaq.*

(iii) *Optimisation of the DMSO and $MgCl_2$ concentration for the amplification of the anti-cTnI x anti-MPO bsAb using Phusion® Taq DNA polymerase. DMSO concentration was varied from 2-5% (v/v) while the $MgCl_2$ concentration was 1.5 – 4mM. 3mM $MgCl_2$ with 4% (v/v) DMSO provided the strongest amplification at approximately 2400bp.*

(iv) *DMSO-$MgCl_2$-optimised large-scale amplification of anti-cTnI x anti-MPO bispecific antibody using Phusion® DNA polymerase.*

(v) *Purified full construct resolved on a 1% (w/v) agarose gel.*

6.4.11 Completion of 'proof-of-concept' studies

The 'proof-of-concept' study for this bispecific antibody generation strategy was a collaborative effort. Initial antibody construction applying SOE-style PCR technology was completed as part of this project. Completion of the 'proof-of-concept' study is on-going for application in the generation of a prostate cancer-specific bispecific

antibody. The work described in this chapter shows the successful generation of a 2400bp product (Figure 6.99), thus completing the first step in the 'proof-of-concept' study and the overall aim of this chapter. The next step in the 'proof-of-concept' study should involve cloning this construct into an expression vector and suitable expression host. Optimisation of expression to ensure maximum expression output will be essential followed by purification of the expressed construct. A standard IMAC purification would be suitable if the construct is cloned into a pComb His-tagged vector allowing straightforward one-step purification. The key to proving the success of this bispecific antibody generation strategy is to complete functional testing and characterisation of the bispecific antibody expressed and purified. Some potential characterisation approaches are presented in the following section.

6.5 Chapter discussion, conclusion and future direction of the bispecific antibody generation strategy

Bispecific antibody generation is becoming an integral part of research world-wide focusing on the improvement of current diagnostic assays and treatment approaches and striving to introduce novel technologies. A bispecific/bifunctional strategy was devised for implementation in a number of projects in Professor Richard O' Kennedy's Lab. Through personal communication it was decided that the expertise of antibody library construction obtained from work on this project would be implemented for the initial 'proof-of-concept' studies for this bispecific antibody generation approach. This strategy involved optimizing conditions for the amplification of two scAbs and the incorporation of SOE-PCR technology, which has been described previously (chapter 4 and 5) for the construction of anti-SFRP-2 and anti-PSMA scFv libraries, for the generation of a 2400bp product corresponding to the overlap of two scAbs.

A growing repertoire of different bsAb fragment formats have been described that lack some or all of the antibody constant domains. For many bsAb fragments the heavy and light chains are connected with short peptide linker sequences that can allow efficient expression of the bsAb in a single host cell. However, further engineering may be necessary to minimize the formation of unwanted antibody species during production (Tan *et al.*, 1998 and Igawa *et al.*, 2010) or to improve the stability of bsAb fragments (Perchiacca & Tessier, 2012). ScFv fragments (Spiess *et al.*, 2015) are the most commonly used building blocks in the generation of bsAbs. The bispecific antibody construction approach presented in this chapter involves two scAbs. A scAb is traditionally generated by incorporating a constant chain to the C-terminal of the V_L region of a scFv fragment. As demonstrated in chapter 4 of this thesis, the expression of scFv antibodies in *E. coli* is not always successful and can in some cases lead to very low antibody yield. Reformatting the scFv antibodies to scAbs dramatically improved the expression of both anti-SFRP-2 and anti-PSMA antibodies. In addition, scAbs can improve the stability of the antibody fragment. Taking these results into consideration the scAb construct comprised more appealing characteristics over the scFv construct and hence was incorporated into the bsAb generation approach presented here.

The first step in the construction of this bispecific antibody was to build the anti-cTnI and anti-MPO scAbs. This construction involved numerous optimisation studies to ensure correct formation of the scAb constructs. Similar to protein expression, when amplifying a gene of interest, optimisation studies may need to be completed in order to achieve clean and precise amplification. The main issue encountered in this study was the amplification of non-specific bands alongside the amplified target band. Non-specific amplification can occur for a number of reasons such as the use of inappropriate parameter settings for amplification. The annealing temperature, extension and initial denature times may need to be optimised. Additionally, in some cases, the presence of contaminating bands in a PCR can be as a result of inappropriate $MgCl_2$/$MgSO_4$ (depending on the buffer applied), primer or dNTP concentrations. Previous studies have demonstrated that the most important parameters for efficient, specific amplification of target DNA were denaturation time and temperature, stringent annealing temperatures and magnesium chloride concentration (Harris & Jones, 1997).

Post optimisation studies the anti-cTnI scAb was generated in the V_L-V_H-C_H format, and the anti-MPO in the V_H-V_L-C_L format successfully. ScFv fragments can be constructed in either V_H–V_L or V_L–V_H orientations (Lu *et al.*, 2004). However, the V domain orientation can sometimes impact antigen binding (Lu *et al.*, 2004; Albrecht *et al.*, 2006). The orientation of the two scFv antibodies presented in this chapter may need to be optimised in future 'proof-of-concept' studies if issues with expression or target binding arise. Using SOE-PCR technology the two scAbs were successfully overlapped to generate the target 2400bp product completing this section in the 'proof-of-concept' study.

The next step in the 'proof-of-concept' study will be to clone the anti-cTnI x anti-MPO bsAb into an appropriate expression vector and commence optimisation of expression of this bispecific antibody. The *E. coli* host would be ideal in terms of cost and time for expressing this construct, however, substantial time should be spent on optimizing the conditions used for expression. Temperature and IPTG concentration for induction should be critically assessed over a range of time points. Addition of agents such as glycerol or magnesium to the expression medium may be necessary to improve expression. The bispecific antibody could be purified by virtue of the 6xHis

tag encoded on the pComb3x vector (if this vector is used for cloning) by immobilised metal affinity chromatography (IMAC), allowing for one-step purification, post-optimisation of purification conditions. The type of buffer, buffer pH and temperature used throughout the purification of this construct should be optimised.

The key to proving the success of this bispecific antibody generation strategy will be the binding studies completed on the purified product. ELISA and SPR analysis should be implemented at this stage of the 'proof-of-concept' studies in order to determine the ability of this bispecific antibody to bind its target antigens. Figure 6.100, below, illustrates some potential approaches that could be taken with ELISA formats to characterise the bispecific antibody. The two scAbs (anti-cTnI scAb and anti-MPO scAb) generated should be expressed and purified along-side the bispecific antibody construct and used as positive controls in this analysis. In addition to having specificity for two different cardiac markers this bispecific antibody has a self-signalling capability, which is advantageous for analysis in an ELISA format, as the anti-MPO Ab is an anti-peroxidase antibody, thus addition of myeloperoxidase/peroxidase with associated substrate can provide a self-signalling bispecific antibody.

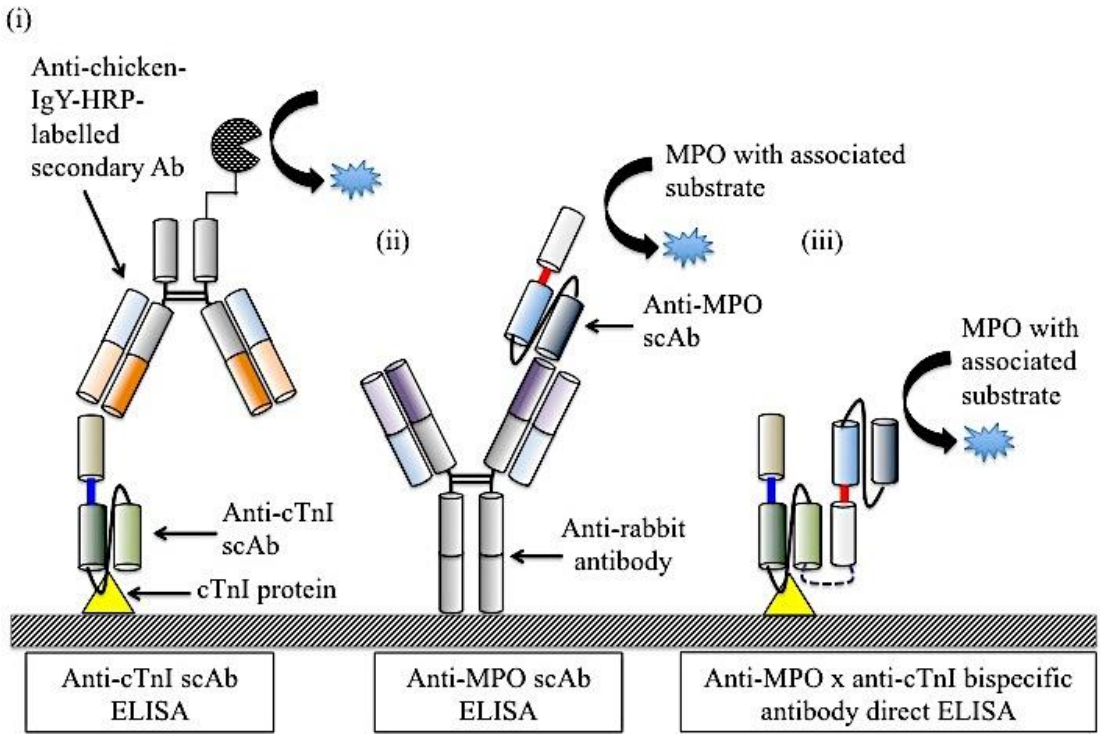

Figure 6.98. ELISA analysis for functionality testing of the bispecific antibody.

(i) *Indirect ELISA to test the functionality of the anti-cTnI scAb. The cTnI antigen is represented by a yellow triangle. An ELISA plate will be coated with 1µg of cTnI antigen. The plate will be blocked using 5% (w/v) Milk marvel in PBS. Varying dilutions of the anti-cTnI scAb will then be used to probe the cTnI antigen. A HRP-labelled anti-chicken-IgY- secondary antibody will then be applied to the plate. After incubation at 37 °C for 1 hour a 3,3',5,5'-Tetramethylbenzidine (TMB) substrate will be applied to the plate. The absorbance will be read at 450 nm.*

(ii) *ELISA to test the functionality of the anti-MPO scAb. The MPO antibody clone used to generate the anti-MPO scAb was raised in rabbit. Therefore, to test the functionality of the anti-MPO scAb the ELISA plate will be coated with an anti-rabbit antibody. The plate will be blocked using 5% (w/v) Milk marvel in PBS. The anti-MPO scAb will then be added to the ELISA plate. Incubate the plate at 37 °C for 1 hour. As mentioned previously, the anti-MPO Ab is an anti-peroxidase antibody, thus addition of myeloperoxidase/peroxidase with associated substrate can provide a self-signalling bispecific antibody (i.e. the addition of a secondary labelled antibody is not required). The absorbance will be read at 450 nm post addition of appropriate substrate.*

(iii) *ELISA to test the functionality of the anti-cTnI x anti-MPO bispecific antibody. An ELISA plate will be coated with 1µg of cTnI antigen.*

(iv) *The plate will be blocked using 5% (w/v) Milk marvel in PBS. Varying dilutions of the anti-cTnI x anti-MPO bispecific antibody will then be used to probe the cTnI antigen. After incubation at 37 °C for 1 hour a peroxidase substrate will then be added and the absorbance read at 450 nm.*

SPR screening can provide a wealth of information for any antibody screening/binding analysis. For the 'proof-of-concept' studies, it is essential to determine whether this bispecific antibody is capable of binding both targets simultaneously. The most appropriate assay set-up for screening this bispecific antibody using SPR would be to capture the purified antibody using an anti-HA immobilized chip surface. Some SPR machines such as the ProteOn™ XPR36 System have a function that allows a 'delayed injection' option. Using this option both targets could be assessed at the same time. CTnI could be injected first, followed by MPO or vice-versa. Negative and positive controls should be included in this screening to ensure true binding is observed. Figure 6.101 and 6.102 below outlines suggested approaches for future screening. Other screening approaches could be applied using SPR systems, such as the Biacore, that do not facilitate this 'delayed injection' option. One of the analytes could be immobilised on to the Biacore chip surface using amine-coupling chemistry. The bispecific antibody could be captured by the immobilised analyte. The second analyte could then be introduced to determine if two binding events take place.

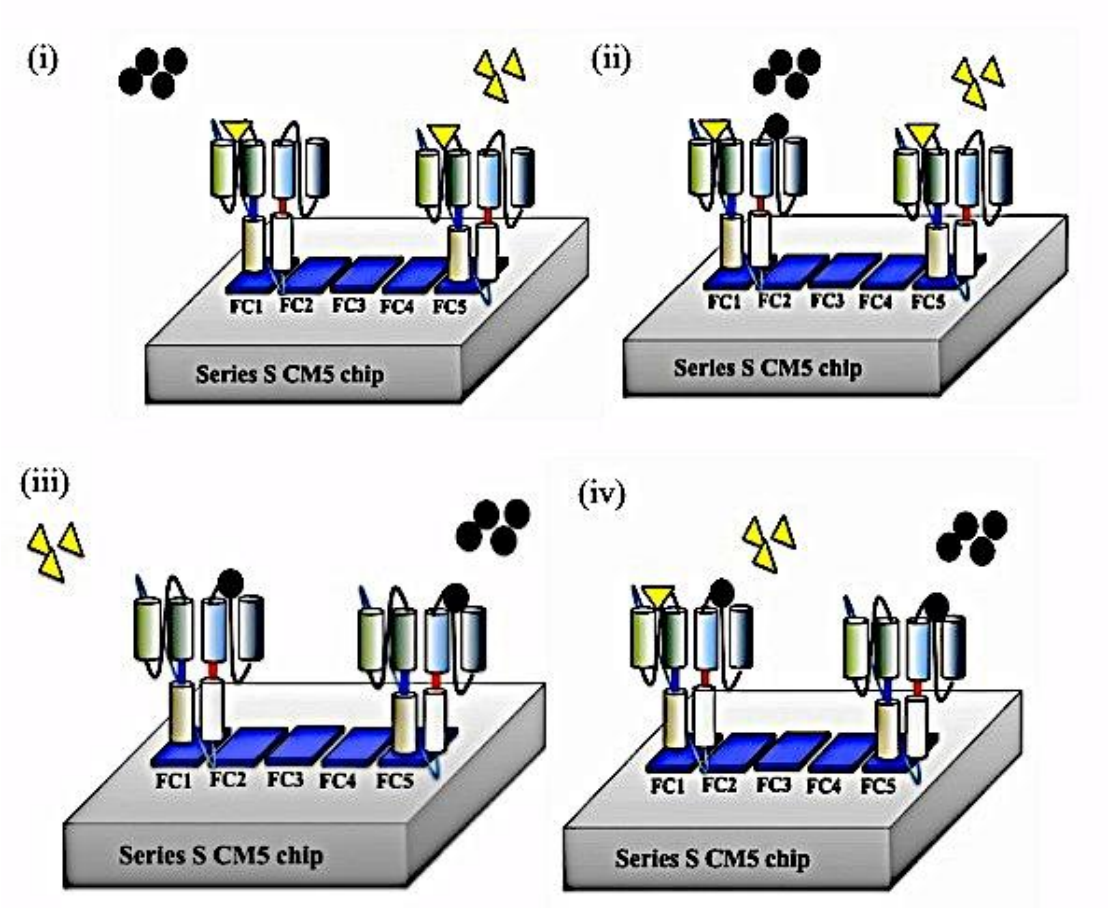

Figure 6.99. SPR analysis for functionality testing of the anti-cTnI x anti-MPO bispecific antibody.

(a) *Analysis of the binding interaction between the anti-HA captured bispecific antibody and its target analytes using a 'delayed injection' option, where cTnI (yellow triangle) is injected first (i), followed by MPO (ii) (black circle).*

(b) *Analysis of the binding interaction between the anti-HA captured bispecific antibody and its target analytes using a 'delayed injection' option, where MPO (black circle) is injected first (iii), followed by cTnI (iv) (yellow triangle).*

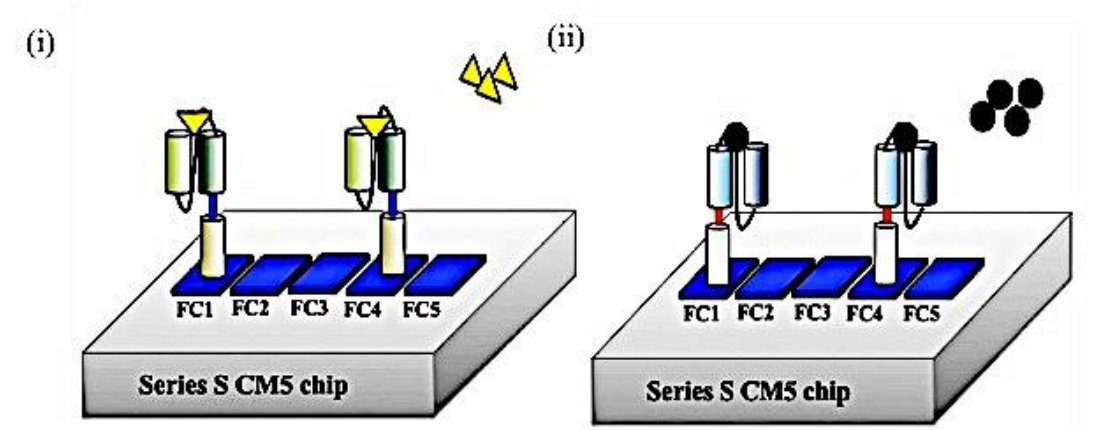

Figure 6.100. SPR analysis for functionality testing of the control mono-specific anti-MPO and anti-cTnI scAb.

(a) *Anti-cTnI scAb capture on anti-HA surface, followed by anti-cTnI analyte (cTnI protein (yellow triangle) capture.*

(b) *Anti-MPO scAb capture on anti-HA surface, followed by anti-MPO analyte (MPO protein (black circle) capture. Using an anti-HA immobilized chip surface, the monospecific antibodies could be captured followed by the addition of varying concentration of the target analyte to assess binding interaction. The information obtained from this control screen could then be compared to the bispecific screen to determine the effect that reformatting the monospecific antibodies into bispecific antibodies has had on binding affinity to cTnI or MPO.*

There are many additional screening options available for characterizing this bispecific antibody. The approaches presented here are suggestions, which could be adapted or expanded to include a more vigorous screen. If the 'proof-of-concept' studies behind this strategy are successful, this approach could ameliorate the shortcomings associated with traditional approaches to produce bispecific antibodies. This generation strategy could allow for the production of homogenous batches of bispecific antibodies, ameliorating the problem of heterogeneity associated with some current approaches, such as 'knob-into-hole' (Klein *et al.*, 2012). Additionally, this construct is readily available for expression in *E. coli*, which as described previously in chapter 3 of this thesis, is a quick and cost-effective approach to recombinant antibody expression. If the pComb expression vector is applied, purification could be achieved using IMAC, as the pComb vector contains a His-tag. This strategy is flexible and could be applied to generate a plethora of disease-specific bispecific

antibodies with the potential to improve current diagnostic approaches and downstream aid in the treatment of disease.

Chapter 7
Overall conclusion

7.1 Overall summary and conclusion

Prostate cancer is a significant cause of illness and death in males. Current detection strategies, described in detail in section 1.5 of this thesis, do not detect the disease at an early stage and cannot distinguish aggressive versus non-aggressive prostate cancer leading to over-treatment of the disease and associated morbidity. Thus, prostate cancer is a disease that would benefit from the discovery and development of novel biomarkers for both early detection and treatment selection. This thesis shows the generation of two antibodies against key markers in prostate cancer, namely SFRP-2 and PSMA for use in IHC that could assist in early diagnosis of the disease and provide critical information for stratification and clinical intervention.

The main aim of chapter 3 was to design and produce a high quality recombinant SFRP-2 protein, of the required quality for use in an effective immunisation campaign, using a novel expression system. SFRP-2 is a novel marker in prostate cancer and paucity of quality antigen and antibody is an impediment to research on this marker. In general, the available reagents are polyclonal in nature and are not targeted to specific histochemically relevant epitopes. Polyclonal antibodies are known for batch-to-batch variation and this can, in turn, affect IHC results. A monoclonal or recombinant antibody would provide more specific and reliable SFRP-2 detection by IHC for clinical utilization. Previous studies completed emphasize the problems encountered in producing a soluble SFRP-2 protein suitable for immunisation. The formation of inclusion bodies was the basis for the insolubility of the generated SFRP-2 protein. Inclusion bodies usually form within prokaryotic systems when heterologous eukaryotic proteins are being over-expressed. In this chapter, current advances in recombinant protein expression technologies that enhance soluble eukaryotic protein expression in *E. coli* were explored, however, each system has its limitations. Using a novel expression system, developed 'in-house', which takes advantage of the favourable expression and solubility profile of fatty acid binding protein (FABP), highly soluble chimeric SFRP-2 protein was produced. This protein was subsequently utilised as a primary antigen to induce a SFRP-2-specific immune response in an avian host. Due to the novelty of this work an IDF was generated and is now being examined for patentability with initial responses indicating significant potential and possible commercial value.

In chapter 4, the most common epigenetic aberrations in PCa are highlighted, and the effects that these aberrations have on genes that regulate the WNT signalling pathway, such as SFRP-2, is described. SFRP-2 had been previously found to be hypermethylated in prostate cancer following Quantitative Methylation-Specific PCR analysis. Furthermore, IHC results propose SFRP-2 to be a useful marker for predicting prognosis and biochemical recurrence particularly in patients with advanced prostate cancer (O'Hurley *et al.*, 2011). However, further methylation and immunohistochemical analysis is required on more PCa tumours with follow-up to highlight the importance of SFRP-2 as a marker for the disease. Successful generation and characterisation of anti-SFRP-2 polyclonal antibodies and two recombinant SFRP-2 fragment antibody formats was achieved using high-throughput assay screening with 'state-of-the-art' multiplexed surface-plasmon resonance-based instrumentation and standard analytical techniques. Furthermore, issues associated with scFv expression in *E. coli* were overcome by reformatting the fragment antibody to a scAb. Reformatting the scFv to a scAb significantly improved the expression of this antibody providing a purified antibody yield ~60 times greater than that obtained for the scFv. The purified antibody is currently being utilized in IHC analysis of prostate tissue in Beaumont Hospital to further address the significance of this marker for PCa detection.

Prostate–specific membrane antigen (PSMA) is the most well-established, highly specific prostate epithelial cell membrane marker known. Pathology studies, carried out to date, indicate that virtually all-prostate cancers express PSMA. Moreover, PSMA expression increases progressively in higher-grade cancers, metastatic disease and castration-resistant prostate cancer (CRPC). The ability to selectively detect PSMA overexpression in prostate cancer offers the promise for new avenues of diagnosis and earlier therapeutic intervention for patients at risk of an aggressive metastatic stage of the disease. Over the past two decades, PSMA is a molecular target whose use has resulted in some of the most productive work toward imaging and treating prostate cancer, in addition to diagnosing the disease. Chapter 5 of this thesis describes the successful generation of a recombinant anti-PSMA scAb, which was demonstrated to match the performance of current commercially available polyclonal antibodies in ELISA, WB and dot blot. An IHC investigation of prostate tissue is underway employing this antibody in Beaumont Hospital.

IHC plays as important role in diagnostic surgical pathology of the prostate. Given the advantageous characteristics associated with SFRP-2 and PSMA as biomarkers for PCa, employing these antibodies into routine IHC analysis for the diagnosis of this disease, singly, or in combination with other PCa-specific antibodies, such as AMACR or STEAP, may significantly improve PCa diagnosis and the ability to distinguish between benign and malignant disease.

Bispecific antibodies are quickly becoming an integral part of antibody research. A bispecific/bifunctional antibody generation strategy was devised in Professor O' Kennedy's lab that utilizes PCR technology and primer design for the overlap of two scAb constructs with specificity for two different targets. Throughout this project, PCR technology was applied for cloning, antibody construction and reformatting and gene amplification. Taking this into consideration, it was decided that the skills gained throughout this work would be utilized to complete the first part in the 'proof-of-concept' studies for this bispecific antibody generation strategy, which was to build the bispecific antibody using PCR technology and specifically designed primers. This was successfully achieved, leading to the generation of a 2400bp product corresponding to two scAbs overlapped. The second part in the 'proof-of-concept' studies in currently underway in a separate project for the generation of an anti-prostate cancer-specific bispecific antibody.

In conclusion, this thesis has presented a novel expression system that overcomes issues associated with current recombinant protein expression technologies and allows the production of highly soluble recombinant protein. Furthermore, the successful generation of two PCa-specific antibodies was achieved, which could aid in predicting prognosis and biochemical recurrence particularly in patients with advanced prostate cancer. The concept of bispecific antibodies for therapeutic and diagnostic application is introduced and the first step in the 'proof-of-concept' studies behind a novel bispecific antibody generation approach was successfully investigated. All of the technologies generated, and the associated antibodies, are now being further evaluated for their diagnostic and commercial potentials.

Chapter 8 Appendices

8. 1 General molecular methods

8.1.1 Ethanol precipitation of DNA

Ethanol precipitation was carried out at -20 °C overnight (O/N) or at -80 °C for two hours depending on the time requirement. To a 1.5mL Eppendorf tube containing the DNA to be precipitated the following was added:

0.1X the volume of sodium acetate, pH5.2

2X the volume of 100% (v/v) molecular grade ethanol (ice cold)

1µL glycogen

Tubes were agitated and placed at the relevant temperature for the desired length of time. The DNA was then pelleted by centrifugation at 12,000 x g for 30 minutes at 4 °C, washed once with 70% (v/v) ice-cold ethanol as above, air dried and resuspended in an appropriate volume of molecular grade water (mol. G. H_2O).

8.1.2 Agarose electrophoresis

Various percentage gels (w/v) were prepared by weighing out the desired amount to give the required percentage in grams of agarose. The weighed agarose was added to 1X Tris-acetate-EDTA (TAE) (pH 8.3) buffer and heated in a microwave (2-3 minutes) until dissolved, allowed to cool, before adding 1X SYBR™ safe DNA gel stain. The gel was then allowed to set in the appropriate gel box with the inserted comb. Gel electrophoresis was carried out using a Bio-Rad PowerPac™ HC in 1X TAE-buffer (pH 8.3) at 85V for between 45 and 60 minutes. Once sufficient separation of the DNA band of interest was achieved, the run was stopped and the band was excised.

8.1.3 DNA Gel extraction and purification using Nucleo-spin gel and PCR clean up kit

The required DNA agarose gel was prepared and run as described in section 8.1.2. The DNA bands were then cut out of the gel under UV light using a scalpel. The cut out agarose was placed into a clearly labelled 1.5mL Eppendorf tube and weighed. For every 100mg of agarose 200µL of Buffer NTI was added. The agarose was then allowed to dissolve at 50°C, vortexing every 2-3 minutes (agarose should dissolve in 15-20 minutes). A NucleoSpin® gel and PCR clean up column was placed into a 2mL collection tube, and the sample loaded on to the column. The sample was centrifuged for 30 seconds at 11,000 x g. The flow-through was discarded and 700µL of Buffer NT3 was applied to the column to wash the silica membrane. The column was

centrifuged as before and the supernatant was discarded. The NucleoSpin® gel and PCR clean up column was placed into a fresh 1.5mL Eppendorf tube clearly labelled. 15-30µL of Buffer NE or deionised H_2O (previously heated to 70°C) was added to the column. The samples were incubated at room temperature for 2-3 minutes, followed by centrifugation at 11,000 x g for 1 minute. Purified DNA was obtained as the eluate. The concentration of eluted DNA was then obtained using a Nanodrop.

8.1.4 LB Agar plate preparation

The components necessary for LB agar plate preparation (section 2.1.4) were weighed out and added to a 1L bottle. The top of the bottle was covered with aluminum foil and labeled with autoclave tape. The medium was then autoclaved according to the autoclave's specifications. After autoclaving, the solution was allowed to cool to ~55°C. The appropriate concentration of antibiotic was added to the solution once cooled and ~20mL of LB agar was poured per 10cm polystyrene petri dish. The lids were placed on the plates and the plates were allowed to cool for 30-60 minutes (until solidified). The bottom of each plate was labeled with the antibiotic used, the date and sealed with parafilm at 4°C.

8.1.5 DNA and protein quantification using a NanoDrop 1000 UV-Vis Spectrophotometer

1 µL of molecular grade water was applied to initialize the spectrophotometer followed by 1µL of the blank (the 'blank' is the solution that the DNA or protein sample was re-suspended in, but with no DNA added. 1 - 2 µL of the DNA/protein sample was placed onto the pedestal. The lid was closed and then the sample was analysed once the measure button was clicked. A concentration value was then obtained. The purity of each sample using the NanoDrop is measured under the 260/280 column. A good purity ranges from 1.80-2.00.

8.1.6 Isolation of low-copy plasmids using a NuceloSpin® Plasmid DNA purification kit

An overnight culture (10mL super broth (SB) supplemented with relevant antibiotic) was prepared from a single transformed colony, or glycerol stock, and incubated at 37°C at 220rpm overnight. Bacterial cells were collected by centrifugation at 4,000 x g at 4°C for 30 minutes. The plasmid was then purified using NucleoSpin® Plasmid kit, as per manufacturers' guidelines. Purified plasmid was resuspended in 15µL of molecular grade H_2O and quantified using the NanoDrop ND^{TM} 1000 nucleic acid DNA 50-setting.

8.1.7 NuceloBond® Xtra high-copy plasmid purification (Midi, Maxi)

A starter culture of 5mL of SB medium was inoculated with a single colony picked from a freshly streaked agar plate containing the appropriate antibiotic and incubated overnight at 37°C, 220rpm. The cells were pelleted through centrifugation at 4,000 x g for 10 minutes at 4°C. The plasmid was then purified using NucleoBond® Xtra Mid, as per manufacturers' guidelines. Purified plasmid was resuspended in a final volume of 15µL mol. G. H_2O and quantified using the NanoDrop ND^{TM} 1000 nucleic acid DNA 50-setting.

8.1.8 Preparation of bacterial cell stocks

Cell stocks were prepared in either 1.5mL tubes or 96-well culture plates dependent on the number required.

1.5mL tubes: overnight cultures (2mL SB with relevant antibiotic and 1% (v/v) glucose) were grown at 37°C while shaking at 220rpm and the cells were collected by centrifugation at 4,000 x g at 4°C for 30 minutes. The supernatant was then discarded and the cells were resuspended in SB medium containing 10% (v/v) glycerol and 100µL was transferred to a number of 1.5mL (screw thread) tubes and stored long term at -80°C.

96 well plates: overnight cultures (150µL SB with relevant antibiotic and 1% (v/v) glucose) were grown at 37°C while shaking at 220rpm. The following day 25µL was removed for expression in 96-deep well plates and replaced with 25µL of 80% (v/v) glycerol and placed at -80°C for long term storage.

8.1.9 Lysis of E. coli cells for small-scale analysis and purification

Cells were lysed using 1mg/mL lysozyme, from chicken egg white, in a 1X PBS solution. The cell pellets were thawed at 37°C in a water bath and resuspended with 1/10 the culture volume (small-scale) or 2.5mL per 1g cell paste (large-scale) lysis buffer (1mg/mL lysozyme in 1X PBS). The samples were left at room temperature (RT) for 30 minutes. Post incubation the cells were alternated from -80°C to 37°C for a minimum of three times. Cellular debris was collected by centrifugation at 12,000 x g at 4°C for 30 minutes and the supernatant separated.

8.1.10 Sonication of E. coli cells for purification

Cells were grown and expressed as described previously. The pellets stored at -80°C were thawed at 37°C and resuspended in the appropriate equilibration buffer (~10mLs) and placed on ice. The sample kept on ice was sonicated at an amplitude of

40% for 6 second pulses for 3 minutes. The cell extract was centrifuged at 12,000 x g for 30 minutes. The supernatant was filtered through a 0.20µm syringe filter and this was the filtered lysate used for purification.

8.1.11 Restriction enzyme digest of DNA

Restriction enzyme digestion is a commonly used technique for molecular cloning and is also used to quickly check the identity of a plasmid by diagnostic digest.

In a sterile PCR tube the following were combined:

- DNA (~1-5µg for molecular cloning)
- Restriction Enzyme(s)
- Buffer
- BSA (if recommended by manufacturer)
- Molecular grade H_2O up to total volume

The sample was mixed gently by pipetting up and down and incubated at the appropriate temperature (dependent on the restriction enzymes being used) for the recommended time (as per manufactures' guidelines). Once complete the digested sample was ethanol precipitated as described previously and purified through gel extraction.

8.1.12 Ligation of DNA into a vector

The final step in the construction of a recombinant plasmid is connecting the insert DNA (gene or fragment of interest) into a compatibly digested vector backbone. This is accomplished by covalently connecting the sugar backbone of the two DNA fragments. This reaction, called ligation, is performed using the T4 DNA ligase buffer and enzyme. The DNA ligase catalyzes the formation of covalent phosphodiester linkages, which permanently join the nucleotides together. After ligation, the insert DNA is physically attached to the backbone and the complete plasmid can be transformed into bacterial cells for propagation.

Ligations were carried out with a number of vector and inserts using the general ligation reaction conditions (Table 5). Standard ligation reaction components are outlined below in Table 5.

Table 64. General ligation reaction components.

Component	Ligation	Control
Vector DNA	Xµg	X µg
Insert DNA	Yµg	-----
Ligation buffer	1X	1X
Mol. G. H_2O	To 100µL	To 100µL
T4 DNA Ligase (400U/µL)	10U/µg	10U/µg

This reaction was then incubated at room temperature (RT) overnight. The following day the PCR tube containing the ligation reaction was transferred to a PCR cycler and incubated at 65°C for 20 minutes in order to deactivate the reaction. The sample was then ethanol precipitated overnight as described in section 8.1.1 followed by a gel extraction and purification (section 8.1.3).

8.1.13 Transformation using chemically competent cells

Chemically competent cells were removed from the -80°C freezer and thawed on ice (for approximately 5 minutes). LB agar plates (containing the appropriate antibiotic) were taken out of the fridge (4°C) and placed in a 37°C incubator to pre-heat. 1-2µL of DNA (usually 10pg to 100ng) was added to a sterile 1.5mL tube containing 50µL of the appropriate chemically competent cells. The competent cell/DNA mixture was then placed on ice for 30 minutes.

The transformation tube was then heat shocked by placing the bottom 1/2 to 2/3 of the tube into a 42°C water bath for 30-60 seconds (42 seconds is usually ideal, but this varies depending on the competent cells being used). The tubes were placed back on ice for a further 5 minutes. 250µl of pre-warmed SOC medium (without antibiotic) was added to the tube and the sample was then placed in the 37°C shaking incubator for 1 hour (outgrowth) (***Note:*** *This outgrowth step allows the bacteria time to generate the antibiotic resistance proteins encoded on the plasmid backbone so that they will be able to grow once plated on the antibiotic containing agar plate. This step is not critical for Ampicillin resistance but is much more important for other antibiotic resistances.)* The transformation was then added onto a 10cm LB agar plate containing the appropriate antibiotic. 100µL and 10µL of the transformation was

added to two separate agar plates. Once dry the plates were incubated at 37°C overnight.

8.1.14 Optimisation of recombinant protein expression

Optimisation of the expression of recombinant proteins was undertaken at numerous stages throughout this work. Various lengths of induction time and Isopropyl-β-D-thiogalactoside (IPTG) concentrations were evaluated with a number of different constructs, and temperatures. An overview of the experimental layout of these expression studies are described by the generic flow contained in Figure 6.103 with refinements or modifications to the protocol noted in the relevant sections. The samples taken were centrifuged after an appropriate induction time and the pellets were retained at -80°C until required. The cell pellets were treated similarly during lysis and loaded onto SDS-PAGE gels for side-by-side comparison with an un-induced cell control (0 mM IPTG).

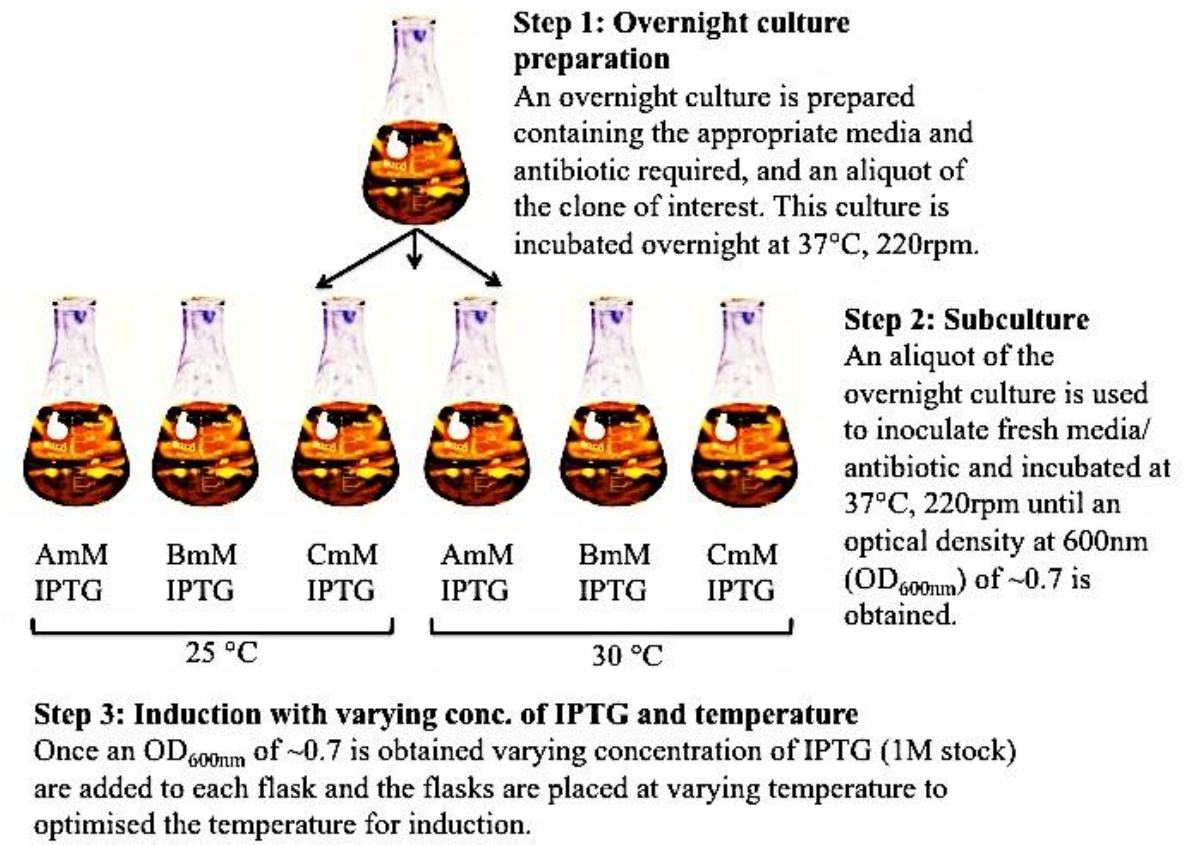

Figure 8.101. Generic time course experiment for expression of recombinant proteins.

A single colony or glycerol stock was inoculated in 10mL of medium containing antibiotic and grown overnight at 37°C, while shaking at 220rpm. The overnight culture was sub-cultured into fresh medium containing antibiotic and grown until an optical density at 600nm (OD_{600nm}) of ~0.7 was reached. Once an OD_{600nm} of 0.7 was obtained the flasks were split and varying concentrations of IPTG was added to each flask. Optimisation of induction length and temperature were then monitored simultaneously, in addition to optimisation of IPTG concentration. Visualisation of the results via SDS-PAGE and Western Blotting (see section 8.1.16 and 8.1.17 for more information) allowed the identification of the optimum expression conditions.

8.1.15 Purification of produced recombinant proteins

Numerous purification strategies were undertaken throughout this work. The cells were grown and expressed as described in the relevant section and lysed, as described in section 8.1.9/8.1.10. The choice of buffers varied and specific buffers for particular purifications are contained within the relevant section. The buffer recipes for protein purification can be found in section 2.1.5.2.

His Bind Ni^{2+} charged resin (Novagen) slurry (1–2mL) was added to a 10mL chromatography column and allowed to settle, corresponding to a 0.5 – 1mL resin bed. The resin was washed thoroughly with 10mL of equilibration buffer (or 10-15 column volumes (CV)). 30µL of the unfiltered lysate was transferred to a sterile PCR tube and labelled unfiltered lysate for SDS page and Western Blot analysis. The remaining lysate was then passed through 0.45µm and 0.20µm syringe filters. A 30µL sample of this filtered lysate was then transferred to a sterile PCR tube and labelled filtered lysate (or FL). The cleared lysate was applied to the column and a sample of the flow through (F1) was retained for SDS-PAGE and Western blotting analysis. The column was washed with 10CV wash buffer (or a combination of wash buffers) and samples were retained for analysis (W1 up to W3). The retained protein was eluted with 4mL elution buffer into 1mL neutralisation buffer or 10 x 150µL neutralisation buffer in 1.5mL tubes. The 5mL eluted sample, or protein-containing samples, were buffer exchanged against PBS (with 0.02% (w/v) NaN_3) using a Vivaspin 6 column with an appropriate molecular weight cut-off. The protein content of the purified sample was determined using a NanoDrop™ 1000 and the protein was stored at -20°C in several aliquots clearly labelled. A sample of the pure protein, unfiltered lysate and filtered lysates, "flow-through" and washes were then analysed by SDS-PAGE and Western blotting (WB).

8.1.16 SDS-PAGE

Assessment of protein expression and purification steps were carried out by SDS-PAGE and western blot (WB) analysis using the buffers described in section 2.1.5.1.

Proteins were separated using 12.5% (w/v) SDS-PAGE gels to analyse purity and to determine the apparent molecular weight. The gel consisted of a resolving gel (12.5%) and a stacking gel (4.5%). These gels were left to polymerise between two clean glass plates. After the stacking gel was poured, a comb was inserted to make wells in preparation for loading of protein samples. The samples were prepared by adding appropriate volumes of 4X SDS loading buffer. A 20µg quantity of each protein sample in a total volume of 10µL or lysate diluted with loading buffer to 1X in a volume of 10µL, were prepared. The gels were placed in an electrophoresis apparatus (Bio-Rad) and submerged in electrophoresis buffer. A page ruler protein ladder and the protein samples were loaded to the wells. The apparatus was attached to a power supply and a voltage of 120V was applied to the gel for 60 minutes. The

gels were allowed to run until the tracker dye had reached the bottom of the gel. The gels were then removed and stained using Instant Blue (MyBio) and allowed to develop for ~ 1 hour. Protein bands began to appear after ~15 minutes. The Instant Blue dye was then washed off the gel using 1X PBS. The gels were imaged using a Biorad gel imager.

8.1.17 Western blotting

Where a western blot was required the SDS-PAGE gels were setup and run as described in section 8.1.16 with one SDS-PAGE gel being placed in western blot transfer buffer (section 2.1.5.1) in place of the Instant Blue stain. The gel, absorbent paper and nitrocellulose (cut to the gel dimension) were all placed in the transfer buffer for 10 minutes.

A four-layer sandwich consisting of filter paper, nitrocellulose membrane, SDS-PAGE gel and filter paper was assembled (outlined in Figure 8.104). All the air bubbles were removed by carefully rolling each of the layers with a disposable plate spreader. Proteins were transferred from the acrylamide gel to the nitrocellulose using a Trans-Blot Semi-Dry Transfer cell (Bio-Rad) at 15V for 21 minutes. The nitrocellulose membrane was then carefully transferred into a large weighing boat containing 20mL of 5% (w/v) PBS milk marvel (PBSM) solution and blocked for 1 hour at RT or overnight at 4°C with agitation. Any excess blocking solution was removed from the membrane via three washes with PBST and three washes with PBS. Next the blocked membrane was incubated with 10mL of 1% (w/v) PBSM solution with 0.05% (v/v) tween20 (PBSTM) containing a 1 in 2,000 dilution of the relevant primary antibody for 1 hour at RT with gentle agitation. The antibody solution was then discarded and the membrane washed in PBST (x3) and PBS (x3). The membrane was then probed with a secondary antibody if necessary. The secondary antibody was prepared and incubated in the same manner as the primary. Development of the specific complex was achieved via the addition of liquid 3, 3', 5, 5'-tetramethylbenzidine (TMB) substrate and stopped by multiple washes with distilled water (dH_2O).

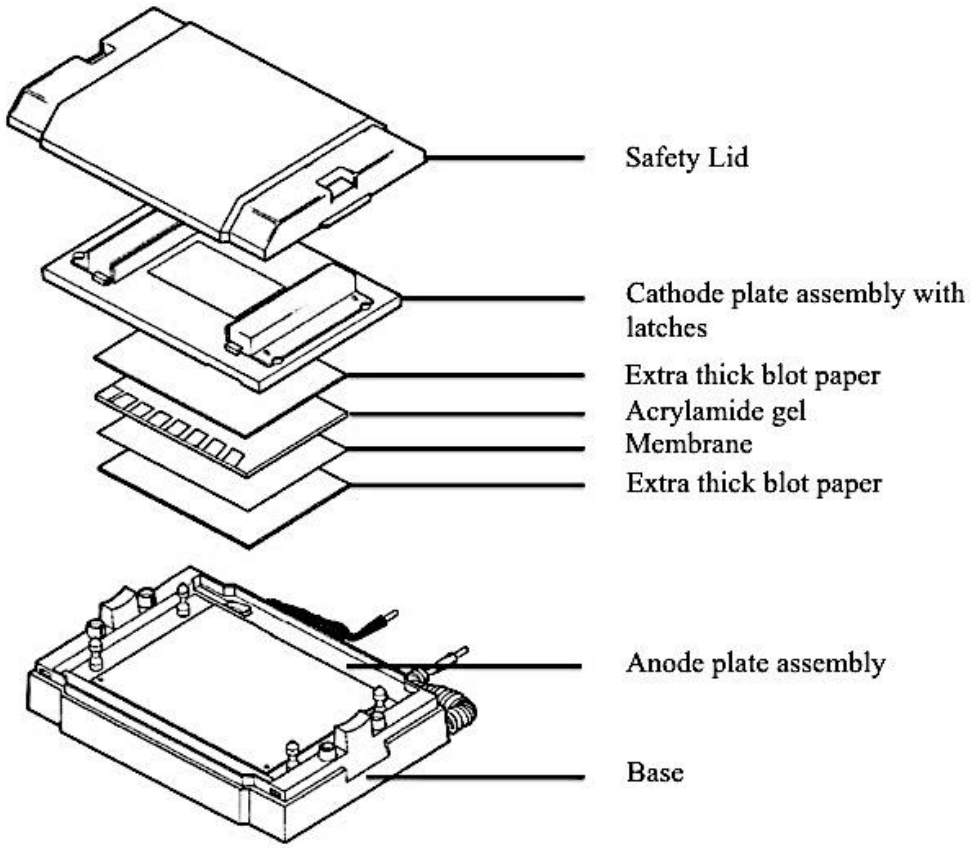

Figure 8.102. Schematic representation of a semi-dry transfer system used for western blotting.

(Adapted from http://www.bio-rad.com)

8.1.18 Biacore 4000 maintenance

The Biacore instrument was cleaned using a 'super desorb' program at 25°C. This method involves cleaning the unit thoroughly prior to starting an assay. It is imperative that the instrument is properly sanitized to remove any residual protein, thus, ensuring high-quality data and complete confidence in results generated. A maintenance chip was docked and primed 5 times with desorb solution 1 (0.5 % (v/v) sodium dodecyl sulphate (SDS)), once with water, 5 times with desorb solution 2 (50mM glycine, pH 9.5), and finally, 5 times with water.

Bibliography

Bibliography

Ahmad, Z. A., Yeap, S. K., Ali, A. M., Ho, W. Y., Alitheen, N. B., Hamid, M. scFv antibody: principles and clinical application. *Clin. Dev. Immunol.* 2012; 2012: 980250.

Akhtar, N. H., Pail, O., Saran, A., Tyrell, L., & Tagawa, S. T. Prostate-specific membrane antigen-based therapeutics. *Adv. Urol.* 2011; 2012: 973820.

Albany, C., Alva, A. S., Aparicio, A. M., Singal, R., Yellapragada, S., Sonpavde, G., Hahn, N. M. Epigenetics in prostate cancer. *Prostate Cancer.* 2011; 2011: 580318.

Albrecht, H., Denardo, G. L., & Denardo, S. J. Monospecific bivalent scFv-SH: effects of linker length and location of an engineered cysteine on production, antigen binding activity and free SH accessibility. *J. Immunol. Methods.* 2006; 310: 100-116.

Andris-Widhopf, J., Rader, C., Steinberger, P., Fuller, R., Barbas C.F. Methods for the generation of chicken monoclonal antibody fragments by phage display. *J Immunol Methods.* 2000; 242: 159-81.

Arnau, J., Lauritzen, C., Petersen, G. E., Pedersen, J. Current strategies for the use of affinity tags and tag removal for the purification of recombinant proteins. *Protein Expr. Purif.* 2006; 48: 1-13.

Auf der Maur, A., Escher, D., Barberis, A. Antigen-independent selection of stable intracellular single-chain antibodies. *FEBS Lett.* 2001; 508: 407-412.

Aus, G., Abbou, C. C., Bolla, M., Heidenreich, A., Schmid, H. P., van Poppel, H., Wolff, J., & Zattoni F. EAU guidelines on prostate cancer. *Eur. Urol.* 2005; 48: 546-51.

Bach, H., Mazor, Y., Shaky, S., Shoham-Lev, A., Berdichevsky, Y., Gutnick, D. L., Benhar, I. *Escherichia coli* maltose-binding protein as a molecular chaperone for recombinant intracellular cytoplasmic single-chain antibodies. *J. Mol. Biol.* 2001; 312: 79-93.

Balk, S. P., Ko, Y. J., & Bubley, G. J. Biology of prostate-specific antigen. *J. Clin. Oncol.* 2003; 21: 383-391.

Barbas, C. F., Burton, D. R., Scott, J. K., Silverman, G. J. Phage display: A laboratory manual, 1st Edition, 736 pp, Cold Spring Harbor Laboratory press, 2001.

Baumgart, L. A., Gerling, G. J., & Bass, E. J. Characterizing the range of simulated prostate abnormalities palpable by digital rectal examination. *Cancer Epidemiol.* 2010; 34: 79-84.

Beekman, J. M., Cooney, A. J., Elliston, J. F., Tsai, S. Y., Tsai, M. J. A rapid one-step method to purify baculovirus-expressed human estrogen receptor to be used in the analysis of the oxytocin promoter. *Gene.* 1994; 146: 285-289.

Ben Jemaa, A., Bouraoui, Y., Oueslati, R. Insight into the heterogeneity of prostate cancer through PSA-PSMA prostate clones: mechanisms and consequences. *Histol. Histopathol.* 2014; 29: 1263-1280.

Bernacki, K. D., Fields, K. L., Roh, M. H. The utility of PSMA and PSA immunohistochemistry in the cytologic diagnosis of metastatic prostate carcinoma. *Diagn. Cytopathol.* 2014; 42: 570-575.

Bird, C. R., & Thorpe, R. (2002) Purification of immunoglobulin Y (IgY) from chicken eggs, 1009-1011, In: Walker, J. M., Bird, C. R., Thorpe, R., Editors. The Protein Protocols Handbook, 2nd Edition, Humana Press.

Birch, J. R., & Racher, A. J. Antibody production. *Adv. Drug Deliv. Rev.* 2006; 58: 671-685.

Birtalan, S., Zhang, Y., Fellouse, F. A., Shao, L., Schaefer, G., & Sidhu, S. S. The intrinsic contributions of tyrosine, serine, glycine and arginine to the affinity and specificity of antibodies. *J. Mol. Biol.* 2008; 377: 1518-1528.

Borrebaeck, C. A. Antibodies in diagnostics - from immunoassays to protein chips. *Immunol. Today.* 2000; 21: 379-82.

Bostwick, D. G., Liu, L., Brawer, M. K., & Qian, J. High-Grade Prostatic Intraepithelial Neoplasia. *Rev. Urol*. 2004; 6: 171–179.

Bostwick, D. G., Pacelli, A., Blute, M., Roche, P., Murphy G. P. Prostate specific membrane antigen expression in prostatic intraepithelial neoplasia and adenocarcinoma: a study of 184 cases. *Cancer.* 1998; 82: 2256–2261.

Bouchelouche, K., Choyke, P. L., & Capala, J. Prostate Specific Membrane Antigen—A Target for Imaging and Therapy with Radionuclides. *Discov. Med.* 2010; 9: 55–61.

Bovolenta, J., Welsh, A., Agarwal, S., Killiam, E., Baquero, M., Hanna, J., Anagnostou, V., & Rimm, D. Antibody validation. *Biotechniques.* 2003; 48: 197-209.

Bovolenta, P., Esteve, P., Ruiz, J. M., Cisneros, E., & Lopez-Rios, J. Beyond Wnt inhibition: new functions of secreted frizzled-related proteins in development and disease. *J. Cell Sci.* 2008; 121: 737-746.

Brandão, J. G., Scheper, R. J., Lougheed, S. M., Curiel, D. T., Tillman, B. W., Gerritsen, W. R., van den Eertwegh, A. J., Pinedo, H. M., Haisma, H. J., de Gruijl, T. D. CD40-targeted adenoviral gene transfer to dendritic cells through the use of a novel bispecific single-chain Fv antibody enhances cytotoxic T cell activation. *Vaccine.* 2003; 21: 2268-2272.

Brawer, M. K., Meyer, G. E., Letran, J. L., Bankson, D. D., Morris, D. L., Yeung, K. K., & Allard, W. J. Measurement of complexed PSA improves specificity for early detection of prostate cancer. *Urology*. 1998; 52: 372-378.

Brischwein, K., Schlereth, B., Guller, B., Steiger, C., Wolf, A., Lutterbuese, R., Offner, S., Locher, M., Urbig, T., Raum, T., Kleindienst, P., Wimberger, P., Kimmig, R., Fichtner, I., Kufer, P., Hofmeister, R., da Silva, A. J., Baeuerle, P. A. MT110: a novel bispecific single-chain antibody construct with high efficacy in eradicating established tumours. *Mol. Immunol.* 2006; 43: 1129-1143.

Brooks, J. D., Weinstein, M., Lin, X., Sun, Y., Pin, S. S., Bova, G. S., Epstein, J. I., Isaacs, W. B., Nelson, W. G. CG island methylation changes near the GSTP1 gene in prostatic intraepithelial neoplasia. *Cancer Epidemiol. Biomarkers Prev.* 1998; **7**: 531-536.

Brownback, K. R., Renzulli, J., Delellis, R., & Myers, J. R. Small-cell prostate carcinoma: A retrospective analysis of five newly reported cases. *Indian J. Urol.* 2009: 25: 259-263.

Bühler, P., Wolf, P., Gierschner, D., Schaber, I., Katzenwadel, A., Schultze-Seemann, W., Wetterauer, U., Tacke, M., Swamy, M., Schamel, W. W., Elsässer-Beile, U. A bispecific diabody directed against prostate-specific membrane antigen and CD3 induces T-cell mediated lysis of prostate cancer cells. *Cancer Immunol. Immunother.* 2008; 57: 43-52.

Buhmann, R., Simoes, B., Stanglmaier, M., Yang, T., Faltin, M., Bund, D., Lindhofer, H., Kolb, H. J. Immunotherapy of recurrent B-cell malignancies after allo-SCT with Bi20 (FBTA05), a trifunctional anti-CD3 x anti-CD20 antibody and donor lymphocyte infusion. *Bone Marrow Transplant.* 2009; 43: 383-397.

Büssow, K., Scheich, C., Sievert, V., Harttig, U., Schultz J., Simon B., Bork, P., Lehrach, H., & Heinemann, U. Structural genomics of human proteins – target selection and generation of a public catalogue of expression clones. *Microb. Cell Fact.* 2005; 4: 21-34.

Butt, T. R., Edavettal, S. C., Hall, J. P., Mattern, M. R. SUMO fusion technology for difficult-to-express proteins. *Protein Expr. Purif.* 2005; 43: 1-9.

Byrne, J. C., Downes, M. R., O'Donoghue, N., O'Keane, C., O'Neill, A., Fan, Y., Fitzpatrick, J. M., Dunn, M., Watson, R. W. 2D-DIGE as a strategy to identify serum markers for the progression of prostate cancer. *J. Proteome Res.* 2009; 8: 942-957.

Byrne, H., Conroy, P. J., Whisstock, J. C., O'Kennedy, R. J. A tale of two specificities: bispecific antibodies for therapeutic and diagnostic applications. *Trends Biotechnol.* 2013; 31: 621-632.

Cairns, P., Esteller, M., Herman, J. G., Schoenberg, M., Jeronimo, C., Sanchez-Cespedes, M., Chow, N. H., Grasso, M., Wu, L., Westra, W. B., Sidransky, D. Molecular detection of prostate cancer in urine by GSTP1 hypermethylation. *Clin. Cancer Res.* 2001; 7: 2727-2730.

Cameron, E. E., Bachman, K. E., Myöhänen, S., Herman, J. G., Baylin, S. B. Synergy of demethylation and histone deacetylase inhibition in the re-expression of genes silenced in cancer. *Nat. Genet.* 1999; 21: 103-107.

Cardillo, T. M., Karacay, H., Goldenberg, D. M., Yeldell, D., Chang, C. H., Modrak, D. E., Sharkey, R. M., & Gold, D. V. Improved targeting of pancreatic cancer: experimental studies of a new bispecific antibody, pretargeting enhancement system for immunoscintigraphy. *Clin. Cancer Res.* 2004; 10: 3552-3561.

Catalona, W. J., Partin, A. W., Sanda, M. G., Wei, J. T., Klee, G. G., Bangma, C. H., Slawin, K. M., Marks, L. S., Leob, S., Broyles, D. L., Shin, S. S., Cruz, A. B., Chan, D. W., Sokoll, L. J., Roberts, W. L., Van Schaik, R. H. N., Mizrahi, I. A. A multicenter study of [-2]pro-prostate specific antigen combined with prostate specific antigen and free prostate specific antigen for prostate cancer detection in the 2.0 to 10.0 ng/mL prostate specific antigen range. *J. Urol.* 2011; 185: 1650-1655.

Cattamanchi, A., Smith, R., Steingart, K. R., Metcalfe, J. Z., Date, A., Coleman, C., Marston, B. J., Huang, L., Hopewell, P. C., & Pai, M. Interferon-gamma release assays for the diagnosis of latent tuberculosis infection in HIV-infected individuals: a systematic review and meta-analysis. *J. Acquir. Immune Defic. Syndr.* 2011; 56: 230-238.

Chames, P. & Baty, D. Bispecific antibodies for cancer therapy: the light at the end of the tunnel. *mAbs.* 2009; 1: 539-547.

Chan, P. K., Ng, K. C., Chan, R. C., Lam, R. K., Chow, V. C., Hui, M., Wu, A., Lee, N., Yap, F. H., Cheng, F. W., Sung, J.J., & Tam, J. S. Immunofluorescence assay for serologic diagnosis of SARS. *Emerg. Infect. Dis.* 2004; 10: 530-532.

Chen, Y. P., Qiao, Y. Y., Zhao, X. H., Chen, H. S., Wang, Y., & Wang, Z. Rapid detection of hepatitis B virus surface antigen by an agglutination assay mediated by a bispecific diabody against both human erythrocytes and hepatitis B virus surface antigen. *Clin. Vaccine Immunol.* 2007; 14: 720-725.

Cheng, Y. Y., Yu, J., Wong, Y. P., Man, E. P., To, K. F., Jin, V. X., Li, J., Tao, Q., Sung, J. J., Chan, F. K., Leung, W. K. Frequent epigenetic inactivation of secreted frizzled-related protein 2 (SFRP2) by promoter methylation in human gastric cancer. *Br. J. Cancer.* 2007; 97: 895–901.

Choo, A. B., Dunn, R. D., Boady, K. W., & Raison, R. L. Soluble expression of a functional recombinant cytolytic immunotoxin in insect cells. *Protein Expr. Purif.* 2002; 24: 338-347.

Chu, D. C., Chuang, C. K., Fu, J. B., Huang, H. S., Tseng, C. P., Sun, C. F. The use of real-time quantitative polymerase chain reaction to detect hypermethylation of the CpG islands in the promoter region flanking the GSTP1 gene to diagnose prostate carcinoma. *J. Urol*. 2002; 167: 1854-1858.

Clackson, T., & Lowman, H. B. (2007) Phage Display: A Practical Approach, pp. 332, Oxford University Press, Oxford.

Cochlovius, B., Kipriyanov, S. M., Stassar, M. J., Christ, O., Schuhmacher, J., Strauss, G., Moldenhauer, G., Little, M. Treatment of human B cell lymphoma xenografts with a CD3 x CD19 diabody and T cells. *J. Immunol.* 2000; 165: 888-895.

Conroy, P. J., Hearty, S., Leonard, P., & O'Kennedy, R. J. Antibody production, design and use for biosensor-based applications. *Semin. Cell Dev. Biol.* 2009; 20: 10-26.

Cosgrove, M. S., Boeke, J. D., & Wolberger, C. Regulated nucleosome mobility and the histone code. *Nat. Struct. Mol. Biol.* 2004; 11: 1037–1043.

Costa, S., Almeida, A., Castro, A., & Domingues, L. Fusion tags for protein solubility, purification and immunogenicity in *Escherichia coli*: the novel Fh8 system. *Front. Microbiol*. 2014; 5: 1-20.

Crawford, E. D., Ventii, K., Shore, N. D. *Oncology*. 2014; 28: 135-42.

Dabbs, D. *Immunohistology of the Prostate, Bladder, Testis and Kidney*, 2nd Edition, 509-610 pp, Diagnostic Immunohistochemistry, Elsevier, 2006.

Damber, J. E., & Aus, G. Prostate cancer. *Lancet* 2008; 371: 1710-1721.

Davis, G. D., Elisee, C., Newham, D. M., Harrison, R. G. New fusion protein systems designed to give soluble expression in *Escherichia coli*. *Biotechnol. Bioeng.* 1999; 65: 382-388.

Davis, J. L., Huang, L., Worodria, W., Masur, H., Cattamanchi, A., Huber, C., Miller, C., Conville, P. S., Murray, P., & Kovacs, J. A. Nucleic acid amplification tests for diagnosis of smear-negative TB in a high HIV-prevalence setting: a prospective cohort study. *PLoS One.* 2011; 6: e16321.

Demain, A. L., & Vaishnav, P. Production of recombinant protein by microbes and higher organisms. *Biotechnol. Adv.* 2009; 27: 297-306.

De Marco, V., Stier, G., Blandin, S., de Marco, A**.** The solubility and stability of recombinant proteins are increased by their fusion to NusA. *Biochem. Biophys. Res. Commun.* 2004; 322: 766-771.

De Marco, A., & De Marco, V. Bacteria co-transformed with recombinant proteins and chaperones cloned in independent plasmids are suitable for expression tuning. *J. Biotechnol.* 2004; 109: 45–52.

DeMarzo, A. M., Nelson, W. G., Isaacs, W. B., & Epstein, J. I. Pathological and molecular aspects of prostate cancer. *Lancet.* 2003; 361: 955-964.

Denekamp, J., Dasu, A., Waites, A. Vasculature and microenvironmental gradients: the missing links in novel approaches to cancer therapy. *Adv. Enz. Regul.* 1998; 38: 281–299.

Dettmar, K., Seitz-Merwald, I., Lindemann, C., Schroeder, P., Seimetz, D., Atz, J. Transient lymphocyte decrease due to adhesion and migration following catumaxomab (anti-EpCAM x anti-CD3) treatment *in vivo. Clin. Transl. Oncol.* 2012; 14: 376-381.

Diaw, L., Woodson, K., & Gillespie J. W. Prostate Cancer Epigenetics: A Review on Gene Regulation. *Gene Regul. Syst. Bio.* 2007; 1: 313–325.

di Guan C., Li P., Riggs P. D., Inouye H. Vectors that facilitate the expression and purification of foreign peptides in *Escherichia coli* by fusion to maltose-binding protein. *Gene.* 1988; 67: 21–30.

Dong, D., Liu, H., Xiao, Q., Li, R. Affinity purification of egg yolk immunoglobulins (IgY) with a stable synthetic ligand. *J. Chromatogr. B Analyt. Technol. Biomed. Life Sci.* 2008; 870: 51-4.

Douette, P., Navet, R., Gerkens, P., Galleni, M., Lévy, D., Sluse, F. E. *Escherichia coli* fusion carrier proteins act as solubilizing agents for recombinant uncoupling protein 1 through interactions with GroEL. *Biochem. Biophys. Res. Commun.* 2005; 333: 686-693.

Dreier, T., Lorenczewski, G., Brandl, C., Hoffmann, P., Syring, U., Hanakam, F., Kufer, P., Riethmuller, G., Bargou, R., Baeuerle, P. A. Extremely potent, rapid and costimulation-independent cytotoxic T-cell response against lymphoma cells catalyzed by a single-chain bispecific antibody. *Int. J. Cancer.* 2002; 100: 690-697.

Dümmler, A., Lawrence, A. M., de Marco, A. Simplified screening for the detection of soluble fusion constructs expressed in *E. coli* using a modular set of vectors. *Microb. Cell Fact.* 2005; 4: 34-44.

Dyson, M. R., Shadbolt, S. P., Vincent, K. J., Perera, R. L., McCafferty, J. Production of soluble mammalian proteins in *Escherichia coli*: identification of protein features that correlate with successful expression. *BMC Biotechnol.* 2004; 4: 32-40.

Edwards, J. L. Diagnosis and management of benign prostatic hyperplasia. *Am. Fam. Physician.* 2008; 77: 1403-1410.

Einhauer, A., & Jungbauer, A. The FLAG peptide, a versatile fusion tag for the purification of recombinant proteins. *J. Biochem. Biophys. Meth.* 2001; 49: 455–465.

Eissler, N., Ruf, P., Mysliwietz, J., Lindhofer, H., Mocikat, R. Trifunctional bispecific antibodies induce tumour-specific T cells and elicit a vaccination effect. *Cancer Res.* 2012; 72: 3958–3966.

Els Conrath, K., Lauwereys, M., Wyns, L., Muyldermans, S. Camel single-domain antibodies as modular building units in bispecific and bivalent antibody constructs. *J. Biol. Chem.* 2001; 276: 7346-7350.

Esposito, D., & Chatterjee, D. K. Enhancement of soluble protein expression through the use of fusion tags. *Curr. Opin. Biotechnol.* 2006; 17: 353–358.

Ewert, S., Huber, T., Honegger, A., Plückthun, A. Biophysical properties of human antibody variable domains. *J. Mol. Biol.* 2003; 325: 531-553.

Filella, X., & Giménez, N. Evaluation of [-2] proPSA and Prostate Health Index (phi) for the detection of prostate cancer: a systematic review and meta-analysis. *Clin. Chem. Lab. Med*. 2013; 51: 729-739.

Forsberg, G., Forsgren, M., Jaki, M., Norin, M., Sterky, C., Enhorning, A, Larsson, K., Ericsson, M. & Bjork, P. Identification of framework residues in a secreted recombinant antibody fragment that control production level and localization in *Escherichia coli*. *J. Biol. Chem.* 1997; 272: 12430-12436.

Fox, J. D., Kapust, R.B., Waugh, D. S. Single amino acid substitutions on the surface of *Escherichia coli* maltose-binding protein can have a profound impact on the solubility of fusion proteins. *Protein Sci.* 2001; 10: 622-630.

Fu, X. Y. Extracellular accumulation of recombinant protein by *Escherichia coli* in a defined medium. *Appl. Microbiol. Biotechnol.* 2010; 88: 75–86.

Gaberc-Porekar, V., & Menart, V. Perspectives of immobilized-metal affinity chromatography. *J. Biochem. Biophys. Methods.* 2001; 49: 335–360.

Gada, K. S., Patil, V., Panwar, R., Majewski, S., Tekabe, Y., & Khaw, B. A. Pretargeted gamma imaging of murine metastatic melanoma lung lesions with bispecific antibody and radiolabeled polymer drug conjugates. *Nucl. Med. Commun.* 2011; 32: 1231-1240.

Galeffi, P., Lombardi, A., Pietraforte, I., Novelli, F., Di Donato, M., Sperandei, M., Tornambé, A., Fraioli, R., Martayan, A., Natali, P. G., Benevolo, M., Mottolese, M., Ylera, F., Cantale, C., Giacomini, P. Functional expression of a single-chain antibody to ErbB-2 in plants and cell-free systems. *J. Transl. Med.* 2006; 4: 39.

Gao, C., Mao, S., Kaufmann, G., Wirsching, P., Lerner R. A., Janda, K. D. A method for the generation of combinatorial antibody libraries using pIX phage display. *Proc. Natl. Acad. Sci. U. S. A.* 2002; 99: 12612-12616.

Barbas, C. F., Burton, D. R., Scott, J. K., Silverman, G. J. Phage display: A laboratory manual, 1st Edition, 736 pp, Cold Spring Harbor Laboratory press, 2001.

Gartner, L. P., Hiatt, J. L. Color textbook of histology, 2nd Edition, 577pp, Saunders, 2001.

Giles, R., H., Van Es, J.,H., Clevers, H. Caught up in a Wnt storm: Wnt signaling in cancer. *Biochem. Biophys. Acta.* 2003; 1653: 1-24.

Gilgunn, S., Conroy, J. P., Saldova, R., Rudd, M. P., & O'Kennedy, J. R. Aberrant PSA glycosylation - a sweet predictor of prostate cancer. *Nat. Rev. Urol.* 2013; 10: 99-107.

Goering, W., Kloth, M., Schulz, W. A. DNA methylation changes in prostate cancer. *Methods Mol. Biol.* 2012; 863: 47-66.

Gold, D. V., Goldenberg, D. M., Karacay, H., Rossi, E. A., Chang, C. H., Cardillo, T. M., McBride, W. J., & Sharkey, R. M. A novel bispecific, trivalent antibody construct for targeting pancreatic carcinoma. *Cancer Res.* 2008; 68: 4819-4826.

Goldenberg, D. M., Sharkey, R. M., Paganelli, G., Barbet, J., & Chatal, J. F. Antibody pretargeting advances cancer radioimmunodetection and radioimmunotherapy. *J. Clin. Oncol.* 2006; 24: 823-834.

Gomes, I. M., Arinto, P., Lopes, C., Santos, C. R., Maia, C. J. STEAP1 is overexpressed in prostate cancer and prostatic intraepithelial neoplasia lesions, and it is positively associated with Gleason score. *Urologic Oncology: Seminars and Original Investigations*. 2014; 32: 53e23-53e29.

Gonzalgo, M. L., Pavlovich, C. P., Lee, S. M., Nelson, W. G. Prostate cancer detection by GSTP1 methylation analysis of postbiopsy urine specimens. *Clin. Cancer Res.* 2003; 9: 2673-2677.

Gonzalgo, M. L., & Isaacs, W. B. Molecular pathways to prostate cancer. *J. Urol.* 2003; 170: 2444-2452.

Goulding, C. W., Perry, L. J. Protein production in *Escherichia coli* for structural studies by X-ray crystallography. *J. Struct. Biol.* 2003; 142:133–143.

Graziano, R. F., & Guptill, P. Chemical production of bispecific antibodies. *Methods Mol. Biol.* 2004; 283: 71-85.

Gregorakis, A. K., Holmes, E. H., Murphy, G. P. Prostate-specific membrane antigen: current and future utility. *Semin. Urol. Oncol.* 1998; 16: 2-12.

Griffiths, A. D., Malmqvist, M., Marks, J. D., Bye, J. M., Embleton, M. J., McCafferty, J., Baier, M., Holliger, K. P., Gorick, B. D., Hughes-Jones, N. C. Human anti-self antibodies with high specificity from phage display libraries. *EMBO J.* 1993; 12: 725-734.

Grosse-Hovest, L., Müller, S., Minoia, R., Wolf, E., Zakhartchenko, V., Wenigerkind, H., Lassnig, C., Besenfelder, U., Müller, M., Lytton, S. D., Jung, G., Brem, G. Cloned transgenic farm animals produce a bispecific antibody for T cell-mediated tumour cell killing. *Proc. Natl. Acad. Sci. U. S. A.* 2004; 101: 6858-6863.

Gruen, M., Bommert, K., Bargou, R. C. T-cell-mediated lysis of B cells induced by a CD19xCD3 bispecific single-chain antibody is perforin dependent and death receptor independent. *Cancer Immunol. Immunother.* 2004; 53: 625-632.

Guan, Y., Zheng, B. J., He, Y. Q., Liu, X. L., Zhuang, Z. X., Cheung, C. L., Luo, S. W., Li, P. H., Zhang, L. J., Guan, Y. J., Butt, K. M., Wong, K. L., Chan, K. W., Lim, W., Shortridge, K. F., Yuen, K. Y., Peiris, J. S., & Poon, L. L. Isolation and

characterization of viruses related to the SARS coronavirus from animals in southern China. *Science.* 2003; 302: 276-278.

Guo, H., Lin, J., Wen, X., M., Yang, J., Qian, W., Deng, Z., Q., Ma, J., C., Tang, C., Y., An, C., Liu, Q., Zhou, H., Qian, J. Decreased SFRP2 expression is associated with intermediate and poor karyotypes in de novo acute myeloid leukemia. *Int J Clin Exp Pathol.* 2014; 7: 4695-703.

Guttikonda, S., Tang, X. L., Yang, B. M., Armstrong, G. D., & Suresh, M. R. Monospecific and bispecific antibodies against *E. coli* O157 for diagnostics. *J. Immunol. Methods.* 2007; 327: 1-9.

Haisma, H. J., Grill, J., Curiel, D. T., Hoogeland, S., van Beusechem, V. W., Pinedo, H. M., Gerritsen, W. R. Targeting of adenoviral vectors through a bispecific single-chain antibody. *Cancer Gene Therapy*. 2000; 7: 901-904.

Han, M., Piantadosi, S., Zahurak, M. L., Sokoll, L. J., Chan, D. W., Epstein, J. I., Walsh, P.C., & Partin, A. W. Serum acid phosphatase level and biochemical recurrence following radical prostatectomy for men with clinically localized prostate cancer. *Urol.* 2001; 57: 707-11.

Hanahan, D., & Weinberg, R. A. Hallmarks of cancer: the next generation. *Cell*. 2011; 144: 646–674.

Harris, S., & Jones, D. B. Optimisation of the polymerase chain reaction. *Br. J. Biomed. Sci.* 1997; 54: 166-73.

Hayashi, H., Asano, R., Tsumoto, K., Katayose, Y., Suzuki, M., Unno, M., Kodama, H., Takemura, S., Yoshida, H., Makabe, K., Imai, K., Matsuno, S., Kumagai, I., Kudo, T. A highly effective and stable bispecific diabody for cancer immunotherapy: cure of xenografted tumours by bispecific diabody and T-LAK cells. *Cancer Immunol. Immunother.* 2004; 53: 497-509.

Hayes, J. D., Pulford, D. J. The glutathione S-transferase supergene family: regulation of GST and the contribution of the isoenzymes to cancer chemoprotection and drug resistance. *Crit. Rev. Biochem. Mol. Biol.* 1995; 30: 445-600.

Healy, D. A., Hayes, C. J., Leonard, P., McKenna, L., O'Kennedy, R. Biosensor developments: application to prostate-specific antigen detection. *Trends Biotechnol.* 2007; 25: 125-131.

Heideman, D.A., van Beusechem, V. W., Offerhaus, G. J., Wickham, T. J., Roelvink, P. W., Craanen, M. E., Pinedo, H. M., Meijer, C. J., Gerritsen, W. R. Selective gene transfer into primary human gastric tumours using epithelial cell adhesion molecule-targeted adenoviral vectors with ablated native tropism. *Hum. Gene Ther.* 2002; 13: 1677-1685.

Hemmerle, T., Wulhfard, S., Neri, D. A critical evaluation of the tumour-targeting properties of bispecific antibodies based on quantitative biodistribution data. *Protein Eng. Des. Sel.* 2012; 25: 851-854.

Hessels, D., & Schalken, J. A. Urinary biomarkers for prostate cancer: a review. *Asian J. Androl.* 2013; 15: 333-339.

Hodek, P., & Stiborova, M. Chicken antibodies – superior alternative for conventional immunoglobulins. *Proc. Indian Natl. Sci Acad. B.* 2003; 69: 461-468.

Ho, M., Nagata, S., Pastan, I. Isolation of anti-CD22 Fv with high affinity by Fv display on human cells. *Proc.. Natl. Acad. Sci. U. S. A.* 2006; 102: 9637–9642.

Hoffman, R. M. Clinical practice. Screening for prostate cancer. *N. Engl. J. Med.* 2011; 365: 2013-2019.

Holliger, P., & Hudson, P. J. Engineered antibody fragments and the rise of single domains. *Nat. Biotechnol.* 2005; 23: 1126-1136.

Holmes, D. Buy buy bispecific antibodies. *Nat. Rev. Drug Discov.* 2011; 10, 798-800.

Hu, J., Qin, H., Sharma, M., Cross, T. A., Gao, F. P. Chemical cleavage of fusion proteins for high-level production of transmembrane peptides and protein domains containing conserved methionines. *Biochim. Biophys. Acta.* 2008; 1778: 1060-1066.

Huang, Y. S., & Chuang, D. T. Mechanisms for GroEL/GroES-mediated folding of a large 86-kDa fusion polypeptide in vitro. *J. Biol. Chem.* 1999; 274: 10405-10412.

Huang, Z., Li, L., Wang, J. Hypermethylation of SFRP2 as a potential marker for stool-based detection of colorectal cancer and precancerous lesions. *Dig. Dis. Sci.* 2007; 52: 2287–2291.

Hubert, R. S., Vivanco, I., Chen, E., Rastegar, S., Leong, K., Mitchell, S. C., Madraswala, R., Zhou, Y., Kuo, J., Raitano, A. B., Jakobovits, A., Saffran, D. C., Afar, D. E. H. STEAP: A prostate-specific cell-surface antigen highly expressed in human prostate tumours. *Proc. Natl. Acad. Sci. U. S. A.* 1999; 96: 14523-14528.

Igawa, T., Tsunoda, H., Kikuchi, Y., Yoshida, M., Tanaka, M., Koga, A., Sekimori, Y., Orita, T., Aso, Y., Hattori, K., Tsuchiya, M. VH/VL interface engineering to promote selective expression and inhibit conformational isomerization of thrombopoietin receptor agonist single-chain diabody. *Protein Eng.Des. Sel.* 2010; 23: 667-677.

Ihlaseh-Catalano, S. M., Drigo, S. A., De Jesus, C. M. N., Domingues, M. A. C., Trindade Filho, J. C. S., De Camargo, J. L. V., Rogatto, S. R. STEAP1 protein overexpression is an independent marker for biochemical recurrence in prostate carcinoma. *Histopathol.* 2013; 63: 678-685.

Isaacs, W., & Kainu, T. Oncogenes and tumour suppressor genes in prostate cancer. *Epidemiol. Rev.* 2001; 1: 36-41.

Israeli, R. S., Powell, C. T., Corr, J. G., Fair, W. R., & Heston, W. D. W. Expression of the prostate-specific membrane antigen. *Cancer Research.* 1994; 54: 1807-1811.

Issaq, H. J., Waybright, T. J., & Veebstra, T. D. Cancer biomarker discovery: Opportunities and pitfalls in analytical methods. *Electrophoresis.* 2010; 32: 967-975.

Jefferis, R. Glycosylation of recombinant antibody therapeutics. *Biotechnol. Prog*. 2005; 21: 11-16.

Jeronimo, C., Usadel, H., Henrique, R., Oliveira, J., Lopes, C., Nelson, W. G., Sidransky, D. Quantitation of GSTP1 methylation in non-neoplastic prostatic tissue and organ-confined prostate adenocarcinoma. *J. Natl. Cancer Inst.* 2001; 93: 1747-52.

Jiang, Z., Woda, B. A., Rock, K. L., Xu, Y., Savas, L., Khan, A., Pihan, G., Cai, F., Babcook, J. S., Rathanaswami, P., Reed, S. G., Xu, J., Fanger, G. R. P504S a new molecular marker for the detection of prostate carcinoma. *Am. J. Surg. Pathol.* 2001; 25: 1397-1404.

John, T. T., Bashir, J., Burrow, C. T., & Machin, D. G. Squamous cell carcinoma of the prostate-a case report. *Int. Urol. Nephrol.* 2005; 37: 311-313.

Jung, K., Brux, B., Lein, M., Rudolph, B., Kristiansen, G., Hauptmann, S., Schnorr, D., Leoning, S. A., & Sinha, P. Molecular forms of prostate-specific antigen in malignant and benign prostatic tissue: biochemical and diagnostic implications. *Clin. Chem.* 2000; 46: 47-54.

Kammila, S., Das, D., Bhatnagar, P. K., Sunwoo, H. H., Zayas-Zamora, G., King, M., & Suresh, M. R. A rapid point of care immunoswab assay for SARS-CoV detection. *J. Virol. Methods.* 2008; 152: 77-84.

Kaplan, W., Hüsler, P., Klump, H., Erhardt, J., Sluis-Cremer, N., Dirr, H. Conformational stability of pGEX-expressed *Schistosoma japonicum* glutathione S-transferase: a detoxification enzyme and fusion-protein affinity tag. *Protein Sci.* 1997; 6: 399-406.

Kapust, R. B., & Waugh, D. S. *Escherichia coli* maltose-binding protein is uncommonly effective at promoting the solubility of polypeptides to which it is fused. *Protein Sci.* 1999; 8: 1668-1674.

Karayi, M. K., & Markham, A. F. Molecular biology of prostate cancer. *Prostate Cancer Prostatic Dis.* 2004; 7: 6-20.

Karlsson, R., & Larsson, A. Affinity measurement using surface plasmon resonance. *Methods Mol. Biol.* 2004; 248: 389-415.

Kellner, C., Bruenke, J., Stieglmaier, J., Schwemmlein, M., Schwenkert, M., Singer, H., Mentz, K., Peipp, M., Lang, P., Oduncu, F., Stockmeyer, B., Fey, G. H. A novel CD19-directed recombinant bispecific antibody derivative with enhanced immune effector functions for human leukemic cells. *J. Immunother.* 2008; 31: 871-884.

Keyaerts, E., Vijgen, L., Maes, P., Neyts, J., & Van Ranst, M. Growth kinetics of SARS-coronavirus in Vero E6 cells. *Biochem. Biophys. Res. Commun.* 2005; 329: 1147-1151.

Khaw, B. A., Tekabe, Y., & Johnson, L. L. Imaging experimental atherosclerotic lesions in ApoE knockout mice: enhanced targeting with Z2D3-anti-DTPA bispecific antibody and 99mTc-labeled negatively charged polymers. *J. Nucl. Med.* 2006; 47: 868-876.

Kiess, A. P., Minn, I., Chen, Y., Hobbs, R., Sgouros, G., Mease R. C., Pullambhatla, M., Shen, C. J., Foss, C. A., & Pomper, M. G. Auger Radiopharmaceutical Therapy Targeting Prostate-Specific Membrane Antigen. *J. Nucl. Med.* 2015; 56: 1401–1407.

Kipriyanov, S. M., Moldenhauer, G., Martin, A. C., Kupriyanova, O. A. & Little, M. Two amino acid mutations in an anti-human CD3 single chain Fv antibody fragment that affect the yield on bacterial secretion but not the affinity. *Protein Eng.* 1997; 10: 445-453.

Kipriyanov, S. M., Cochlovius, B., Schäfer, H. J., Moldenhauer, G., Bähre, A., Le Gall, F., Knackmuss, S., Little, M. Synergistic anti-tumour effect of bispecific CD19 x CD3 and CD19 x CD16 diabodies in a preclinical model of non-Hodgkin's lymphoma. *J. Immunol.*. 2002; 169: 137-144.

Kipriyanov, S.M., Moldenhauer, G., Braunagel, M., Reusch, U., Cochlovius, B., Le Gall, F., Kouprianova, O. A., Von der Lieth, C. W., Little, M. Effect of domain order on the activity of bacterially produced bispecific single-chain Fv antibodies. *J. Mol. Biol.* 2003; 330: 99-111.

Klein, C., Sustmann, C., Thomas, M., Stubenrauch, K., Croasdale, R., Schanzer, J., Brinkmann, U., Kettenberger, H., Regula, J. T., & Schaefer, W. Progress in overcoming the chain association issue in bispecific heterodimeric IgG antibodies. *MAbs.* 2012; 4: 653–663.

Knappik, A., & Pluckthun, A. Engineered turns of a recombinant antibody improves its *in vivo* folding. *Protein Eng.*. 1995; 8: 81–89.

Knudsen, B. S., Vasioukhin, V. Mechanisms of prostate cancer initiation and progression. *Adv. Cancer Res.* 2010; 109: 1-50.

Köhler, G., & Milstein, C. Continuous cultures of fused cells secreting antibody of predefined specificity. *Nature.* 1975; 256: 495-497.

Komiya, Y., & Habas, R. Wnt signal transduction pathways. *Organogenesis.* 2008; 4: 68-75.

Kontermann, R. E. Bispecific Antibodies. Springer; 2011. ISBN 978-3-642-20909-3.

Kontermann, R. Dual targeting strategies with bispecific antibodies. *MAbs.* 2012; 4: 182-197.

Kontermann, R. E., & Brinkmann U. Bispecific antibodies. *Drug Discov. Today*. 2015; 20: 838-47.

Korn, T., Müller, R., Kontermann, R. E. Bispecific single-chain diabody-mediated killing of endoglin-positive endothelial cells by cytotoxic T lymphocytes. *J. Immunother.* 2004; 27: 99-106.

Kudou, M., Ejima, D., Sato, H., Yumioka, R., Arakawa, T., Tsumoto, K. Refolding single-chain antibody (scFv) using lauroyl-L-glutamate as a solubilization detergent and arginine as a refolding additive. *Protein Expr. Purif.* 2011; 77: 68–74.

Larue, L., & Delmas, V. The WNT/Beta-catenin pathway in melanoma. *Frontierst Biosci.* 2006; 11: 733-742.

LaVallie, E. R., Diblasio, E. A., Kovacic, S., Grant, K. L., Schendel, P. F., Mccoy, J. M. A thioredoxin gene fusion expression system that circumvents inclusion body formation in the *Escherichia coli* cytoplasm. *Biotechnol.* 1993; 11: 187–193.

LaVallie, E. R., Lu, Z., Diblasio-Smith, E. A., Collins-Racie, L. A., McCoy, J. M. Thioredoxin as a fusion partner for production of soluble recombinant proteins in *Escherichia coli. Methods Enzymol.* 2000; 326: 322-340.

Lee, W. H., Morton, R. A., Epstein, J. I., Brooks, J. D., Campbell, P. A., Bova, G. S., Hsieh, W. S., Isaacs, W. B., Nelson, W. G. Cytidine methylation of regulatory sequences near the pi-class glutathione S-transferase gene accompanies human prostatic carcinogenesis. *Proc. Natl. Acad. Sci. USA.* 1994; 91: 11733-11737.

Leek, J., Lench, N., Maraj, B., Bailey, A., Carr, I. M., Andersen, S., Cross, J., Whelan, P, MacLennan, K. A., Meredith, D. M. Prostate-specific membrane antigen: evidence for the existence of a second related human gene. *Br. J. Cancer.* 1995; 72: 583-588.

Leonard, J.P., Schuster, S. J., Emmanouilides, C., Couture, F., Teoh, N., Wegener, W. A., Coleman, M., Goldenberg, D. M. Durable complete responses from therapy with combined epratuzumab and rituximab: final results from an international multicenter, phase 2 study in recurrent, indolent, non-Hodgkin lymphoma. *Cancer.* 2008; 113: 2714-2723.

Lerner, R. A. Manufacturing immunity to disease in a test tube: the magic bullet realized. *Angew. Chem. Int. Ed Engl.* 2006; 45: 8106-25.

Loffler, A., Gruen, M., Wuchter, C., Schriever, F., Kufer, P., Dreier, T., Hanakam, F., Baeuerle, P. A., Bommert, K., Karawajew, L., Dörken, B., Bargou, R. C. Efficient elimination of chronic lymphocytic leukaemia B cells by autologous T cells with a bispecific anti-CD19/anti-CD3 single-chain antibody construct. *Leukemia.* 2003; 17: 900-909.

Li, L. C., Carroll, P. R., Dahiya, R. Epigenetic changes in prostate cancer: implication for diagnosis and treatment. *J. Natl. Cancer Inst.* 2005; 97: 103-115.

Lu, D., Jimenez, X., Witte, L., Zhu, Z. The effect of variable domain orientation and arrangement on the antigen-binding activity of a recombinant human bispecific diabody. *Biochem. Biophys. Res. Commun*. 2004; 318: 507-513.

Lilja, H., Oldbring, J., Rannevik, G., Laurell C-B. Seminal vesicle-secreted proteins and their reactions during gelation and liquefaction of human semen. *J. Clin Invest* 1987; 80: 281-285

Lin, X,. Tascilar, M., Lee, W. H., Vles, W. J., Lee, B. H., Veeraswamy, R., Asgari, K., Freije, D., van Rees, B., Gage, W. R., Bova, G. S., Isaacs, W. B., Brooks, J. D., DeWeese, T. L., De Marzo, A. M., Nelson, W. G. GSTP1 CpG island hypermethylation is responsible for the absence of GSTP1 expression in human prostate cancer cells. *Am. J. Pathol*. 2001; 159: 1815-1826.

Lopez-Beltran, A., Mikuz, G., Luque, R. J., Mazzucchelli, R., & Montironi, R. Current practice of Gleason grading of prostate carcinoma. *Virchows Arch.* 2006; 448: 111-118.

Luo, J., Zha, S., Gage, W. R., Dunn, T. A., Hicks, J. L., Bennett, C. J., Ewing, C. M., Platz, E. A., Ferdinandusse, S., Wanders, R. J., Trent, J. M., Isaacs, W. B., De Marzo, A. M. Alpha-methylacyl-CoA racemase: a new molecular marker for prostate cancer. *Cancer Res.* 2002; 62: 2220–2226

Lustig, B., & Behrens, J. The Wnt signaling pathway and its role in tumour development. *J. Cancer Res. Clin. Oncol.* 2003; 129: 199–221.

Lytton, B. Prostate cancer: a brief history and the discovery of hormonal ablation treatment. *J. Urol*. 2001; 165: 1859-1862.

Madu, C. O., & Lu, Y. Novel diagnostic biomarkers for prostate cancer. *J. Cancer*. 2010; 1: 150-177.

Maia, C. J. B., Socorro, S., Schmitt, F., Santos, C. R. STEAP1 is overexpressed in breast cancer and down-regulated by 17-beta-estradiol in MCF-7 cells and in the rat mammary gland. *Endocrine*. 2008; 34: 108-16.

Majumdar, S., Chanda, S., Ganguli, B., Mazumder, D. N., Lahiri, S., Dasgupta, U. B. Arsenic exposure induces genomic hypermethylation. *Environ. Toxicol.* 2010; 25: 315–318.

Makarov, D. V., Loeb, S., Getzenberg, R. H., & Partin, A. W. Biomarkers for prostate cancer. *Annu. Rev. Med.* 2009; 60: 139-151.

Maletz, K., Kufer, P., Mack, M., Raum, T., Pantel, K., Riethmüller, G., Gruber, R. Bispecific single-chain antibodies as effective tools for eliminating epithelial cancer cells from human stem cell preparations by redirected cell cytotoxicity. *Int. J. Cancer* 2001; 93: 409-416.

Manafi, M., & Kremsmaier, B. Comparative evaluation of different chromogenic/fluorogenic media for detecting *Escherichia coli* O157:H7 in food. *Int. J. Food Microbiol.* 2001; 71: 257-262.

Marblestone, J. G., Edavettal, S. C., Lim, Y., Lim, P., Zuo, X., Butt, T. R. Comparison of SUMO fusion technology with traditional gene fusion systems: enhanced expression and solubility with SUMO. *Protein Sci.* 2006; 15: 182-189.

Maruvada, P., Wang, W., Wagner, P. D., & Srivastava, S. Biomarkers in molecular medicine: cancer detection and diagnosis. *Biotechniques.* 2005; 6: 9-15.

Maynard, J., & Georgiou, G. Antibody engineering. *Annu. Rev. Biomed. Eng*. 2000; 2: 339-376.

McBride, W. J., Zanzonico, P., Sharkey, R. M., Norén, C., Karacay, H., Rossi, E. A., Losman, M. J., Brard, P. Y., Chang, C. H., Larson, S. M., & Goldenberg, D. M. Bispecific antibody pretargeting PET (immunoPET) with an ^{124}I-labeled hapten-peptide. *J. Nucl. Med.* 2006; 47: 1678-1688.

McCall, A.M., Shahied, L., Amoroso, A. R., Horak, E. M., Simmons, H. H., Nielson, U., Adams, G. P., Schier, R., Marks, J. D., Weiner, L. M. Increasing the affinity for tumour antigen enhances bispecific antibody cytotoxicity. *J. Immunol*. 2001; 166: 6112-6117.

McNeal, J. E. Normal histology of the prostate. *Am. J. Surg. Pathol.* 1988; 12: 619-633.

Mhawech-Fauceglia, P., Zhang, S., Terracciano, L., Sauter, G., Chadhuri, A., Herrmann, F. R., Penetrante, R. Prostate-specific membrane antigen (PSMA) protein expression in normal and neoplastic tissues and its sensitivity and specificity in prostate adenocarcinoma: an immunohistochemical study using multiple tumour tissue microarray technique. *Histopathol.* 2007; 50: 472-483.

Mikolajczyk, S. D., Song, Y., Wong, J. R., Matson, R. S., & Rittenhouse, H. G. Are multiple markers the future of prostate cancer diagnostics. *Clin. Biochem.* 2004; 27: 519-528.

Milstein, C., & Cuello, A. C. Hybrid hybridomas and their use in immunohistochemistry. *Nature.* 1983; 305: 537-540.

Mine, Y., & Kovacs-Nolan, J. Chicken egg yolk antibodies as therapeutics in enteric infectious disease: A review. *J. Med. Food.* 2002; 5: 159-169.

Mine, Y., & Yang, M. Recent advances in the understanding of egg allergens: Basic, industrial, and clinical perspectives. *J. Agric. Food Chem.* 2008; 56: 4874-4900.

Minner, S., Wittmer, C., Graefen, M., Salomon, G., Steuber, T., Haese, A., Huland, H., Bokemeyer, C., Yekebas, E., Dierlamm, J., Balabanov, S., Kilic, E., Wilczak, W., Simon, R., Sauter, G., Schlomm, T. High level PSMA expression is associated with

early PSA recurrence in surgically treated prostate cancer. *The Prostate.* 2011; 71: 281-288.

Mitchell, D. A., Marshall, T. K., Deschenes, R. J. Vectors for the inducible overexpression of glutathione S-transferase fusion proteins in yeast. *Yeast.* 1993; 9: 715-722.

Morgan, G., & Levinsky, R., J. Monoclonal antibodies in diagnosis and treatment. *Arch. Dis. Child.* 1985; 60: 96–98.

Müller, D., & Kontermann, R. E. Bispecific antibodies for cancer immunotherapy: Current perspectives. *BioDrugs.* 2010; 24: 89-98.

Nallamsetty, S., & Waugh, D.S. Mutations that alter the equilibrium between open and closed conformations of *Escherichia coli* maltose-binding protein impede its ability to enhance the solubility of passenger proteins. *Biochem. Biophys. Res. Commun.* 2007; 364: 639–644.

Narat, M. Production of antibodies in chickens. *Food Tech. Biotech. 2003;* 41: 259-267.

Nelson, P. N., Reynolds, G. M., Waldron, E. E., Ward, E., Giannopoulos, K., & Murray, P. G. Monoclonal antibodies. *Mol. Pathol.* 2000; 53: 111-117.

Nettelbeck, D.M., Miller, D. W., Jérôme, V., Zuzarte, M., Watkins, S. J., Hawkins, R. E., Müller, R., Kontermann, R. E. Targeting of adenovirus to endothelial cells by a bispecific single-chain diabody directed against the adenovirus fiber knob domain and human endoglin (CD105). *Mol. Ther.* 2001; 3: 882-891.

Nettelbeck, D.M., Rivera, A. A., Kupsch, J., Dieckmann, D., Douglas, J. T., Kontermann, R. E., Alemany, R., Curiel, D. T. Retargeting of adenoviral infection to melanoma: combining genetic ablation of native tropism with a recombinant bispecific single-chain diabody (scDb) adapter that binds to fiber knob and HMWMAA. *Int. J. Cancer.* 2004; 108: 136-145.

Nichol, M. B., Wu, J., Huang, J., Denham, D., Frencher, S., Jacobsen, S. J. Cost-effectiveness of Prostate Health Index for prostate cancer detection. *BJU International*. 2011; 110: 353-362.

Nieba, L., Honegger, A., Krebber, C., & Pluckthun, A. Disrupting the hydrophobic patches at the antibody variable/constant domain interface: improved in vivo folding and physical characterization of an engineered scFv fragment. *Protein Eng.* 1997; 10: 435-444.

Nilsson, F., Tarli, L., Viti, F., Neri, D. The use of phage display for the development of tumour targeting agents. *Adv. Drug Deliv. Rev.* 2000; 43: 165-96.

Nisonoff, A., & Rivers, M. M. Recombination of a mixture of univalent antibody fragments of different specificity. *Arch. Biochem. Biophys.* 1961; 93: 460-462.

Nogueira, L., Corradi, R., & Eastham, J. A. Prostate-specific antigen for prostate cancer detection. *International Braz. J. Urol.* 2009; 35: 521-531.

Ntais, C., Polycarpou, A., & Tsatsoulis, A. Molecular epidemiology of prostate cancer: androgens and polymorphisms in androgen-related genes. *Eur. J. Endocrinol.* 2003; 149: 469-477.

Oberwalder, M., Zitt, M., Wontner, C., Fiegl, H., Goebel, G., Kohle, O., Muhlmann, G., Ofner, D., Margreiter, R., Muller, H. M. SFRP2 methylation in fecal DNA - A marker for colorectal polyps. *Int. J. Colorectal Dis.* 2008; 23: 15–19.

O'Brien, P. M., & Aitken, R. Antibody Phage Display: Methods and Protocols, Methods in Molecular Medicine, 178 pp, 2nd Edition, Human Press, 2002.

Ohlin, M., & Zouali, M. The human antibody repertoire to infectious agents: implications for disease pathogenesis. *Mol. Immunol.* 2003; 40: 1-11.

Ohta, M., Hamako, J., Yamamoto, S., Hatta, H., Kim, M., Yamamoto, T., Oka, S., Mizuochi, T., Matsuura, F. Structures of asparagine-linked oligosaccharides from hen egg-yolk antibody (IgY). Occurrence of unusual glucosylated oligo-mannose type oligosaccharides in a mature glycoprotein. *Glycoconj. J.* 1991; 8: 400-13.

O'Hurley, G., Perry, A. S., O'Grady, A., Loftus, B., Smyth, P., O'Leary, J. J., Sheils, O., Fitzpatrick, J. M., Hewitt, S. M., Lawler, M., Kay, E. W. The role of secreted frizzled-related protein 2 expression in prostate cancer. *Histopathol.* 2011; 59: 1240-1248.

O'Keefe, D. S., Su, S., Bacich, D. J., Horiguchi, Y., Luo, Y., Powell, C. T., Zandvliet, D., Russell, P. J., Molloy, P. L., Nowak, N. J., Shows, T. B., Mullins, C., Vonder Haar, R. A., Fair, W. R., Heston, W. D. Mapping, genomic organization and promoter analysis of the human prostate-specific membrane antigen gene. *Biochem. Biophys. Acta.* 1998; 1443: 113–127.

Ou J. N., Torrisani J., Unterberger A., Provencal N., Shikimi K., Karimi M., Ekstrom T. J., & Szyf M. Histone deacetylase inhibitor Trichostatin A induces global and gene-specific DNA demethylation in human cancer cell lines. *Biochem. Pharmacol.* 2007; 73: 1297–1307.

Özen, H., & Sözen, S. PSA isoforms in prostate cancer detection. *Europ. Urol. Supplements.* 2006; 5: 495-499.

Pacheco, B., Crombet, L., Loppnau, P., & Cossar, D. A screening strategy for heterologous protein expression in *Escherichia coli* with the highest return of investment. *Protein Expr. Purif.* 2012; 81:33-41.

Parashar, A., Sarkar, S., Ganguly, A., Sharma, S. K., & Suresh, M. R. Bispecific Antibodies for Diagnostic Applications. In *Bispecific Antibodies* (1st Edition) (Kontermann, R.E., ed), pp. 349-367, Springer Berlin Heidelberg, 2011.

Patil, V., Gada, K., Panwar, R., Varvarigou, A., Majewski, S., Weisenberger, A., Ferris, C., Tekabe, Y., & Khaw, B. A. Imaging small human prostate cancer xenografts after pretargeting with bispecific bombesin-antibody complexes and targeting with high specific radioactivity labeled polymer-drug conjugates. *Eur. J. Nucl. Med. Mol. Imaging.* 2012; 39: 824-839.

Perchiacca, J. M., Tessier, P. M. Engineering aggregation-resistant antibodies. *Annu. Rev. Chem. Biomol. Eng.* 2012; 3: 263-86.

Perner, S., Hofer, M. D., Kim, R., Shah, R. B., Li, H., Möller, P., Hautmann, R. E., Gschwend, J. E., Kuefer, R., Rubin, M. A. Prostate-specific membrane antigen expression as a predictor of prostate cancer progression. *Human Pathol.* 2007; 38: 696-701.

Perry, A. S., Watson, R. W. G., Lawler, M., & Hollywood, D. The epigenome as a therapeutic target in prostate cancer. *Nature Revs Urol*. 2010; 7: 668–680.

Perry, A. S., O'Hurley, G., Raheem, O. A., Brennan, K., Wong, S., O'Grady, A., Kennedy, A. M., Marignol, L., Murphy, T. M., Sullivan, L., Barrett, C., Loftus, B., Thornhill, J., Hewitt, S. M., Lawler, M., Kay, E., Lynch, T., Hollywood, D. Gene expression and epigenetic discovery screen reveal methylation of SFRP2 in prostate cancer. *Int. J. Cancer.* 2013; 132:1771-1780.

Pescovitz, M. D. Rituximab, an anti-cd20 monoclonal antibody: history and mechanism of action. *Am. J. Transplant.* 2006; 6: 859-866.

Plückthun, A., Skerra, A. Expression of functional antibody Fv and Fab fragments in *Escherichia coli. Methods Enzymol.* 1989; 178: 497-515.

Pontari, M. A., & Ruggieri, M. R. Mechanisms in prostatitis/chronic pelvic pain syndrome. *J. Urol.* 2004; 172: 839-845.

Poon, L. L., Guan, Y., Nicholls, J. M., Yuen, K. Y., & Peiris, J. S. The aetiology, origins, and diagnosis of severe acute respiratory syndrome. *Lancet Infect. Dis.* 2004; 4: 663-671.

Prajapati, A., Gupta, S., Mistry, B., & Gupta, S. Prostate stem cells in the development of benign prostate hyperplasia and prostate cancer: emerging role and concepts. *Biomed. Res. Int.* 2013; 2013: 1-10.

Prensner, J. R., Rubin, M. A., Wei, J. T., & Chinnaiyan, A. M. *Sci Transl Med.* 2012; 4: 127.

Pryor, K. D., & Leiting, B. High-level expression of soluble protein in *Escherichia coli* using a His(6)-tag and maltose-binding-protein double-affinity fusion system. *Protein Expr. Purif.* 1997; 10: 309–319.

Rajasekaran, A. K., Anilkumar, G., Christiansen, J. J. Is prostate-specific membrane antigen a multifunctional protein? *Am. J. Physiol. Cell Physiol.* 2005; 288: C975-981.

Ramos, R., Domingues, L., Gama, F. M. *Escherichia coli* expression and purification of LL37 fused to a family III carbohydrate-binding module from *Clostridium thermocellum*. *Protein Expr. Purif.* 2010; 71: 1–7.

Ramos, R., Moreira, S., Rodrigues, A., Gama, M., & Domingues, L. Recombinant expression and purification of the antimicrobial peptide magainin-2. *Biotechnol. Prog.* 2013; 29: 17–22.

Ren-Heidenreich, L., Davol, P. A., Kouttab, N. M., Elfenbein, G. J., Lum, L. G. Redirected T-cell cytotoxicity to epithelial cell adhesion molecule-overexpressing adenocarcinomas by a novel recombinant antibody, E3Bi, *in vitro* and in an animal model. *Cancer.* 2004; 100: 1095-1103.

Reusch, U., Le Gall, F., Hensel, M., Moldenhauer, G., Ho, A. D., Little, M., Kipriyanov, S. M. Effect of tetravalent bispecific CD19xCD3 recombinant antibody construct and CD28 costimulation on lysis of malignant B cells from patients with chronic lymphocytic leukemia by autologous T cells. *Int. J. Cancer*. 2004; 112: 509-518.

Ristau, B. T., O'Keefe, D. S., Bacich, D. J. The prostate-specific membrane antigen: Lessons and current clinical implications from 20 years of research. *Urologic. Oncol.* 2013; 1-8.

Rogers, C. G., Yan, G., Zha, S., Gonzalgo, M. L., Isaacs, W. B., Luo, J., De Marzo, A. M., Nelson, W. G., Pavlovich, C. P. Prostate cancer detection on urinalysis for alpha methylacyl coenzyme a racemase protein. *J. Urol.* 2004; 172: 1501-1503.

Ross, J. S., Sheehan, C. E., Fisher, H. A., Kaufman, R. P., Kaur, P., Gray, K., Webb, I., Gray, G. S., Mosher, R., Kallakury, B. V. Correlation of primary tumour prostate-specific membrane antigen expression with disease recurrence in prostate cancer. *Clin. Cancer Res.* 2003; 9: 6357–6362.

Rossi, E.A., Sharkey, R. M., McBride, W., Karacay, H., Zeng, L., Hansen, H. J., Goldenberg, D. M., Chang, C. H. Development of new multivalent-bispecific agents for pretargeting tumour localization and therapy. *Clinical Cancer Research : an official journal of the American Association for Cancer Research*. 2003; 9: 3886S-3896S.

Rousset, R., Mack, J. A., Wharton, K. A., Axelrod, J. D., Cadigan, K. M., Fish, M. P., Nusse, R., Scott, M. P. Naked cuticle targets dishevelled to antagonize Wnt signal transduction. *Genes Dev.* 2001; 15: 658–671.

Rubenstein, A. B., & Rubnitz, M. E. Transitional cell carcinoma of the prostate. *Cancer.* 1969; 24: 543-546.

Rubin, M. A., Zhou, M., Dhanasekaran, S. M., Varambally, S., Barrette, T. R., Sanda, M. G., Pienta, K. J., Ghosh, D., Chinnaiyan, A. M. alpha-Methylacyl coenzyme A racemase as a tissue biomarker for prostate cancer. *JAMA.* 2002; 287: 1662-1670.

Rudert, F., Visser, E., Gradl, G., Grandison, P., Shemshedini, L., Wang, Y., Grierson, A., Watson, J. pLEF, a novel vector for expression of glutathione S-transferase fusion proteins in mammalian cells. *Gene.* 1996; 169: 281-282

Sadeghi, M. M. H., Rabbani, M., Rismani, E., Moazen, F., Khodabakhsh, F., Dormiani, K., & Khazaei, Y. Optimization of the expression of reteplase in *Escherichia coli*. *Res. Pharm. Sci.* 2011; 6: 87–92.

Saito, T., Mitomi, H., Imamhasan, A., Hayashi, T., Mitani, K., Takahashi, M., Kajiyama, Y., Yao, T. Downregulation of sFRP-2 by epigenetic silencing activates the β-catenin/Wnt signaling pathway in esophageal basaloid squamous cell carcinoma. *Virchows Arch.* 2014; 464: 135-43.

Sarkar, S., Tang, X. L., Das, D., Spencer, J. S., Lowary, T. L., & Suresh, M. R. A bispecific antibody based assay shows potential for detecting tuberculosis in resource constrained laboratory settings. *PLoS One.* 2012; 7: e32340.

Schade, R., Calzado, E. G., Sarmiento, R., Chacana, P. A., Porankiewicz-Asplund, J., Terzolo, H. R. Chicken egg yolk antibodies (IgY-technology): a review of progress in production and use in research and human and veterinary medicine. *Altern. Lab. Anim.* 2005; 33:129-154.

Schmidt, T. G. M., & Skerra, A. One-step affinity purification of bacterially produced proteins by means of the strep tag and immobilized recombinant core streptavidin. *J. Chromatogr. A.* 1994; 676: 337–345.

Schmidt-Ott, K. M., Barasch, J. WNT/beta-catenin signaling in nephron progenitors and their epithelial progeny. *Kidney Int.* 2008; 74: 1004-1008.

Seimetz, D., Lindhofer, H., Bokemeyer, C. Development and approval of the trifunctional antibody catumaxomab (anti-EpCAM x anti-CD3) as a targeted cancer immunotherapy. *Cancer Treat. Rev.* 2010; 36: 458-467.

Selius, B. A., & Subedi, R. Urinary retention in adults: diagnosis and initial management. *Am. Fam. Physician.* 2008; 77: 643-650.

Sharkey, R. M., Karacay, H., McBride, W. J., Rossi, E. A., Chang, C. H., & Goldenberg, D. M. Bispecific antibody pre-targeting of radionuclides for immuno single-photon emission computed tomography and immunopositron emission tomography molecular imaging: an update. *Clin. Cancer Res.* 2007; 13: 5577s-5585s.

Shen, M. M., & Abate-Shen, C. Molecular genetics of prostate cancer: new prospects for old challenges. *Genes Dev.* 2010; 24: 1967-2000.

Shi, Y., He, B., You, L., Jablons, D., M. Roles of secreted frizzled-related proteins in cancer. *Acta. Pharmacol. Sin.* 2007; 28: 1499-504.

Skerra, A., Plückthun, A. Assembly of a functional immunoglobulin Fv fragment in *Escherichia coli. Science.* 1988; 240:1038-1041.

Smith, D. B., & Johnson K. S. Single-step purification of polypeptides expressed in *Escherichia coli* as fusions with glutathione-*S*-transferase. *Gene*. 1988; 67: 31–40.

Smith, M. R., Kabbinavar, F., Saad, F., Hussain, A., Gittelman, M. C., Bilhartz, D. L., Wynne, C., Murray, R., Zinner, N. R., Schulman, C., Linnartz, R., Zheng, M., Goessl, C., Hei, Y., Small, E., Cook, R., & Higano, C. S. Natural history of rising serum prostate-specific antigen in men with castrate nonmetastatic prostate cancer. *J. of Clin. Oncol*. 2005a; 23: 2918 – 2925.

Smith, J., Kontermann, R. E., Embleton, J., & Kumar, S. Antibody phage display technologies with special reference to angiogenesis. *FASEB J*. 2005b; 19: 331-341.

Sokoll, L. J., Chan, D. W., Mikolajczyk, S. D., Rittenhouse, H. G., Evans, C. L., Linton, H. J., Mangold, L. A., Mohr, P., Bartsch, G., Klocker, H., Horninger, W., & Partin, A.W. Proenzyme PSA for the early detection of prostate cancer in the 2.5-4.9 ng/mL total PSA range: preliminary analysis. *Urol.* 2003; 61: 274-276.

Sonoda, H., Kumada, Y., Katsuda, T., & Yamaji, H. Effects of cytoplasmic and periplasmic chaperones on secretory production of single-chain Fv antibody in *Escherichia coli*. *J. Biosci. Bioeng.* 2011; 111: 465–470.

Stewart, E.J., Aslund, F., & Beckwith, J. Disulfide bond formation in the *Escherichia coli* cytoplasm: an *in vivo* role reversal for the thioredoxins. *EMBO J.* 1998; 17: 5543–5550.

Stewart, D. J. Wnt signaling pathway in non-small cell lung cancer. *J. Natl. Cancer Inst.* 2014; 106: djt356.

Sui, C., Wang, G., Chen, Q., Ma, J. Variation risks of SFRP2 hypermethylation between precancerous disease and colorectal cancer. *Tumour Biol.* 2014; 35: 10457-65.

Sunwoo, H. H., Palaniyappan, A., Ganguly, A., Bhatnagar, P. K., Das, D., El-Kadi, A. O., & Suresh, M. R. Quantitative and sensitive detection of the SARS-CoV spike protein using bispecific monoclonal antibody-based enzyme-linked immunoassay. *J. Virol. Meth.* 2013; 187: 72-78.

Surana, R., Sikka, S., Cai, W., Shin, E. M., Warrier, S. R., Tan, H. J., Arfuso, F., Fox, S. A., Dharmarajan, A. M., Kumar, A. P. Secreted frizzled related proteins: Implications in cancers. *Biochim. Biophys. Acta.* 2014; 1845: 53-65.

Suresh, M. R., Cuello, A. C., Milstein, C. Advantages of bispecific hybridomas in one-step immunocytochemistry and immunoassays. *Proc Natl Acad Sci U S A.* 1986; 83: 7989-93.

Suzuki, H., Toyota, M., Carraway, H., Gabrielson, E., Ohmura, T., Fujikane, T., Nishikawa, N., Sogabe, Y., Nojima, M., Sonoda, T., Mori, M., Hirata, K., Imai, K., Shinomura, Y., Baylin, S. B., Tokino, T. Frequent epigenetic inactivation of Wnt antagonist genes in breast cancer. *Br. J. Cancer*. 2008; 98: 1147-1156.

Sweat, S. D., Pacelli, A., Murphy, G. P., & Bostwick, D. G. Prostate-specific membrane antigen expression is greatest in prostate adenocarcinoma and lymph node metastases. *Urolology* 1998; 59: 3192-3198.

Tabesh, A., Teverovskiy, M., Pang, H. Y., Kumar, V. P., Verbel, D., Kotsianti, A., & Saidi, O. Multi-feature prostate cancer diagnosis and Gleason grading of histological images. *IEEE Trans. Med. Imaging.* 2007; 26: 1366-1378.

Tagawa, S. T., Beltran, H., Vallabhajosula, S., Goldsmith, S. J., Osborne, J., Matulich, D., Petrillo, K., Parmar, S., Nanus, D. M., & Bander, N. H. Anti-Prostate Specific Membrane Antigen-based Radioimmunotherapy for Prostate Cancer. *Cancer.* 2010; 116: 1075–1083.

Taichman, R. S., Loberg, R. D., Mehra, R., & Pienta, K. J. The evolving biology and treatment of prostate cancer. *J. Clin. Invest.* 2007; 117: 2351-2361.

Takemura, S., Kudo, T., Asano, R., Suzuki, M., Tsumoto, K., Sakurai, N., Katayose, Y., Kodama, H., Yoshida, H., Ebara, S., Saeki, H., Imai, K., Matsuno, S., Kumagai, I. A mutated superantigen SEA D227A fusion diabody specific to MUC1 and CD3 in targeted cancer immunotherapy for bile duct carcinoma. *Cancer Immunol. Immunother.* 2002; 51: 33-44.

Tan, P. H., Sandmaier, B. M., Stayton, P. S. Contributions of a highly conserved VH/VL hydrogen bonding interaction to scFv folding stability and refolding efficiency. *Biophys. J.* 1998; 75: 1473-1482.

Tang, X. L., Peppler, M. S., Irvin, R. T., & Suresh, M. R. Use of bispecific antibodies in molecular velcro assays whose specificity approaches the theoretical limit of immunodetection for Bordetella pertussis. *Clin. Diagn. Lab Immunol.* 2004; 11: 752-757.

Taira, A., Merrick, G., Wallner, K., & Dattoli, M. Revising the acid phosphatatse test for prostate cancer. *Oncol.* 2007; 21: 1003-1010.

Tekabe, Y., Einstein, A. J., Johnson, L. L., & Khaw, B. A. Targeting very small model lesions pretargeted with bispecific antibody with 99mTc-labeled high-specific radioactivity polymers. *Nucl. Med. Commun.* 2010; 31: 320-327.

Terpe, K. Overview of tag protein fusions: from molecular and biochemical fundamentals to commercial systems. *Appl. Microbiol. Biotechnol.* 2003; 60: 523-533.

Terpe, K. Overview of bacterial expression systems for heterologous protein production: from molecular and biochemical fundamentals to commercial systems. *Appl. Microbiol. Biotechnol.* 2006; 72: 211-222.

Thanendrarajan, S., Kim, Y., Schmidt-Wolf, I. G. Understanding and Targeting the Wnt/β-Catenin Signaling Pathway in Chronic Leukemia. *Leuk. Res. Treatment.* 2011; 2011: 1-10.

Thompson, I. M., Goodman, P. J., Tangen, C. M., Lucia, M. S., Miller, G. I., Ford, I. G., Lieber, M. M., Cespedes, R. D., Atkins, J. N., Lippman, S. M., Carlin, S. M., Ryan, A., Szczepanek, C. M., Crowley, J. J., Coltman, C. A. The influence of finasteride on the development of prostate cancer. *N. Engl. J. Med.* 2003; 17349: 215-224.

Thompson, I. M., Ankerst, D. P., Chi, C., Lucia, M. S., Goodman, P. J., Crowley, J. J., Parnes, H. L., & Coltman, C. A. Operating characteristics of prostate-specific antigen in men with an initial PSA level of 3.0 ng/ml or lower. *JAMA.* 2005; 294: 66-70.

Tilley, P. A., Kanchana, M. V., Knight, I., Blondeau, J., Antonishyn, N., & Deneer, H. Detection of Bordetella pertussis in a clinical laboratory by culture, polymerase chain reaction, and direct fluorescent antibody staining; accuracy, and cost. *Diagn. Microbiol. Infect. Dis.* 2000; 37: 17-23.

Tizard, I. The avian antibody response. *Semin. Avian Exot. Pet.* 2002; 11: 2-14.

Tomme, P., Boraston, A., Mclean, B., Kormos, J., Creagh, A. L., Sturch, K. Characterization and affinity applications of cellulose-binding domains. *J. Chromatogr. B.* 1998; 715: 283–296.

Troyer, J. K., Beckett, M. L., Wright, G. L. Detection and characterization of the prostate-specific membrane antigen (PSMA) in tissue extracts and body fluids. *Int. J.Cancer.* 1995; 62: 552-558.

Turner, A. P. Biosensors: sense and sensibility. *Chem. Soc. Rev.* 2013; 42: 3184-3196.

Turner, P., Holst, O., Karlsson, E. N. Optimized expression of soluble cyclomaltodextrinase of thermophilic origin in *Escherichia coli* by using a soluble fusion-tag and by tuning of inducer concentration. *Protein Expr. Purif.* 2005; 9: 54-60.

Uematsu, K., He, B., You, L., Xu, Z., McCormick, F., Jablons, D. M. Activation of the Wnt pathway in non small cell lung cancer: evidence of dishevelled overexpression. *Oncogene.* 2003; 22: 7218-7221.

Van Beusechem, V. W., Grill, J., Mastenbroek, D. C., Wickham, T. J., Roelvink, P. W., Haisma, H. J., Lamfers, M. L., Dirven, C. M., Pinedo, H. M., Gerritsen, W. R. Efficient and selective gene transfer into primary human brain tumours by using single-chain antibody-targeted adenoviral vectors with native tropism abolished. *J Virol.* 2002; 76: 2753-2762.

Vaillancourt P., Zheng C. F., Hoang D. Q., & Briester L. Affinity purification of recombinant proteins fused to calmodulin or to calmodulin-binding peptides. *Appl. Chimeric Genes Hybrid Proteins Pt. A.* 2000; 326: 340–362.

Varma, M., & Jasani, B. Diagnostic utility of immunohistochemistry in morphologically difficult prostate cancer: review of current literature. *Histopathol.* 2005; 47: 1-16.

Vasan, S. S. Ageing male and testosterone: current status and treatment guidelines. *Indian J. Urol*. 2006; 22: 15-22.

Veeck, J., Noetzel, E., Bektas, N., Jost, E., Hartmann, A., Knüchel, R., Dahl, E. Promoter hypermethylation of the SFRP2 gene is a high-frequent alteration and tumour-specific epigenetic marker in human breast cancer. *Mol. Cancer.* 2008; 7: 83-93.

Velonas, V. M., Woo, H. H., dos Remedios, C. G., & Assinder, S. J. Current status of biomarkers for prostate cancer. *Int. J. Mol. Sci.* 2013; 14: 11034-11060.

Hodnik, V., Anderluh, G. Toxin Detection by Surface Plasmon Resonance. *Sensors* 2009; 9: 1339-1354.

Vera, A., González-Montalbán, N., Arís, A., Villaverde, A. The conformational quality of insoluble recombinant proteins is enhanced at low growth temperatures. *Biotechnol. Bioeng*. 2007; 96: 1101–1106.

Wang, D., & Tang, D. Hypermethylated *SFRP2* gene in fecal DNA is a high potential biomarker for colorectal cancer noninvasive screening. *World J. Gastroenterol.* 2008; 14: 524–531.

Warr, G. W., Magor K. E., Higgins, D. A. IgY: clues to the origins of modern antibodies. *Immunol. Today.* 1995; 16: 392-8.

Waugh, D. S. Making the most of affinity tags. *Trends Biotechnol.* 2005; 23: 316-320.

Weiner, L. M, Surana, R., & Wang, S. Antibodies and cancer therapy: versatile platforms for cancer immunotherapy. *Nat. Rev. Immunol.* 2010; 10: 317–327.

Weisbart, R.H., Wakelin, R., Chan, G., Miller, C. W., Koeffler, P. H. Construction and expression of a bispecific single-chain antibody that penetrates mutant p53 colon cancer cells and binds p53. *Int. J. Oncol.* 2004; 25: 1113-1118.

Wolf, E., Hofmeister, R., Kufer, P., Schlereth, B., Baeuerle, P. A. BiTEs: bispecific antibody constructs with unique anti-tumour activity. *Drug Discov. Today.* 2005; 10: 1237-1244.

Wright, G. L., Grob, B. M., Haley, C., Grossman, K., Newhall, K., Petrylak, D., Troyer, J., Konchuba, A., Schellhammer, P. F., & Moriarty, R. Upregulation of prostate-specific membrane antigen after androgen- deprivation therapy. *Urol.* 1996; 48: 326-334.

Wright, G. L., Haley, C., Beckett, M. L., Schellhammer, P. F. Expression of prostate-specific membrane antigen in normal, benign and malignant prostate tissues. *Urologic. Oncol.* 1995; 1: 18-28.

Wu, C., Ying, H., Grinnell, C., Bryant, S., Miller, R, Clabbers, A., Bose, S., McCarthy, D., Zhu, R. R., Santora, L., Davis-Taber, R., Kunes, Y., Fung, E.,

Schwartz, A., Sakorafas, P., Gu, J., Tarcsa, E., Murtaza, A., Ghayur, T. Simultaneous targeting of multiple disease mediators by a dual-variable-domain immunoglobulin. *Nat. Biotechnol*. 2007; 25: 1290-1297.

Wuest, T., Moosmayer, D., Pfizenmaier, K. Construction of a bispecific single chain antibody for recruitment of cytotoxic T cells to the tumour stroma associated antigen fibroblast activation protein. *J. Biotechnol*. 2001; 92: 159-168.

www.who.int/topics/tuberculosis/en/ Global tuberculosis report, 2012. (Accessed in January 2014).

www.ncri.ie. Trends in Irish cancer Incidence, 1994-2012. (Accessed in Sept. 2015).

Xiao, Z., Adam, B. L., Cazares, L. H., Clements, M. A., Davis, J. W., Schellhammer, P. F., Dalmasso, E. A., & Wright, G. L. Quantitation of serum prostate-specific membrane antigen by a novel protein biochip immunoassay discriminates benign from malignant prostate disease. *Cancer Res.* 2001; 61: 6029-33.

Xiong, D., Xu, Y., Liu, H., Peng, H., Shao, X., Lai, Z., Fan, D., Yang, M., Han, J., Xie, Y., Yang, C, Zhu, Z. Efficient inhibition of human B-cell lymphoma xenografts with an anti-CD20 x anti-CD3 bispecific diabody. *Cancer Lett.* 2002; 177: 29-39.

Yam, W. C., Chan, K. H., Poon, L. L., Guan, Y., Yuen, K. Y., Seto, W. H., & Peiris, J. S. Evaluation of reverse transcription-PCR assays for rapid diagnosis of severe acute respiratory syndrome associated with a novel coronavirus. *J. Clin. Microbiol.* 2003; 41: 4521-4524.

Yamada, H., Tsuzuki, T., Maeda, N., Yamauchi, Y., Yoshida, S., Ishida, R., Nishikimi, T., Yokoi, K., Kobayashi, H. Alpha methylacyl-CoA racemase (AMACR) in prostate adenocarcinomas from Japanese patients: Is AMACR a "race" -dependent marker. *Prostate*. 2013; 73: 54-59.

Yamashita, M., Yamate, M., Li, G. M., & Ikuta, K. Susceptibility of human and rat neural cell lines to infection by SARS-coronavirus. *Biochem. Biophys. Res. Commun.* 2005; 334: 79-85.

Yang, D., Holt, G. E., Velders, M. P., Kwon, E. D., Kast, W. M. Murine six-transmembrane epithelial antigen of the prostate, prostate stem cell antigen, and prostate-specific membrane antigen: prostate-specific cell-surface antigens highly expressed in prostate cancer of transgenic adenocarcinoma mouse prostate mice. *Cancer Res.* 2001; 61: 5857-5860.

Yang, X., Noushmehr, H., Han, H., Andreu-Vieyra, C., Liang, G., Jones, P. A. Gene reactivation by 5-aza-2′-deoxycytidine–induced demethylation requires SRCAP–mediated H2A.Z insertion to establish nucleosome depleted regions. *PLoS*. 2012; 8: e1002604.

Young, C. L., Britton, Z. T., Robinson, A. S. Recombinant protein expression and purification: a comprehensive review of affinity tags and microbial applications. *Biotechnol. J.* 2012; 7: 620-634.

Zhang, Y. B., Howitt, J., McCorkle, S., Lawrence, P., Springer, K., Freimuth, P. Protein aggregation during overexpression limited by peptide extensions with large net negative charge. *Protein Expr. Purif.* 2004; 36: 207-216.

Ziada, A., Rosenblum, M., & Crawford, E. D. Benign prostatic hyperplasia: an overview. *Urol.* 1999; 53: 1-6.